AD-A198 910

ORT DOCUMENTATION PAGE

1a. REPORT SECURITY CLASSIFICATION: Unclassified	1b. RESTRICTIVE MARKINGS:
2a. SECURITY CLASSIFICATION AUTHORITY:	3. DISTRIBUTION/AVAILABILITY OF REPORT: Unlimited
2b. DECLASSIFICATION/DOWNGRADING SCHEDULE:	
4. PERFORMING ORGANIZATION REPORT NUMBER(S):	5. MONITORING ORGANIZATION REPORT NUMBER(S):
6a. NAME OF PERFORMING ORGANIZATION: Stanford University; 6b. OFFICE SYMBOL (If applicable):	7a. NAME OF MONITORING ORGANIZATION: Office of Naval Research
6c. ADDRESS (City, State and ZIP Code): Edward L. Ginzton Laboratory, W.W. Hansen Laboratories of Physics, Stanford, CA 94305	7b. ADDRESS (City, State and ZIP Code): Metallurgy and Ceramics Program, 800 N. Quincy Street, Arlington, VA 22217
8a. NAME OF FUNDING/SPONSORING ORGANIZATION; 8b. OFFICE SYMBOL (If applicable):	9. PROCUREMENT INSTRUMENT IDENTIFICATION NUMBER: N00014-79-C-0222
8c. ADDRESS (City, State and ZIP Code):	10. SOURCE OF FUNDING NOS. — PROGRAM ELEMENT NO.; PROJECT NO.; TASK NO.; WORK UNIT NO.
11. TITLE (Include Security Classification): Elastic Domain Wall Waves in Ferroelectric Ceramics and Single Crystals	
12. PERSONAL AUTHOR(S): B. A. Auld	
13a. TYPE OF REPORT: Final Report; 13b. TIME COVERED: FROM 2/1/79 TO 1/31/88; 14. DATE OF REPORT (Yr., Mo., Day): 1988 July; 15. PAGE COUNT: 67	
16. SUPPLEMENTARY NOTATION	
17. COSATI CODES — FIELD; GROUP; SUB. GR.	18. SUBJECT TERMS (Continue on reverse if necessary and identify by block number): Composites, Piezoelectric, Transducers, Electrostriction, Signal Processing, Adaptive Filters, Surface Acoustic Waves, Sonar, Mode Suppression, Boundary Layer Noise.

19. ABSTRACT (Continue on reverse if necessary and identify by block number)

This report reviews research on acoustic guided waves along poling transitions in counter-poled ferroelectric ceramics, signal processing with programmable electrostrictive SAW transducers, improved performance and mode suppression in periodic piezoelectric/epoxy composites, programmable acoustic and optical gratings in ferroelastic crystals. It concludes with projections and needs for future work on electrostrictive transducers and periodic composites for hydrophone applications. Particular attention is paid to new materials amd structures for the transducers, and to the potential of periodic composites for spatial filtering of turbulent boundary layer noise in hydrophones.

20. DISTRIBUTION/AVAILABILITY OF ABSTRACT: UNCLASSIFIED/UNLIMITED ☒ SAME AS RPT. ☐ DTIC USERS ☒	21. ABSTRACT SECURITY CLASSIFICATION: Unclassified
22a. NAME OF RESPONSIBLE INDIVIDUAL: B. A. Auld	22b. TELEPHONE NUMBER (Include Area Code): 415-723-0264; 22c. OFFICE SYMBOL: Professor Research

DD FORM 1473, 83 APR — EDITION OF 1 JAN 73 IS OBSOLETE.

Unclassified
SECURITY CLASSIFICATION OF THIS PAGE

ELASTIC DOMAIN WALL WAVES IN FERROELECTRIC CERAMIC AND SINGLE CRYSTALS

Final Report
for the period
February 1 1979 - January 31 1988

Sponsored by the Office of Naval Research under
Contract No. N00014-79-C-0222

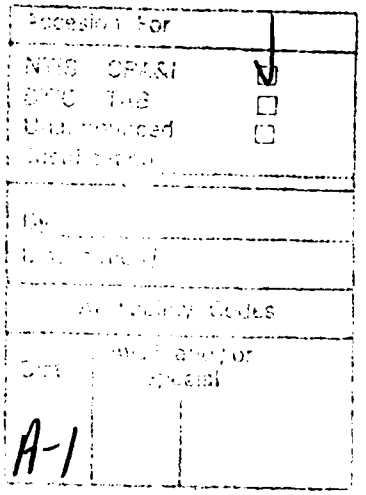

July 1988

Principal Investigator
B. A. Auld

Edward L. Ginzton Laboratory
W. W. Hansen Laboratories of Physics
Stanford University
Stanford, California 94305

TABLE OF CONTENTS

I. INTRODUCTION

The initial aim of the research was to investigate use of new types of elastic waves as probes for examining the material properties of piezoelectric and electrostrictive types of ferroelectric ceramics and single crystals. This was for the purpose of shedding light on the effectiveness and general characteristics of fabrication techniques, as well as exploring basic physical mechanisms playing a role in the technology of this class of materials. In the category of relevant physical mechanisms, one can cite poling phenomena and grain boundary effects. This study was considered generally as influencing improvements of new materials. A possible spin-off could be the invention of switchable elastic interface waveguides for electronic signal processing.

Elastic interface waves can exist on either natural or artificial domain wall structures– ferroelectric and ferroelastic natural domain walls in single crystals, interfaces between glue-bonded materials with different elastic properties, or at the transition region between counterpoled parts of a single piece of ferroelectric ceramic. The last case provides an artificial domain wall geometry having the switchable properties of natural domain walls.

The material interfaces discussed above may be introduced *extrinsically* by introducing actual inclusions of a second material phase (by glue bonding different materials together, or by embedding inclusions in a polymer matrix), or *intrinsically* by altering the material properties with a selectively applied electric field or stress. In the second case, one can distinguish between: (1) intrinsic material inhomogeneities introduced by poling patterns of electrical polarization into remanent-type ferroelectrics (such as PZT or PLZT), (2) intrinsic inhomogeneities introduced by selective electric field biasing of relaxor-type ferroelectrics (such as PMN), and (3) arrays of ferroelastic domains introduced and switched by applied stress patterns. Materials with intrinsic inhomogeneities offer exciting possibilities for realizing a variety of planar signal routing and processing devices on small ferroelectric wafers, fabricated by simple inexpensive poling and biasing techniques. Such devices may be either slowly or rapidly switched and programmed, according to the choice

of either a remanent-type or a relaxor-type ferroelectric material.

During the second half of this program the scope of the research was extended beyond the guidance of elastic waves along natural and artificial domain wall interfaces. Specifically, the emphasis was shifted gradually to transduction in both extrinsic and intrinsic types of piezoelectric composites. The following topics have been investigated in detail:

(i) elastic resonance, transduction, and propagation in two-phase composites of extrinsic type, such as the PZT-plastic composites used in hydrophones.

(ii) programmable elastic wave transduction and signal processing, and optical signal processing in relaxor ferroelastics such as PMN and PLZT; and

(iii) optical and elastic wave signal processing with programmable domain wall structures in ferroelastic crystals, especially neodymium pentaphosphate.

Also, several trends and promising directions for the future have been identified: possible tailoring of composite piezoelectrics for spatial and temporal filtering of flow noise in sonar receivers, development of thick relaxor ferroelectric films for programmable SAW and STW transducers, investigation of the kinetics of domain wall motion in ferroelastics in connection with domain wall devices and better understanding of new ferroelectric materials.

II. GENERAL REVIEW

The initial phase of this project was an in-depth study of elastic wave propagation by the transition zone region in differentially-poled piezoelectric ceramics. It was shown that the elastic wave is strongly confined to the transition zone because of the well-known ducting effect, where a region of slower velocity than its surroundings acts as a waveguide. The wave slowing occurs in a transition region because the polarization goes to zero and, with it, the piezoelectric coupling. That is to say, the piezoelectric stiffening, which acts to increase the elastic velocity, is on the average below zero within a transition zone. As a result of the strong confinement in a typical transition zone,

the wave has a strong cumulative interaction with the zone, and is therefore sensitive to changes in the zone structure. The zone structure may be characterized by its width, profile curve, and piezoelectric coupling. In turn, these macroscopic parameters depend on microscopic structural features, such as grain size, domain wall mobility and symmetry of the constitutive polycrystals, and also on the macroscopic material properties, such as stiffness, loss and coercive fields. In this part of the research effort the effects of the above factors were investigated in different ferrites, and prototypes of several potential device applications of transition-zone waveguides were built and tested.

In the second phase of this research the investigation was expanded into other techniques for controlling elastic wave propagation and resonance by artificially controlled inhomogenities in material properties. Here, the emphasis shifted from wave guidance by intrinsically-induced material "ducts" to: (1) the optimization of material properties for piezeoelectric transduction by combining two phases to produce a composite that has superior properties to either of the individual phases, taken separately; (2) electronically programmable linear electromechanical coupling by spatially inhomogeneous dc biasing of nonpiezolectric,—i.e., electrostrictive—ceramics; and (3) filtering and scattering of optical and acoustic waves, for signal processing applications, by using arrays of domain walls created and tuned in ferroelastic crystals by externally applying mechanical, electrical and optical patterns of spatial excitation.

(a) COUNTERPOLED CERAMICS

Structure of Ferroelectric Ceramics

In our study of elastic domain wall waves in differentially poled ceramics, we have chosen to concentrate on the widely popular and commercially available ceramics known collectively as PZT. These ceramics are all derived from the system PbO-ZrO_2-TiO_2, hence the acronym PZT. When these three constituents are mixed and reacted in the appropriate way [1], a compound consisting of $PbZrO_3$ and $PbTiO_3$ in solid solution results. This solid solution is the basis of PZT, and subsequently undergoes grinding, forming, and firing to

become the final ceramic body. The firing process is essentially a densification process which decreases ceramic porosity, creates intergranular bonds, and generally increases the strength of the ceramic. In addition, the firing process causes some grain growth by solid state diffusion, and this can be utilized to adjust the grain size in the final body [2].

The basic polycrystalline structure of a typical PZT ceramic is a randomly distributed collection of grains, each of which is a single ferroelectric crystal. The properties of the ceramic body as a whole are largely determined by features of the single crystal grain, such as grain size, crystal symmetry, and domain wall mobility. These features are all strongly dependent on the balance of the $PbZrO_3$ to $PbTiO_3$ in the grain as well as the presence of additional dopants. To obtain materials with high dielectric constant and strong electromechanical coupling, all PZT's have a composition within a few percent of 53.5% $PbZrO_3$ and 46.5% $PbTiO_3$ [3]. This particular balance constitutes a morphotropic phase boundary in the $PbZrO_3$–$PbTiO_3$ system, and the ceramic properties dramatically peak at this boundary. In addition, the crystal symmetry of the ceramic grains changes from rhombohedral to tetragonal as this boundary is crossed, with the tetragonal symmetry occurring on the $PbTiO_3$ side of the boundary. It is found that the dielectric constant and coupling factors have their highest values just on the tetragonal side of the phase boundary. Therefore, most of the commercially available PZT's have tetragonal grain symmetry, such as PZT-4 with 47% $PbTiO_3$ and 53% $PbZrO_3$, and PZT-5A with 48% $PbTiO_3$ and 52% $PbZrO_3$ [3]. Nevertheless, proximity to the phase boundary is important, and too much $PbTiO_3$ will favor a more highly distorted tetragonal structure which is difficult to pole [4]. We have found that grain symmetry is an important factor in transition zone formation.

Aside from the balance of $PbZrO_3$ and $PbTiO_3$ in a particular PZT ceramic, the presence of additives can have an important effect on the ceramic material properties. Substitutions for Pb^{+2}, Zr^{+4}, and Ti^{+4} are all possible, with different material properties resulting from each. An isovalent substitution of Sr^{+2} for Pb^{+2} is made in PZT-4, which has the composition $Pb_{0.94}Sr_{0.06}Ti_{0.47}Zr_{0.53}O_3$. This substitution lowers the Curie

temperature 9.5°C for every atom percent of strontium added, and hence raises the dielectric constant at room temperature [5]. Additionally, as a result of this substitution, the ceramic becomes harder to depole by mechanical or electrical means. Consequently, PZT-4 is a difficult material to counterpole, and is not ideally suited for differentially poled waveguide applications.

Ceramics that are difficult to pole and counterpole are often composed of grains having high rigidity and immobile domain walls. For a typical multi-domain crystal grain, reorientation proceeds by domain wall motion, with domains oriented along unfavorable directions shrinking as the domain walls move in from either side [6]. Hence, the mobility of the domain walls is an important factor in grain reorientation. In addition, for the majority of grains, a high degree of crystal deformation is involved in these reorientation processes [7], and the extent to which the reorientation can proceed is largely determined by the intergranular elastic boundary conditions [8]. If the grains are fairly compliant, the deformation of grains undergoing reorientation can be accommodated by neighboring grains, and the counterpoling process will proceed relatively easily. If the grains are highly rigid and the intergranular bonds are strong, grains undergoing reorientation will be "clamped" by neighboring grains, and the counterpoling process will be inhibited.

The substitution of electron-donor additives into a PZT solid solution is a common way to bring about greatly enhanced domain wall mobility within the grains, resulting in a ceramic which is much easier to pole and counterpole [9]. PZT-5A amd PZT-5H are examples of ceramics possessing electron-donor dopants. In PZT-5A, Nb^{+5} is added to the solid solution, replacing Ti^{+4} or Zr^{+4} in the lattice, and yielding a composition $Pb_{0.988}(Ti_{0.48}Zr_{0.52})_{0.976}Nb_{0.024}O_3$. For every two Nb^{+5} added there occurs one Pb^{+2} vacancy in the lattice. This vacancy facilitates easy domain wall motion in the grain, which in turn gives rise to a family of related properties characteristic of electron-donor doped ceramics [10]. Some of the more important properties include: reduced elastic stiffness, increased dielectric constant, high electromechanical coupling constant, low coercive field,

relatively square hysteresis loops, low mechanical Q and high dielectric loss [9]. In these materials, the domain wall mobility allows the grain to easily deform in response to applied field or pressure. This responsiveness accounts for the high dielectric constant and electromechanical coupling observed in these materials. The ease with which the grain deforms to accommodate an applied stress indicates that the ceramic should be very compliant, and the grains will be unable to store large amounts of stress. Therefore, a counterpoling stress in one region of the ceramic should not be transferred to the outlying regions, but instead should be absorbed by easily deformed grains in the immediate region.

The mobility of the domain walls and the inability of the ceramic to store large amounts of internal stress also account for the low coercive field and relatively square hysteresis loops of these materials [9]. Because the intergranular elastic constraints are significantly reduced, the ceramic's hysteresis loop is closer to that of an unconstrained single grain, and resembles the relatively square crystal loop. The nature of the hysteresis loop is another important feature which will have direct relevance to transition zone formation.

Finally, the low mechanical Q and high dielectric loss of these materials arise directly from the domain wall mobility [10]. An elastic wave or alternating electric field in the ceramic will cause the responsive domain walls to vibrate, thereby absorbing energy from the wave or field. Though this high loss can be a desirable feature for a broadband ultrasonic transducer, it is a disadvantage when using PZT-5A or PZT-5H for elastic waveguides.

Another interesting class of PZT ceramics is obtained if we substitute an electron-acceptor additive to the solid solution. Such an additive replaces a given ion with an ion of lower valence. For example, in PZT-8, a small amount of Fe^{+3} is substituted in sites occupied by Zr^{+4} or Ti^{+4}. These electron-acceptor substitutions cause the appearance of oxygen vacancies in the lattice, resulting in a shrinkage of cell size [11]. Ceramics in this family have a different set of properties than those with electron-donor additives.

These properties include: high coercive field, more difficult to pole and counterpole, high mechanical Q and low dielectric loss [11]. These properties are all believed to arise from the shrinkage and distortion of the unit cells by oxygen vacancies, which effectively "pins" domain walls in place, thereby making grain reorientation more difficult, and preventing the compliant grain behavior characteristic of the electron-donor doped ceramics. Therefore, a great deal of internal stress can be stored in these ceramics, so that a regional counterpoling stress will be transferred by the material to surrounding poled regions of ceramic. Because the material is unable to absorb this stress by domain wall motion, the material will be relatively stiff and will have a high mechanical Q.

Another important effect of electron-acceptor doping in PZT is the inhibition of grain growth during ceramic firing [11]. Typical grain sizes in unmodified PZT and electron-donor doped PZT range from 5 to 10 μm whereas the grain size in PZT-8 is about 1 μm [12]. It is believed that the lattice shrinkage in the electron-acceptor ceramics such as PZT-8 make grain growth by diffusion during the firing process more difficult. As a small grained ceramic, we have found PZT-8 to have some interesting properties relevant to transition zone waveguide fabrication.

So far we have discussed the properties of the isovalently doped ceramic PZT-4, the electron-donor doped ceramics PZT-5A and PZT-5H, and the electron-acceptor doped ceramic PZT-8. All of these ceramics are modified solid solutions of $PbZrO_3$–$PbTiO_3$ lying just on the tetragonal side of the morphotropic phase boundary. We have performed differential poling on all of these ceramics, and explain and classify each transition zone in terms of the ceramic's material properties.

In addition to the ceramics listed above, we have studied specimens of the ceramic PZT-7A. This ceramic is one of the few commercially available PZT's which has rhombohedral grain symmetry, lying on the $PbZrO_3$ side of the $PbZrO_3$–$PbTiO_3$ phase boundary [3]. Because of this different crystal symmetry, the reorientations occurring in each rhombohedral grain are fundamentally different than those in a tetrogonal grain.

In a rhombohedral crystal, there exist eight possible directions along which the crystal polarization can be oriented, corresponding to the body diagonals of the unit cell [7]. In a tetragonal crystal, there exist only six allowed polarization directions, corresponding to orientations parallel to the cell edges [7]. Initially in a ferroelectric ceramic, the crystal grains will be randomly distributed among all of the allowed polarization states. When an electric poling field is applied, the grains will attempt to reorient along the direction allowed by symmetry which is closest to the direction of poling. If all domains are reoriented in such a manner, then it follows for tetragonal symmetry that 1/6 of the domains experienced no switching, 1/6 experienced 180° switching, and 2/3 experienced 90° switching. Similarly, for rhombohedral symmetry, 1/8 of the domains would experience no switching, 1/8 would have 180° switching, 3/8 would have 71° switching, and 3/8 would have 109° switching. From these results, it follows that a perfectly poled ceramic having rhombohedral grain symmetry would possess a polarization 86.6% of the maximum single crystal value, compared with 83.1% for the tetragonal grain cramic [7].

In both types of ceramic, the 180° reorientation of domains does not alter the state of strain of a grain with respect to the rest of the ceramic body. As a result, these reorientations proceed relatively unimpeded by elastic constraints, and it is observed that all of the allowed 180° reorientations are achieved in a typical poling process [7]. In contrast, 90° reorientations, occurring in a tetragonal grain ceramic, are often quite difficult to achieve because of the change in strain state accompanying the reorientation. Intergranular elastic constraints will attempt to keep the grain in its initial state of strain, and may block reorientations involving changes in this state. For a typical unmodified tetragonal PZT, one study reported that only 44% of all possible 90° reorientations occurred during poling [7]. In the rhombohedral grain ceramic, where there is no 90° switching, only 71° and 109° reorientations account for changes in strain state. In a typical rhombohedral specimen, it is observed that 65% of the allowed 71° and 109° reorientations occur during poling [7]. Hence, 71° and 109° reorientations in rhombohedral

grains occurred more readily than did 90° reorientations in tetragonal grains. These results suggest that reorientation strain is more easily accommodated in a rhombohedral grain ceramic than it is in a tetragonal grain ceramic.

Though this argument is by no means rigorous, and may not apply for ceramics where additional domain wall mobility and strain relief is achieved by additives, it indicates that in its "unmodified" state, a rhombohedral grain may respond to a counterpoling field in a more compliant way than a tetragonal grain would. As such, a regional counterpoling stress should have a more localized effect in a rhombohedral grain ceramic, since the relatively compliant rhombohedral grains will locally absorb the stress in the vicinity of the counterpoled region, and not distribute the stress over a broad area as in the stiffer tetragonal case. To test this hypothesis, we chose to differentially pole the rhombohedral grain ceramic PZT-7A and compare the resulting transition zone with those in the tetragonal grain ceramic.

Transition Zones in Differentially Poled Ceramics

Understanding the way in which a ferroelectric ceramic responds to a locally applied electric field is of prime importance in the fabrication of elastic domain wall waveguides. If we wish to select an appropriate ferroelectric ceramic for a particular waveguide application based on a manufacturer's list of material properties, we must be able to predict the type of transition zone that the ceramic will support. The formation of a transition zone in a ferroelectric ceramic is a complex process which should be governed by the same underlying intragranular and intergranular forces that control the more commonly measured material properties, such as stiffness, loss, coercive field, etc. We have studied transition zones in a number of commercially available PZT ceramics and attempt to correlate various aspects of these zones with the underlying material properties that control their formation.

Fig. 1 shows two remanent polarization profiles, representing transition zones in PZT-4 and PZT-5H. In both cases, a uniformly poled, 1/4" thick ceramic plate was partially electroded, and suitable counterpoling fields were applied to bring about reorientation

in the electroded region. In this figure, the initial electric polarization was negative throughout the ceramic, and the counterpoled region lies to the left of the origin. It is apparent from the figure that the PZT-4 transition zone is significantly broader than the PZT-5H zone.

In choosing a ferroelectric ceramic for a differentially poled waveguide application, it is important to understand the intrinsic granular material properties which govern transition zone formation. These intrinsic properties, strongly affected by stoichiometry of the $PbZrO_3$–$PbTiO_3$ solid solution and the nature of any additives, include intragranular domain wall mobility, grain size, and grain symmetry, as well as the permittivity, stiffness, and coercive field characterizing each single crystal domain. These properties give rise to the overall macroscopic material properties which characterize the ceramic body as a whole. Some of the macroscopic properties relevant to elastic domain wall propagation and device applications are listed in Table 1 for the ceramics studied. Five commercially available PZT's were investigated, along with one type of barium titanate ceramic for comparison.

The electromechanical shear coupling constant k_{15} for the ceramics studied are listed in the first row of Table 1. PZT ceramic is typified by relatively high coupling constants in general, and the ceramics PZT-4, PZT-5H, and PZT-5A were found to have the highest. The large coupling in these materials arises from the commercial PZT's proximity to the morphotropic phase boundary in the $PbZrO_3$–$PbTiO_3$ system. It was shown in previous reports that a higher k_{15} results in a more strongly guided domain wall wave with a slower phase velocity. This can be a desirable feature in a transition zone waveguide so long as the acoustic wavelength remains longer than the transition zone width. When the wavelength becomes comparable to the transition zone width, higher order modes begin to appear, and materials with larger k_{15} will become multimode at lower frequency than those with smaller k_{15}.

The mechanical Q of the material, designated Q_M in Table 1, is a very important factor

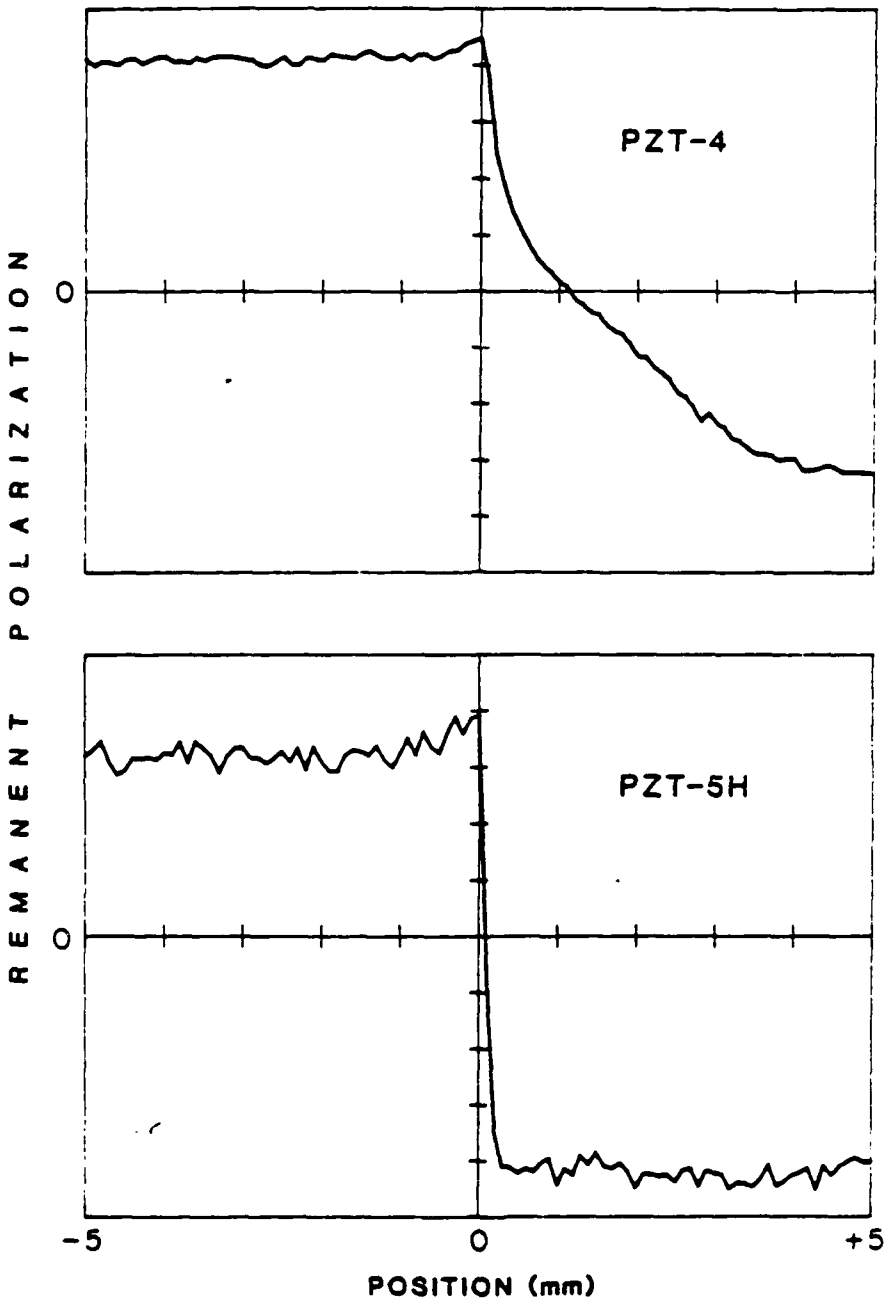

FIGURE 1

Remanent polarization profiles measured in two differentially poled ceramics. In both profiles,the original ceramic polarization was negative, and the left half space represents the counterpoled region. TOP: 1/4" thick PZT-4 plate counterpoled with $E = 47.6$ kV/in for 10 minutes at $T = 140°$ C. BOTTOM: 1/4" thick PZT-5H plate counterpoled with $E = 20$ kV/in for 1 minute at room temperature.

TABLE OF MATERIAL PROPERTIES

	PZT-4	PZT-5H	PZT-8	PZT-7A	PZT-5A	$BaTiO_3$
k_{15}	0.71	0.67	0.60	0.63	0.69	0.45
c_{44}^D	5.18	4.22	4.51	4.72	3.97	5.85
Q_M	500	65	1100	600	75	600
E_c	35-45	16	40-50	19	21	40
T_c	328°	190°	300°	350°	365°	115°

Units and Description of Symbols:

c_{44}^D = elastic stiffness, 10^{10}Newton/m^2

k_{15} = shear coupling factor, (dimensionless)

Q_M = mechanical Q, (dimensionless)

E_c = coercive field, kV/inch

T_c = Curie temperature, °C

TABLE 1

Selected material properties for the ceramics studied.

to consider when using PZT as a waveguide material. From the table, it is evident that Q_M varies dramatically among the commercially available PZT's, ranging from PZT-8 with a Q_M of 1100 to PZT-5H with a Q_M of 65. Since domain wall mobility is a predominant loss mechanism in PZT [11], it follows that Q_M should be related to domain wall mobility in these ceramics. As was discussed above, PZT-5H and PZT-5A are both electron-donor doped ceramics and possess high domain wall mobility. Therefore, as shown in Table 1, Q_M for these materials is considerably lower than the Q_M in ceramics without this doping. For waveguide applications, it is desirable to have material with a high mechanical Q. From that consideration alone, PZT-4, PZT-8, PZT-7A, and $BaTiO_3$ are seen to be good choices for waveguide material. Nevertheless, the mechanical Q's of PZT-5H and PZT-5A are still high enough so as to permit use at frequencies up to roughly 1 MHz. Based on the Q_M values, the shear wave attenuation in PZT-5H at 1 MHz will be approximately 2 dB/cm, which might be acceptable for a delay line of only a few centimeters in length. However, at 5 MHz, this attenuation will climb to at least 10 dB/cm (more if Q_M decreases with frequency) which is unacceptable in a delay line material. In contrast, PZT-8 will support a shear wave with an attenuation of 0.1 dB/cm at 1 MHz, and 0.5 dB/cm at 5 MHz, and constitutes a better choice for a delay line material.

The formation of a transition zone in a differentially poled ceramic is governed by counterpoling forces. From the remanent polarization profiles of Fig. 1, it is clear that these counterpoling forces are not strictly confined to a partially electroded region, but extend beyond the electrode edge into the surrounding unelectroded ceramic. The extent to which these counterpoling forces affect the surrounding unelectroded ceramic determines the structure of the transition zone.

There are two types of force fields arising from the counterpoling process that extend from the partially electroded region into the surrounding ceramic. One is a fringing electric field emanating from the partial electrodes, and the other is a mechanical stress field which arises when one part of a ceramic undergoes a deformation with respect to another.

Though it is difficult to separate these two effects experimentally, since a ceramic which is responsive to electric fringing fields will often support far-reaching mechanical stress fields, it is worthwhile to address these fields individually for the purpose of discussion.

The electric counterpoling fields are fairly uniform and parallel at points well within the electroded region. However,these parallel field lines are distorted near the electrode edge, and extend into the unelectroded region of the ceramic. Therefore, if the fringing fields are strong enough, counterpoling and depoling can occur far from the electrode edge. For this reason, it is wise to apply electric fields which are no stronger than necessary to achieve counterpoling in the electroded region of the ceramic. In this way, the fringing fields can be kept below the threshold for counterpoling, and the effect of these fringing fields on transition zone formation can be minimized.

Of course, electric fringing is only one factor contributing to the breadth of the typical transition zone. The other factor which must be considered is the strong mechanical stress to which the transition zone region is subjected. A region undergoing counterpoling will progress through a range of polarization states, with each state corresponding to a distribution of poling induced strain within the ceramic. The ceramic in the electroded region first becomes depoled before proceeding to its final counterpoled state. The large change in strain state accompanying this process will result in a corresponding mechanical stress within the ceramic. If the grains are very compliant, or intragranular domain wall mobility is great, then the grains can become easily deformed and poling stress is relieved. On the other hand, if the ceramic possesses rigid, stiff grains, and the domain walls are relatively immobile, then the grains will store the poling stress, and a local stress will be more evenly distributed throughout the ceramic.

A ceramic undergoing a regional counterpoling procedure will be subject to inhomogeneous mechanical stresses. Axial compression and tension accompanying domain reorientation in the partially electroded region will create a strong vertical shearing strain in the vicinity of the electrode edge. In a relatively stiff ceramic, this shearing strain will

cause a correspondingly strong shearing stress which extends beyond the electrode edge to cause depoling in the unelectroded region. In a relatively compliant ceramic, the shearing strain will be "absorbed" by compliant grains in the vicinity of the electrode edge, so that the stress arising from this shearing strain far from the edge will be greatly reduced. From these stress considerations alone, it would follow that the more compliant, electron-donor doped ceramics, such as PZT-5A and PZT-5H, should form narrower transition zones. The more rigid unmodified and electron-acceptor doped ceramics, such as PZT-4 and PZT-8, respectively, should form wider zones based on this argument.

In an attempt to quantify the correlation of transition zone width to ceramic stiffness, we sought an easily measured stiffness parameter which could be logically related to the mechanical depoling stress occurring in the partially electroded geometry. Because of the predominant component of shear strain which will occur near the electrode edge during axial tension and compression in the electroded region, we considered the elastic stiffness constant c_{44}^D. This linear stiffness constant gives the amount of shear stress arising when a ceramic is deformed by a shear strain. As such, it is reasonable to assume that the mechanical depoling stress generated in a ceramic by a shear poling strain may be related to this value.

In Table 1, we listed the values of c_{44}^D for the six ceramics studied. These values were obtained from the manufacturer's specification sheet accompanying the materials. Based on this parameter alone, we would expect PZT-5A, with $c_{44}^D = 3.97 \times 10^{10}$ Newton/m^2, to have the narrowest zone width (which it does) with PZT-5H, with $c_{44}^D = 4.22 \times 10^{10}$ Newton/m^2, to have the next narrowest (which it does). On the other hand, PZT-4, possessing a very wide transition zone, has a very large stiffness, $c_{44}^D = 5.18 \times 10^{10}$ Newton/m^2, and PZT-8, with an intermediate transition zone width, has an intermediate stiffness, $c_{44}^D = 4.51 \times 10^{10}$ Newton/m^2. To further test this correlation, we obtained a 1/8" thick piece of $BaTiO_3$ ceramic from Channel Industries having a stiffness $c_{44}^D = 5.85 \times 10^{10}$ Newton/m^2. Because of this high stiffness, we expected to find a ceramic having a very

wide transition zone. Counterpoling the $BaTiO_3$ piece with the lowest field possible to avoid fringing effects (approximately 40 kV/in for 3 minutes at $T = 70°C$), we observed the transition zone width in this ceramic, almost 5 mm in only a 1/8" thick plate, to be far the largest of any measured. This supported the notion that c_{44}^D scales with zone width.

To summarize the findings regarding zone width and ceramic stiffness, we compiled our data in the plot of Fig. 2. The figure shows the transition zone width 2α plotted as a function of ceramic stiffness c_{44}^D. We have defined 2α as the distance between the point having 75% of maximum positive polarization and the point having 75% of maximum negative polarization. The points plotted represent transition zones measured on plates of varying thickness and varying counterpoling conditions. The symbols describing the different plate thicknesses are listed in the upper left corner of the plot. The counterpoling conditions were chosen to suit the ceramic under test, and the aim was to create a suitably counterpoled specimen using as small an electric field and as low a poling temperature as possible.

When interpreting this plot, care must be taken to note the variations in plate thickness which can also affect zone width. For example, it is clear from the figure that a wide variation of values 2α are possible in PZT-8, depending on the plate thickness. Nevertheless, by comparing results from plates of like thicknesses, the trend of increasing zone width with increasing ceramic stiffness is evident. Comparing just the measurements of 1/4" samples (solid dots), we see an increasing trend of zone width with stiffness. Furthermore, we can infer that a hypothetical 1/4" thick piece of $BaTiO_3$ would have a transition zone at least as wide as the zone in a 1/8" thick piece, so that the 1/4" sample point for $BaTiO_3$ would support the increasing trend established by the other 1/4" samples. We can also infer that 1/8" plates of PZT-5A and PZT-5H would have zone widths no greater than those in the 1/4" plates, so that a similar increasing trend could be inferred from the 1/8" sample points alone (ignoring the PZT-7A point for the moment).

A sample of the ceramic PZT-7A, the only rhombohedral grained ceramic in the group,

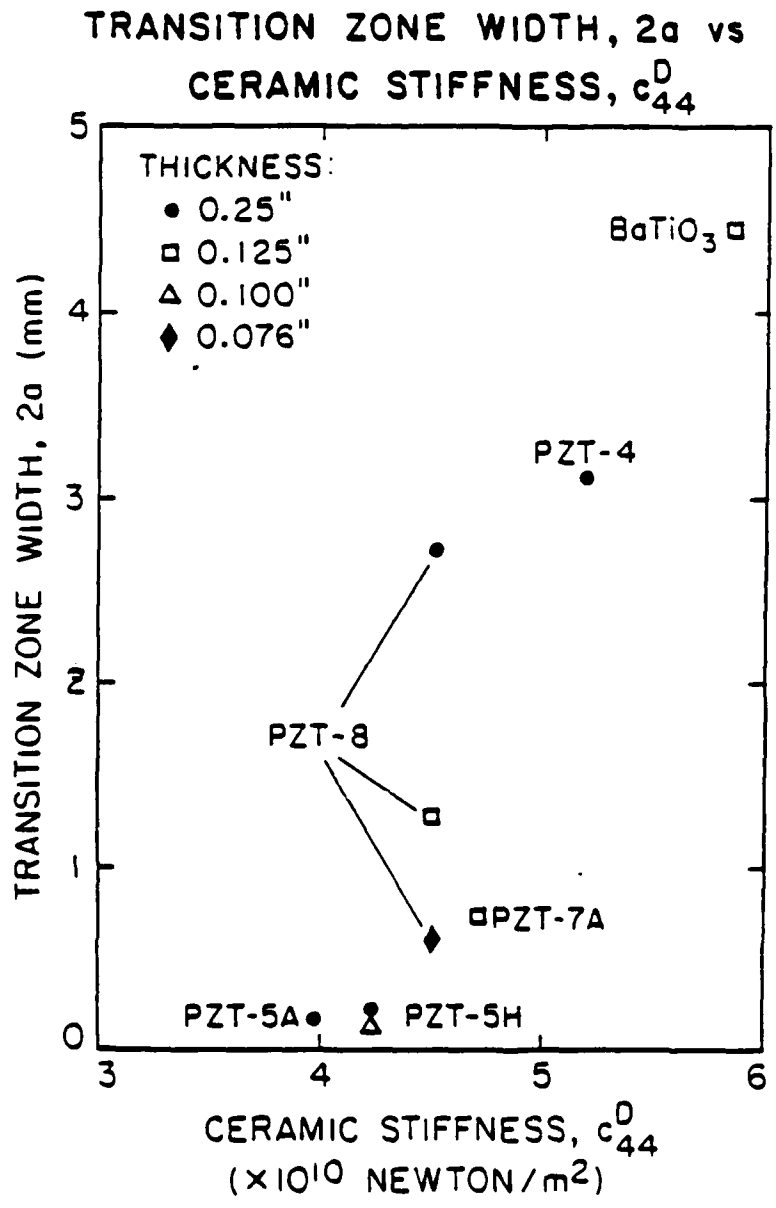

FIGURE 2

Compilation of transition zone width data measured from remanent polarization profiles plotted as a function of shear stiffness c_{44}^D for the various ceramics studied.

was also differentially poled to examine the relation of transition zone width to c_{44}^D in this ceramic. This measured value, plotted as a function of c_{44}^D in Fig. 2, is less than the zone width measured in a PZT-8 plate of the same thickness, and hence represents a ceramic which does not fit the established trend of increasing zone width with c_{44}^D. Because PZT-7A has a higher c_{44}^D than PZT-8, we would have expected PZT-7A to support a wider zone than PZT-8.

A possible reason for this narrower than expected transition zone lies in the rhombohedral grain symmetry of PZT-7A. The assumption that the nonlinear stiffnesses governing polarization reversal could be qualitatively related to a linear stiffness c_{44}^D was made without regard for the underlying grain symmetry in the ceramic. As was described earlier, there are eight possible orientation directions allowed in a rhombohedral grain, as opposed to six in a tetragonal grain. It was shown that it was therefore possible to get a larger net polarization along a given axis, and that the strain-related 71° and 109° reorientations in this symmetry could in practice be achieved with greater ease than the 90° reorientations in a tetragonal grain. Therefore, the rhombohedral grain ceramic should be more reversible than a tetragonal grain ceramic having the same linear stiffness. In other words, given a rhombohedral and tetragonal grain ceramic with the same c_{44}^D, the nature of rhombohedral grain reorientation will make the rhombohedral ceramic more compliant in the nonlinear regime where reorientation takes place. Hence, it is reasonable that the rhombohedral ceramic PZT-7A, being linearly stiff, will have a more compliant nature when subjected to counterpoling fields, and a narrower transition zone will result.

The results of this study can be implemented as a set of "design rules" governing the selection of material for differentially poled ceramic waveguides. To achieve a narrow transition zone so that low dispersion and single mode operation can be obtained, the ideal ceramic sample should have the following properties: small thickness to minimize fringing, relatively square hysteresis loop to minimize the ceramic response to fringing, low stiffness to minimize the mechanical depoling stress outside of the electroded region. In addition,

the ceramic should possess high mechanical Q for lossless waveguide behavior, and large coupling k_{15} for stronger guidance.

The ceramics PZT-5A and PZT-5H were deemed excellent because of the narrow, well-defined transition zones they were capable of supporting. However, their low Q's restricted their use to frequencies below 1 MHz. In addition, PZT-5A demonstrated severe problems with cracking along the transition zone, and was therefore eliminated as a practical ceramic for any differential poling applications. Occasionally, cracking occurred in the PZT-5H zones, but this was much less frequent. Because of the large volume resistivity of PZT-5A and PZT-5H, these ceramics are much more likely to crack during poling operations than the more conductive, lower resistivity ceramics such as PZT-4 and PZT-8. Potentially destructive local strains and electric fields arising in high resistivity ceramics can grow very large, since the flow of compensation charge which would reduce these nonuniformities in a conducting ceramic is limited. For this reason, differential poling in a high resistivity ceramic may be inherently difficult. However, a visual inspection of the PZT-5A used in this work (C-5500 obtained from Channel Industries) revealed gross inhomogeneities and imperfections in the material, which may have been the primary reason for the transition zone cracking observed in this ceramic. The ceramics PZT-4 and $BaTiO_3$ were found to possess inconveniently wide transition zones for practical single mode waveguide operation, and were eliminated on that ground alone. Zone widths of 3 to 5 mm, like those observed in these ceramics, would give rise to many propagating waveguide modes at the frequencies we are interested in, and are therefore unsuitable for our applications.

From this work, the ceramics PZT-7A and PZT-8 emerged as the most serious contenders for single mode elastic domain wall waveguide applications around 1 MHz. Both materials support relatively narrow transition zones, and have sufficiently high Q and k_{15} for relatively lossless, well-guided elastic waves. PZT-7A has the unique feature that the transition zone can be displaced by applying a moderate strength electric field (10 to 15 kV/in) at *room temperature*. This property is especially attractive for directional

coupler devices.

PZT-7A Variable Directional Couplers

Having previously demonstrated and reported the principle of domain wall wave coupling between parallel transition zones in PZT-5H, we proceeded to design a working directional coupler. PZT-7A was chosen for this purpose because the transition zone can be shifted at room temperature by application of an electric field. This allowed the coupling to be varied. Measurements on this device are reported in Publication 9, and in H. A. Kunkel, "Elastic Domain Wall Waves in Ferroelectric Ceramics," Ph.D. Thesis, Department of Applied Physics, Stanford University, June 1985.

(b) PZT/EPOXY COMPOSITES

Stanford composite research under this program was performed in close collaboration with T. R. Gururaja and others at The Pennsylvania State University, and with W. A. Smith and A. Shoulov at Philips Laboratories. This work was aimed at exploring potential applications in ultrasonic transduction (for medical and nondestructive evaluation instrumentation) of the piezoelectric composite materials for hydrophone applications, developed under Navy support at Penn State. The success of this endeavor is evident from the number of publications by ourselves and others in the recent literature and symposium proceedings, as well as the number of companies now producing these materials for ultrasonic arrays.

Theory

The initial goal was to investigate the high frequency dynamic behavior of 3:1 connected PZT-epoxy composites in plate transducer configurations, to better understand the physics of these materials, and to explore their exploitation for applications other than hydrophones. But progress made in formulating a general Floquet (or space harmonic expansion) theory of elastic vibrations in composites now makes it possible to extend the goals of this research. The dynamic behavior of composite materials consisting of *general* periodic lattices of inclusions in a matrix can be analyzed using this theory, which has been

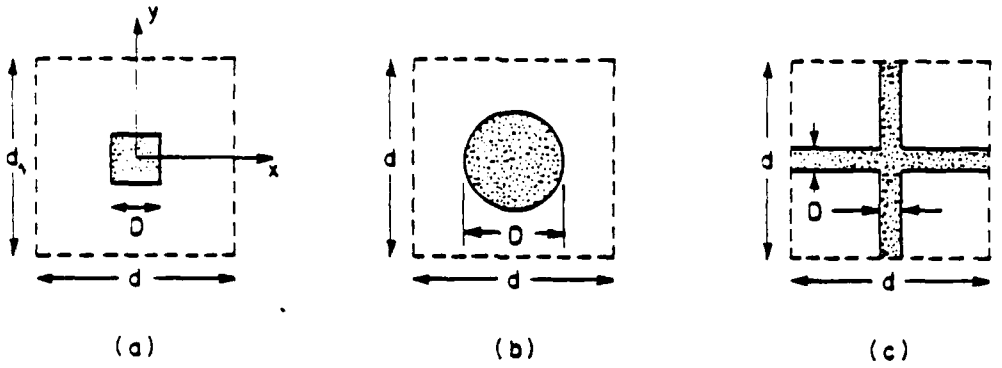

FIGURE 3

Two-dimensional unit cell geometries. Area of unit cell is A. Area of PZT (shaded) is a.

tested in certain specific configurations against experimental results. A capability now exists for quantitatively studying and exploiting periodic composite materials (whether piezoelectric or nonpiezoelectric) in meeting Navy needs for improved, more reliable and cost-effective techniques for detecting, generating, and controlling acoustic vibrations in liquids and solid structures—including specifically the development of anechoic structures and the control of undesirable noise in detectors.

Explicit calculations have been made for the "superlattice" unit cell geometries shown in Fig. 3. Although the general formulation is capable of treating Floquet waves propagating in arbitrary directions, attention was initially focused on wave propagation either normal to the plane of the periodicity (xy-plane) or parallel to that plane. These propagation directions correspond, in the first case, to the longitudinal thickness resonances of a composite transducer and, in the second case, to lateral resonances of the transducer. Lateral resonances occur in all transducers [12]. However, certain resonances in composite transducers are enhanced by Bragg-scattering from the lateral periodicity, and by phase-matched coupling of the electrical excitation to selected lateral resonances through the periodically distributed piezoelectric coupling.

Figure 4(a) gives a typical input impedance versus frequency curve, measured on a Penn State sample and showing three strong resonances. Here, f_ℓ is the longitudinal thickness resonance and f_{t1}, f_{t2} are the two dominant lateral standing wave resonances—along the unit cell edge and the unit cell diagonal, respectively (Fig. 4(b)). Since the sample is uniformly electroded, the piezoelectric elements (shown stippled in Figs. 3 and 4(b)) are driven in phase, so that the elastic vibrations excited must also be in phase at these points. This means that the lateral resonances observed in Fig. 4(a) consist of standing waves with one full-wavelength spacing between the piezoelectric elements—along the unit edge for f_{t1} and along the unit cell diagonal for f_{t2}. Such standing wave patterns are shown schematically in Fig. 5(a) for f_{t1} and (b) for f_{t2}. These patterns will be discussed more fully below, in connection with laser probe measurements of the motion of composite resonators.

Our study of lateral resonances in composite transducers was initially approached by assuming wave propagation in the xy-plane of an infinite composite. The model was further simplified by supposing that only a z-polarized elastic displacement existed, reducing the elastic wave function to a scalar form similar to that appearing in electronic band theory. In a first approximation, coupled mode theory (which retains only simultaneously "resonant" space harmonics) is used to find the edges of the stopbands for wave propagation in the composite medium. Stopband edges are located at frequencies where Bragg-scattering resonances occur between certain planes of PZT rods (Bragg planes) in the periodic arrays of rods. (Resonances occur at frequencies for which the Bragg planes are spaced by integral multiples of $\lambda/2$ for the z-polarized shear wave assumed in the model.) These "Bragg" resonances are just the enhanced lateral resonances referred to above.

At $\lambda/2$ spacing between the Bragg planes, the resonant wave functions are standing waves along the unit cell edge, the unit cell diagonal, and perpendicular to the higher Bragg planes. These resonances cannot, however, be excited piezoelectrically in a uniformly electroded sample because neighboring PZT rods vibrate 180° out of phase. The lowest

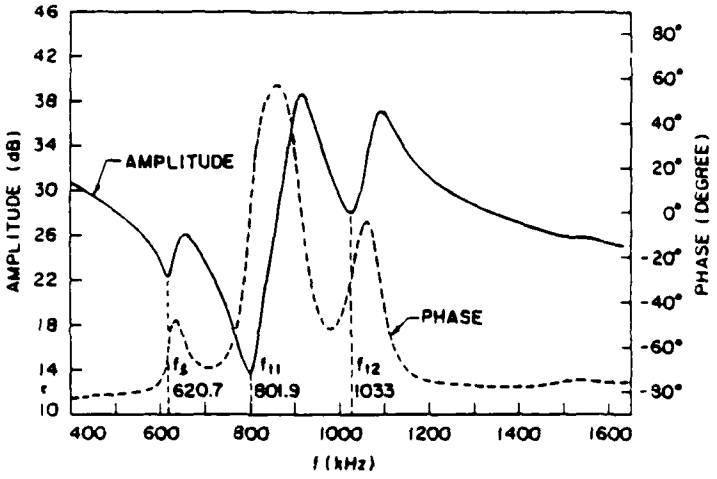

FIGURE 4

Resonance spectrum of a periodic composite plate resonator: (a) Typical measured impedance curve; (b) Corresponding standing wave patterns.

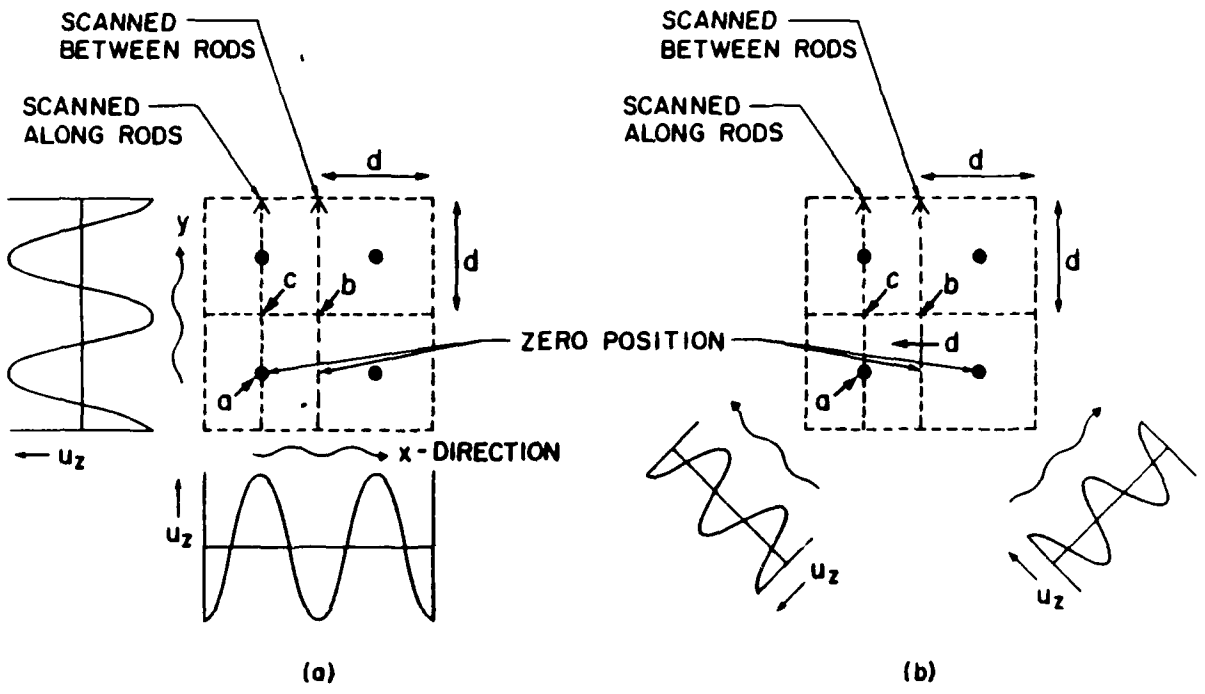

FIGURE 5

Unit cell geometries and laser scanpaths for $d = \lambda$ Bragg resonances: (a) Standing waves along cell edge (f_{t1}; (b) Standing waves along cell diagonal f_{t2}.

lateral mode that can be excited piezoelectrically in this geometry is that which occurs when the edge of the unit cell equals one full wavelength (f_{t1} in Fig. 4). At this resonant frequency several allowed Bragg-scattering resonances occur, but only the mode shown in Fig. 5 has the PZT rods all vibrating in phase [13]. For the longitudinal thickness resonance (f_ℓ in Fig. 4), Bragg-scattering resonances do not appear, because there is no periodicity of the medium along the z-propagation direction. In this case the simplest model is a z-propagation longitudinal wave with properties determined by $\overline{\rho}$ and $\overline{c}_{33}$ (spatial averages over the unit cell), and with weakly excited space harmonics because no resonance of the space harmonics can occur. In other words, the Bragg-scattering condition cannot be satisfied.

Comparison of experimentally measured resonant frequencies with those calculated from the simple model described above gives good agreement for the longitudinal thickness mode but only fair agreement for the lateral modes [14]. One reason for this is that the theory uses a spatial average of the density and the elastic stiffness constants c_{IJ} to model the effective properties of the medium at low frequencies, where scattering from the periodicity is unimportant. This corresponds to the *constant strain model* for the static (or low frequency) behavior of a composite. If a particular strain component (the J-th) has the same value (S_J) in the plastic matrix and in the PZT rod, the average I-th component of stress over the unit cell is (see Fig. 4)

$$\left(\frac{(A-a)(c_{IJ})_{\text{plastic}} + a(c_{IJ})_{\text{PZT}}}{A}\right) S_J = \overline{c}_{IJ} S_J, \tag{1}$$

corresponding to the spatial averaging of the stiffness c_{IJ}. For the longitudinal thickness resonance (f_ℓ) the plastic matrix and the PZT rods vibrate like springs in parallel, and the model reduces to this constant strain description at low frequencies.

For the lateral resonances in Fig. 4(b), the plastic and the PZT are elastic members connected in series, so that the stress (not the strain) is common to both; and the low frequency behavior of the medium is best represented by the *constant stress model.* In this case the counterpart of Eq. (1) is

$$\left(\frac{(A-a)(s_{IJ})_{\text{plastic}} + a(s_{IJ})_{\text{PZT}}}{A}\right) T_J = \overline{s}_{IJ} T_J, \tag{2}$$

for the average strain over the unit cell. Vibrations of the composite material at low frequencies are now most accurately calculated from the spatially averaged compliances $\overline{s}_{IJ}$, rather than the $\overline{c}_{IJ}$.

Another reason for the observed discrepancies between experiments and the theory is that the stress-free boundary conditions at the surfaces of the plate have not been considered. This point was discussed briefly in Reference 15. It was noted there that additional coupling among the space harmonics occurs at the boundaries, and that new

plane wave terms (not contained in the original set of space harmonics) are also generated by elastic mode boundary coupling.

The Floquet theory of wave propagation in an infinite isotropic elastic composite with two-dimensional periodicity (summarized in Reference 13) is not adequate for a complete treatment of the composite plate transducer problem, because it does not include plate boundary conditions. As was noted in the previous paragraph, the addition of boundary conditions to the theory introduces a number of complications. Several attempts have been made to follow this approach. However, it was found that (because of additional boundary couplings introduced between space harmonic orders and between different polarizations of the same space harmonic order) this is not a useful way to implement the coupled mode approximation for composite plates or to iterate the coupled approximation up to solutions of increased accuracy.

A solution to the above difficulty is found by taking the basis functions of the Floquet solution to be Lamb and SH waves of the plate, rather than plane waves. This procedure has been carried out in detail for the case of a composite plate with material parameter periodicity along one direction (x). Details of the analysis are given in Y. Wang, "Waves and Vibrations in Elastic Superlattice Composites," Ph.D. Thesis, Department of Applied Physics, Stanford University, December 1986. In this theory, simultaneous "resonance" (Bragg-scattering) may occur *either* between space harmonics of the *same* Lamb wave species, *or* between space harmonics of *different* Lamb wave species. This adds a great many stopbands in the wave dispersion curves. Nevertheless, the Lamb wave approach, as distinct from the plane wave approach, does give a clear-cut method for describing and studying the stopband (or resonance) structure of the composite plate.

An additional feature of the Lamb wave formulation is that it leads to the average compliance (constant stress) material description of Eq. (2), rather than the average stiffness (constant strain) description of Eq. (1). It therefore more accurately represents the lateral resonances in a composite plate. This point is confirmed by the comparison of

theory and experiment in the following subsection.

Experiment

Comparisons of theory and experiment have been made using resonance spectra of the electric input impedance (Fig. 4) and laser probe measurements of elastic resonance vibration patterns over a unit cell of the composite. The second class of measurements has proved to be a powerful tool for positively identifying and classifying resonances. For reasons mentioned in the previous section, only the resonances f_t, f_{t1} and f_{t2} of Fig. 4(b) are strongly excited in a uniformly electroded sample, and comparisons are made for only these resonances.

Many laser probe measurements have been performed, but only one example will be given here (Fig. 6). The figure shows recorded amplitude and phase of the vibration amplitude measured along a path between the rods in Fig. 5. Experimentally observed amplitude maxima in Fig. 6 are seen to occur at the zero position and at point b of Fig. 5(a). In Fig. 5(a), superposition of the $x-$ and y-directed standing waves predicts a zero at the zero position and a maximum at point b. In Fig. 5(b), superposition of the two standing waves predicts maximum amplitudes at both the zero position and at point b. The latter behavior is in agreement with the experimental result in Fig. 6. It can also be seen by superposing the two standing waves in Fig. 5(b) that the vibration maximum at the zero position and that at point b are 180° out of phase, again in agreement with the experiment of Fig. 6. This comparison clearly identifies the motion as belonging to the diagonal resonance of part (b) in Fig. 5. Corroboration is provided by measurements taken at points a, c and d in Fig. 5, which were also found to be consistent with the superposed standing wave patterns in Fig. 5(b).

The above laser probe technique was used at Stanford to identify the vibration patterns of the resonances observed in certain selected samples among those listed in Table 2. For these particular samples, the resonance spectra (as in Fig. 4(a)) measured at both Stanford and Penn State were found to be in close agreement. Most of the sample frequencies listed

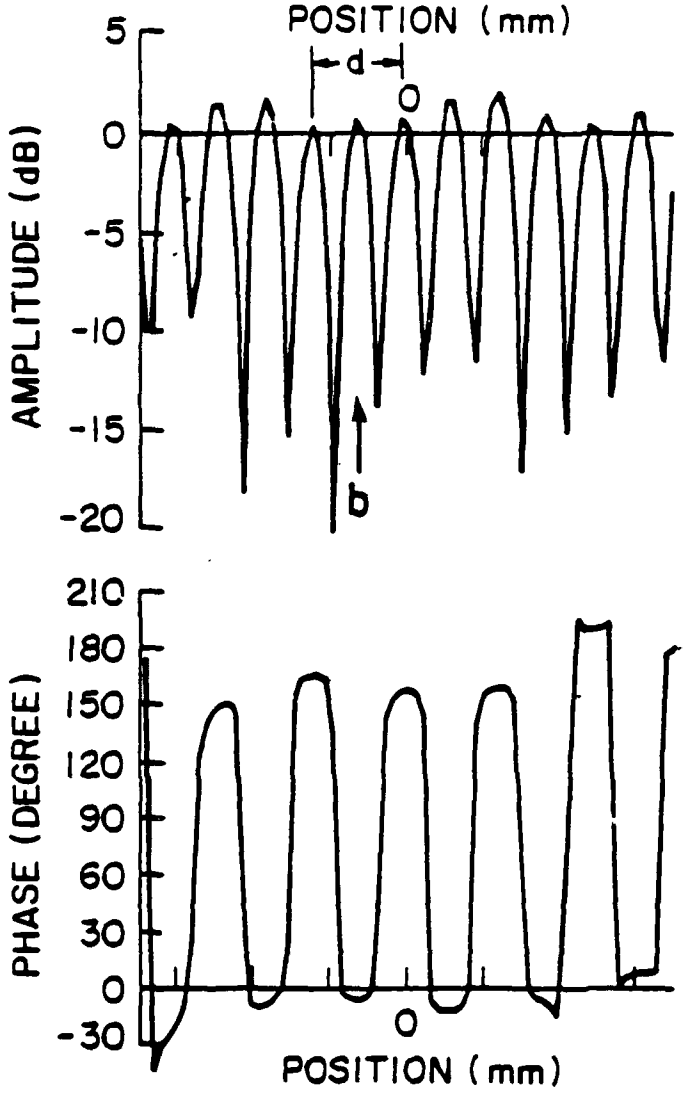

FIGURE 6

Laser scan measurement of acoustic displacement at f_{t2}, scanned between the rods (Fig. 5(b)).

in Table 2 were measured at Penn State only, and the resonant mode identification was made by comparison with samples that were laser-probed.

In Table 2, the piezoelectric rods are of PZT-5A and the polymer of Spurrs epoxy. Material parameters used in comparing theory and experiment are $\rho = 7.75 \times 10^3$ Kg/m^3, $V_\ell = 4032$ m/s, $V_s = 2263$ m/s for PZT-5A, and $\rho = 1.14 \times 10^3$ Kg/m^3, $V_\ell = 2207$ m/s, $V_s = 1003$ m/s for Spurrs epoxy. The parameters for PZT-5A were obtained from the manufacturer's data, using piezoelastically-stiffened elastic constants and assuming isotropy. Spurrs epoxy parameters were measured at Stanford, using pulse echo methods to determine the velocities. Frequencies listed in the table are the antiresonance frequencies for the longitudinal thickness mode (f_1) and the resonance frequencies for the lateral modes (f_2, f_3). In Fig. 4(a), the resonance frequencies are points of impedance minimum and the antiresonance frequencies are points of impedance maximum. A resonance frequency corresponds approximately to the *short-circuit* natural frequency of the freely vibrating piezoelectric resonator mode, and an anti-resonance frequency to the *open-circuit* natural frequency of the free resonator mode. Since our composite theory does not yet include piezoelectricity, the choice of which experimental frequency to compare with theory is not immediately obvious. Our choice was based on the following considerations: In the Mason model for a parallel plate transducer/resonator, the open circuit (or antiresonance) frequencies correspond to pure $n\lambda/2$ standing waves across the plate [16]; for this reason, the antiresonance frequencies are chosen to compare with the theory of the longitudinal thickness resonance ($f_1 \equiv f_\ell$). For the lateral resonances (f_2, f_3), the standing waves are parallel to the electrode faces (Fig. 4(b)) and the choice between resonance and antiresonance frequencies is not clear at this point; consequently, the resonance frequencies were chosen simply because they give a better fit to the theory.

It was noted above that the constant strain model is more appropriate for calculating the longitudinal thickness resonances, while the constant stress model is more appropriate for the lateral resonances. Figures 7-12 compare theory and experiment for these two cases.

TABLE 2

Resonant Modes for PZT Rod-Polymer Composites*

(The numbers on the left correspond to the points plotted in Figs. 7-12)

Label of Plotted Point	Sample Number	% PZT	Thickness b (mm)	Spacing d (mm)	f_1 (anti-resonance) (KHZ)	f_2 (resonance) (KHZ)	f_3 (resonance) (KHZ)	Frequency Plotted
1	128**	10%	1.9	1.27	-	804	1096	f_2
2	2	5%	2.59	1.58	-	604	786	f_2
3	128**	10%	1.9	1.27	-	804	1096	f_3
4	10	5%	4.0	1.76	321.6	485	691	f_2
5	2	5%	2.59	1.58	-	604	786	f_3
6	11	5%	4.8	1.75	275.6	449	-	f_2
7	223	20%	2.54	0.90	612	894	-	f_2
8	122**	10%	3.64	1.27	-	662	1006	f_2
9	222	20%	3.05	0.90	519	830	-	f_2
10	12	5%	5.9	1.76	231.8	437	730	f_2
11	10	5%	4.0	1.76	321.6	485	691	f_3
12	130**	10%	5.15	1.27	296	644	-	f_2
13	228	20%	3.95	0.90	408	828	-	f_2
14	122**	10%	3.64	1.27	-	622	1006	f_3
15	12	5%	5.9	1.76	231.8	437	730	f_3
16	227	20%	4.60	0.90	353	886	-	f_2
17	226	20%	5.15	0.90	309	825	-	f_2
18	10	5%	4.0	1.76	321.6	485	691	f_1
19	11	5%	4.8	1.75	275.6	449	-	f_1
20	12	5%	5.9	1.76	231.8	437	730	f_1
21	130**	10%	5.15	1.27	296	644	-	f_1
22	227	20%	4.60	0.90	353	886	-	f_1
23	223	20%	2.54	0.90	612	894	-	f_1
24	228	20%	3.95	0.90	408	828	-	f_1
25	222	20%	3.05	0.90	519	830	-	f_1
26	226**	20%	5.15	0.90	309	825	-	f_1

*Measurements by T.R. Gururaja, Materials Research Laboratory, The Pennsylvania State University.

**Sample also tested at Stanford University.

Figures 7-9 represent the dispersion curves for the symmetric Lamb modes* calculated from spatially averaged stiffnesses (the constant strain model). On these curves the frequencies of the longitudinal thickness resonances for samples in Table 2 are plotted at $\beta b = 0$. They lie very close to the $\beta b = 0$ intercept of the second symmetric Lamb mode, a point that corresponds to the longitudinal thickness resonance in a homogeneous plate. Plots of lateral resonance frequencies (at $\beta = 2\pi/d$, corresponding to the resonance conditions in Fig. 4(b), lie far below the Lamb waves spectrum in Figs. 7-9. This is unreasonable physically because the lateral resonances correspond to Lamb waves that are Bragg scattered by planes of piezoelectric rods; and these points are therefore not shown.

In Figs. 10-12, the curves are Lamb wave spectra calculated from spatially-averaged compliances (i.e., the constant stress model). The experimental longitudinal thickness resonances (f_1) are now seen to be in poor agreement with the theory, but the lateral resonances (f_2, f_3) (plotted at $\beta = 2\pi/d$) lie close to the lower modes of the symmetric Lamb spectrum. The experimental points are distributed along the dispersion curves and trace out the Lamb wave dispersion curves quite accurately.

Discussion

Experimental points plotted in Figs. 7-12 clearly show the expected behavior—i.e., longitudinal thickness resonances are best represented by the constant strain model and lateral resonances by the constant stress model, for volume percentages of PZT as large as 20%. In this comparison, the longitudinal thickness resonance is analyzed by completely neglecting any coupling into other space harmonics, and the lateral resonances are analyzed by the coupled mode approximation. These approximations are expected to be somewhat inaccurate, even in the 5% volume ratio case, and this fact may account for some of the disagreement observed in Figs. 7-12. Continuing analysis should add more and more space harmonics to the calculation until there is no further change in the result.

* Antisymmetric modes cannot be excited in plates driven by PZT rods poled normal to the plane of the plate.

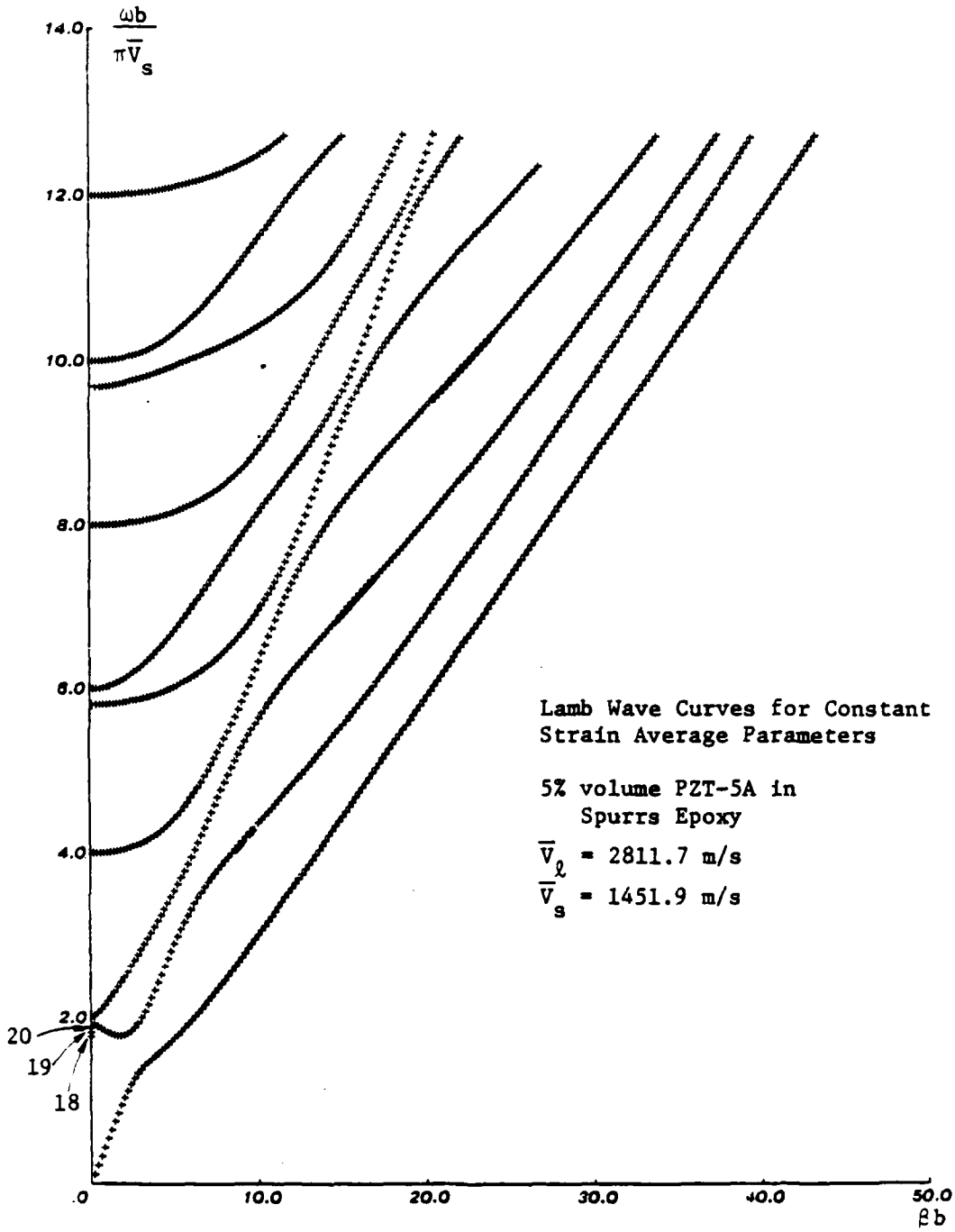

FIGURE 7

Comparison of constant strain model with experiment (5% volume ratio).

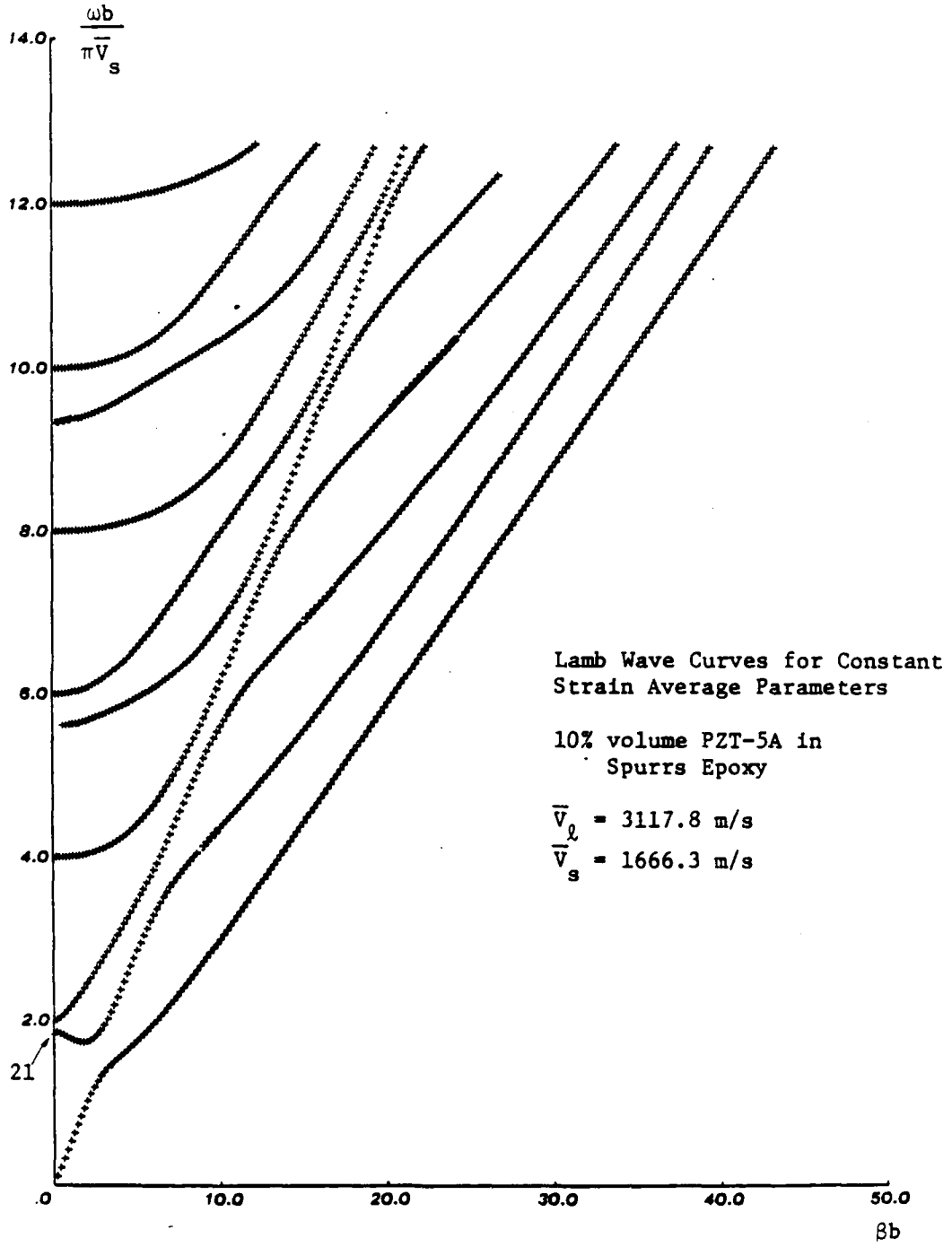

FIGURE 8

Same as Fig. 7 (10% volume ratio).

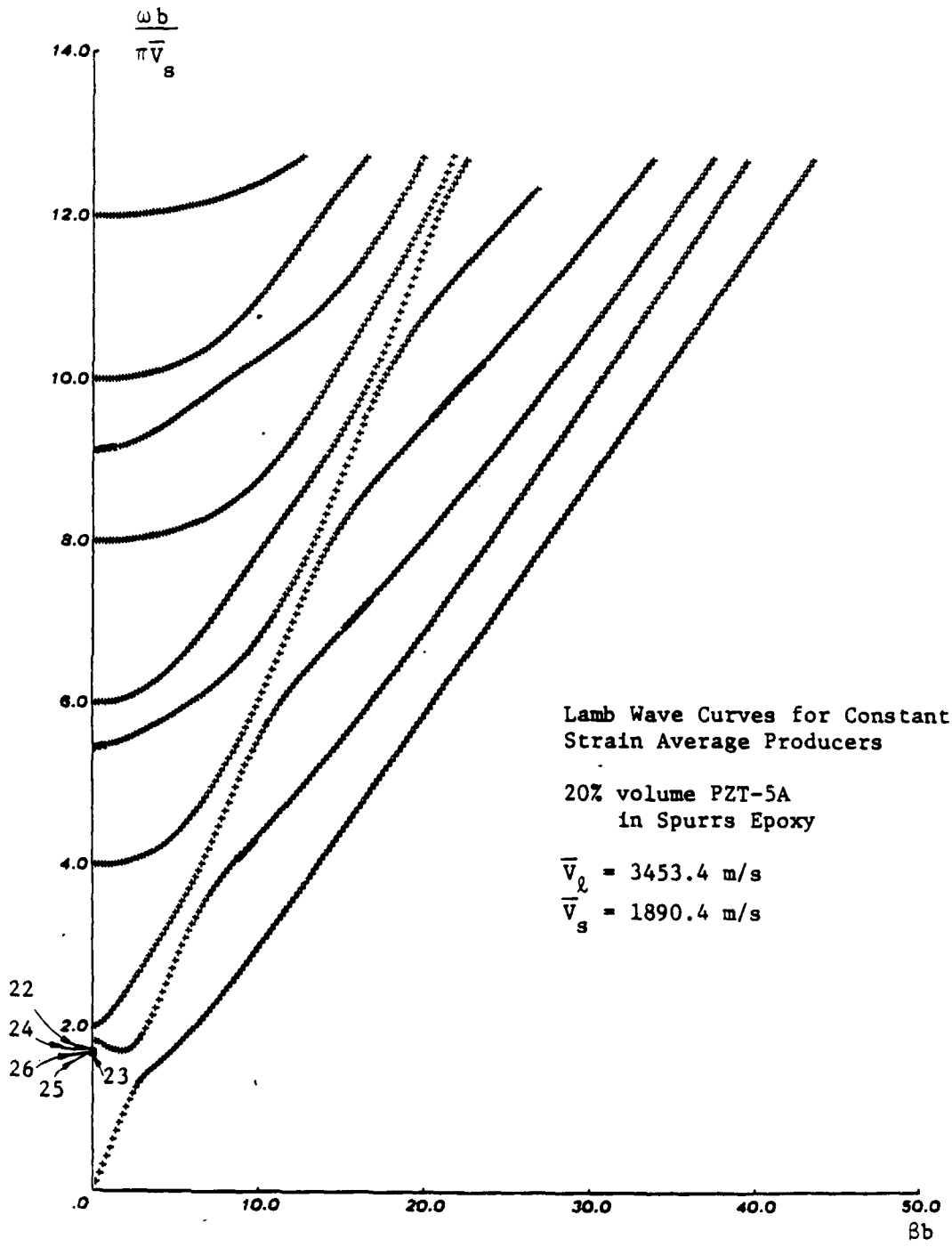

FIGURE 9

Same as Fig. 7 (20% volume ratio).

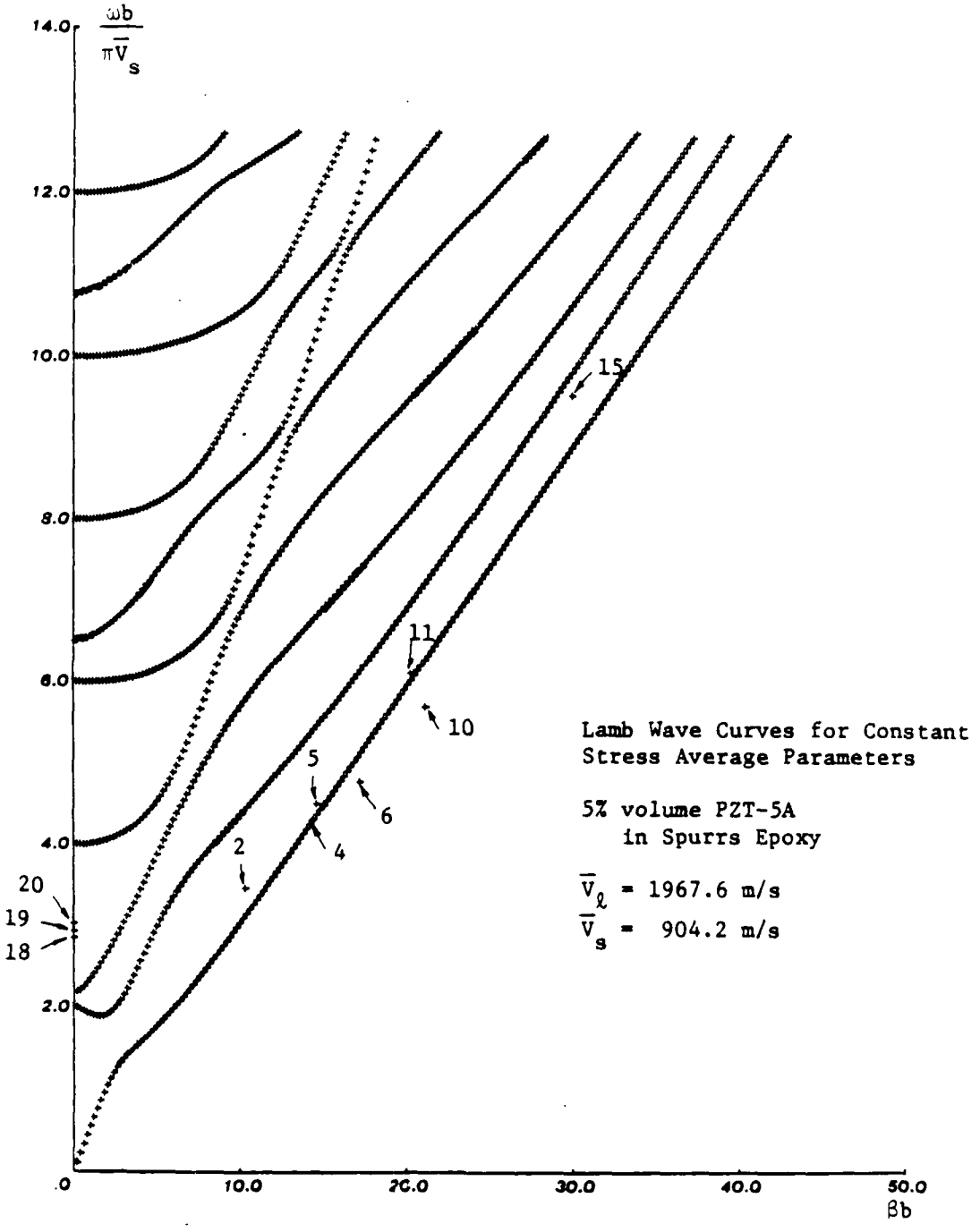

FIGURE 10

Comparison of constant stress model with experiment (5% volume ratio).

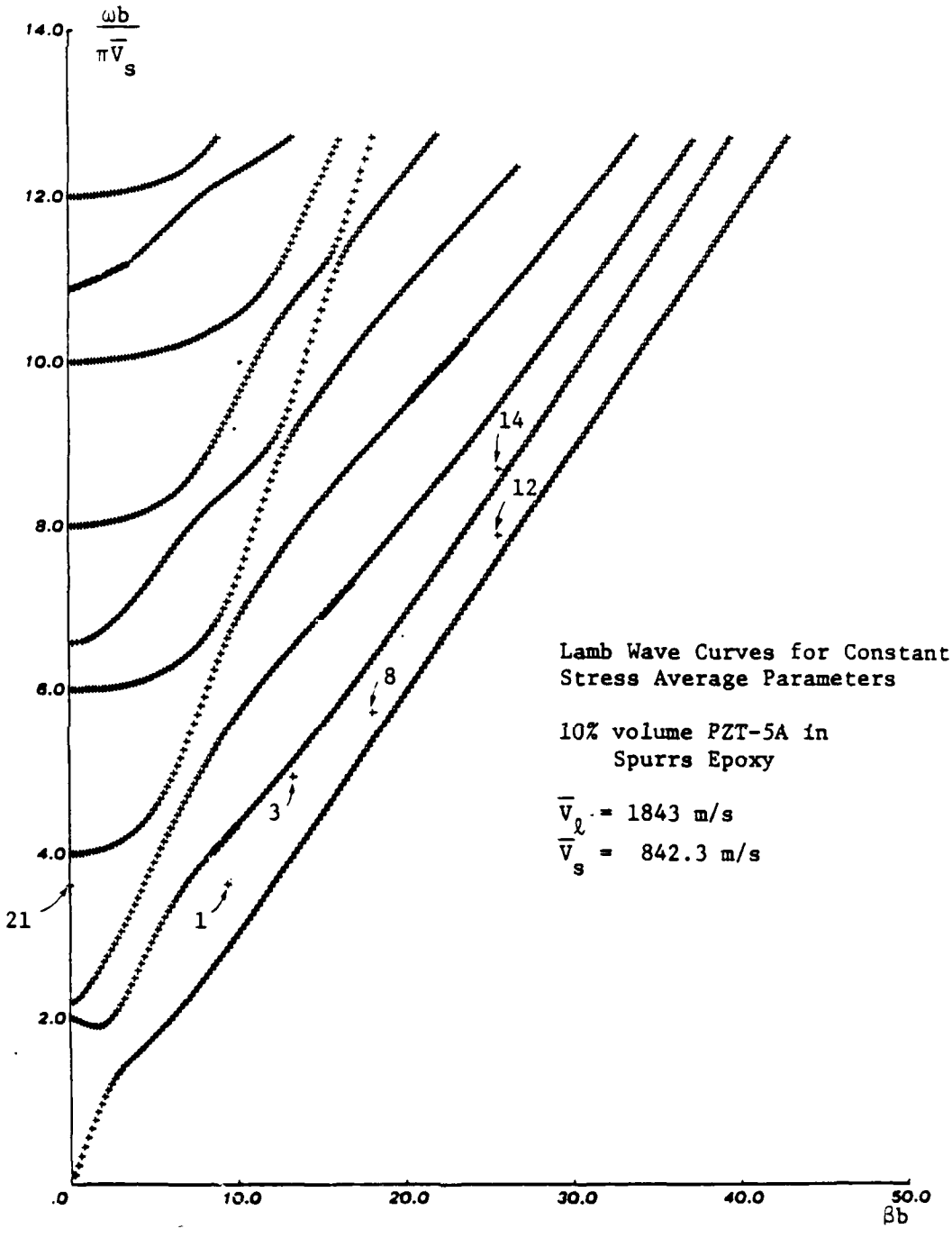

FIGURE 11

Same as Fig. 10 (10% volume ratio).

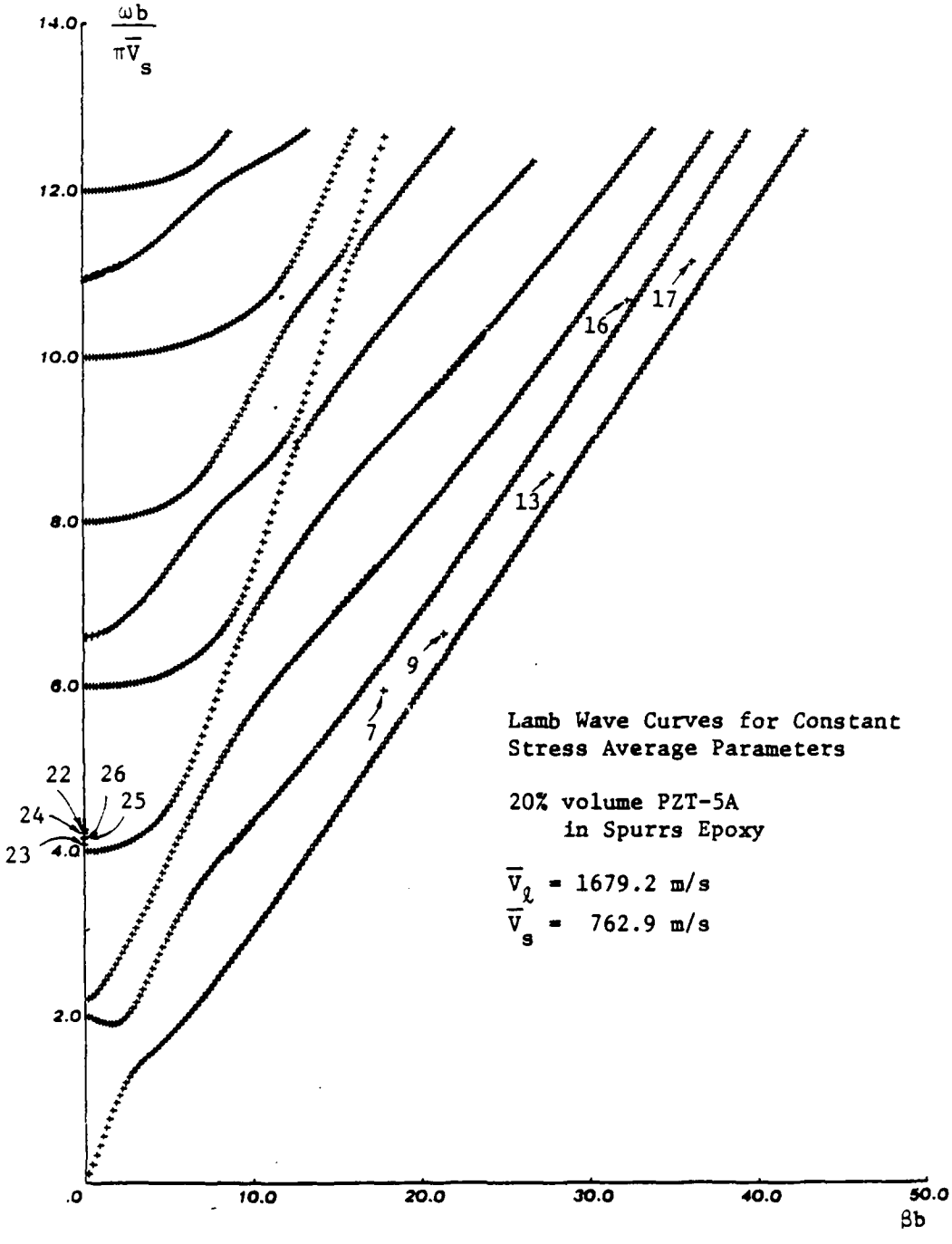

FIGURE 12

Same as Fig. 10 (20% volume ratio).

Another possible source of error is the incomplete treatment of piezoelectricity and anisotropy in the PZT. One important consequence of piezoelectric coupling was discussed above, with respect to the choice of the longitudinal thickness antiresonance for comparison with theory. The theoretical basis for choosing to compare lateral mode experiments with theory on the basis of resonance frequencies has not yet been formulated. Another area of uncertainty is how best to characterize piezoelectric stiffening of the elastic constants in a composite medium.

Despite these unresolved questions, agreement of theory and experiment in Figs. 7-12 is quite sufficient to permit drawing practical conclusions and to explain and predict various aspects of the behavior of composites. In many experimental resonance curves a number of small supplementary resonances are observed above and below f_{t1} and f_{t2}. These can be explained by observing that there is coupling among all Lamb waves in all orders of space harmonic, and that additional couplings occur in the two-dimensional version of the equation. Bragg resonances therefore occur for the higher order Lamb modes, but are weakly excited by the electrodes.

(c) PROGRAMMABLE ELECTROSTRICTIVE TRANSDUCERS

Electrostriction

The various devices considered in this research were constructed on the nonpiezoelectric ceramic substrates lead magnesium niobate (PMN) and lead lanthanum zirconate titanate (PLZT). Piezoelectricity is present only in certain noncentrosymmetric crystallographic classes, whereas electrostriction effects are present in all dielectrics. In electrostriction, the elastic strain is proportional to the square of the applied electric field. Usually this effect is viewed as a small electric field correction to the piezoelectric constants. However, if the material is nonpiezoelectric, then electrostriction is the dominant electromechanical coupling effect [17,18]. PMN and PLZT are very strong electrostrictors, and it is this property that makes them useful for electromechanical devices. These two materials have the perovskite crystal structure with a centrosymmetric arrangement of

atoms in the unit cell which forces them to be nonpiezoelectric. However, they exhibit an induced piezoelectric coupling comparable to that of the PZT piezoelectrics when biased with fields on the order of one kV per millimeter. Unfortunately, their very large dielectric constants (9000 for PMN and 4000 for PLZT) reduces their electromechanical coupling coefficients.

A simple one-dimensional geometry (an infinite electroded plate) and elementary electrostatics can be used to show that electrostriction exists in all dielectric solids [19]. Before charges are placed on the electrodes, the solid is stress free. When a voltage source is connected to the electrodes, charge will flow onto the conductor surfaces. Once current flow ceases, the voltage source is disconnected. The surface charge distribution on the conductor and dielectric surfaces is shown in the figure. At this point, an electric field exists in the vacuum and in the dielectric solid. The field in the vacuum is related to the field in the dielectric

$$E_o = \epsilon E/\epsilon_o$$

We can use the principle of virtual work to compute the force on the dielectric. We make a virtual displacement of the dielectric surface. Under these conditions the force is

$$\text{Force/Area} = \epsilon(\epsilon/\epsilon_o - 1)E^2/2 \approx \epsilon_o\epsilon_r^2 E^2/2$$

where ϵ_r is the relative permittivity and the last term is for materials with large permittivity. This is the case for both PMN and PLZT ceramics used in this research.

This stress will cause a material deformation in the direction of the virtual displacement. That is, the material undergoes an elongation in the direction of the field. Since the material strain is linearly related to the stress, the strain is proportional to the electric field squared. We see that the material properties desired are large dielectric constant and large compliance constants. In addition to the electrostriction effects, all dielectrics may also exhibit the quadratic electrooptic effect. This effect is a change in the dielectric permittivity proportional to the square of an applied electric field. (In some cases, such as PMN, higher order permittivity changes occur even at low applied fields.)

Previous Research Using PMN and PLZT Ceramics

Most of the previous interest in PMN devices was because of its large static strain produced by a DC electric bias field. In fact, the major emphasis has been on mechanical positioners [20]. For this application, research has concentrated on laminate processing techniques. Previous work on PLZT ceramics centered on the effect of a large bias field on the dielectric permittivity at optical wavelengths. PLZT ceramic is optically transparent and the electrooptic constants are relatively large. In addition, it is possible to manufacture the ceramic in very large sizes with good optical quality. For just this reason, it has been used in both commercial and military applications [21]. For example, large viewports (100 mm diameter) for flashblindness protection of pilots' eyes have been in service since the late 1970's. In this application and in other commercial applications, the main interest has been in two-state devices. That is, the device is either fully "ON" or fully "OFF" and the orientation of the optic axis is constant. These shutters can be switched between 20% and 0.1% transmission in less than 50 microseconds. The present research is concerned with the small signal biased behavior of both materials.

Acoustic Devices

These devices are electrically biased piezoelectric devices [22]. For our materials, the material strain versus applied electric field is a quadratic relation (i.e., electrostrictive). An electric bias is applied and the small signal variations about this bias point are used in the devices. Simple calculus predicts that the slope is proportional to the bias field. This response is applicable even in cases where the variables of interest are higher rank tensors (strain, a second rank tensor, and electrostriction, a fourth rank tensor). The biased behavior of the small signal response is linear—i.e., a piezoelectric-like relation exists between the small signal strain and the small signal electric field. The proportionality constant, which determines the strength of the transduction of mechanical to electrical energy, is under external control, unlike the situation in a normal piezoelectric. In addition, the sign of the transducer coupling constant follows the sign of the bias field.

This effect was used in the present research mainly in surface acoustic wave (SAW) devices, but it also occurs in electrostrictive bulk wave transducers. Either the traditional parallel plate geometry or the van der Pauw interdigital geometry [23,24] can be used for biased electrostrictive bulk wave transducers. Both PMN and PLZT substrates were used. However, because of the poor material quality of the PMN sample available for the research, the PMN SAW device performance was substandard.

For SAW transducers two different biasing geometries have been studied. The first uses a conventional PZT-like orientation in which the z-axis (or poling axis) is perpendicular to the major surface of the substrate. In this case the interdigital transducer (IDT) signal electrodes are on one surface and the biasing electrodes are on the opposite surface (Fig. 13). This geometry is most like conventional SAW technology. It was used to illustrate the basics of programmable SAW operation and a matched filter application in these electrostrictive substrates. The second biasing geometry has both sets of electrodes on the same surface. A serpentine electrode (or meander line) for the bias is interleaved between the fingers of IDT electrodes for the RF signal (Fig. 14). This meander line biasing geometry greatly reduces the biasing voltage magnitude, and is therefore more suitable for applications that require RF time-varying bias fields, such as rapidly programmable finger weighting and electromechanical mixing applications.

Advantage of Electrostrictive Materials for Programmable Device Operation

The major advantage of using electrostrictive and electrooptic effects to generate spatially varying material properties is that the resulting devices are electrically programmable. Of course, programmable acoustic and microwave devices already exist. However, this programmability is accomplished through external active circuitry. That is, external switching circuits and/or variable gain amplifiers are needed. For example, in programmable microwave devices, active components (like diodes) require biasing components and blocking inductors to isolate these biasing components from the

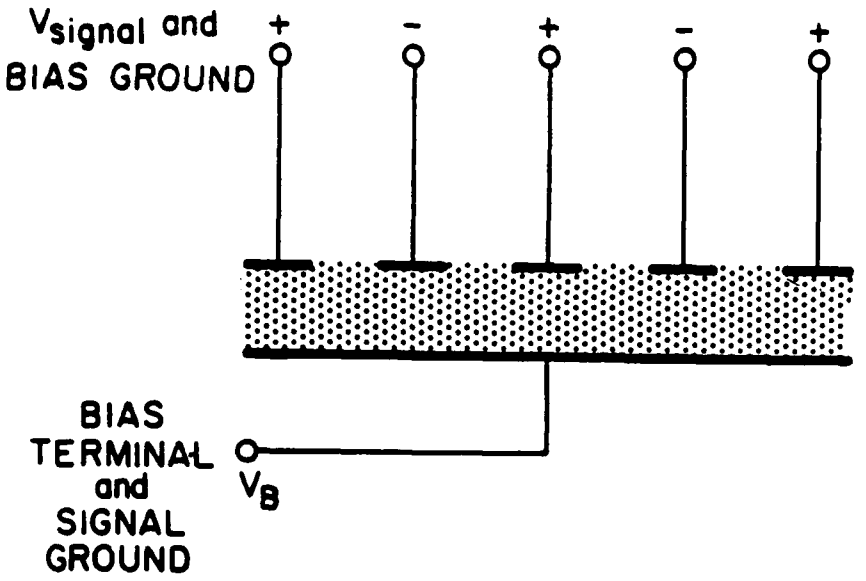

FIGURE 13

Back electrode bias structure

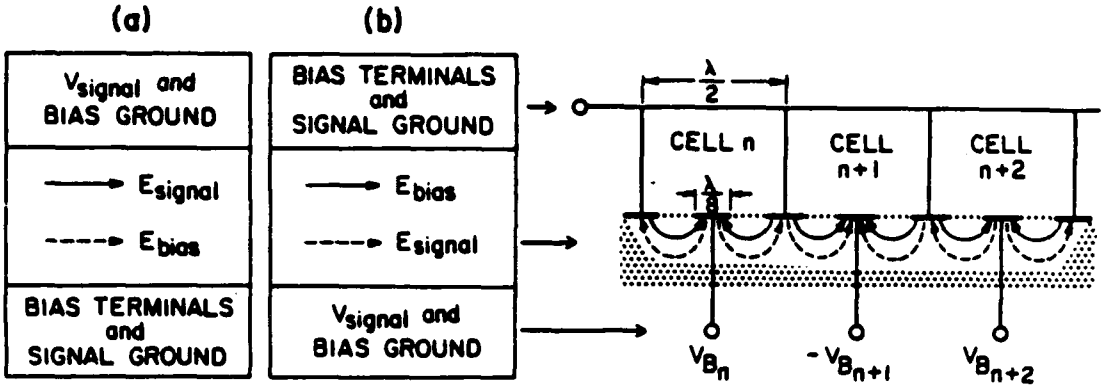

FIGURE 14

Split finger bias structure: (a) Programmable weighting; (b) Fixed uniform weighting.

transmission line. These circuits are usually quite complex and usually complicate device operation since they perturb the basic device operation. The present devices achieve programmability "internal" to the device itself with the only external electronics required for the programming being the bias voltage supply and associated bias electrodes. In the devices discussed here, these biasing electrodes need not be part of the signal electrodes and so do not perturb the signal response. Thus, this type of programmability is achieved in a more "natural" and unobtrusive way.

Future Materials Research

Finally, more materials research is required to produce substrates with better properties than those used in this research. For example, a material with large electrostrictive coefficients, but also vanishingly small quadratic electrooptic coefficients, would greatly improve the operation of the acoustic devices. For signal processing acoustic devices, lower acoustic losses at higher frequencies would be very desirable.

Reports on the performance of these biased electrostrictive SAW devices are given in Publications 16, 20, 25, and also in G. Laguna, "Applications Using Electrically Alterable Material Properties in Large Dielectric Constant Ceramics," Ph.D. Thesis, Department of Electrical Engineering, Stanford University, June 1986. A brief review of the principles, and an extensive analysis of potential sonar applications, is given in a report "Applications of Surface Acoustic Wave Circuits to Acoustic Signal Processing, Especially for Sonar"—written by a visiting scientist from Thomson Sintra, P. F. Delval. A copy of this report is attached.

(d) ACOUSTIC REFLECTION GRATINGS IN NEODYMIUM PENTAPHOSPHATE

Periodic arrays of ferroelastic domains were previously produced in the ferroelastic crystal, neodymium pentaphosphate (NPP) [25], which is a monoclinic, $2/m$ point symmetry ferroelastic single crystal material. A ferroelastic is a material which exhibits at least two states of spontaneous strain which may be switched by an applied stress. The two

distinct strain states, called ferroelastic domains, exhibit distinct physical properties, and the boundaries between domains, or domain walls, are therefore surfaces of abrupt change in material properties. The abrupt change in elastic and optical properties at a domain wall results in an interface which reflects optical and acoustic waves [26,27,28]. These periodic gratings are stable in the absence of any external force. Arrays of approximately 25 micron period have been seen to be stable up to the Curie point of 145°C. It is of particular interest to note that these arrays are highly periodic and tunable over a range from 100 to 0.5 micron period (see Ref. 25), making them excellent candidates for device applications.

In the present program, acoustic and optical applications of these gratings, as tunable acoustic and optical filters, were investigated. Acoustic reflections for longitudinal waves were calculated to be 6.06% in amplitude at normal incidence. Experimental and theoretical results were obtained for longitudinal wave filtering by a grating tuned from 54 periods, at 95.1 microns each, to 69 periods, at 74.8 microns each.

Since NPP is a high gain infrared laser material, and the ferroelastic domain walls have excellent short term stability, there exists the possibility of constructing a tunable grating filter with optical gain. In the experiments performed, quasi-cw gains of 30% were observed. But there was a discrepancy with theoretical predictions because of gain quenching by "up conversion." To overcome this limitation it is necessary to use a pulsed pump or to substitute La or Y for some of the Nd in the crystal.

Publications 17 and 23 relate to this work. Full detail is available in S. W. Meeks, "Optical and Acoustic Device Applications of Ferroelastic Crystals," Ph.D. Thesis, Department of Applied Physics, Stanford University, March 1986.

III. ACTIVITIES 1987-1988

During the period, a Final Report (attached) was prepared by P.F. Delval of Thomson Sintra covering his research on electrostrictive SAW devices for sonar signal processing, performed under this program at Stanford.

Major emphasis has been put on examining the material property requirments for improved electrostrictive SAW transducers. The second topic under study has been applications of composite materials for spurious mode suppression in ultrasonic transducers, and on the spatial and spectral (spatial and temporal) frequency responses of both ultrasonic and hydrophone transducers. Spatial and spectral filtering is of obvious interest in connection with the problem of hydrophone flow noise, and may also have some relevance to signal processing for ultrasonic imaging. There already exists a considerable literature on spatial filtering in the study of turbulent boundary layer (flow) noise. But impact on this problem of emerging composite transducer technologies is not yet clear.

(a) MATERIAL RESEARCH REQUIRED FOR IMPROVED ELECTROSTRICTIVE SAW TRANSDUCERS

Two issues must be addressed before satisfactory transducers of this kind can be properly understood and developed. First, improved materials are required, with better control of surface conditions. Second, new electrode configurations must be realized, for more efficient excitation.

Material Development

One of the striking results of experiments performed under this program was the difference between SAW transducers on PMN and PLZT substrates. For bulk wave transducers, PMN appears to have a larger coupling constant. But in a SAW transducer PMN exhibited a short-time decay of the signal after application of the bias. Transmission is reduced to approximately 10% several seconds after the bias is applied. If the bias is removed for a period of the order of a minute the system appears to recover, and repeats the cycle. This phenomenon was not observed in PMN bulk wave transducers, nor in PLZT

transducers of either type. In PMT SAW transducers the phenomenon changed with the periodicity of the SAW transducers.

No satisfactory explanation of this effect was found. Measurements of ϵ versus temperature were made by W. Schulze, but gave no relevant information. Our samples are being sent to S. Kurtz at Penn State for further investigation.

New Transducer Structures

Theoretical studies reported in Publication 25 showed that the transducer structures shown in Fig. 15 have approximately the same coupling strength as in Fig. 13, but allow the coupling to be controlled at each individual finger. To realize such structures it will be necessary to develop high quality relaxor thick films that can be grown over the bottom layer of fingers on a nonferroelectric substrate. This technology is being actively researched at the present time using metallo-organic decomposition, sputtering, etc., and promising results have been obtained for some materials.

(b) PIEZOELECTRIC COMPOSITE MATERIALS

Spurious Mode Reduction in Ultrasonic Transducers

The composite materials considered here are periodic arrays of piezoelectric elements in a nonpiezoelectric matrix with different elastic properties. PZT-epoxy composites are mainly the composites to be discussed here. For applications in high-frequency ultrasonics, these composite materials have aroused interest because of their high electrical coupling, low acoustic impedance, and reduced mechanical crosstalk in arrays. Composite transducers, therefore, have high sensitivity and broad bandwidth. An optimal design of piezoelectric composite transducers requires understanding of the high frequency vibration behavior of the composite medium itself.

Most currently used composite transducers are thin plastic plates, which have imbedded in them a two-dimensional periodic array of piezoceramic rods with the poling direction normal to the plate. They are used in the longitudinal thickness mode, driven by applying an electric field to the rods. Since the composite periodicity occurs only in

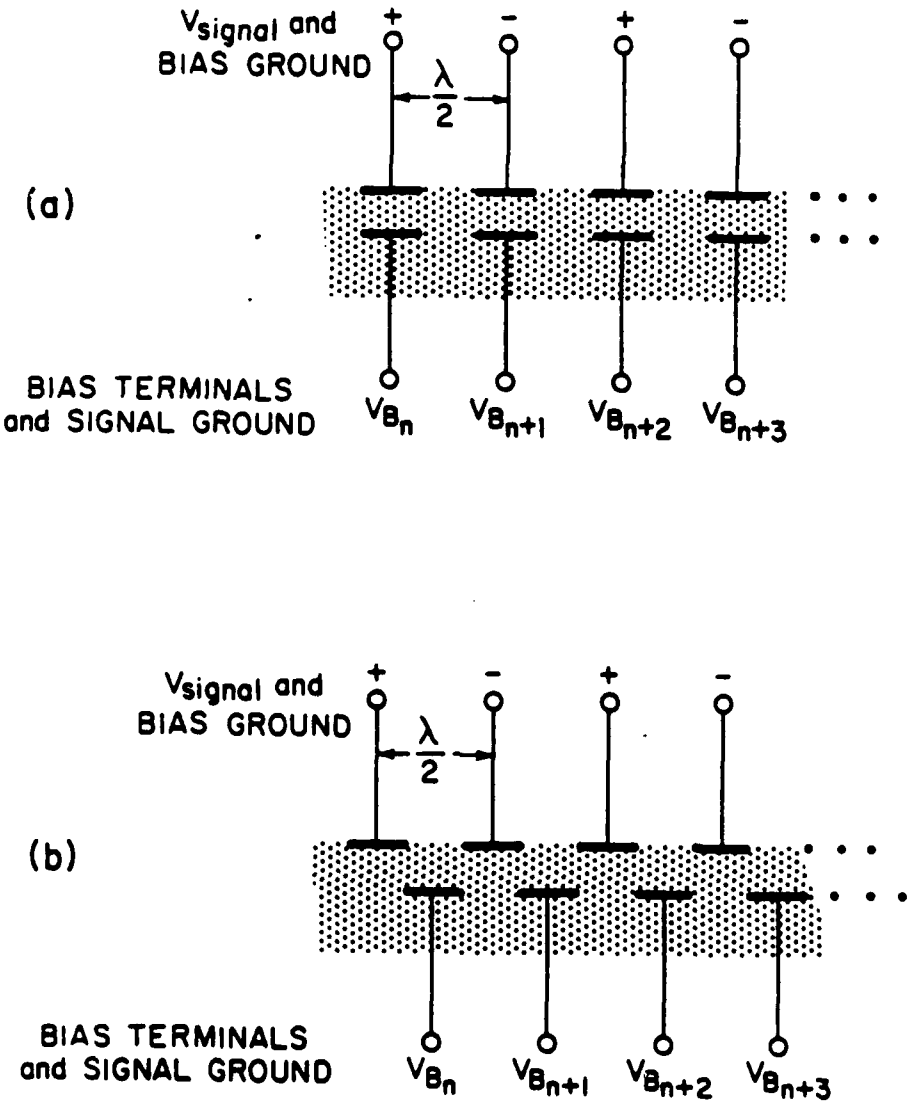

FIGURE 15

Buried electrode bias structure.

(a) In-line. (b) Offset.

the plane of the plate, the stopbands exist only for propagation in the plane of the plate, and do not have a direct effect on the longitudinal thickness mode. However, the lateral stopbands (where the attenuation can be very large) do play an important role in reducing crosstalk between image array elements, as well as eliminating transducer resonances. The presence of a lateral resonance near the thickness resonance can cause a serious reduction of the electromechanical coupling. In the design process care must be taken to reduce mechanical crosstalk between different electrodes on an imaging array, and to control the lateral resonances of the structure in order to get high efficiency. The best design avoids placing any of the narrow passbands at the same frequency as the thickness resonance of the transducer.

In composite transducer design two kinds of lateral resonances must be considered: (i) those that are piezoelectrically coupled to the transducer electrically, and (ii) those that do not couple piezoelectrically but are excited mechanically at the sides of the transducer plate. Category (i) resonances are located at the edges of stopbands where the piezoelectric elements of the composite all vibrate in phase. These correspond to the 2π Bragg scattering points, where the spacing of the Bragg planes of the superlattice is a multiple of λ. It has been shown [15] that these resonances occur at the upper and lower stopband edges and that the piezoelectrically coupled resonance is at the upper bandedge. This corresponds to comparisons of theory and experimental observations of lateral resonances in the input impedance of composite transducers. Resonances in category (ii) arise from mechanical coupling between the thickness mode and lateral modes at the stress-free edges of the transducer. They are not excited piezoelectrically because the piezoelectric elements do not vibrate in phase; they are located at the edges of stopbands corresponding to $\lambda/2$ Bragg plane spaces, or lie entirely within the passbands for lateral mode propagation. No lateral resonances of any kind appear inside the stopbands. This latter feature, illustrated in Fig. 16 for a one-dimensional composite, is of the utmost importance in transducer design. Inside the stopband there exist only evanescent decaying waves, so that no standing

wave resonances exist when k_o is an integral multiple of π/ℓ. The same suppression mechanism occurs in a two-dimensional composite, where stopbands correspond to the various angled Bragg scattering planes of the lattice. Two are illustrated in Fig. 17. The Bragg frequencies differ for all of the stopbands; but the stopbands are very wide in ceramic/epoxy materials and tend to overlap. Suppression of standing waves in various directions therefore eliminates a wide range of lateral resonances in disk transducers.

The ratio of transducer thickness to composite period must be controlled so that no resonances of category (i) appear close in frequency to the thickness resonance. If this condition is not satisfied, coupling to the thickness resonance is seriously reduced. Suppressing mechanical coupling of the thickness mode to lateral modes of category (ii) can be achieved by placing the thickness mode frequency inside one or more of the stopbands, where all lateral resonances are suppressed. This avoids reduction of thickness mode coupling and distortion of the radiated beam due to strong lateral mode excitation.

Composite ultrasonic transducers are now being developed by a number of companies, and the suppression of lateral modes predicted by the above discussion has now been realized. A presentation noting this result was given by Mr. Clyde Oakley of Echo Ultrasound, at the March 1988 Review Meeting of the ONR Program on Piezoelectric and Electrostrictive Materials for Transducer Applications at the Materials Research Laboratory, Pennsylvania State University.

Spatial and Spectral Filtering in Transducers

Reduction of noise due to turbulent boundary layer (TBL) flow is a longstanding problem in sonar arrays. Turbulent flow along the ship generates a pressure field P_{FN} with a very wide spatial and temporal spectrum, acting on the hydrophone of the array (Fig. 18). The response to this field must be distinguished from the pressure field of the sonar signal P_{S}, which is at the resonant response frequency of the hydrophones. Although P_{FN} has only a small part of its spectrum resonantly coupled into the hydrophone outputs, it still poses a problem because of its extremely high level (30-50 dB above P_{S}).

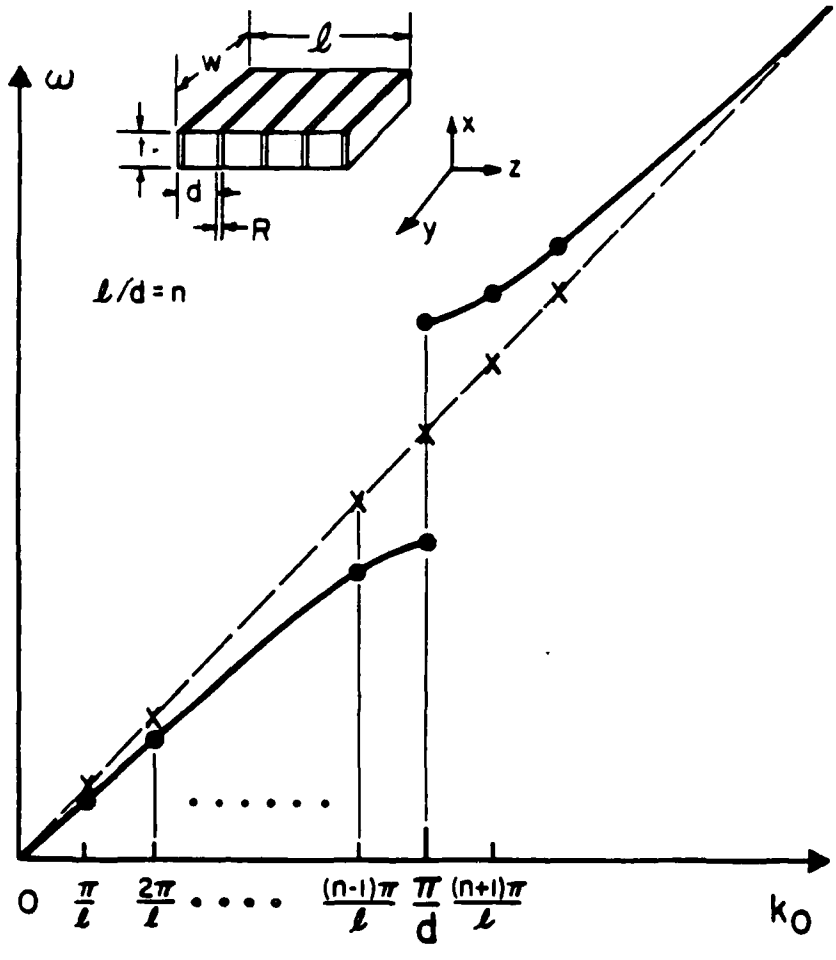

FIGURE 16

Resonance mode spectra for homogeneous and composite one-dimensional resonators.

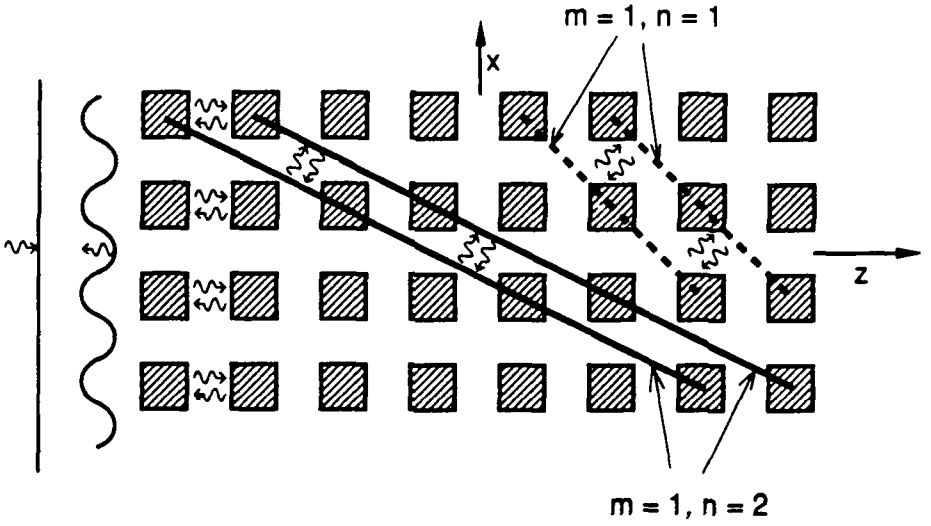

FIGURE 17

Examples of Bragg scattering planes in a two-dimensional composite.

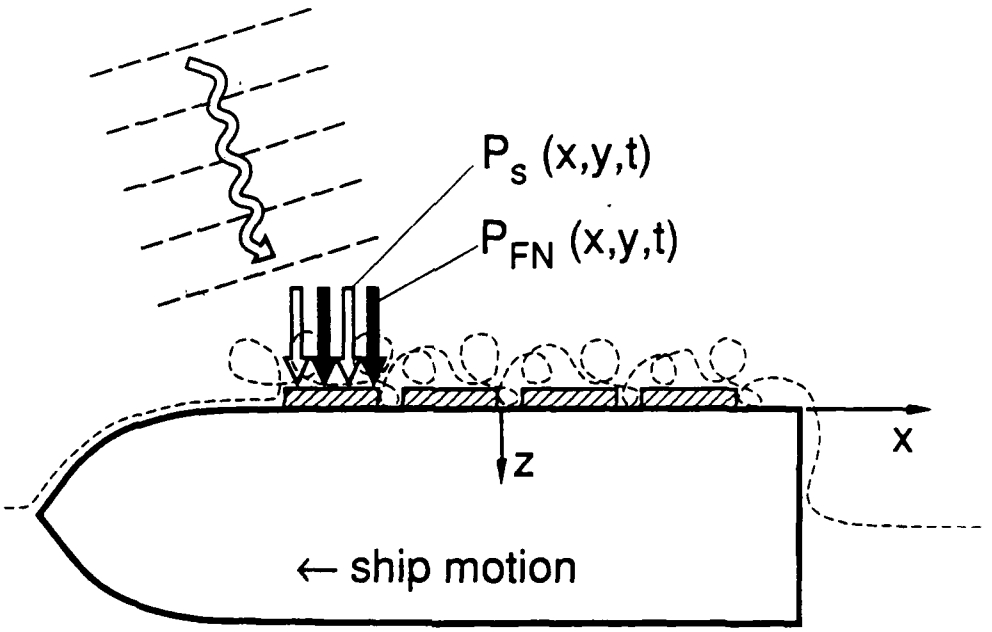

FIGURE 18

Turbulent boundary layer (TBL) flow noise.

A question to be posed is the following: Can the unique resonant frequency response of a periodic composite be exploited to reduce the effect of TBL flow by appropriate spatial and temporal filtering? There already exists an extensive literature concerning TBL pressure fields and their interaction with structures (see, for example, [29],[30],[31],[32]); but the response to turbulent flow of a composite hydrophone does not appear to have been examined.

The references cited in the previous paragraph discuss in detail the spatial and spectral frequency spectrum $P(\omega, \mathbf{k})$ of P_{FN} in Fig. 18. This spectrum has a smoothly-varying background variation with ω and $\mathbf{k}$, plus a convection contribution that varies inversely as some power of the quantity

$$\omega - \mathbf{k} \cdot \mathbf{U}_c$$

where $\mathbf{U}_c$, the convection velocity, is approximately equal to the ship's velocity. This convection term makes the largest contribution to the TBL flow noise and forms a "convective noise ridge" in the ω, k plane, where k is the component of $\mathbf{k}$ parallel to $\mathbf{U}_c$. Figure 19 shows the approximate form of the contours of the convection noise spectrum as a function of ω and k. There is still considerable uncertainty as to the relative amplitude of the flow noise near the origin, because of experimental difficulties with background noise in this region. A constant-ω slice through the convection noise ridge is as illustrated in Fig. 20, which assumes a typical convection velocity of 50 ft/s and a frequency of one kiloherz. The peak of the ridge lies along a line defined by

$$k = k_h = \omega / U_c$$

Wave numbers k_L, k_S, and k_F on the horizontal scale are for bulk longitudinal waves, bulk share waves, and flexural waves in a 1 in. thick steel plate. The wave number in water is k_A.

Figure 21 illustrates dispersion curves (ω versus β) for dilatational Lamb waves in a ceramic epoxy hydrophone plate. Only the dilatational waves excite a potential difference

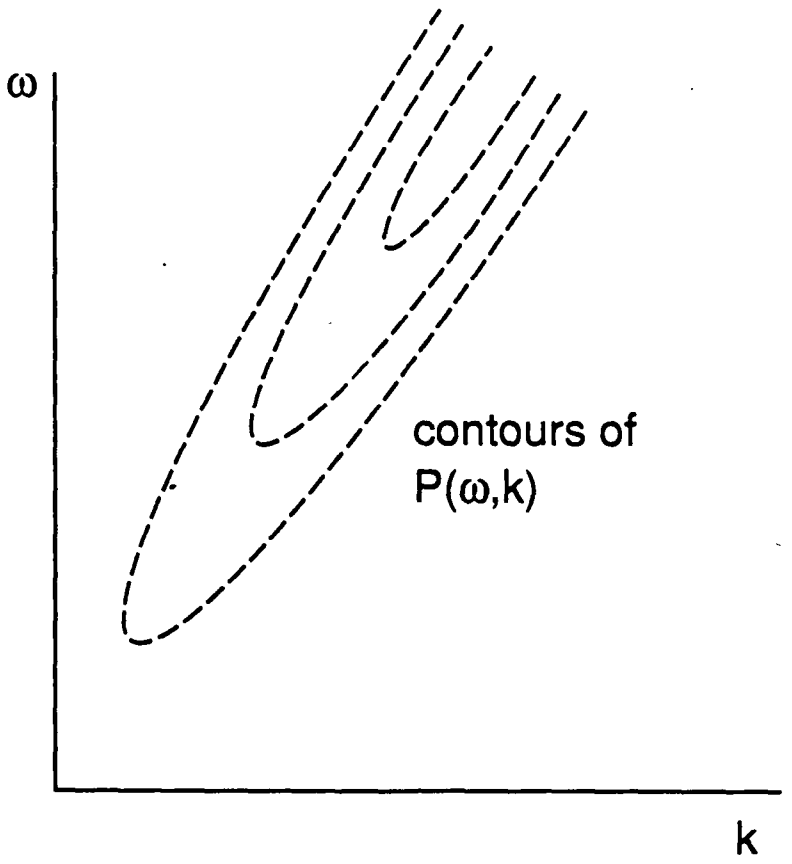

FIGURE 19

Schematic representation of the convective noise ridge in the ω, k plane.

between the surface electrodes (Fig. 22). The flexural waves considered in [32] do not couple piezoelectrically to the electrodes. For a homogeneous plate, the $\omega - \beta$ diagram contains only the branches starting on the vertical axis. The other branches represent space harmonics generated by the periodicity. In the actual dispersion curves of the composite, the first dilatational Lamb mode curve runs through the π and 2π stopbands denoted by vertical lines. In Fig. 21 the uniform thickness resonance of the hydrophone is at the vertical intercept of the second Lamb mode. This is the sonar operating frequency.

To qualitatively understand the interaction of TBL flow noise with a composite hydrophone, Figs. 19 and 20 must be overlaid on Fig. 21. The slope of the lowest Lamb wave branch has a ratio of ω to β approximately equal to the bulk shear velocity in the

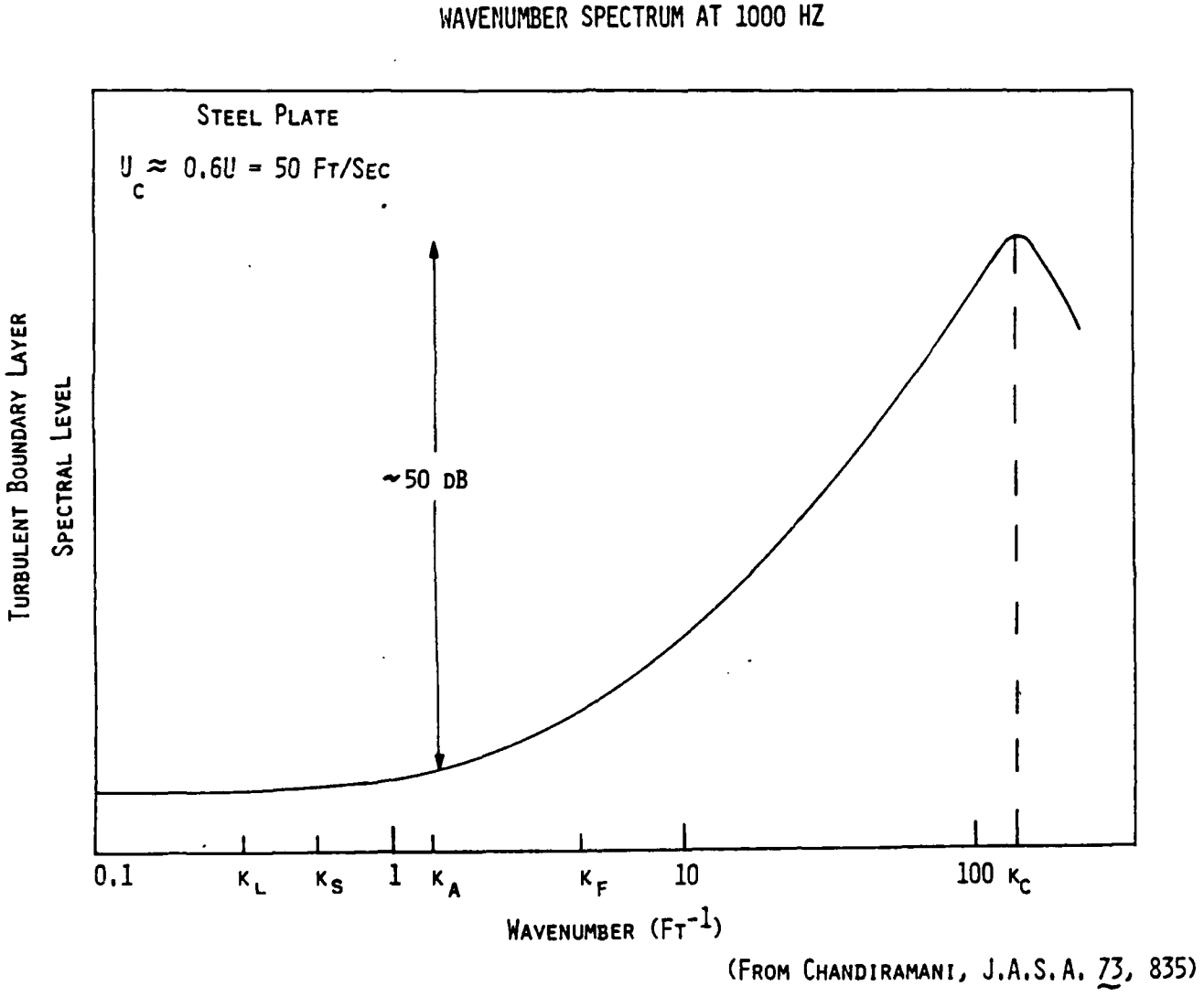

(FROM CHANDIRAMANI, J.A.S.A. 73, 835)

FIGURE 20

Section through Figure 19

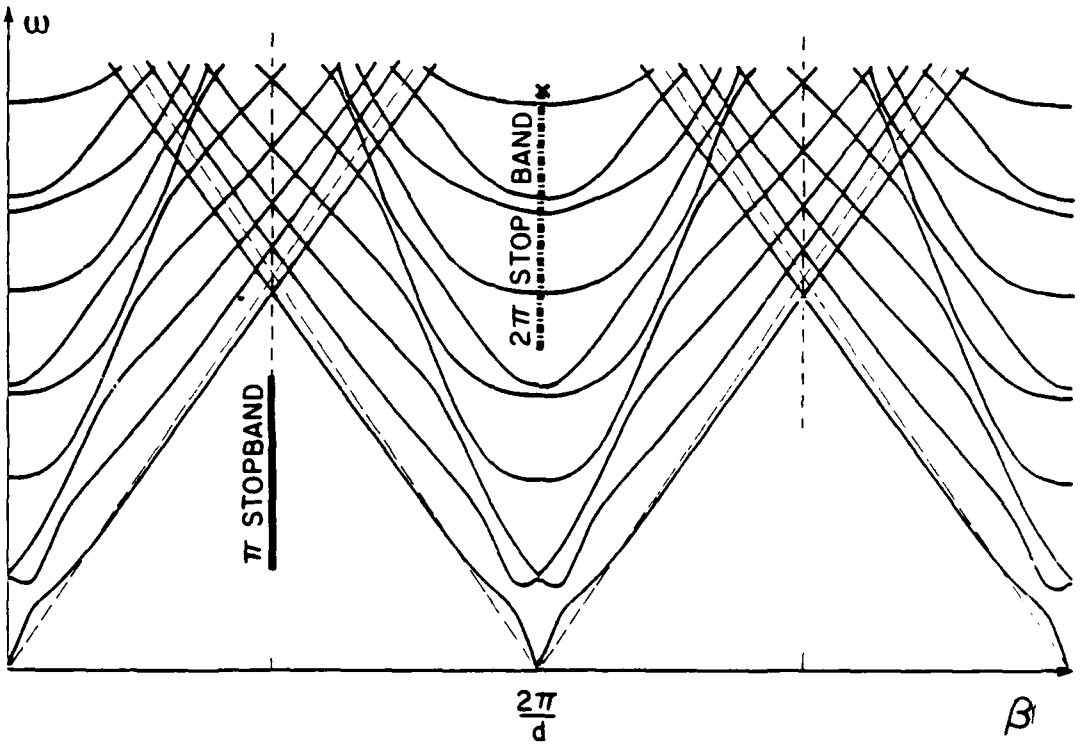

FIGURE 21

Typical composite plate dispersion curves.

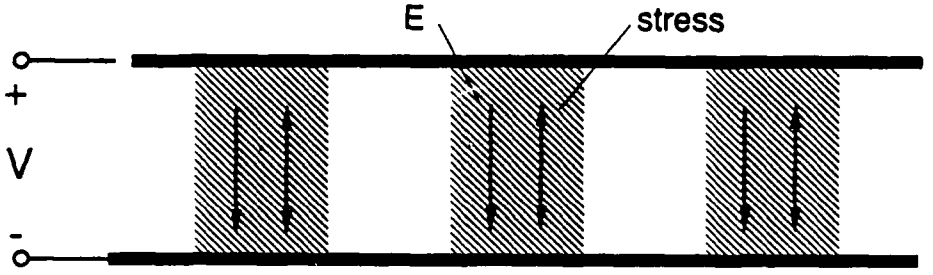

FIGURE 22

Piezoelectric coupling in a composite plate.

plate (corresponding to k_S in Fig. 20). From Fig. 20 the slope of the convective flow noise ridge in Fig. 19 is therefore approximately one five-hundredth of the ω/β for the first Lamb wave. Off-resonance excitation of the plate waves by the TBL noise can be estimated from the separation between the space harmonic dispersion curves in Fig. 21 and the overlay line of the convective noise ridge. It is clear from this figure that the first space harmonic of the first dilatational mode crosses the noise ridge at

$$\beta \approx 2\pi/d$$

so that the first space harmonic is resonantly excited there by the TBL noise. This should increase the noise output of the hydrophone, but at a frequency far below the sonar frequency. Resonant excitation at the sonar frequency can only occur at a very high order space harmonic, and this can probably be nulled by appropriate dimensional choices.

The periodic arrangement of the piezoelectric elements in Fig. 22 provides a spatial frequency filter action, as in [29] and [30], and could be used to provide spatial filter rejection of flow noise in the sonar frequency band. To do this properly will require detailed consideration of the space harmonic spectrum in Fig. 21.

IV. REFERENCES

[1] Bernard Jaffe, William R. Cook, Jr., and Hans Jaffe, *Piezoelectric Ceramics*, (Academic Press, New York, 1971), pp. 253–256.

[2] *ibid*, pp. 259–261.

[3] Private communication with Mr. Mel Kullin of Channel Industries, Santa Barbara, California.

[4] Reference 1, p. 140.

[5] Reference 1, pp. 148–149.

[6] M. Hayashi, *J. Phys. Soc. Japan* **33**, 616 (1972).

[7] Don Berlincourt and Helmut H. A. Krueger, *J. Appl. Phys.* **30**, 1804 (1959).

[8] M. E. Lines and A. M. Glass, *Principles and Applications of Ferroelectrics and Related Materials*, (Clarendon Press, Oxford, 1977), p. 532.

[9] Reference 1, pp. 154–158.

[10] R. Gerson *J. Appl. Phys.* **31**, 188 (1960).

[11] Reference 1, pp. 158–159.

[12] S. Ikegami, I. Ueda, and S. Kobayashi, *J. Acous. Soc. Am.* **55**, 339 (1974).

[13] B. A. Auld, H. A. Kunkel, Y. A. Shui, and Y. Wang, *Proc. 1983 IEEE Ultrasonics Symposium*, 554 (1984).

[14] T. R. Gururaja, W. L. Schulze, L. E. Cross, B. A. Auld, Y. A. Shui, and Y. Wang, *Ferroelectrics*, **54**, 183 (1983).

[15] B. A. Auld, Y. Shui, and Y. Wang, *J. de Physique* **45**, 159 (1984).

[16] B. A. Auld, *Acoustic Fields and Waves in Solids*, Vol. I, pp. 324–327 (New York: Wiley-Interscience, 1984).

[17] V. N. Celyi and B. B. Seuruk, *Sov. Phys.-Crystallogr.* **28**, 548 (1983).

[18.] K. Uchino and L. E. Cross, *J. Appl. Phys.* **19**, L171 (1980).

[19] J. D. Jackson, *Classical Electrodynamics*, (New York: Wiley, 1982).

[20] S. J. Jang, "Electrostrictive Ceramics for Transducer Applications," Ph.D. thesis at Pennsylvania State Univ., 1979.

[21] G. H. Haertling, Chairman, "PLZT Goggles," 1979 IEEE Int'l SAF, **27**, 173–202.

[22] B. A. Auld, P. Delval, G. Laguna, D. F. Thompson, and W. J. Wang, *Proc. IEEE Ultrasonics Symposium*, 217 (1987).

[23] K. Nakamura, H. Shimizu, and N. Sato, *IEEE Trans.* **SU-30**, 345 (1983).

[24] L. J. van der Pauw, *Appl. Phys. Lett.* **9**, 129 (1966).

[25] S. W. Meeks and B. A. Auld, *Appl. Phys. Lett.* **47**, 102 (1985).

[26] S. W. Meeks, B. A. Auld, P. Maccagno, and A. Miller, *Ferroelectrics* **50**, 245 (1983).

[27] S. W. Meeks and B. A. Auld, *Proc. Ultrasonics Symposium*, 535 (1983).

[28] T. Tsukamoto, J. Hatano, and H. Futama, *J. Phys. Soc. Jpn.* **51**, 3948 (1982).

[29] G. Maidanik and D.W. Jorgensen, *J. Acous. Soc. Am.* **42**, 494 (1967).

[30] G. Maidanik, *J. Acous. Soc. Am.* **42**, 1017 (1967).

[31] W.K. Blake and D.M. Chase, *J. Acous. Soc. Am.* **42**, 862 (1981).

[32] K.L. Chandiramani, *J. Acous. Soc. Am.* **73**, 835 (1983).

V. PRESENTATIONS AND VISITS

March 1987. B.A. Auld attended the Annual Review of the ONR Program on Piezoelectric and Electrostrictive Materials for Transducer Applications at the Materials Research Laboratory, Pennsylvania State University.

December 1987. B.A. Auld visited NRL, Orlando, Florida and presented a seminar on "The Spatial and Temporal Frequency Response of Composite Hydrophones."

Marh 1988. B.A. Auld attended the Annual Review of the ONR Program on Piezoelectric and Electrostrictive Materials for Transducer Applications, at the Materials Research Laboratory, Pennsylvania State University.

VI. PUBLICATIONS

1. B. A. Auld, "Wave Propagation and Resonance in Piezoelectric Materials," (Invited), *J. Acoust. Soc. Am.* **70** 1577-1585 (December 1981).
2. B. A. Auld, S. Ayter, M. Tan, and D. Hauden, "Filter Detection of Phase-Modulated Laser Probe Signals," *Elect. Lett.* **17**, 662-662 (September 1981).
3. B. A. Auld and H. A. Kunkel, "Laser Probe Measurements of Material Properties and Elastic Vibration Distributions in Counterpoled Ceramics," *Ferroelectrics* **38**, 971-974 (1981).
4. B. A. Auld and H. A. Kunkel, "Laser Probe Investigation of Guided Acoustic Interface Waves in Differentially Poled Ceramics," *Proc. 1981 IEEE Ultrasonics Symposium*, 438-443 (1982).
5. H. A. Kunkel and B. A. Auld, "The Use of Guided Acoustic Interface Waves in the Study of Differentially Poled Piezoelectric Ceramics," *Ferroelectrics* **51**, 99-104 (1983).
6. T. R. Gururaja, W. A. Schulze, L. E. Cross, B. A. Auld, Y. A. Shui, and Y. Wang, "Resonant Modes of Vibration in Piezoelectric PZT-Polymer Composites with Two Dimensional Periodicity," *Ferroelectrics* **54**, 183-186 (1983).
7. B. A. Auld, Y. A. Shui, and Y. Wang, "Elastic Wave Propagation in Three-

Dimensional Periodic Composite Materials," *J. de Physique* **45**, 159-163 (1984).

8. B. A. Auld, H. A. Kunkel, Y. A. Shui, and Y. Wang, "Dynamic Behavior of Periodic Piezoelectric Composites," *Proc. 1983 IEEE Ultrasonics Symposium*, 554-558 (1984).
9. H. A. Kunkel and B. A. Auld, "Acoustic Interface Waveguide Directional Couplers," *Proc. 1983 IEEE Ultrasonics Symposium*, 562-565 (1984).
10. B. A. Auld and Y. Wang, "Acoustic Wave Vibrations in Periodic Composite Plates," *Proc. IEEE Ultrasonics Symposium*, 528-532, (1984).
11. S.W. Meeks, B.A. Auld, and R.E. Newnham, "Ferroelastic Bubbles and Periodic Gratings in Neodymium Pentaphosphate," *Jap. J. Appl. Phys.* **24**, 568-570 (1985).
12. S. W. Meeks and B. A. Auld, "Periodic Domain Walls and Ferroelastic Bubbles in Neodymium Pentaphosphate," *Appl. Phys. Lett.* **47**, 102-104 (1985).
13. News Report "Ferroelasticity Comes of Age," *Nature* **316**, 481 (8 August 1985).
14. T. R. Gururaja, W. A. Schulze, L. E. Cross, R. E. Newnham, B. A. Auld, and Y. Wang, "Piezoelectric Composite Materials for Ultrasonic Transducer Applications, Part I: Resonant Modes of Vibration of PZT Rod-Polymer Composites," *IEEE Trans. Son. and Ultrason.* **SU-32**, 481-498 (1985).
15. B. A. Auld,"Rayleigh Wave Propagation," in *Rayleigh-Wave Theory and Application*, eds. E. A. Ash and E. G. S. Paige, (Springer-Verlag, 1985), pp. 12-28.
16. George R. Laguna, Pierre F. Delval, and B. A. Auld, "Electronic Control of SAW Transducers in Electrostrictive Ceramics," *Proc.* 1985 IEEE Ultrasonics Symposium, 207-211 (1986).
17. S. W. Meeks, L. Clarke, and B. A. Auld, "Tunable Bulk Acoustic Reflection Gratings in Neodymium Pentaphosphate," *Proc.* 1985 IEEE Ultrasonics Symposium, 325-328 (1986).
18. Y. Wang and B. A. Auld, "Acoustic Wave Propagation in One-Dimensional Periodic Composites," *Proc.* 1985 IEEE Ultrasonics Symposium, 637-641 (1986).

19. W. A. Smith, A. Shaulov, and B. A. Auld, "Tailoring the Properties of Composite Piezoelectric Materials for Medical Ultrasonic Transducers," *Proc.* 1985 IEEE Ultrasonics Symposium, 642-647 (1986).

20. George R. Laguna and B. A. Auld, "SAW Transduction in Electrostrictive Substrates," *Proc.* 6th IEEE International Symposium on Applications of Ferroelectrics, 589-592 (1986).

21. B. A. Auld, "High Frequency Piezoelectric Resonators," *Proc. 6th IEEE* International Symposium on Applications of Ferroelectrics, 288-295 (1986).

22. Y. Wang and B. A. Auld, "Numerical Analysis of Bloch Theory for Acoustic Wave Propagation in One-Dimensional Periodic Composites," *Proc.* 6th IEEE International Symposium on Applications of Ferroelectrics, 261-264 (1986).

23. Steven W. Meeks and B. A. Auld, "A Tunable Active Optical Ferroelastic Grating," *Proc.* 6th IEEE International Symposium on Applications of Ferroelectrics, 76-79 (1986).

24. Y. Wang, E. Schmidt, and B. A. Auld, "Acoustic Wave Transmission Through One-Dimensional PZT-Epoxy Composites," *Proc.* 1986 IEEE Ultrasonics Symposium, 685-689 (1987).

25. B. A. Auld, P. Delval, G. Laguna, D. F. Thompson, and W. J. Wang, "SAW Devices on Electrostrictive Substrates," *Proc.* 1986 IEEE Ultrasonics Symposium, 217-232 (1987).

26. S. W. Meeks and B. A. Auld,"Optical and Acoustic Device Applications of Ferroelastic Crystals," in *Advances in Electronics and Electron Physics* **71**, ed. Peter W. Hawkes, Academic Press, Inc. New York (1988).

VII. PATENT DISCLOSURES

1. Invention Disclosure S86067, "Adaptive Filter," P. Delval, B.A. Auld, Y. Wang, and B. Widrow, August 1986.
2. Invention Disclosure S86070, "Split Finger Structures for Weighted Electrostrictive SAW Transducers," B.A. Auld, August 1986.
3. Invention Disclosure S86071,"Programmable SAW Device on Electrostrictive Substrates," George R. Laguna, August 1986.
4. Invention Disclosure S86072, "Time and Space Varying Properties of Acoustic Transduction in Electrostrictive Substrates with Related Applications," B.A. Auld, G. Laguna, and P. Delval, August 1986.
5. Invention Disclosure S86073, "SAW Mixing on Electrostrictive Substrates," G. Laguna, B.A. Auld, and P. Delval, August 1986.

VIII. PERSONNEL

B.A. Auld, Faculty.

Y. Shui, Visiting Professor from the University of Nanjing, August 1982 to August 1983.

P.F. Delval, Visiting Scientist from Thomson-Sintra ASM, September 1985 to August 1986.

H.A. Kunkel, Graduate Student, January 1980 to December 1984; now at Schlumberger Research Laboratory, Ridgefield, Connecticut.

Y. Wang, Graduate Student, September 1981 to December 1986; now at Institute of Physics, UCLA, Marina del Rey, California.

G. Laguna, Graduate Student, September 1983 to March 1986; now at Sandia Laboratory, Albuquerque, New Mexico.

S. Meeks, Graduate Student, October 1984 to December 1985; now at IBM Laboratory, San Jose, California.

IX. Ph.D. THESES

H.A. Kunkel, "Elastic Domain Wall Waves in Ferroelectric Ceramics," June 1985.

S. Meeks, Optical and Acoustic Device Applications of Ferroelastic Crystals," March 1986.

G. Laguna, "Applications Using Electrically Alterable Material Properties in Large Dielecteric Constant Ceramics," June 1986.

Y. Wang,"Waves and Vibrations in Elastic Superlattice Composites," December 1986.

ASM/ETUA/87.054/PDF October 14 1987

Applications of Surface Acoustic Wave Circuits to Acoustic Signal Processing and to Sonar in Particular.

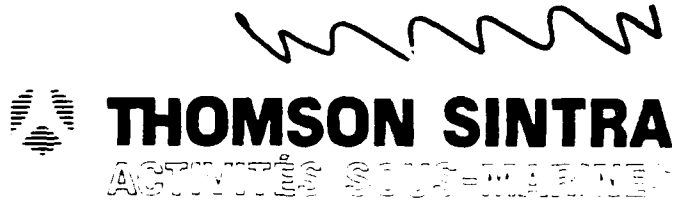

GLOSSARY OF TERMS

A/D: Analog to Digital (conversion, converters, process)

ARMA: Auto Regressive Moving Average (algorithm)

1/2 A.T.R: Printed circuit board format (roughly 10 cm times 20 cm)

B: Bandwidth of a signal

BT: Time Bandwidth product (also TB)

D/A: Digital to Analog (conversion, converters, process)

FET: Field effect transistor

FIR: Finite Impulse Response (filter, usually)

Fo: Central frequency

Fs: Sampling Frequency

FT: Fourier Transform

FFT: Fast Fourier Transform (digital algorithm)

GHz: Giga Hertz

Gops: Giga operations per second

I.D.T.: Inter Digital Transducer

kHz:	kilo Hertz
LMS:	Least Mean Square (algorithm)
LOFAR:	LOw Frequency Analyzing and Recording
MHz:	Mega Hertz
Mops:	Mega operations per second
PLZT:	Lead Lanthanum Zirconate Titanate (ceramics)
PMN:	Lead Magnesium Niobate (ceramics)
P.S.A.W.:	Programmable Surface Acoustic Wave (device or component)
PZT:	Lead Zirconate Titanate (ceramics)
R.M.S.:	Root Mean Square
S.A.W.:	Surface Acoustic Wave (device or component)
T:	Time duration of a signal
TB:	Time Bandwidth product (same as BT)
T.T.L.:	Transistor-Transistor-logic

ACKNOWLEDGMENTS

I would like to thank all the people who helped me, advised me, listened to me or corrected me during this stay at Stanford University. I would like to express my deepest gratitude to Professor Auld for his guidance and advises during this one year study; he leaded me, encouraged me and helped me finding other helpful people. Thank you also to Professor Widrow who discussed with me the adaptive filter applications.

I am grateful to the different people in several companies who listen to my ideas and councelled me; thank you Harper Whitehouse and James Alsup from the Naval Ocean Systems Center, Clifford Carter, Charlie Leblanc, Norman Owsley and Timothy Straw from the Naval Undersea Systems Center, Dave Baird, Howard Jones and Donald Bonnema from E.D.O. Western Corporation (who also provided some ceramics sam- ples for the adaptive filter experiments), Duan Arsenault and Donald Oates from the Lincoln Laboratories.

I am also endebted to Judy Clark, who helped me in different administrative problems and, especially, in the typing of this document.

Finally, thank you to all my friends in the Ginzton Laboratories and especially Daniel Hauden, Mark Gimple, George Laguna, Steve Meeks, Daniel Thompson and June Wang for the hours of fruitful discussions on all kinds of subjects.

TABLE OF CONTENT

CHAPTER 1

Introduction or "Why trying to use S.A.W. devices in Sonar?":

In the last decade, sonar systems have evolved from a detection and navigation equipment to a sophisticated detection - localization - classification one. This drastic change has been mainly influenced by the extraordinary evolution of the digital technology for computers and signal processors. Also of importance were the large progresses made in the design and realization of extremely silent submarine vessels; thus the sonar required more and more capabilities, essentially leading to very large antennae. In the next future, it will be common for advanced Navies to have submarines equipped with sonars having thousands of hydrophones. Nevertheless, during the last few years, the specifications of sonar have outstanded the capabilities of digital technology. Then, sonar engineers have to find out more and more tricks in order to achieve the requirements within the specified volume of electronics or the limited available power or the authorized weight. Conversely, for some applications, the available technology will determine in a way the possible achievable functions, thus forcing engineers to work the way around. Anyhow, several trade-offs have to be chosen and are regularly brought onto the subject because both technologies and operational requirements are always changing.

Radar and Sonar, although very similar in their working principles, have encountered a different kind of evolution [1]. The differences lie mainly in three factors: - operating

frequency range - wave velocity - and medium behavior. The last one (knowing the fact that air is a lot better medium for electro-magnetic waves than water is for acoustic waves) explains why the radar became very quickly a sophisticated tracking and classifying equipment as the sonar was (and mainly still is) a detecting equipment. The first factor is the reason why the radar technology has been analog for decades while the sonar is already partly, if not entirely, digital. For this particular aspect, radar is now using more and more the digital technology as the throughput capability of digital processors is increasing. However, only analog technology can cope with a good part of the signal processing chain. Then the hybrid technology is inherent and not considered as a problem by its own. On the other hand, sonars are digital now from the hydrophones themselves (just after the preamplifier and anti-aliasing filter) up to the TV monitor. Any attempt to go back to some kind of analog technologies encounters a strong opposition. The reason for this is multiform; it goes from physical aspects (such as temperature independance of digital circuits or parasitic natural shieldings) to theoretical reasons (such as a required accuracy or dynamic range for certain computations) without mentioning human reasons (such as the preference to deal with digital signals where only mathematics, and thence logics, are involved). Also, in some aspects, this attempt is viewed as a come-back, not fitting well with these high technology equipments. However, the second difference between sonar and radar, i.e. the wave velocity, must not be forgotten, for it leads to the very different concepts used for antenna design in both fields. Because of the very slow acoustic wave velocity in water (compared to electro-magnetic wave speed in air, and not acoustic wave in air), the rotating antennae have been disgarded very soon in sonar. Instead, sonars are using fixed arrays with phasing, allowing simultaneous beamforming of the hydrophone signals for different looking directions (i.e., simulating a rotating antenna having an infinite speed

of rotation). The important consequence of this fact is that you have to deal with numerous low-frequency channels, on which you have to perform a great variety of signal processing functions, such as filtering, beamforming, spectral analysis, etc.. Even speaking only about conventional signal processing (i.e. non adaptive), the computational load on the digital signal processors exceeds greatly the capabilities; for instance, imagine a linear array of a thousand hydrophones operating in a passive mode with a highest frequency of 6 kHz; to perform the beamforming operation with sufficient spatial resolution and coverage (say 2000 contiguous beams), would mean to have a signal processor capable of achieving a computation throughput of 72 giga-operations per second (an operation being either an addition or a multiplication); there is neither a super computer, nor a powerful signal processor able to cope with this throughput alone; even a set of computers in parallel would not solve this because it is impossible to put many of them without running into other problems. About adaptive signal processing [2,3], the problem is even worse, and are selected the channels on which this specific processing is required.

All these considerations give reasons why many people are doing research on processor architectures like, for instance, the systolic approach; nevertheless, this approach cannot deal with any kind of algorithms. Thus, other people are working on specific algorithms "systolically" implementable and are solving some of the problems; however, there will always be, at least in the coming future, some basic operations in a sonar system; these will be beamforming, Fourier transform (in parts of the system at least), filtering (adaptive or not), and image processing. Depending on the context, some of them are typically hard to implement with a systolic architecture; so, it is worthwile to think about the different ways of achieving such a throughput with conventional architectures. Several people are, then, working

on the way to realize networks of computers working in parallel, and then achieving very large throughput; another approach is to imagine some specific dedicated hardware (like a butterfly operator for FFT) for some repetitive and heavy tasks; one is then generally able to improve the efficiency of the processor. Going further with that idea, a promising alternative is to imagine an analog operator inside a digital hybrid computer ; this operator would, then, relieve the main computer from some heavy tasks; some functions like filtering, Fourier transforms can be very efficiently implemented and the computational speed greatly increased for two reasons: first, the very large bandwidth of analog components allows multiplexing of low-frequency signals on the same device ; secondly, some functions (like filtering) are performed intrinsically by the component rather than decomposed in operations as additions and multiplications; then, the computational rate is boosted by a factor equal to the number of elementary operations per function; this can be significant.

This last approach is chosen in this study; we are going to investigate the use of some analog components in sonar; for several reasons, the choice was made to work on the applications of S.A.W. (surface acoustic wave) devices [4,5] for sonar systems: The excellent disposition of these devices to perform transversal filtering (equivalent to the F.I.R. approach in the digital domain), their easy and relatively cheap technology, their "state of the art" and, at last but not least, the possibility investigated at Stanford University by Professor Auld and his group, of designing and making fully programmable and digitally compatible S.A.W. component (P.S.A.W.)[6]. Furthermore, it was derived that an analog adaptive transversal filter was actually achievable. These S.A.W. components are usually operating between 10 MHz and 1 GHz; it means that some kinds of frequency shifts or multiplications have to be done, but also that several signals

can be multiplexed on the same component, increasing its performances.

The following study will then be split in several parts; first of all, the nature of S.A.W. devices will be investigated; that is how they work, what kinds of signal processing functions are achievable, what the advantages and drawbacks are and also what do they offer in terms of performances (speed, volume, power-consumption). In that chapter, the specific features of the programmable .A.W. components will be described and some insights about how using S.A.W. devices in low-frequency signal processing (from some Hertz to several kiloHertz) will be given. Then, in another chapter, the possible applications of S.A.W. and P.S.A.W. devices in sonar will be scanned; these will determine some particularly promising signal processing blocks that will be investigated further. Also, in a separate chapter, the different constraints and linked trade-offs will be studied. From now on, we have the required knowledge to derive some promising system applications; for that point, the discussions with the Naval Undersea Systems Center in New-London, the Naval Ocean Systems Center in San Diego and E.D.O. Western corporation were very profitable. A last part will then try to make some concluding remarks on this subject and make some openings; these openings will represent either details to be investigated, or some new applications that need some simulations or experimental tests. Also have been added to this report several appendixes : first a bibliography, mainly on S.A.W. technology and also sonar and A/D, D/A problems; second, some more insights about P.S.A.W. and adaptive filter applications; finally, some details about another kind of application, a programmable coupling transducer.

In this report, we have tried to take a sonar engineer approach. From that point of view, it will be helpful as a S.A.W. technology description and as a source of new sonar

signal processing methods. However, the part on the P.S.A.W. devices and the sonar applications can be of interest for any person working on analog techniques and especially S.A.W. ones. Nevertheless, it has to be noted that Professor Auld's group in Stanford is mainly concerned about waves theory. For this study, we needed knowledge of materials science, S.A.W. technology, signal processing and hybrid computer technology. Then, this study could appear incomplete on some of these aspects, since we have been dealing with several of these fields together. But, this report has the merit of existing and pointing out several promising possibilities.

CHAPTER 2

Description of some S.A.W. components

2.1 Conventional S.A.W. devices:

2.1.1 What is a S.A.W. device [4,5]

At the end of the 19th century, Lord Rayleigh discovered some new types of waves in solids; they were to be called Rayleigh waves; these waves are characterized by the fact that they exist only in a very narrow layer, close to the surface where they are generated; usually, this layer measures less than a wavelength; also these waves are characterized by an elliptic motion of the particles. However, only in the early sixties was discovered all the potential applications of surface waves (and especially Rayleigh waves) in piezoelectric crystals for signal processing functions; a specific kind of transducer, the interdigital transducer (I.D.T.), which allows the launching and receiving of an acoustic surface wave, was invented. The whole advantage of the surface acoustic wave concept is that, the wave being confined on the surface, its propagation properties and its amplitude can be altered via some surface electrodes or grooves; also, the velocity of the surface waves in crystals or ceramics is usually about two to three thousand meters per second; being much slower than

electromagnetic waves, some non-negligible delays can be obtained within a very small piece of crystal. Finally, a classical S.A.W. component will include a launching transducer and a receiving transducer ; the spatial patterns described by the transducers will determine the different delays and control the amplitude of the wave. Figure 1 shows some typical features of a S.A.W. component; from this, one can deduce (see appendix 2) that the basic function of a S.A.W. device is transversal filtering (F.I.R.) (see Figure 2). Furthermore, contrariwise to the digital technology, there is no requirement for an uniform sampling of the signal, or uniform locations for the electrodes; thence, some exotic filter, like the chirp filter [7,8] (see figure 3), can be easily achieved. Also, some very narrowband filter can be designed using a resonator structure (see figure 3). All these functions belong to the linear signal processing group; and then, linear materials are needed. For some specific purpose, as convolution, some nonlinear materials [9] are used but we will not investigate this aspect and will consider only linear signal signal processing.

2.1.2 Basic functions of a S.A.W. component

As it was mentioned earlier, the basic function achieved by a S.A.W. component is transverse filtering [8]; it will be shown in this report that many signal processing blocks, in various fields of application, can be designed using one or several transversal filters. Let us talk now about two specific kinds of S.A.W. transversal filters, that are very useful: the bandpass transversal filter and the chirp filter. The first one will be useful for matched filtering

applications or image processing and the second one will lead to the design of very efficient Fourier transformers [10].

2.1.2.1 Transversal filter

A typical bandpass (or lowpass) transversal filter will involve series of delays and weightings ending on a summation; figure 4 shows the Z-transform scheme and the corresponding equation. The realization requires a way of implementing the delays (we already mentioned that this was easily achieved because of the slow acoustic velocity) and the weightings; for this latter purpose, several techniques are available but only one will be described here for reasons of clarity: the overlap method. For further details about these techniques, an abundant bibliography is available and notably [4,5,11,12]. The last step, summation, is directly performed by the electrode shorting (see appendix 2). The overlap method can be roughly described by the linear (at first order) relation between the wave amplitude and the signal on the electrodes; this linearity factor is proportional to the overlap between two adjacent fingers (see figure 5).

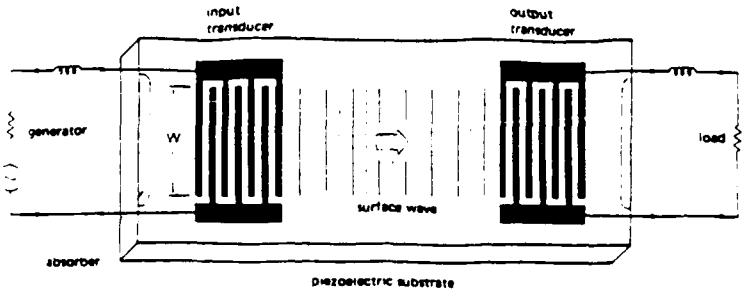

Figure 1: S.A.W. component - General structure

Figure 2: Transversal filter structure

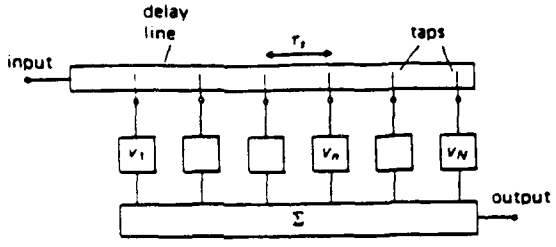

Figure 3: Chirp and resonator filter

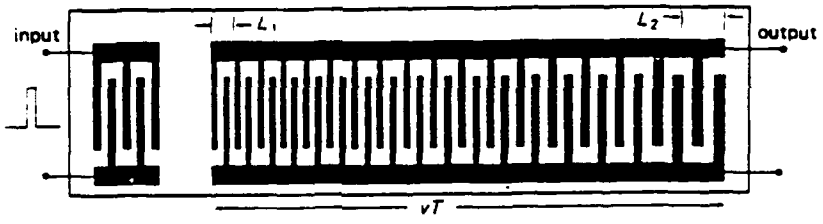

3.a Chirp filter - Linear Frequency modulation

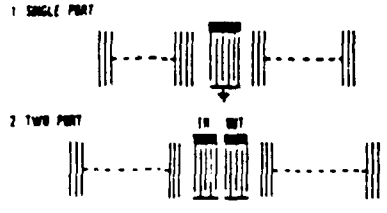

3.b Resonator filter

Thus, by controlling this overlap during the electrode design, one is able to control the impulse function of the filter. One major flaw of S.A.W. filter is then readily apparent since with this technique, as opposed to the digital one, the weights, and thus the impulse response, are fixed, and cannot be changed. Also, another drawback is their inability to transmitt any direct current (or very low-frequency) signal; thence, this filter can only be bandpass and not lowpass; however, by using a carrier signal, it is easy to get around that problem.

The last point concerning the design of a transversal filter is the space-time relationship for the delays; one wavelength corresponds to a time period; also the transducer properly launches or receives only signals having a frequency being half that of the designed spacing; this corresponds to the well-known Nyquist criterion.

Finally, the design of a S.A.W. transversal filter consists in the following steps: - selection of the center (or carrier) frequency and computation of the spacing of the fingers (1 of alternate polarity each half-wavelength); - design of the impulse function of the filter (by conventional means); this gives the number of coefficients of the filter, and then the number of gaps between fingers; endly, the overlap between two fingers is determined by the amplitude of the concerned weight. The next step is then to design a mask (as for printed circuit board) and to lay the electrodes on the substrate, usually via photolithographic deposition techniques. With conventional S.A.W. filters, there is no way to compensate any flaw of the filter, even a minor one. Then, it is unthinkable to change the filter impulse function;

S.A.W. components are non variable by nature.

2.1.2.2 Fourier transformer

A very interesting application of S.A.W. technology concerns the realization of a Fourier transformer; this is possible by using two or three S.A.W. filters. Although these filters are transverse by nature, they differ from the ones described earlier and from the common group of transversal filters; they are called chirp filters and are dispersive, meaning that the delay of the signal is a function of the frequency. Their first application was for pulse compression and expansion for radar. This is the matched filtering operation involving frequency modulated signals. However, by using linear frequency modulated signals, a Fourier transform can be performed very efficiently [4,5,7,8,10,13,14] using the chirp-filter algorithm. It is a very important application because of the very wide use of a FT [15]. Various ways are possible to describe the chirp algorithm [16], but one of them is more closely related to the mathematical operations; it is called the M-C-M, or multiply, convolve, multiply. It is derived in [14] that a Fourier transform could be expressed as in equation 1. Thus, the M-C-M arrangement, shown in figure 6, consists in the pre-multiplication of the input signal by a downchirp signal; the result is then fed into an up-chirp filter for convolution; to obtain the Fourier transform of the input as a function of time, a post-multiplication by another downchirp signal must be performed. The features of the chirp signals and filter must be matched; especially, the magnitudes of the slope (i.e. B/T) need to be identical. Also, the center frequencies, although not necessarily the same, should be consistent one with the others. Furthermore, in

order to perform the full convolution in the up-chirp filter, this filter's response should last twice as long as the input signal. A possible implementation of the chirp algorithm with S.A.W. components is shown on figure 7; the two down-chirp signals are obtained here by impulsing a single down-chirp filter, thus achieving a two filter implementation. The other ways of implementation will differ by the locations of the mixers or by the kind of signal (baseband or modulated) or by the form of the output (again, baseband or modulated or magnitude only). Actually, complex signals (and then, complex transform) can be taken into account by using more filters; a very good discussion of the various possibilities, their advantages and drawbacks is given in [14]. The way to design and manufacture the chirp filter is very similar to the one described earlier for transversal filtering. In [12] is discussed the special way of locating the electrodes.

$$F(\nu) = \exp\left[-j2\pi\alpha t^2\right] \cdot \int_{-\infty}^{+\infty} f(x)\exp(-j2\pi\alpha x^2) \cdot \exp\left(j2\pi\alpha(t-x)^2\right) dx \qquad (1)$$

with $\nu = \alpha.t$

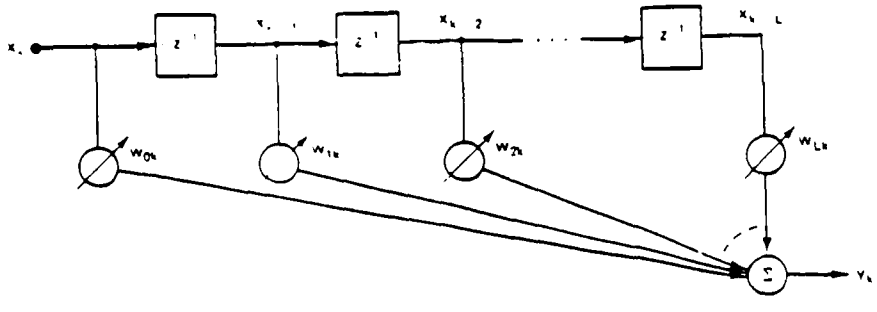

Figure 4: Z-transform of a transversal filter

Figure 5: Overlap and Impulse function

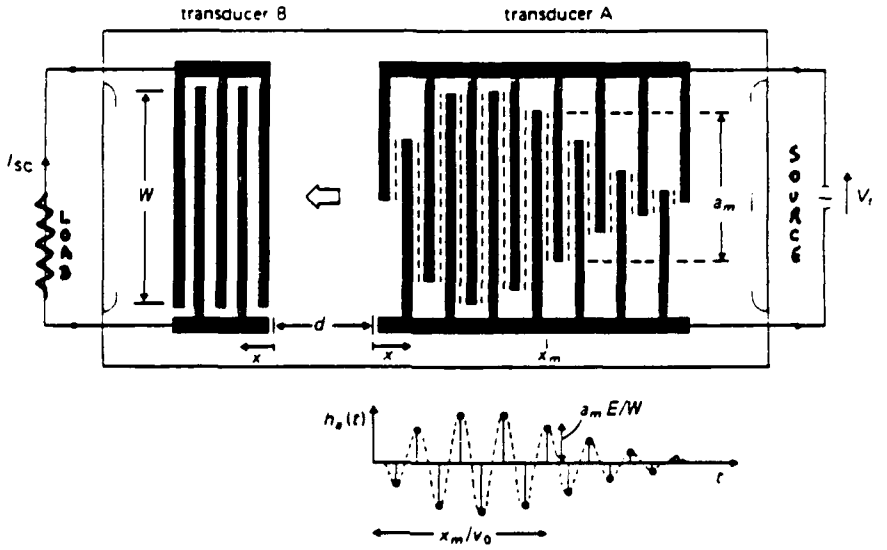

Figure 6: Chirp filter algorithm (MCM) and Fourier transform

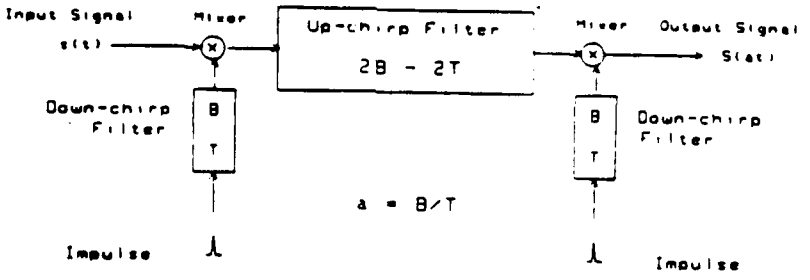

Figure 7: S.A.W. implementation of a Fourier transformer (MCM)

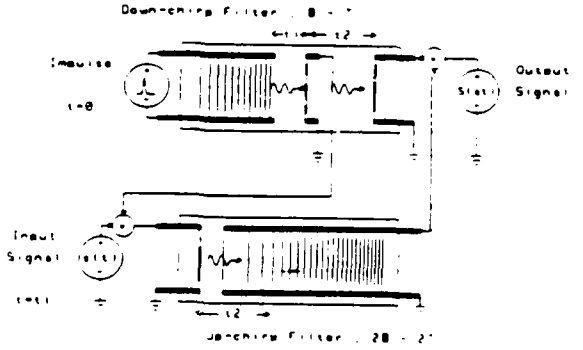

2.1.3 Some characteristics of S.A.W. filters

In this section, we will give some useful figures about the main features of S.A.W. devices. This will allow a better evaluation of their capability for signal processing.

The first, and may be most important, parameter of such a component is its frequency span or operating frequency range; for conventional S.A.W. devices, the center frequency goes from a few MHz to 1 or 2 GHz for the best, while the bandwidth goes from some hundreds of kHz to several hundreds of MHz. For a specific filter, the relative bandwidth (ratio of the bandwidth to the center frequency) varies between a few percent to 30-50 percent, sometimes 100, accordingly to some material properties such as the electromechanical coupling.

Another important feature is the achievable delay; it is usually comprised between a few hundreds of nanoseconds to some tens of microseconds; the resolution of an actual delay usually gives a typical accuracy of 10 degrees RMS on the phase of the signal. On some kinds of filters, it is possible to compensate some of the phase errors once the mask is laid on the substrate (using laser techniques); then an overall accuracy of some degrees is achievable. Other limitation on the accuracy of the component will involve the quality of the material (inhomogeneities), the surface shape (it should be as close as possible to optical polishing), the temperature dependance and the uniformity of the poling for piezoelectrics. This gives a typical accuracy of one part in a million; to be more practical, this could be compared to a digital computer

giving the same accuracy; this will require computations on a 8 bit-word; for some specific applications, it can be as low as 5-6 bits [17]. However, in the remainder, we will consider an equivalent 8-bit accuracy for S.A.W. component. On another hand, for analog circuit, the dynamic range is not related to the accuracy, as it is for a digital processor, through the number of bits (at least for fixed formats); it is rather related to the different noises in the component (such as thermal noise, bulk wave generation, scattering or electromagnetic (E/M) feedthrough) and to the insertion loss of the device; the latter represents the attenuation of the signal power when going through the device (seen as a quadrupole). Typical insertion losses can vary between a few decibels to 20 or 30 decibels ; for some filters or materials, it can go as high as 50 to 60 dB. With a correct design of the device and for a typical case, the other noises can be kept below 80 or 90 dB; this then gives an equivalent maximum dynamic range of 15 bits (with the same idea of comparison that for accuracy [17]); for the remainder, we will consider a 12 to 15 bit dynamic range figure.

The last features that will be briefly described are the volume and power-consumption of these devices; the size is a function of the frequency and of the required delay for the function; it is usually a piece of crystal measuring 1cm by 2 to 5 cm with a thickness of a few millimeters; specifically, it can be larger, especially for chirp filter and the length could be up to 10 cm. On another hand, the power-consumption is usually very small and a typical figure is some milliwatts for driving the filter; long chirp filters may require more but anyhow, less than a watt.

Finally, a typical S.A.W. signal processing device will include the device itself plus an output amplifier to compensate for the low-level outputs, especially when several filters are cascaded as for the Fourier transform application. A bandpass filter will have easily some hundreds of coefficients, thus allowing sharp stopbands characteristics; the time required to perform the filtering will be roughly equal to the time duration of the filter (say 20 microseconds); then, the equivalent number of operations per second is readily into the tens of megaoperation/s for a device smaller than a matchbox! Fourier transformers will need some more space because they involve several filters ; however, on a 1/2 ATR board, you will be able to fit a transformer having an equivalent number of 1024 points, with all its surrounding electronics. This module will perform the FT in roughly twice the length of the filter; then, several hundreds of megaoperations per second are easily achieved this way. Chirp filters have been built with a time bandwidth product (TB) greater than 10000. Conclusively, it seems obvious that these S.A.W. components are very powerful for signal processing.

2.2 Programmable S.A.W. devices [6,18,19,20,21,22]

2.2.1 Why programmability:

We have already mentioned that one of the major drawbacks of the S.A.W. devices was their rigidity; several people have worked on that aspect for a while, some of them successfully. Before going into the d tails of how this is achieved (note that it is not a simple thing), it is useful to wonder why some kind of programmability could be of interest. To adress that, the term programmability should be cleared up ; usually, it is referred to as a programmability of the transfer function of the filter ; however, again, the problem is different if the specifications required adjustments of the weights (and at which speed) or changes in the center frequency. The basic advantage of these features is to be able to use the same device for different functions (and thus, save hardware and prices) or to experiment some new functions and make some adjustments. For instance, you may have a matched filter for a torpedo sonar, and want to change the signal code in order to adapt the sonar to the situation (sinusoidal wave for doppler and frequency modulation for distance); with a programmable transversal filter, the only thing required is to switch from one transfer function to another. Another example is when an operator wants to adjust the parameters of a filter to improve the response on some specific feature; this requires some kinds of up and down adjustments. Remember also that programmability, and software modifications, is the main advantage of the digital technique; basically, this feature allowed this technology to overcome all the others when speed and/or hardware saving was not the principal constraint. The next step in that direction is to

design an analog operator inside a digital hybrid computer; the computer will serve as an interface and give a mean of easy programming, while the analog operator (for instance a S.A.W. filter) will boost the computational capabilities of the processor by taking in charge all the filtering. There, you need a S.A.W. device fully programmable and digitally compatible; for instance a programmable bandpass filter (center frequency, bandwidth, sidelobes level, etc.) or a programmable Fourier transformer (duration, resolution, frequency span, etc.) could fit very well into a digital computer and unload it from these operations. This is exactly the way an array processor will interact with a host mainframe computer. Endly, the ultimate step is the adaptive device; basically, it is a programmable device but with very high programming frequency capability ; furthermore, an adaptation algorithm is needed, but it could be implemented on the digital computer. Nevertheless, the applications of adaptive filters (filter being used in a very broad meaning) are numerous [2]; also, this signal processing requires many computations, these being mainly involved for the filtering rather than for the adaptive process; then, an adaptive S.A.W. filter will be of great usefulness for signal processing.

2.2.2 S.A.W./F.E.T. programmable filters

This kind of filter is the only one, so far, that was called programmable S.A.W. devices; several persons are working on this aspect since several years [20,21,22]. The basic idea is to use independant access of each finger electrode rather than using stripes connecting all the electrodes of the same polarity

(compare figure 1 and figure 8); then, by using the proper electronics, you can attenuate and even turn off the signal coming out of this electrode. The electronics can be relatively simple since it involves only F.E.T. components (hence, the name!). However, with filters having hundreds of taps, the problem becomes more complex and you need all the integrated circuit technology to build a hybrid circuit with a piezoelectric layer and a semiconductor one. This has been done for filters having tens of taps, but beyond, the connectics problem (to go from the piezoelectric to the semiconductor layer) is really tough.

These components represent a breakthrough for conventional rigid S.A.W. filters; however, they have several drawbacks that we will analyse in the following. First, the insulation that you can achieve with this electronics is limited; the on/off ratio is usually about 30 to 40 dB, thus allowing a restricted 30-40 dB dynamic range for the filter's coefficients; this corresponds to about a 6 bit-word on a digital computer. Second, the relationship between the command voltage and the consecutive attenuation is not linear; then, the use of some kinds of conversion tables are required. Last, there is no direct way of achieving a negative coefficient with this technique; actually, even with conventional S.A.W. filters, the way to design a negative tap is to put two electrodes of the same polarity next to each other, rather than having the periodic alternance. The programmability we are speaking about will allow a negative tap to be attenuated, but staying negative; the same is true for a positive tap. Finally, to be able to change the sign of a tap, you need two identical filters, with reverse polarity; hence, by switching the output between the two filters and using the F.E.T.s for attenuation, one

can really program the taps; but now, the device looks rather complicated.

Figure 8: S.A.W./F.E.T. component

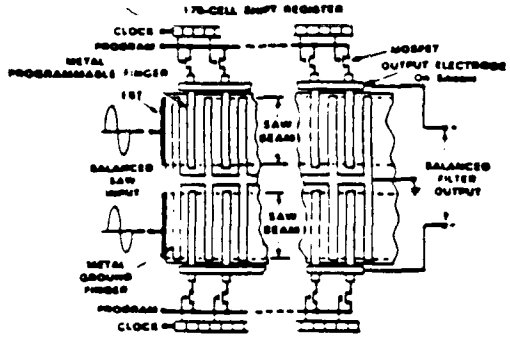

Concluding, all these remarks and the complexity of the manufacturing have prevented this kind of filter from being pushed onto the top.

2.2.3 Truly programmable S.A.W. devices

A few years ago, Professor Auld devised that in order to get programmability for S.A.W. components or for transducers, the best way was to achieve programmability of the piezoelectric coefficients, or of the electromechanical coupling. At first look, it seems rather unthinkable since, usually, poling a ceramic or a crystal requires several minutes, sometimes heat and almost always high voltages. However, it was found that materials like some variety of PZT (lead zirconate titanate) can be poled and depoled in a few minutes, using low voltages (less than 20 volts) and with a designed spatial pattern (given by the poling electrodes). Nevertheless, it is still far from a programmable filter with digital compatibility.

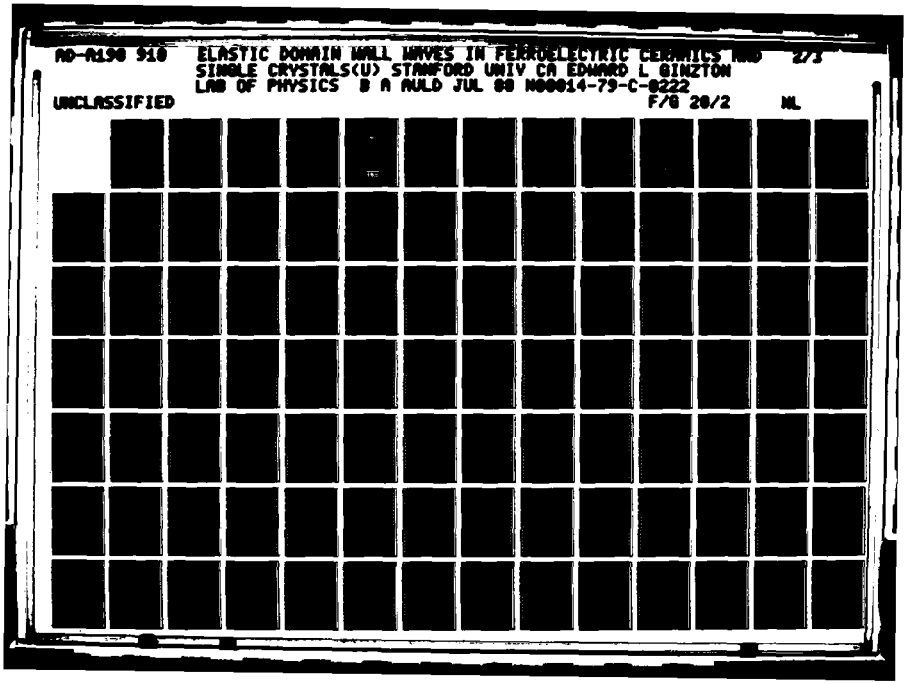
AD-A190 910 ELASTIC DOMAIN WALL WAVES IN FERROELECTRIC CERAMICS AND 2/3
SINGLE CRYSTALS(U) STANFORD UNIV CA EDWARD L GINZTON
LAB OF PHYSICS B A AULD JUL 88 N00014-79-C-0222
UNCLASSIFIED F/G 20/2 NL

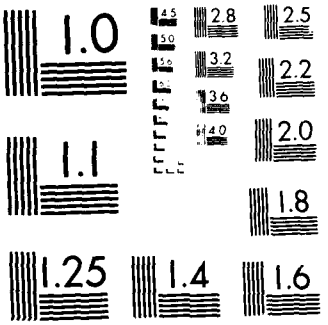
1.0
1.1
1.25
1.4
1.6
1.8
2.0
2.2
2.5
2.8
3.2
3.6
4.0
4.5
5.0

Then, it was deduced that non-piezoelectric materials have to be used. The question is now how to achieve a piezoelectric-like behavior into the material. It was discovered [19] that electrostrictive materials (having a square law relationship between the stress and the applied electric field) can be induced to be piezoelectric by using a D.C. biasing voltage. Furthermore, there is now a linear relation between the electromechanical coupling and the biasing voltage (providing that the dielectric constant is not changing with the DC field, which is one of the specification). Actually, there is a true proportionnality with respect both to the sign and magnitude of the bias; negative coupling was predicted and observed. This represented mainly G. Laguna's Phd thesis and was the background of my study at Stanford. With a correct design of the biasing electrodes, it is possible to achieve an accurate control (each finger pair) with low voltages (less than 10-20 volts). Appendix 2 and [6,18,19] are going further into details about this concept.

2.2.3.1 Biasing configurations

As we mentioned in the last section, the whole idea is here to bias an electrostrictive (i.e., non piezoelectric) material into a piezoelectric-like material, this effect being thoroughly under control of the spatial and temporal distribution of the biasing field. Besides some material problems and some classical S.A.W. design troubles (that will be adressed briefly in a further section), the real new problem is the way to achieve the bias control. Figure 9 shows various possibilities for the bias electrodes on a

piece of substrate. 9(a) represents the first experimented geometry; it works pretty well except for the following inconveniencies: the spatial resolution is low, and the required voltages are high (several hundred volts) in order to get an appreciable effect, because of the large distance between the top and the bottom of the substrate. 9(b) is an attempt to solve this problem by decreasing the distance between the electrodes; it is not simply possible to decrease the thickness since it is needed to avoid generation of spurious modes like plate vibrations; then, this composite structure is required. The manufacturing process become then complicated, especially at high frequency because the thickness of the plate would be no more uniform. Also the connections are troublesome; this solution has never been experimented. 9(c) is known as the meander line structure; it allows to use low voltages (down to 10 volts) and could allow individual control of the finger pairs by using the air-bridges technology for the connections. The experiments gave good results although less promising than 9(a) or 9(d); in addition to the complexity of the connections, the real problem is a low transduction efficiency. 9(d) is the last up-to-date solution; it should combine the advantages of the meander line (low voltages and potential control of each electrode), the efficiency of the 9(a) solution (see appendix 2 for more details) and the mask is not more complicated than for regular split finger S.A.W. devices. The split finger geometry, which is the basis for the design here, is a common solution for reducing the reflections occurring under the electrodes; reflections will cancel themselves between the first and the second finger of each electrode while the wave going through will be unaffected. The design presented on 9(d) takes advantage of this geometry (and its reflections

cancellation) for an efficient implementation of the biases; figure 10 gives an expanded view with the different connections for a transversal filter; the wi's are the filter's coefficients. A device made according to this idea is currently under investigation and very good results are expected. The cross-talk effect (meaning the fact that the bias voltage on one electrode will influence the bias field under the next electrode, and thence the coupling in an undesired way) should be as low as possible here; this cross-talk represents the limitation on the achievable dynamic range for the filter's coefficients; it is expected to be greater than 50 dB, thus leading to an equivalent 8 bits encoding of the weights.

2.2.3.2 Promises of this concept

The promises of this concept for S.A.W. signal processing applications are readily various and exciting. Different kinds of programmable transversal filters can be achieved, with a full control of the impulse response; this can either involve changes in the weights only (negative or positive, with a linear relationship), or also in the center frequency (with integer steps) by selecting the active cells.
Programmable Fourier transformer can be easily designed, with control of the bandwidth and resolution. Also, adaptive transversal filters can be made; an open-loop or feedback loop approach can be chosen with no differences for the concept. In the case of sonar, except for specific application such as torpedo or dipping sonar, the common method involves an open-loop approach since the signal to noise ratio is usually too low for a feedback loop (the convergence time is too

Figure 9: Biasing geometries. (a) top-bottom; (b) layered structure; (c) meander line; (d) split finger transducer

(a)

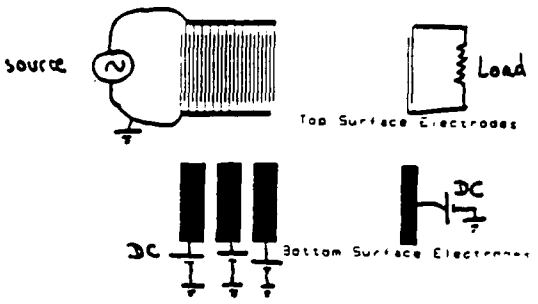

(b)

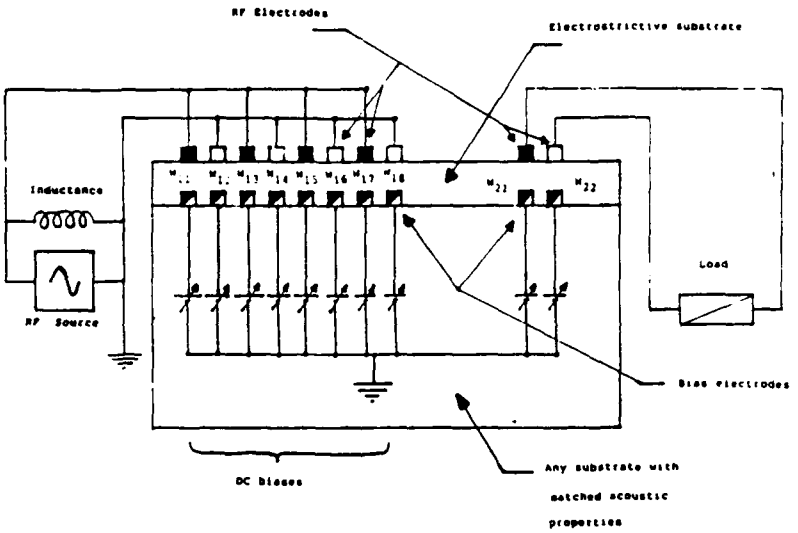

(c)

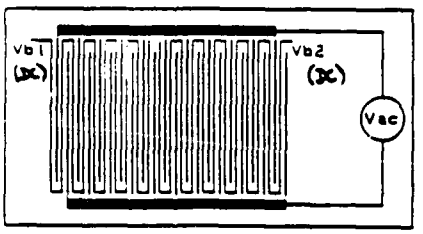

(d)

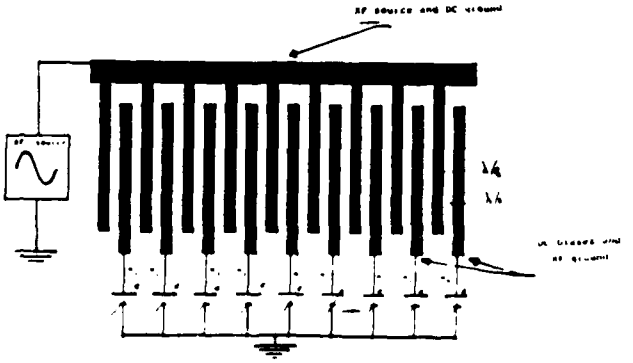

Figure 10: Split finger structure and filter's taps

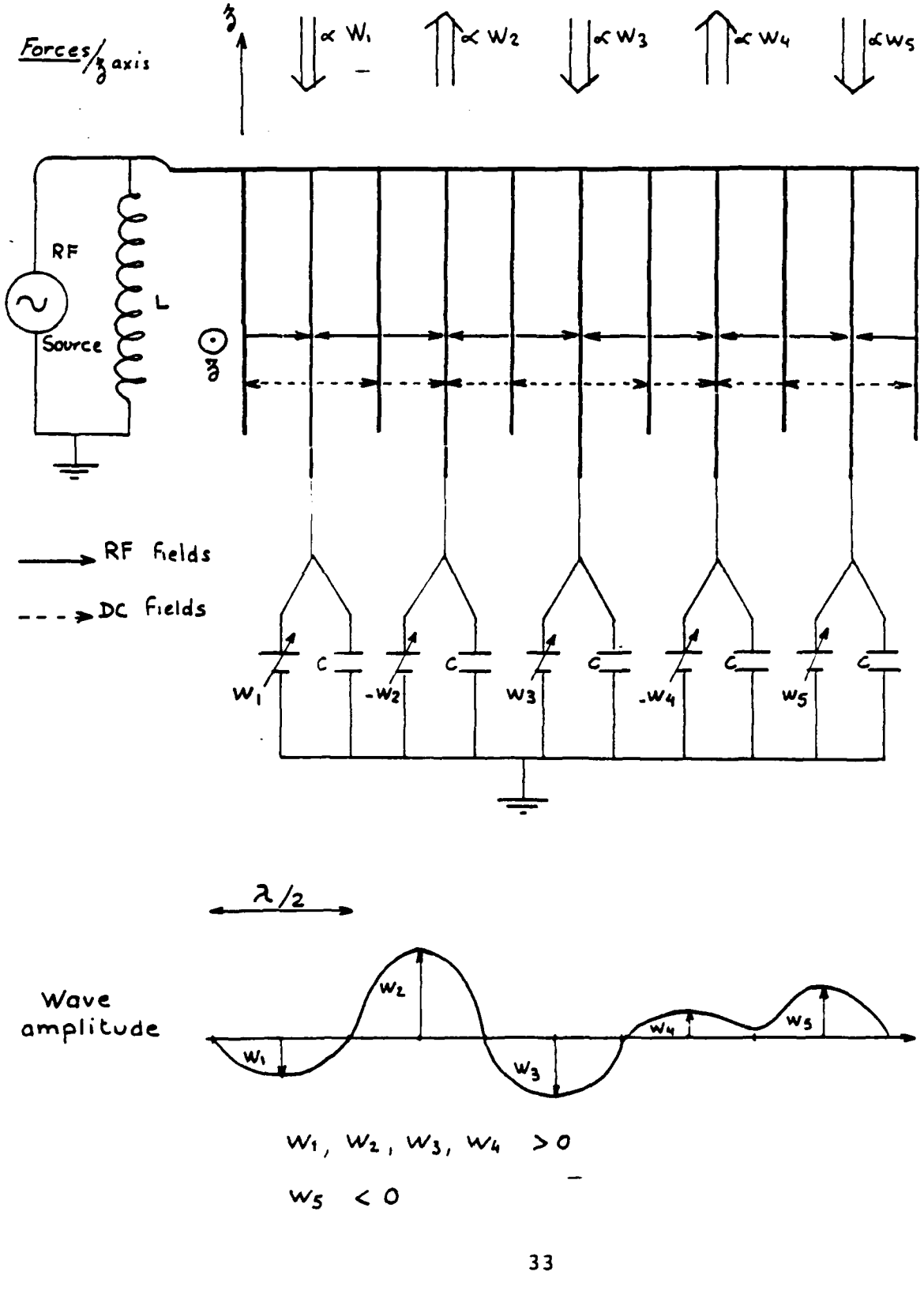

long); it is possible in this case to compute the optimum set of weights on a digital computer and to send them to the filter.

The most important features on the biasing capabilities are the linear relationship between field and coupling, the low-voltages required for the field settings (then compatible with digital to analog converters) and the capacitive geometry of the biasing electrodes. This leads to the very attractive architecture shown in figure 11. Theoretically, in order to set a weight on the filter, the computer has to send the value to the D/A converter, which transmits it to the electrode; the capacitive electrode holds the value for a while, thus allowing the converter to set the voltage on another electrode. Then, according to the programming speed and the characteristics of the D/A converter, a single converter and a multiplexer could be the only required interface electronics; this is truly a digitally compatible S.A.W. filter. In fact, we already mentioned the cross-talk problem ; this means that the relation between voltage and field is not reciprocal and thence, the coupling on one electrode depends on several biasing voltages. Still, the equations being linear, if there are as many biasing electrodes as weights, there is always a solution allowing to achieve the right coupling pattern; however, the solution to the Laplace's equations is needed first. The split finger geometry (9d) should decrease the cross-talk enough to avoid any problem, but this must be considered because of the inherent problem due to the high dielectric constant of highly electrostrictive materials. Also, in the case of the adaptive filter, the feedback loop takes this misadjustment of the weights into account, thus trying to compensate them (i.e. solving Laplace's equations by

approximation). Figure 12 shows the implementation of the adaptive transversal filter; in the first case, the adaptation process could be analog; the voltage source is then just an operational amplifier with the convenient connections. Figure 12 shows also the programming features of a chirp filter,and thence that of a Fourier transformer.

The last important feature concerning the promises is the speed of programming; in this case, there is no real limitation since the material is reacting to two fields, the signal and the bias. Moreover, the response is symmetric and then the bias could also be a high frequency signal; mixing of two signals was predicted and easily observed on experiments; then, programming speed of 10 MHz or up are easily achievable. The actual limitation would rather be the programming electronics; in the digital case, the D/A converter is also a limitation, although some of them are very powerful [23]. If a fully analog option is taken, then the only limitation comes from the material both for the signal and bias. Figure 13 shows an interesting thoroughly analog implementation of an adaptive filter using the L.M.S. algorithm; it is currently under investigation (see appendix 2).

Figure 11: Hybrid architecture

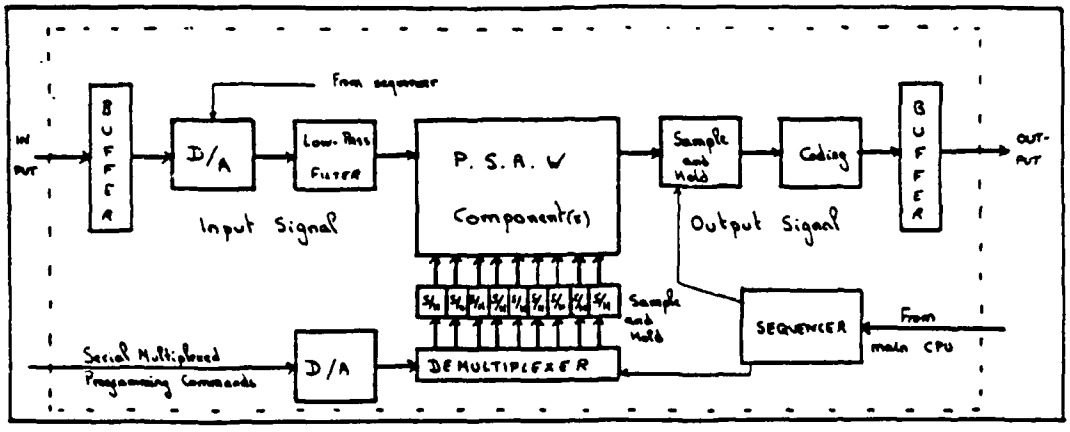

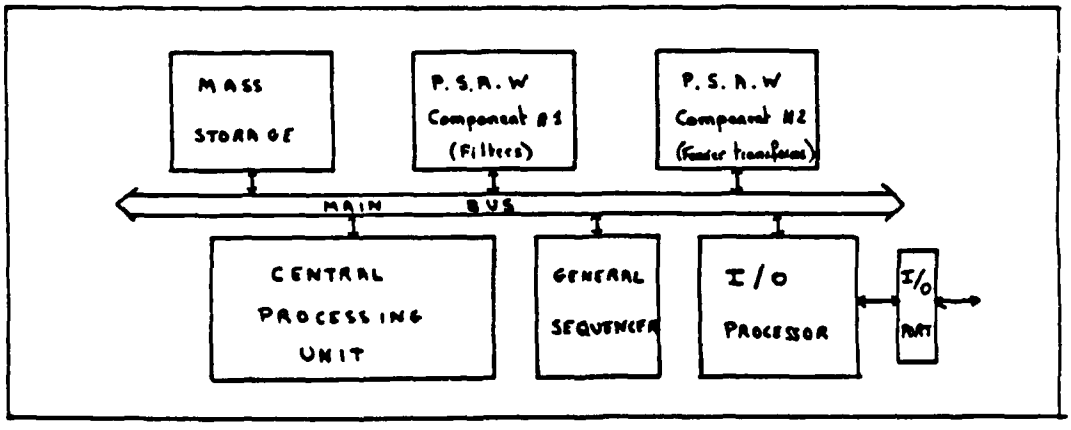

Figure 12: Programming feature and interface. (a) and (b), adaptive filter, feedback and open-loop method. (c) Chirp programming.

(a)

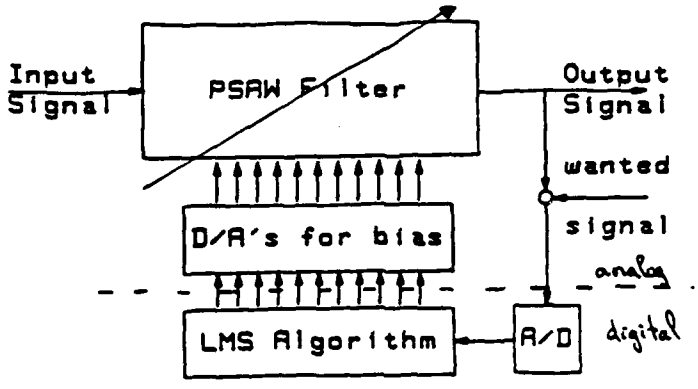

(b)

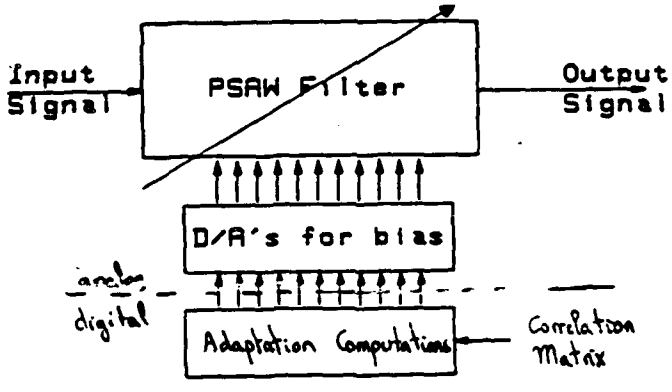

(c)

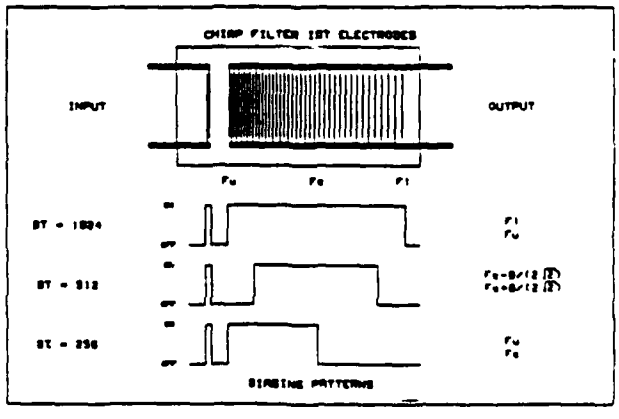

Figure 13: Analog implementation of the L.M.S. adaptive algorithm

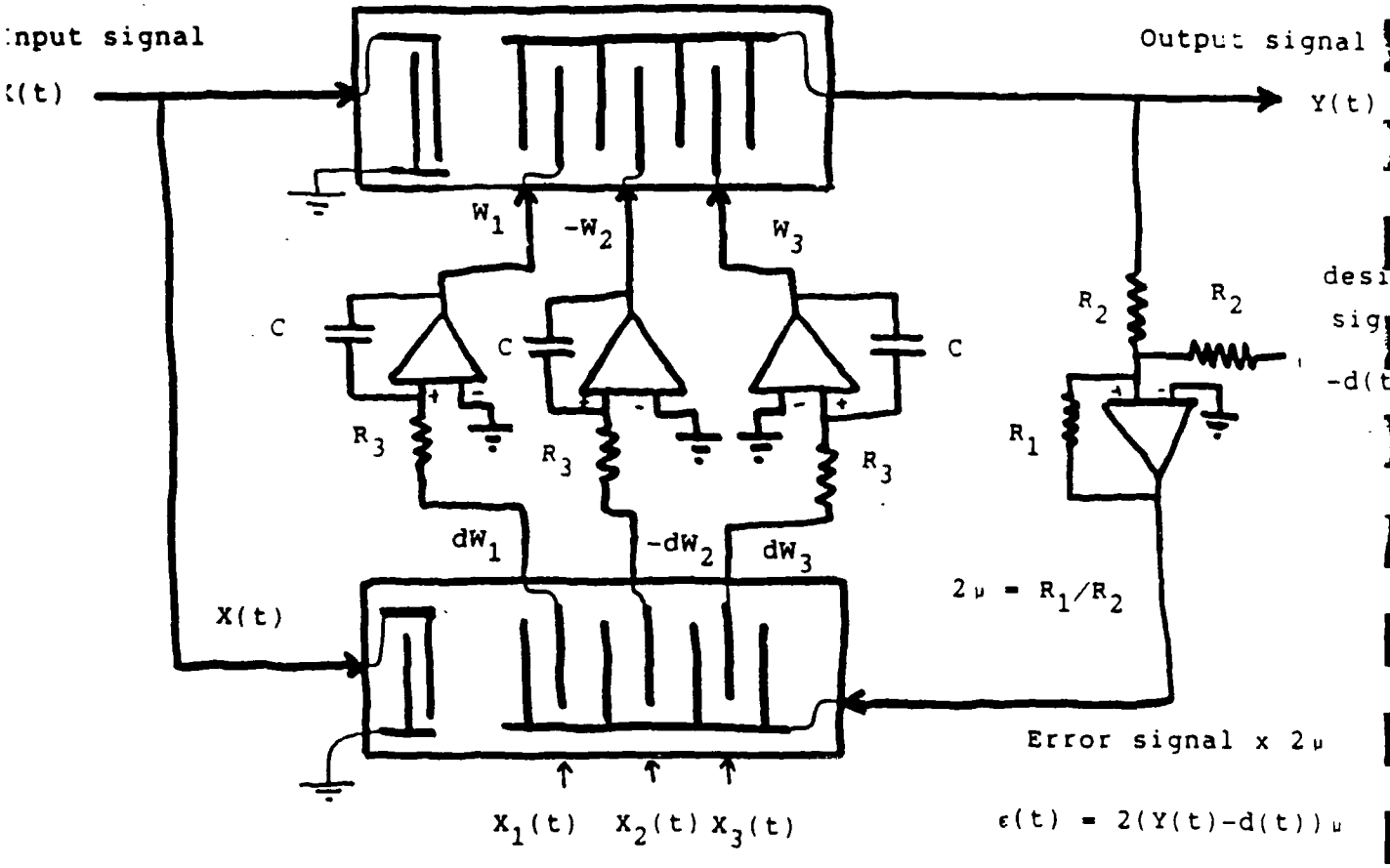

$$dW_i/dt = 2\mu\varepsilon(t)X_i(t)$$

2.2.3.3 Some performances

In this section, some expected or measured performances are scanned. This is brief for several reasons: first of all, these components are still in their childhood, and thus few measurements are available. Then, these figures depend completely on the materials; we have used PMN (lead magnesium niobate) and PLZT (lead lanthanum zirconate titanate) for the first experiments; PLZT, although less coupled than PMN, was the most satisfactory. However, there are still some undesirable effects that can be cancelled by using other materials; some people in Pennstate University are locking for that and it seems completely possible. Also, a good design of the component, by a S.A.W. engineer, would increase greatly the overall performances of the component. Nevertheless, here are some typical figures for these devices. Nowadays, the center frequency on these materials is limited to a few tens of MHz; this is not due to acoustic losses, but rather diffraction because of the grain size in these ceramics; a hot-pressed ceramic, or better, a single crystal grown from these materials should allow a big increase in the center frequency. It seems possible to get to that point since PMN crystal was grown in Japan; the question is how difficult it was and what could be the price. However, in the remainder, an operating frequency higher than 100 MHz will not be considered. The electro-mechanical coupling is rather low, about twice the quartz's one. The induced piezoelectric coefficients can be large but the dielectric constant is also (several thousands); then, the relative bandwidth has to be kept rather small, anyhow less than 50 percent. So, bandwidths larger than 30-50 MHz will not be considered.

Because of the few available measurements, we assumed that the general characteristics of the S.A.W. devices are still true for P.S.A.W. components. That is an insertion loss varying between -10 and -30 dB, an equivalent accuracy (for the signal) of 8 bits and a signal dynamic range of 12-15 bits. Again, the temperature dependance cannot be predicted but the different S.A.W. compensation techniques should still be adequate. For these programmable components have also to be considered the accuracy and dynamic range setting of the weights for a filter, or the on/off ratio. Assuming a good stability of the electrostrictive coefficients, the accuracy of the tap settings should be determined by the external electronics and the cross-talk problem. However, the material being always unperfect, an 8 bit accuracy should again be considered, although it could possibly be better (same cause, same effects). We already mentioned the dynamic range of 8 bits, possibly better (or about 50 dB on/off ratio) and the fast programming speed. Caution must be observed on these components because of their youth; a specific device will have to go through all qualification steps before being readily implemented in a promising application. However, despite the programming features, this should be very similar to a conventional S.A.W. component.

?.3 S.A.W. components and low-frequency signals

We have just seen that S.A.W. components, whether they are programmable or not, work with center frequencies around several tens of Mhz, even hundreds. In the introduction was recalled that a sonar usually operates with a center frequency of some kHz, sometimes less (a few hundred Hertz) or more (a few tens of kHz). The question is then, how to use S.A.W. components for sonar with that big inherent difference? We will adress it in the following to see the different possibilities, advantages and drawbacks. There are two basic ways of achieving this kind of frequency shifting or multiplication: the carrier modulation technique and the time compression technique [13,24,25]. The first one is very well known since it is used in all the radar or communication systems for the transmission of baseband signals. It usually involves an analog mixer (or multiplier) and the output is the product of the input signal with the output of an oscillator, adjusted on the desired center frequency. The technique is very simple, needs very little hardware but it presents in the sonar case two major drawbacks: first, in most cases, the duration of the sonar signal for subsequent analysis is far too long for any S.A.W. devices; several tens of milliseconds to a few seconds can be considered as typical, but we mentioned earlier that a typical S.A.W. device has a delay of 1 to 20 microseconds. The carrier modulation technique, if it increases the frequency range of the signal, does not change at all its duration. Second, analog mixers are usually components with a limited dynamic range and accuracy; then, solutions without such devices, or with as little as possible will be appreciated eventhough the S.A.W. devices themselves bring the same limitations.

The other technique, time compression, requires the use of some kinds of memories; the length of these depends on the compression ratio. The basic idea consists in sampling the signal(s) (if not already done), storing it into memories, and reading it out of the memories at a faster rate than it was written; the output/input ratio is the time compression factor. This processing shrinks the time scale while it expands the bandwidth of the signal (it is easily proven by basic Fourier considerations). Thus, a signal with a duration T and spanning from F1 to F2 in frequency will then be output as a signal with a duration T/k, spanning from kF1 to kF2, where k is the compression factor. The inherent advantage to this technique is the multiplexing capability which is now available; if a signal of duration T can be processed on a S.A.W. component in T/k, it means that k signals can go through the same component by easy multiplexing. Figure 14 shows an example of such an implementation for a sonar case; note that the signals need to be converted into analog signals before going through the component, and digitized again after; notice also that in figure 14, the two techniques, carrier modulation and time compression, are shown; this is possible but not compulsory. For a sonar application with S.A.W. components, the compression factor lies between several hundreds to several thousands; this leads to very efficient and hardware-saving implementation for some typical functions (such as filtering or spectral analysis) when the number of low-frequency channels is large enough; typically, a few hundreds is large enough. An important remark concerning this aspect is that almost only digital memories can be used; that brings up several facts : first, several components are added, especially D/A and A/D converters and maybe the

memories; in the sonar case, digital memories are already required for real-time signal processing and even the fast read-out does not bring more trouble than any other real-time solution ; it can still be troublesome and some kinds of interleaved memories may be required. On another hand, the D/A and A/D just preceding and following the S.A.W. device are added; they can induce some problem for the speed, especially the A/D converters, always slower than their counterparts [23]. Also, the coding and conversions bring some errors, or inaccuracies or noises; thus, this will limit the number of times such conversions may occur in order to stay within tolerances [23,26]. In any case, the less there is D/A and A/D conversions, the better it is. However, remember that the signals are first analog and that in the front end of the sonar, the accuracy is not such a problem that the use of S.A.W. devices is not possible.

A very interesting case to notice concerning these techniques is the beamforming operation; we noticed earlier that the size of the memories is a function of the required compression factor; the size is usually referred to as the time length on one signal; however, for beamforming purpose, all the signals are digitized at the same time from the array and they could be processed as a single signal, i.e. the acoustic wave running into the antenna, and then, at each sampling time, all the data are available. For instance, a Fourier transform can be used for a narrowband beamforming (see following chapters for details); in this case, the N data from the N hydrophones of an array are considered as the N samples of a signal that will go through a N points FT; this operation is repeated with a rate consistent with Nyquist criterion [18]. The S.A.W. component is a very

fruitful alternative to the digital FFT, but it needs some sort of time compression; here, it is easily achieved through the use of a sample-and-hold circuit and a multiplexer. The general scheme is indicated in figure 15; note that there is no need for any kind of conversion, just the sampling which is a very easy operation (a lot faster than any A/D conversion); this means also that the beamforming can be directly performed on the analog samples; the beams are then digitized at the output, but no extra conversion is required if you compare that to the digital implementation. Furthermore, this solution has several other advantages than just the computing speed (see following chapters for details).

Conclusively, there is a possibility for matching the characteristics of the S.A.W. components and the requirements of a sonar; we saw that there were some drawbacks to this, but we will now investigate in the forthcoming chapters the different advantages that they present. First, the general sonar chains will be studied to find out where the S.A.W. devices may fit and then several promising applications will be pointed out.

Figure 14: Time compression for sonar

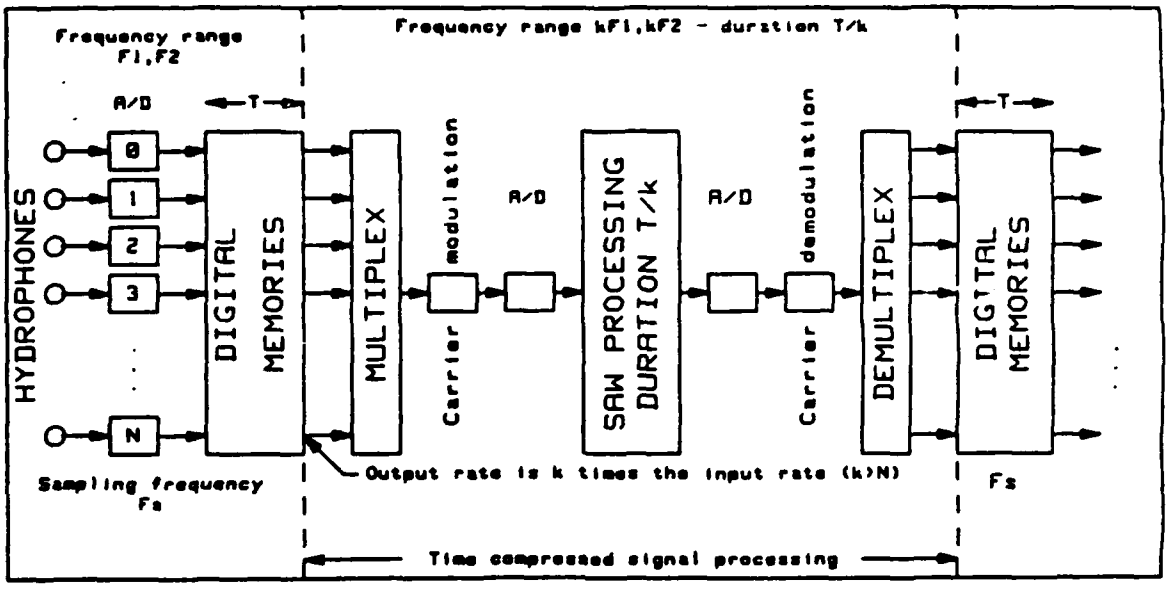

Figure 15: Time compression for beamformer

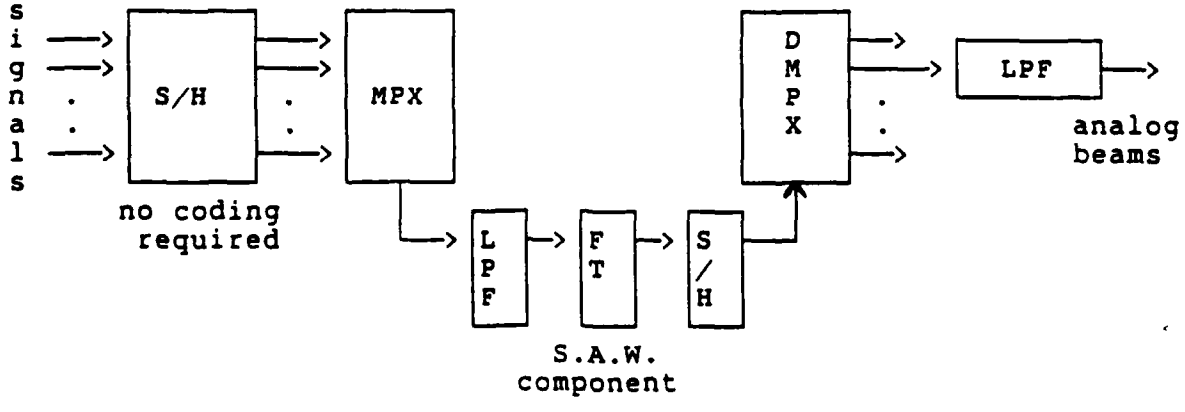

Entirely analog process - The beams are then digitized

CHAPTER 3

Sonar signal processing and S.A.W. components

3.1 Overview of some typical sonar systems:

3.1.1 Background [1,18,27]

In this chapter, we analyze different typical sonar chains in order to find out where S.A.W. components could be adequate, especially for hardware saving. A sonar system is composed of several subsystems, depending on the kind of vessel that is using it; it is certainly different for a missile-launcher submarine and for a helicopter or for a torpedo. For instance, a submarine sonar would comprise a passive search and track sonar, a localization one, a classification equipment, an active sonar for some specific situation, an intercept receiver (to detect other vessels that are using their active sonar); it would also have a depth sounder, a communication equipment, a torpedo alert sonar,etc.. Also, some of these equipments, such as the search and track one, have several antennae working at different frequencies in order to maximise the threat detection probabilities. However, it is possible to classify roughly these sonar subsystems in two groups, the passive and the active ones. As it isusually the case for such classification, there are some equipments that, even though being from one of these two catego-

ries, present some important differences with the main categories; thus, we take them differently into account. In the following sections, some passive and active signal processing chains are investigated in order to study some specific blocks that are relevant of S.A.W. processing. It is to be noted that the actual trend is to emphasize a lot the passive detecting, localizing and classifying sonar; this is by much the most attractive since modern electronics allow the processing of larger and larger antennae, thus theoretically increasing the performances of this sonar; in addition to that, this sonar provides a way to "see without being seen". Then, a large part of the research concerns this kind of equipment and their results drive not only the way to build a modern passive sonar, but also any kind of sonar. This is, in a way, a mistake since what is true for a big and powerful system is not always optimum for a smaller one; hence, there is a need to think about some small equipment to find some efficient implementations. This would lead to low cost sonars that should have a market, in advanced or regular navies from the whole world; trying to use results from a large system studies to small system will never create a competitive equipment; however, it does not mean that large systems have not to be investigated. As a matter of fact, these large systems determine what are the actual possibilities of a modern system, whatever size it could be, and then, they set the limits for each possible sonar to be built.

In the remainder of this chapter, we will deliberately exclude the modern large sonar systems. The motivations are that the higher the goals are, the greater the accuracy that you need on your computations is and this outstands the usual features of analog devices. However, this is only partially true because

the signal is always analog on the antenna; hence, the very front end of a sonar does not require high performance hardware, contrariwise to the popular idea that if 32 bits are required at one level for specific computations, they are also required in all the up-stream calculations! On another hand, the first assertion is still true because large sonar systems become very complicated; then, the hardware usually represents several highly integrated electronics cabinets. The cost of these equipments would be consistent with what modern navies can afford only if they were highly standardized. Modern equipment will be built with high performances standard signal processor to lower maintenance costs. Finally, analog (and among them S.A.W.) components have little chance to exist within such signal processors. Nevertheless, as we will see, they can be excellent outsiders for low-priced equipment where hardware saving is extremely important and where these high technology processors would resemble a hammer used to kill a mosquito!

3.1.2 Passive sonar case

A passive sonar is an equipment whose purpose is to detect, localize and sometimes classify a target by its radiated noise in the ocean. It involves some kind of array of hydrophones followed by an adequate signal processing. Underwater sounds, for this kind of sonar, can be split into two categories: narrowband very low frequency signals (spectral lines, below 1 kHz usually) and large band low and medium frequency signals (between 1 and 10 kHz). The processing varies according to what kind is dominant but it is always similar to the one shown in figure 10, at least for

the detection part; some parameters (such as frequency resolution) are variable. Also, the order in which the operations are performed may vary according to the signal's type but also to some other specifications. More details about the different blocks of figure 16 are given in [18].

We will only address the detection and rough-localization problem since accurate localization and classification (in a sense of "naming" the target) are more complicated problems in which the algorithms need a better accuracy. As a matter of fact, modern large passive sonars must be distinguished from the others because their goals for fine localization and classification are really high. Therefore, even digital computations are pushed to their limits and extremely fast digital signal processors with 32 bits floating point words are required. In order to get fine localization for instance, the processor will deal with the phase of the signals, trying to find out changes in the order of a few degrees; thus, it is already in the accuracy limits of any analog device. Indeed, it is truly a problem for the design of the necessarily analog preamplifiers and it is compulsory to convert the data as soon as possible into a numerical format. Depending on the system, some of the antennae are dedicated to localization or detection or are multipurpose; this determines where S.A.W. component could fit but it will always concern a detection branch then, figure 16 is the one to consider. In this figure, the array can have any geometry although some are more common (e.g., linear planar, circular or spherical) due to localization needs, hardware considerations (towed array for instance) or computing simplifications.

Figure 16: Typical passive sonar signal processing

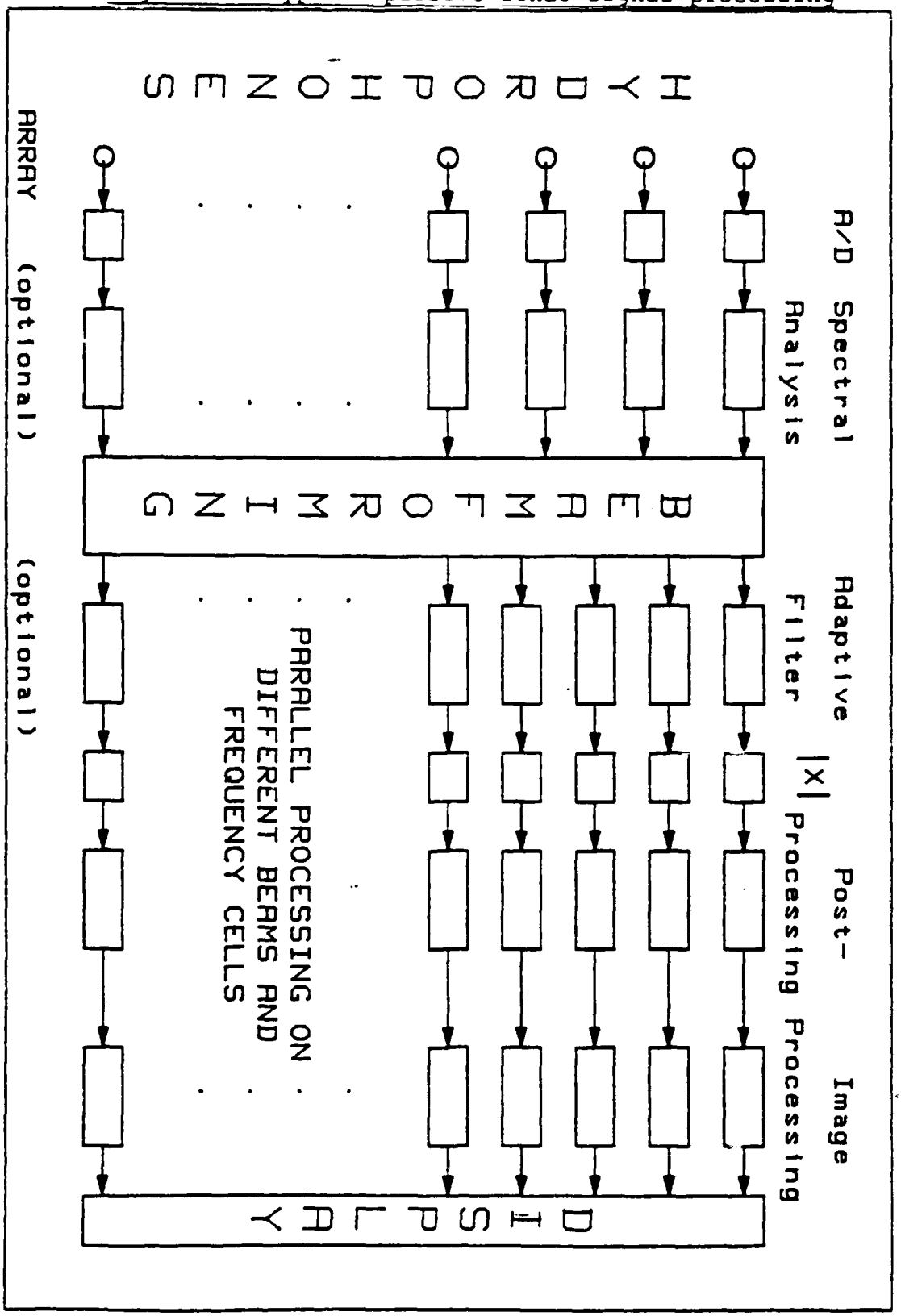

The spectral analysis shown in Fig.16 is optional and dcpends on the signal features (either spectral lines or broadband noise). Nevertheless it can be useful to consider broadband noise as a set of spectral lines. This is wrong in theory, unless the number of spectral lines is infinite, but in practice, this can be considered as true to some extent. With this assumption, one can use special narrow-band techniques (as phase-shift beamforming) for broadband signals, although usually, one then has to recombine the different frequency bins in order to reconstruct the broadband feature.

From Fig.16, it seems that some of these functional blocks, which are mainly linear signal processing operations, can be suitable for SAW use. Particularly, it was already pointed out that Fourier transforms are easily and efficiently implemented on a S.A.W. component; therefore, it can be fruitful to use this component for all the FT involved; this concerns mainly the spectral analysis, but as it was remarked in [18] and is detailed further, the beamforming operation may take the form of a FT for specific array geometry. Thus a FT operator could perform both spectral analysis and beamforming for certain kind of sonar. Also, adaptive filters are often from the transversal type [2]; this is especially true for narrowband interference suppression (e.g., self-generated noise) or any kind of jamming or temporal disturbance; it is less true for spatial filtering where, usually, a combined space-time approach is preferred. Anyhow, there are opportunities here for adaptive transversal filters, especially long and efficient ones; the fact that recursive filters, and mainly ladder structures, are pushed ahead is mainly due to their better digital efficiency: they required less operations to achieve a

specific shape but they are less stable and harder to design. On the end, the image processing block seems promising; again, the functions involved here are mainly transversal filters; moreover, the signal becomes eventually analog for the display and the rate of the display is consistent with the frequency of S.A.W. component. Therefore, it seems interesting to consider their use for this operation. Nevertheless, some practical system considerations need also to be asserted. In order to avoid functional block duplications, some operations shown on figure 16 are shared by the detection, localization and classification chains (as beamforming or spectral analysis). Consequently, they are designed according to the highest quality required by any of these chains. Also, the purpose of the sonar (such as for submarine, helicopter or sonobuoy) has to be considered because it leads to different implementation concepts. For instance, the available volume of electronics dedicated to the sonar, the allowable size of the antennae, and the quantity of units to be built are vastly different for the various purposes of sonars and thus need to be considered. Finally, in some cases (such as dipping or towed sonar), it can be very fruitful to have some electronics in the water-body rather than in the carrier and this requires low-power and compact hardware. These last requirements fit rather well with SAW technology. There are many other practical considerations which depend on the specific case, but they will not be discussed here. In brief, there are opportunities for S.A.W. devices in passive sonars, but they need to be studied on a case by case basis; it is not possible to imagine a standard signal processor having a S.A.W. operator.

3.1.3 Active sonar case

In the active case, the sonar transmits a specific acoustic pulse and then waits for any kind of echo, trying then to interpret it in terms of targets. This is therefore exactly similar to a radar system; again, as we noticed earlier, the differences come from the speed of sound in the water; so, the sonar usually radiates with an omnidirectional pattern and receives the echoes on different simultaneous beams; the joint patterns of these beams cover the whole area illuminated by the transmitter. Thus, again, an active sonar requires a beamformer, and some kind of spectral analysis (for signal reception enhancement). From that point of view, matched filters are used each time a frequency modulated signal is transmitted. Figure 17 shows a typical signal processing chain for an active sonar. It has to be noted that generally, active sonars involve higher frequencies than passive ones; it is due to several factors, but mainly because of the large difficulties encountered to design a powerful low-frequency transducer. Hence, typical search and track sonars use frequencies around 10 kHz while some specific sonar like torpedo's are in the thirties and some mine-sweepers operate at a few hundred kiloHertz. Also, these sonars are characterized by a small relative bandwidth; therefore, narrowband techniques can be readily performed and they fit rather well with S.A.W. components [18], especially for beamforming.

Figure 17: Typical active sonar signal processing

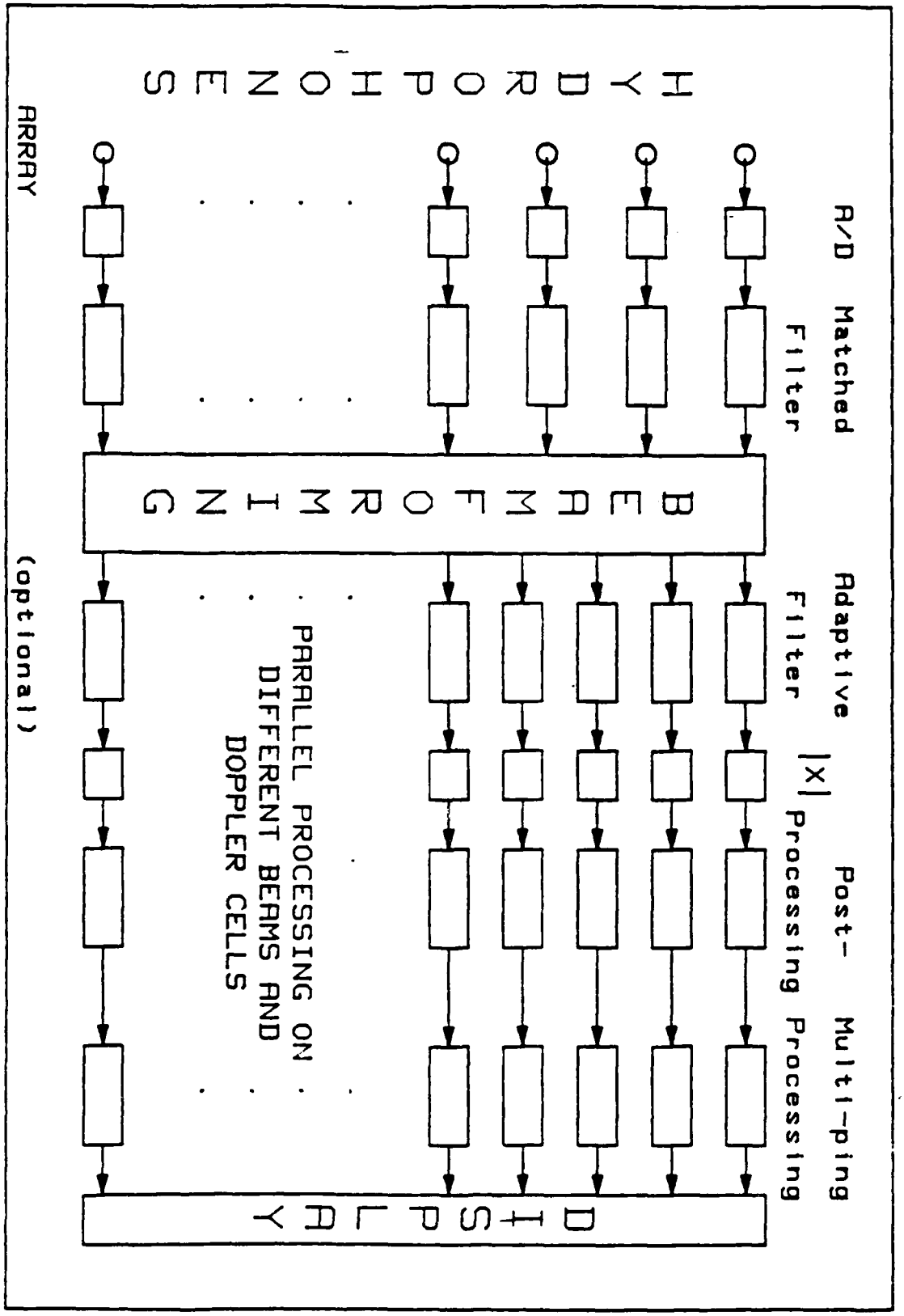

The passive case signal processing blocks are suitable for a S.A.W. component. In addition to those, the matched filter involves only a transversal filter, whose impulse response matches the transmitted signal features; therefore, it is also suitable for S.A.W. devices. The programmability is fruitful since it hardens the sonar (in terms of countermeasures) to change randomly the characteristics of the signal, which implies a change in the matched filter. Also, the kind of image processing is slightly different, involving the processing of several consecutive pulses, but needs again some kinds of transversal filter. Furthermore, active sonar systems are generally smaller than their passive homologues, both on the performances and hardware standpoints; it is unlikely to find, in an active sonar, a localization chain outstanding completely the capabilities of analog devices. Thus, even with fine measurements downstream, the front end of the sonar can accomodate the limited accuracy of S.A.W. devices. On the other hand, dynamic range can be greater than what is offered by S.A.W. devices. Moreover, several active systems use antennae that are towed or dipped or put in a torpedo; then, it is very fruitful to put some electronics in the water body. This implies that the electronics should be very compact, consumming little power and yet, computationally efficient. On another hand, this electronic needs to withstand water environment and high pressure; we actually have no data on this problem; however, in some cases, the electronics inside is still in air with ordinary pressure, thus giving no trouble to the hardware.

Finally, active sonar systems are certainly one of the most promising place for S.A.W. component; however, these systems usually involve less hydrophone

channels than passive ones and, thus, the computational load is less important. Indeed, these sonars are also more concerned about volume, cost and power requirement reduction, because they are installed on less important vessels than submarine. Moreover, the assumption that passive sonars are going to overcome the active ones is only partially true; in many instances, active sonars give a better detection, for a given hardware, and the indiscretion is not that important (helicopter, surface ships, etc.). Also, a great advantage is the intrinsic measure of range, which is only available to sophisticated passive sonars.

3.1.4 Other equipments

In this section are investigated other equipments related to the main sonar system; by these, we mean other sonar type equipments that are processing acoustic waves but from a different point of view than the main passive or active sonars. For instance, intercept receiver, sea-bottom imager, decoy system, underwater telephone, mine avoidance sonar are among this list. Such sonars are characterized by a simple, if not crude, signal processing; sometimes low-power consumption requirement, a small available volume and very often a weak priority versus the main system are also typical; this is not always true though, and for instance, the intercept receiver [18] or a decoy subsystem is of vital importance when the considered detected target is a torpedo. In some cases, the kinds of signals (active transmission) being unknown and very short, it seems hard to perform any kind of sophisticated processing eventhough the best possible performance is required. Basically, for an intercept

receiver, the signal processing mainly involves a detection process; since good performances are expected, several systems have to work simultaneously, therefore leading to a lot of hardware; figure 18 shows such processing. Notice also as it was mentioned in [18] that an intercept receiver usually deals with signals having a frequency within the band 10 kHz to 100 kHz; then, the computational load is quickly important. Moreover, because of this frequency span, this kind of equipment is usually not implemented with standard signal processor; therefore, it would fit to S.A.W. signal processing for any adequate operation such as beamforming (although not likely to happen), spectral analysis (very important) and even for some cases, adaptive filters to avoid multipath problems, and then give better performances.

For a decoy subsystem, the problem is different and still rather new in terms of true sonar; the idea is to cheat a torpedo that started a homing against a submarine or surface ship. One way to do that is to simulate the echoes of the vessel but at the wrong location. A method to perform such operation is to receive the signal transmitted by the torpedo, try to model it and once it is done, send it back to the torpedo with wrong delays. Unfortunately, torpedoes have usually a safeguard feature known as proximity detector; it explodes only if it has indication that a large chunk of metal is around, for instance; otherwise, it starts a new homing. Therefore, it could be promising to do this processing from a released or towed vessel, homing the torpedo to that location and making the torpedo explode by exploding the decoy itself once the target is close enough. This adventurous idea would require a hardware capable of good signal processing (adaptive modeling, which can be

Figure 18: Typical intercept receiver signal processing

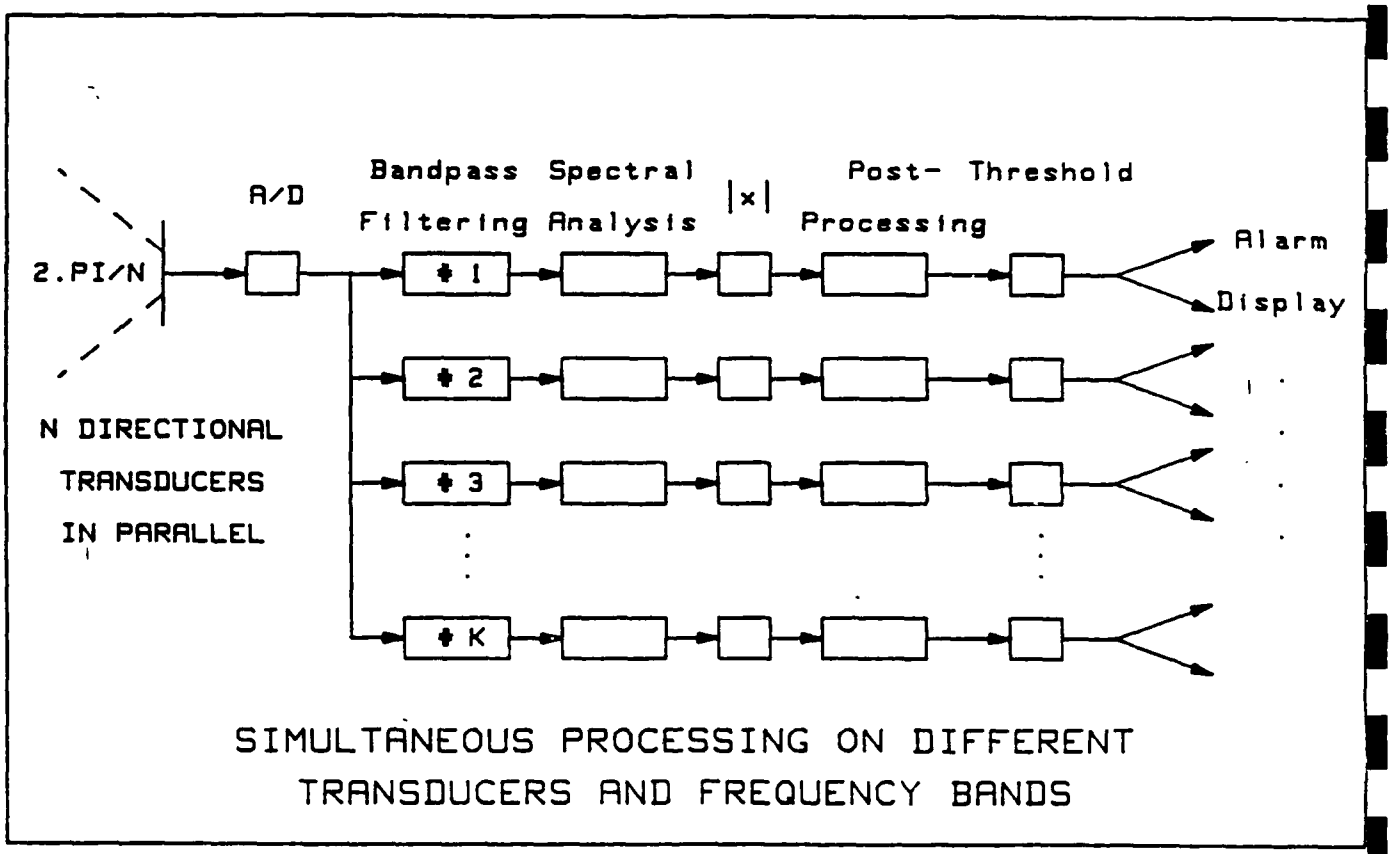

realized with a transversal adaptive filter [2]) and yet needing a small volume and power consumption; this can fit rather well with the S.A.W. technology.

A sea-bottom imager is an equipment whose goal is to picture as closely as possible the ocean bottom; this is either performed for mapping or just for knowing whether a submarine can bottom. This involves usually some kind of scan sonar where a towed water body is mapping the floor, in two directions and the map is reconstructed using synthesis methods (see figure 19). Because of the duration of the process, it is not possible to do the mapping using S.A.W. components for interpolation or reconstruction. On another hand, the prime processing consists in a two-dimensional beamforming which can be achieved using two consecutive Fourier transforms (these equipments are working with narrowband type signals) [13]. Here too, a powerful, yet very compact hardware is required. Also, as it was described for the active sonar case, a matched filter is used, which can be performed via a transversal S.A.W. device.

Figure 19: Sea bottom imaging sonar

Finally, several sonar related equipments need some high speed signal processing that fits with S.A.W. techniques; they involve beamforming with narrowband signals, matched filters, adaptive filters and spectral analysis. The nice point with such equipments is that they are not built using standard processors, they have to be compact, energy saving and cheap; they also already deal with hybrid technology. Therefore, it seems very promising to use S.A.W. devices since they will provide fast signal processing with low power consumption, little volume, and may allow new functions to be performed.

3.2 some promising signal processing applications for S.A.W.

In this section, we will go further into the details of some of the promising signal processing blocks pointed out previously; these blocks are the Fourier transform technique for narrowband beamforming; the spectral analysis; the adaptive filtering and the image processing. It was noticed earlier that these functions were present in several systems where S.A.W. devices are conceivable and that they fitted rather well with S.A.W. technology. Then, in this part, will be described the actual way of implementing these functions with S.A.W. components, the different advantages and drawbacks.

3.2.1 Narrowband beamformer

In reference [18] was described what was the beamforming operation and what were the different algorithms; it was recalled than in the case of a linear array, with uniform spacing and in the case of a narrowband signal (or expected as such), the beamforming equation then become a spatial Fourier transform equation; on figure 19 are recalled the geometry and the consistent equation. The whole advantage of the technique was the possibility to use the FFT algorithm to implement efficiently the operation. Furthermore, the narrowband restriction was easily got around by splitting any broadband signal into a set of narrowband ones by using a temporal FT. This process is very advantageous this way; it was also pointed out that these operations could be carried

using a S.A.W. Fourier transformer with the benefit of the speed and volume. In addition to that were shown some very promising new capabilities due to the conversions between the analog and digital domains.

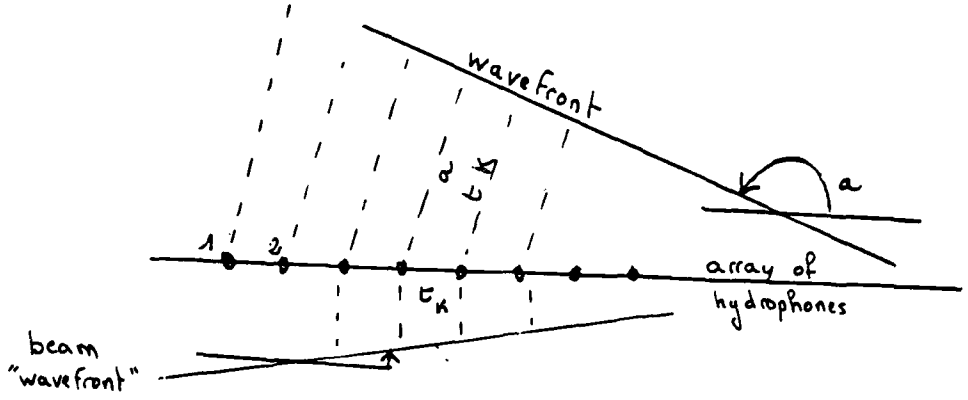

$$V_k = \Sigma_i(a_i \cdot x_i(t - t_k)) = \Sigma_i(a_i \cdot x_i(t) \cdot \exp(-j \cdot 2 \cdot \pi(t_k - t_k^a) \cdot f)) \qquad (2)$$

Figure 19: Line array geometry and beamforming

Let us do a little computation in order to prove the benefit of a S.A.W. approach to this problem: imagine a linear array with a hundred hydrophones, equispaced and a sonar using this array below 6 kHz; a typical signal processing would involve a temporal FFT, to split the signal into spectral lines, and a spatial FFT for the beamforming operation in each frequency cell. Typical figures for the number of points would be 1024 for the temporal FFT and 128 for the spatial one in order to get full coverage; on a digital computer, this straightforward signal processing amounts roughly to 100 Mops, which represents already a very powerful signal processor (we are talking of 100 Mops data flow rate and not theoretical figures deduced from the number of adders or multipliers). Taking commercially available array processors like the Floating Point

System 30, would require the use of four of them simultaneously to absorb the task. A S.A.W. Fourier transformer, designed for the task (i.e. BT=1024 and programmability to perform also the 128 or two non-programmable), would easily perform the temporal and spatial FT in real-time within a piece of crystal measuring 1 by 5 cm (features of the component: frequency 51.2 to 102.4 MHz, duration 20 microseconds). The component with its interfacing electronics would fit on a 1/2ATR board as the digital solution would require several cabinets. The power consumption is also not comparable. It is now obvious why such implementation is promising because of the hardware saving. Notice also that a delay sum beamforming alternative is possible, thus avoiding the need for any Fourier transform; however, a quick calculation gives a computation rate of 460 Mops, far more than the FT technique!

In addition to that, it was remarked in [18] and shown in [28] that the Fourier transform technique for beamforming can be used for less specific geometries like circular or planar or cylindrical (considering them as stack of linear or circular ones). Also, it was proven that this technique employed with S.A.W. components can bring new features as the ability to process non uniformly spaced array or to do automatically, at no cost, any required interpolation for aligning the beams for whatever frequency; this is intensive to do with digital methods.

Furthermore, a new very promising possibility was discovered concerning the use of this technique for linear array; usually, the implementation looks like the one shown in figure 20(a); however, because the involved operations are linear, the scheme in figure

20(b) is also right. Hardware considerations generally dictate one or the other architecture; in the following, we show that the second one, used with S.A.W. components, can be very rewarding.

If the second scheme, figure 20(b), is considered for sonar, it turns out that the signals coming into the Fourier transformer are analog by nature; it was pointed out in chapter 2.3 that for array processing (e.g. beamforming), the time-compression scheme was not required since all the samples were available simultaneously. Therefore, only a multiplexer was required, which leads to a solution without encoding of the samples. This solution is shown in figure 21; the signals sampled on the array are routed on an analog multiplexer which reconstructs a signal similar to the incoming acoustic wave. A low-pass filter is needed to compensate the effect of the spatial (and not temporal) sampling. Again, we find the advantage of this reconstruction in the fact that non uniform sampling are tolerated, because of this low-pass filter, which will "create" the missing samples correctly, as long as the spatial Nyquist criterion is respected, in average. Then the FT is performed efficiently on the S.A.W. component and the output now is a multiplexed version of the beams outputs; this FT has to be performed according to the temporal Nyquist rate and then, every Ts, the output from the S.A.W. device represents the beams covering the whole space, multiplexed temporally. A demultiplexer would give the beams outputs, sampled but not encoded; it is now easy to encode them, and to perform a narrowband filtering (FT or else) to achieve the whole function. Notice, that depending on the length of the link between the antenna and the main sonar, the beams could be transmitted in an analog way,

Figure 20: Two different architectures for processing broadband signals with a FT beamformer

(a)

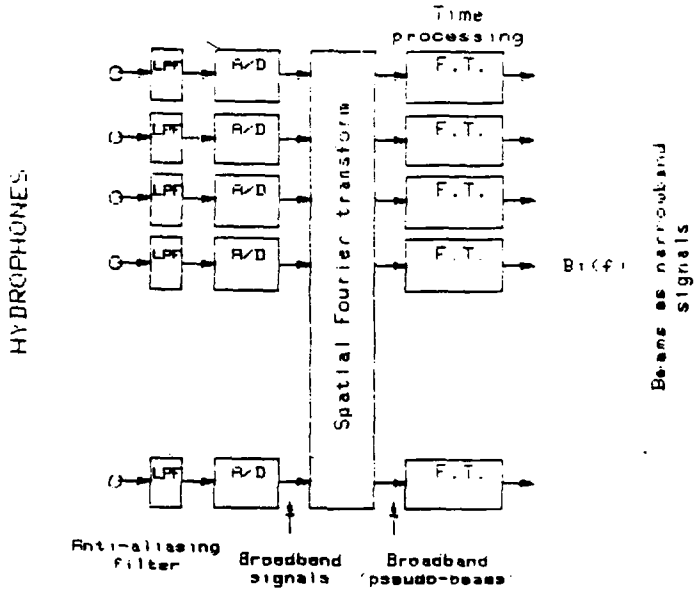

(b)

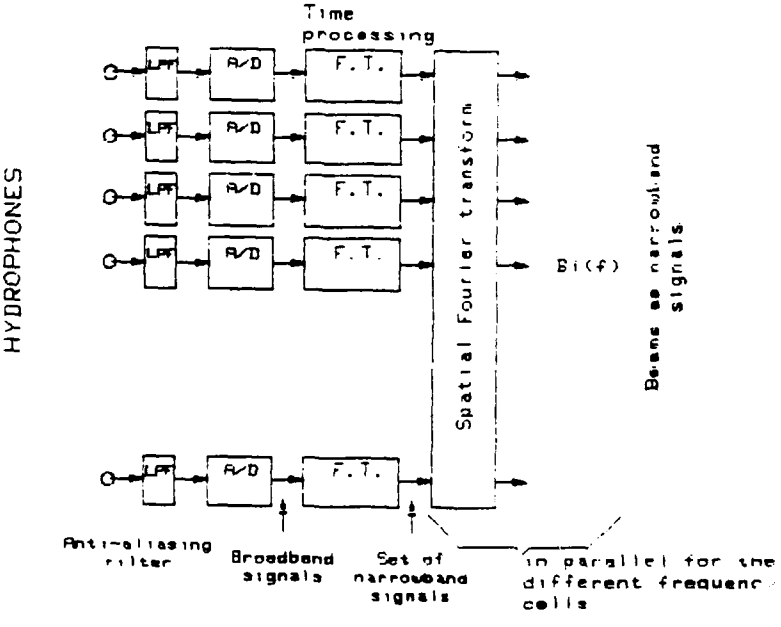

because they are already multiplexed. Anyhow, once the signal is digitized, regular signal processing may follow with the advantage of the beamforming being done at little cost. As a matter of fact, the whole process up to the digitizing could be performed in the antenna itself because multiplexing electronics can already be put into it and the S.A.W. component can be easily put because of its small size. Figure 22 pictures such a case for a towed linear array.

In the example previously discussed, the beamforming has to be performed on 100 hydrophones, at a rate being one FT each 1/18000 second or 18000 FT per second; the time for such a FT was described earlier as 20 microseconds; we then have a safe guard ratio of roughly 3.

3.2.2 Spectral analysis

We mentioned previously that spectral analysis was very common in sonar and that it usually was performed by Fourier transform. Some new methods involve ARMA filtering or eigenvalues analysis or different kinds of models; however, they will not be taken into account for two reasons: first, they are still experimental models, that are supposed to give better results with unstationary phenomena; yet, it is not proven that they will give better results on sonar and it is highly unlikely that they will outperform FT everywhere. Second, they cannot be implemented using S.A.W. devices; therefore, we will consider the spectral analysis in these signal processing chains where FT is adequate; this represents now 99 percent of the sonars, excepting may be the large modern passive

Figure 21: FT analog beamformer at the hydrophone array output

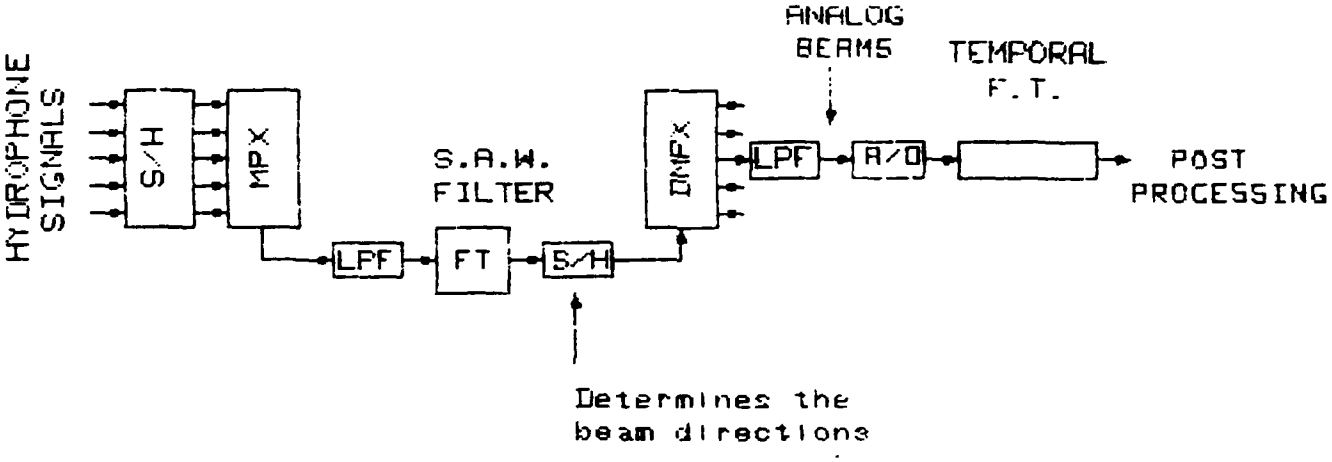

Figure 22: Architecture of the beamforming system for a linear towed array; (a) with digital multiplexed link; (b) with analog multiplexed link

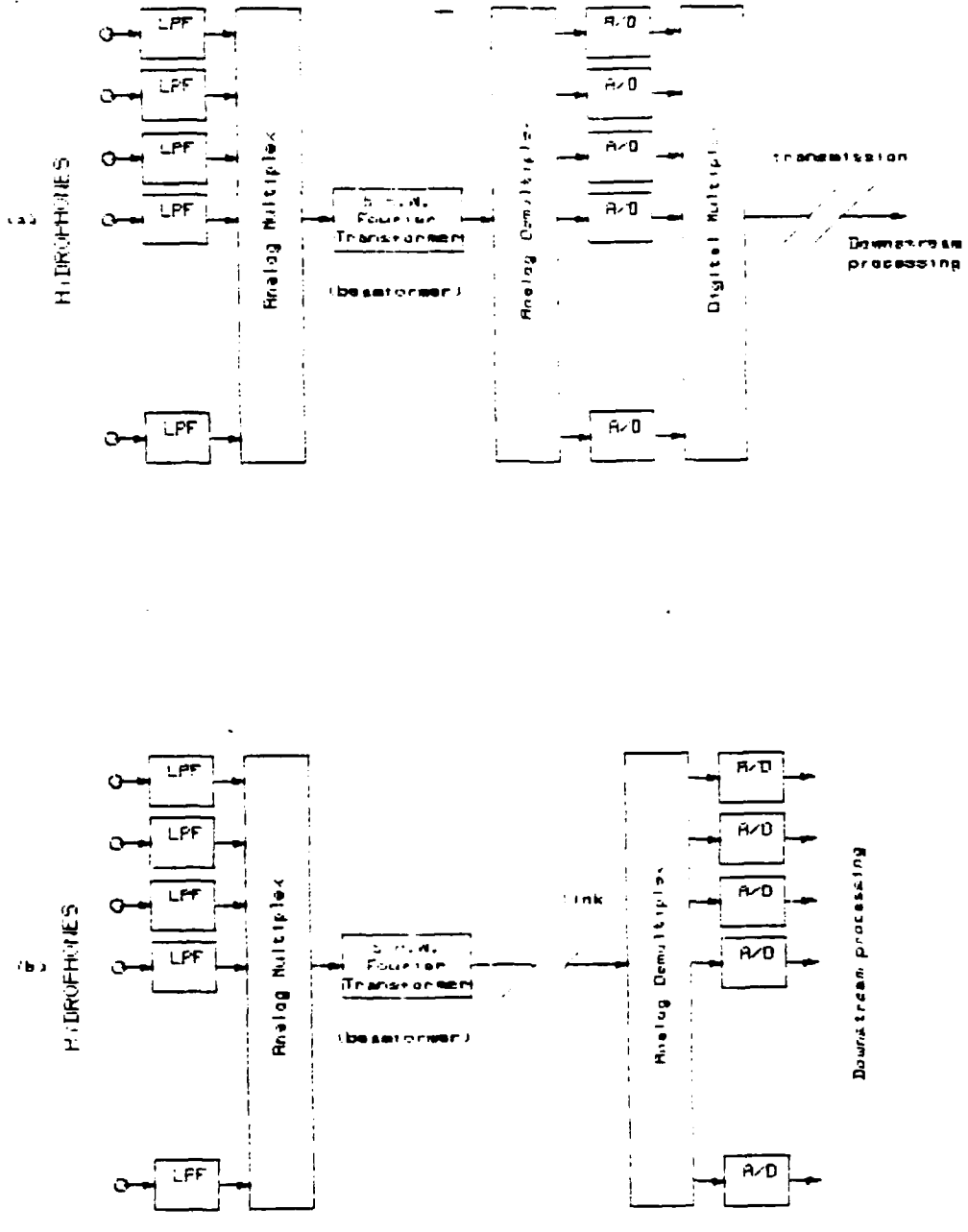

sonar systems.

We already discussed in section 2.2 the different ways of achieving time-compression and/or frequency shifting; a spectral analysis performed via a S.A.W. device will then look like the scheme shown in figure 23; the signal coming from a digital memory is time-compressed, then converted and filtered before going through the Fourier transformer. The basic advantage of this method, as it was already pointed out is the efficiency of the calculations; even with a modest S.A.W. device working in the tens of MHz, the trick is that it performs the FT at this frequency, while digital computers may give you this rate only for elementary operations. Because of the compression factor, typically several hundreds to thousands, a few hundreds of signals can be multiplexed on the same component. Also very promising is the analog nature of the output; it represents continuously the spectrum of the input signal; then by adjusting the A/D conversion process, it is very easy to select some specific frequencies; therefore, sonobuoys could be imagined having a threat spectrum detection feature: just after the spectrum analysis, an A/D conversion adjusted on the spectral lines of the threatening vessel (if known) will give easily access to a yes or no detection; the compactness of a S.A.W. spectrum analyzer, plus the low-power consumption make it a good candidate for such job on a sonobuoy. Some tracking of a specific spectral line can also be readily available without the need for any interpolation, eventhough the spectral line frequency may drift. Adaptive cancellation of some spectral line is also available by a tunable time gater, before the conversion to the digital domain; as a matter of fact, the signal can be converted back to the time domain with an inverse FT, also done with the

Figure 23: Spectral analysis with a S.A.W. device, for sonar applications

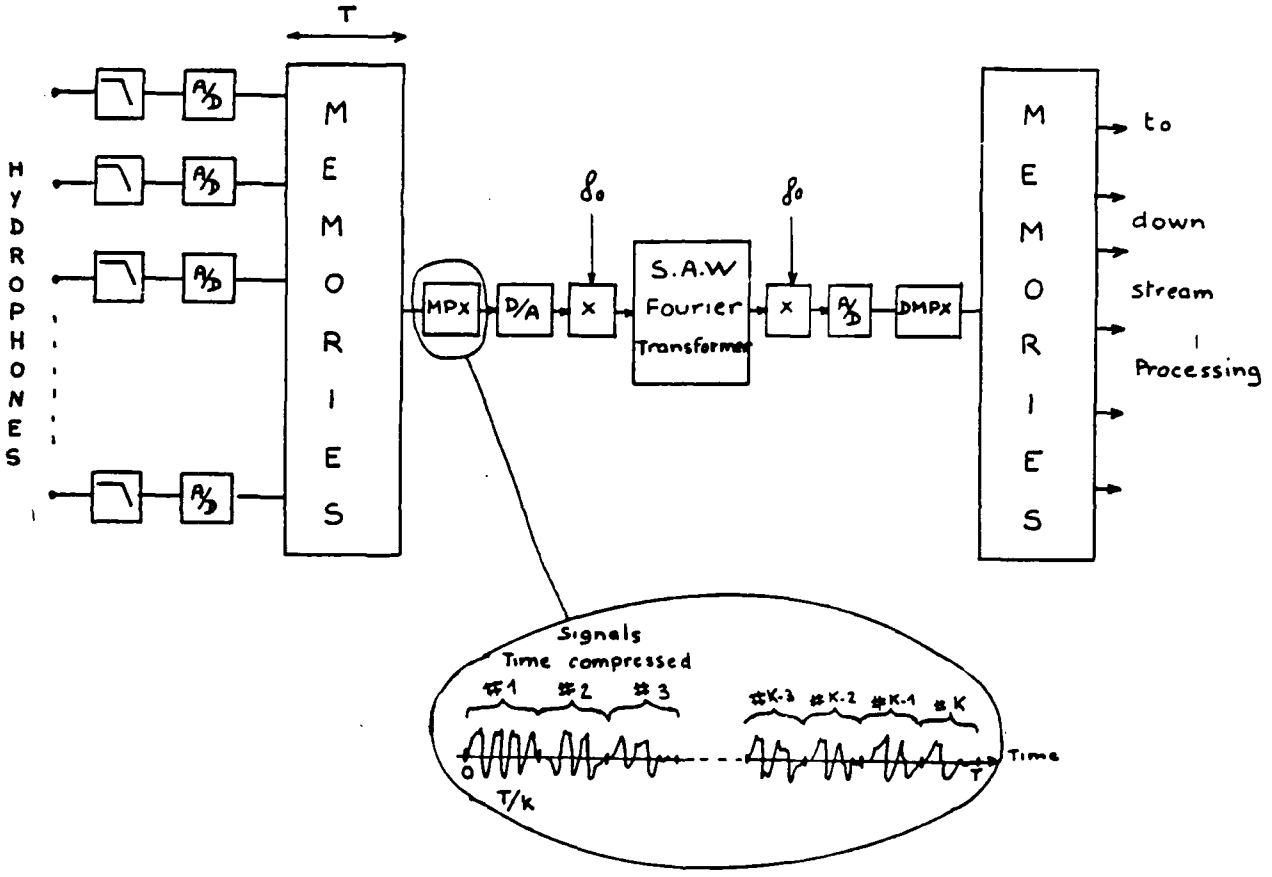

S.A.W. component, after the time gating; this is known as frequency excision and is used in communications [29]; however, the principle may apply for any adaptive cancellation of a narrowband jammer.

In order to design a FT S.A.W. device, you have to know the following remarks: first the transform will be performed in about twice the time length of the signal; second, the bandwidth is determined by the signal's one, and in the sonar case by the compression ratio, which in turn fixes the time length of the input signal; finally, the bandwidth is related to the center frequency by the relative bandwidth limitations for the material; therefore, there is a trade-off to find according to all these parameters. However, in some cases, you may benefit from the different mixing operations (see 2.1.2.2) to adjust the different center frequencies together and thus gain an additional freedom degree. In the case of the programmable S.A.W. components, it is then easy to use the same component for other BT or different frequency span, as long as they are included in the first one (which determines the actual physical limits by the electrodes, see figure 12(c)). This may allow, as it was described in section 3.2.1, to use a single component to perform two different FTs, one with 1024 points and the other with 128. Notice also that there is no more any integer type restriction on the value of BT, or number of points, since it is determined by one's choice of B and T.

3.2.3 Adaptive filters

It was mentioned in section 2.2 that adaptive transversal S.A.W. filters are conceivable, if

not already available. It was also pointed out in section 3.1 that adaptive filtering can be of great use for sonar signal processing; furthermore, it was derived from the properties of such S.A.W. filters that it was very easy to interface such filters with a digital processor by using D/A converters.

In sonar, two structures could be of interest, a temporal filter and a spatial one; the first one deals with reflections or parasitic noise (such as self-generated noise) while the second tries to null out strong jammers on a directivity pattern in order to detect small residual signals. Again, we should find the distinction between array and signal processing; the first one would be possible without time scale shrinking (and thus, possible entirely analog realization), but the second one would need it because of the large difference in time duration for acoustic underwater signals and S.A.W. duration. However, the structures for adaptive array beamforming are more complicated [2] than just a transversal filter on the spatial samples; usually the structure involves some kind of adaptive temporal filter on each channel, before the final summation. Figure 24 shows an adaptive array beamformer with the various adaptive filters; however, it is still quite possible to do that with S.A.W. devices, using again the time compression scheme (section 2.3). The speed of these components again improves the possible implementation by using the same adaptive filter for several channels. The digital processor computes the set of optimum weights according to some kind of signal reference; in the case of antenna beamforming, it is sometimes a beam pointed towards the jammer or reference and sometimes an omnidirectional transducer, thus receiving both the signal and the jammer. In the case of a temporal, non

Figure 24: Adaptive antenna beamforming with S.A.W. devices

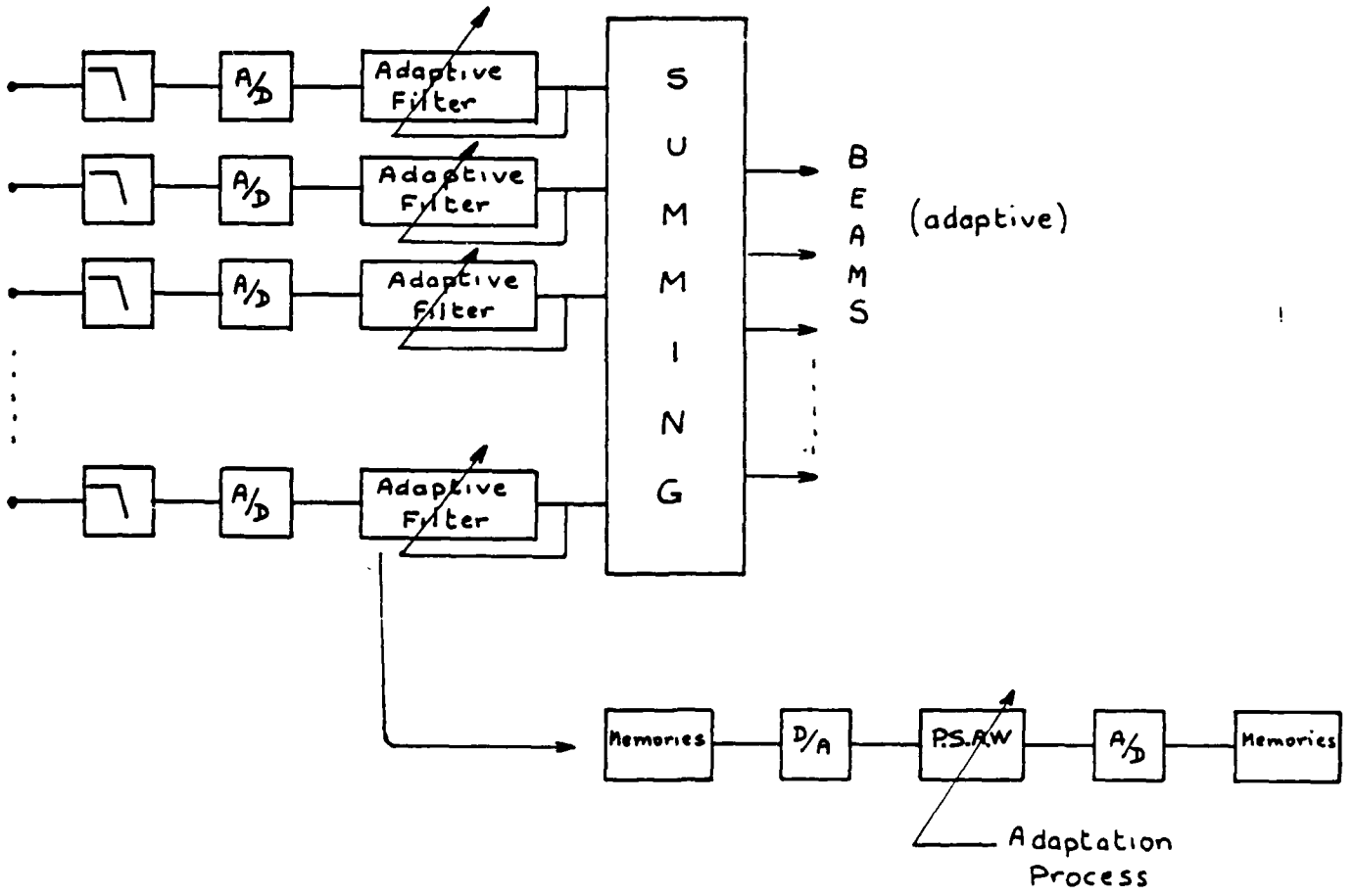

spatially located jammer (as self noise), a specific reference (generally an accelerometer) is used to model the undesireable signal. Such an implementation is shown in figure 25.

Basically, the fact to use S.A.W. device for this purpose has the following promise; generally, such algorithms are still rarely in use because of their large computational loads; it is due mainly to the filtering operation rather than to the adaptation process itself. The fact that S.A.W. devices are suited to perform very quickly transversal filtering, even with very long filters is adequate. Also, the digital computers are more suited than any analog device to perform the adaptation; any kind of algorithm could be used without prejudice to the implementation; the very simple interface required between the processor and the S.A.W. filter is again an advantage. Finally, using adaptive S.A.W. filters may allow to perform adaptive beamforming or interference cancellation in small sonar systems where the available electronics did not allow it with a thorough digital implementation.

3.2.4 Image processing

This aspect of signal processing is usually a whole science by itself; we will not go into details here; there is a very wide litterature on the subject [30,31,32]; unfortunately, it is generally too much oriented towards digital computations; anyhow, we will just describe why such kind of processing can fit with S.A.W. devices and what are the advantages.

25: Interference cancellation with a S.A.W. device

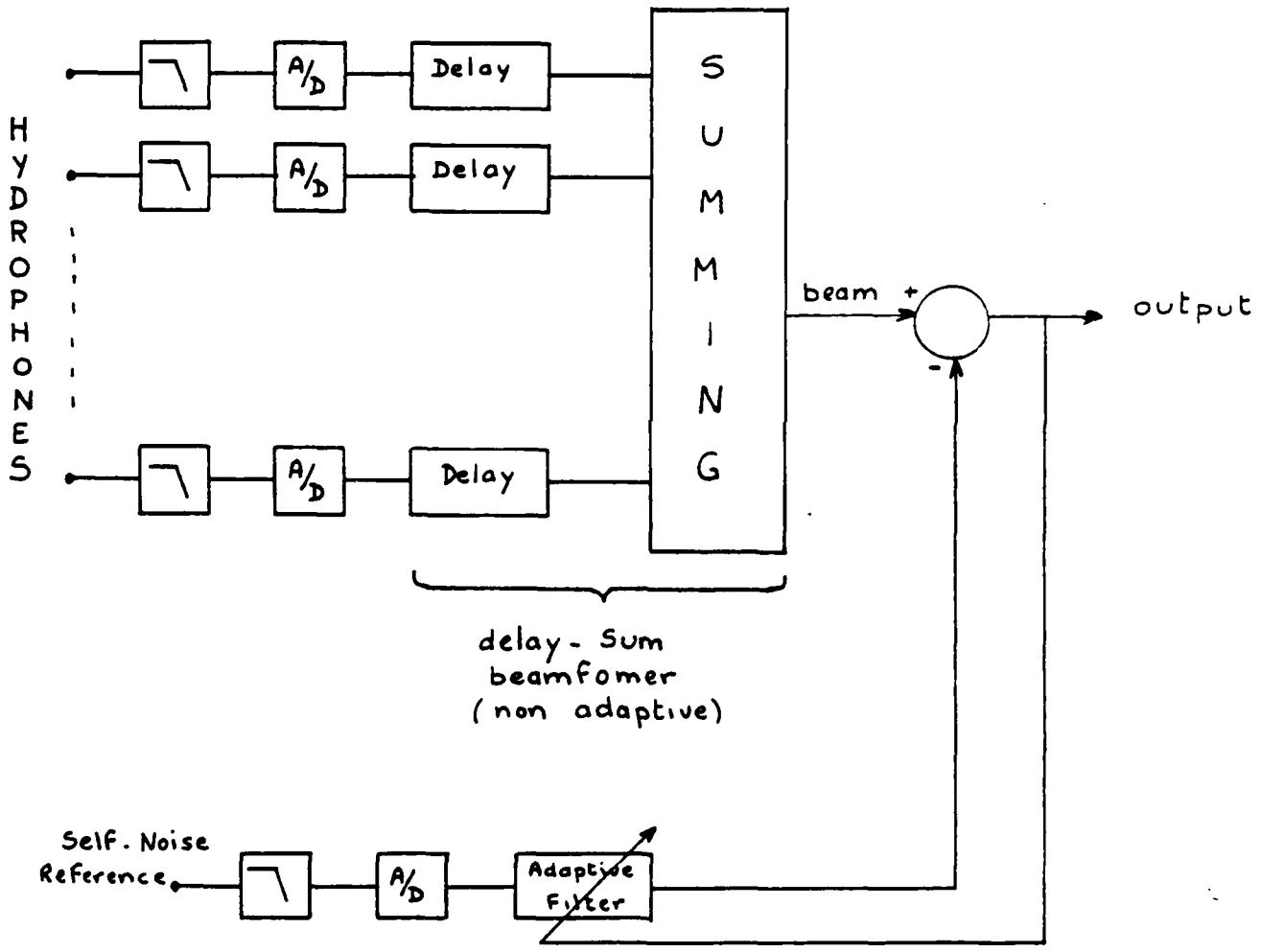

The output of a sonar generally consists of the amplitude of some parameters as a multidimensional function of time, azimuth, frequency, sometimes even elevation. More and more, the sonar operators also deal with outputs coming simultaneously from different antennae; however, this is a typical information processing problem and will not be adressed here. Nevertheless, even with one antenna, the display cannot show simultaneously all the features; then, some cuts, by plane, are displayed, like amplitude of the signal function of time and frequency (LOFAR) or azimuth; these two are shown on figure 26; the nature of these displays makes possible an enhancement of the contrast, and then a better detection process, by assuming some features about these displays. For instance, on an azimuth versus time display (see figure 26 (b)), a target will appear as roughly a straight line or a set of them; in a similar fashion, spectral lines should appear as straight vertical lines, sometimes shimmering because of a slight instability. It is then possible to define some functions (usually two-dimensional) as representative of the desired or tracked features; basic signal processing theory then says that matched filtering of the original picture with that specific function should increase the detection capabilities. On another hand, deconvolution of a two dimensional display is often desired to get rid of some medium effects on the real signal; this problem is usually limited by some kind of instability in the process; it was shown [32] that to insure this stability, a re-convolution of the actual picture with an estimate of the blurring function could be desirable; this involve again some two-dimensional transverse filters.

Figure 26: Typical sonar output charts; (a) LOFAR (b) Azimuth/time

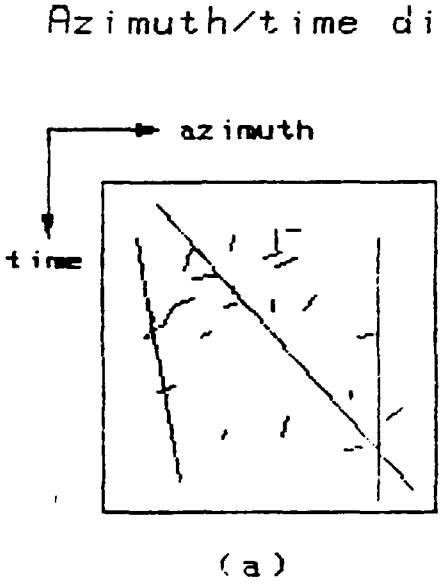

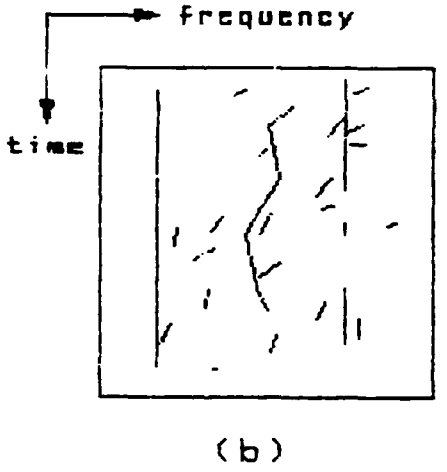

Finally, we have seen very briefly that two dimensional transversal filters are useful for image processing; how can this fit with the one-dimensional transversal filtering capability of S.A.W. devices? Figure 27 shows how data from a three dimensional memories could be adressed to go through a S.A.W. filter before being displayed; the fact is that the pilot signal for a TV monitor is a time signal and is folded on itself in order to give the two-dimensional picture; therefore, by taking this folding into account in the matched filter it is possible to process a two dimensional set of data on a single line transversal filter.

Moreover, the use of S.A.W. devices in that part of a sonar presents several advantages; first, again, the speed of filtering is an interesting feature; second, the frequency band of S.A.W. devices matches very well the frequency band of a video signal (typically, 6 MHz); then the time compression which is anyhow required to go from the digital memories to the TV may be used for S.A.W. purpose; on another hand, there is no need for time expansion after the filtering; it fits with the TV characteristics. Third, the signal has to go through a D/A conversion for display; again, the S.A.W. signal processing will not add specific errors or hardware. Finally, the architecture shown in figure 28 would be adequate; this promising application of S.A.W. devices for sonar could again allow such image processing to be used in moderate size sonar, where the digital alternative is not thinkable, because of volume restrictions.

Figure 27: How to adress three dimensional data with a single line transversal filter

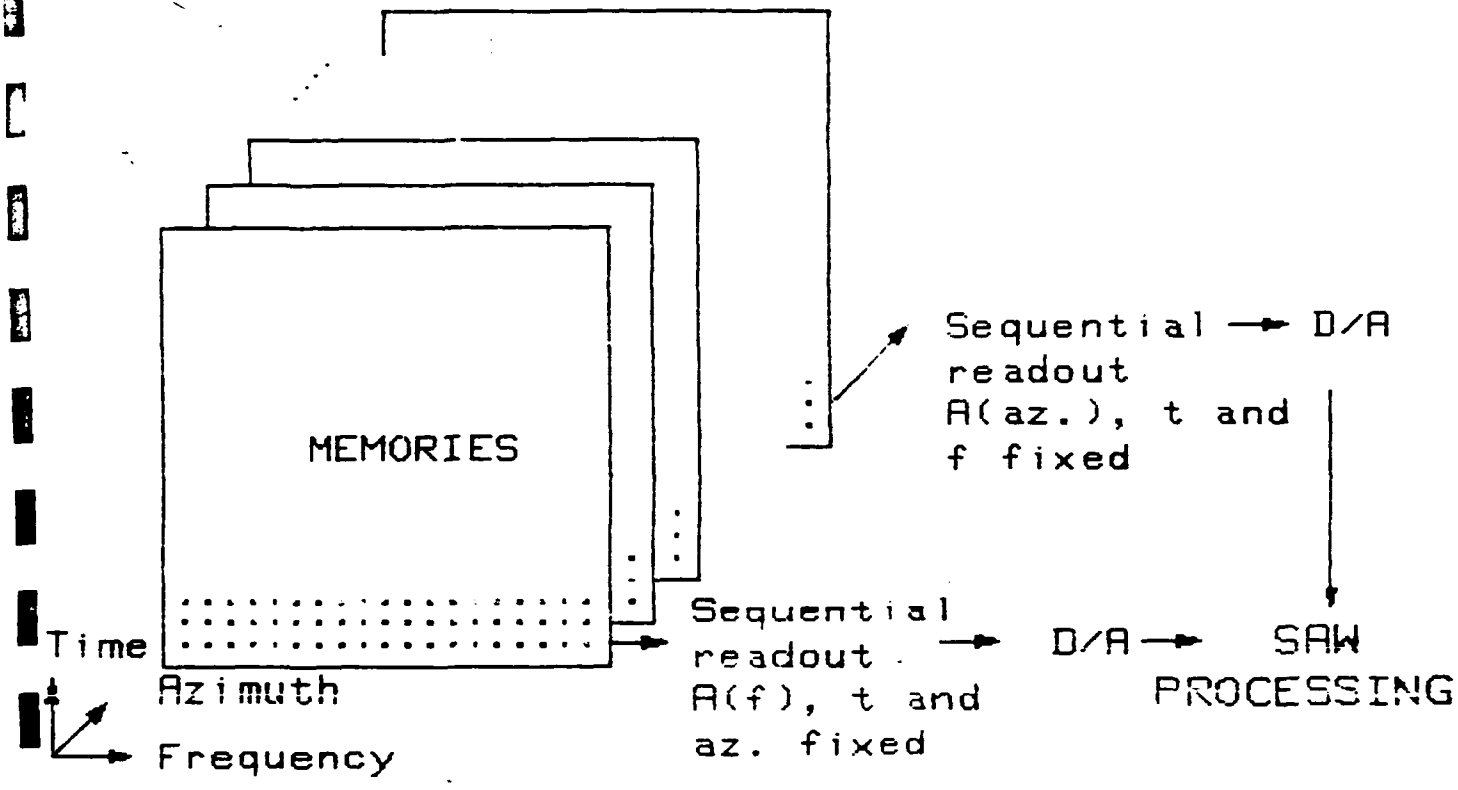

Figure 28: Image processing with a S.A.W. device

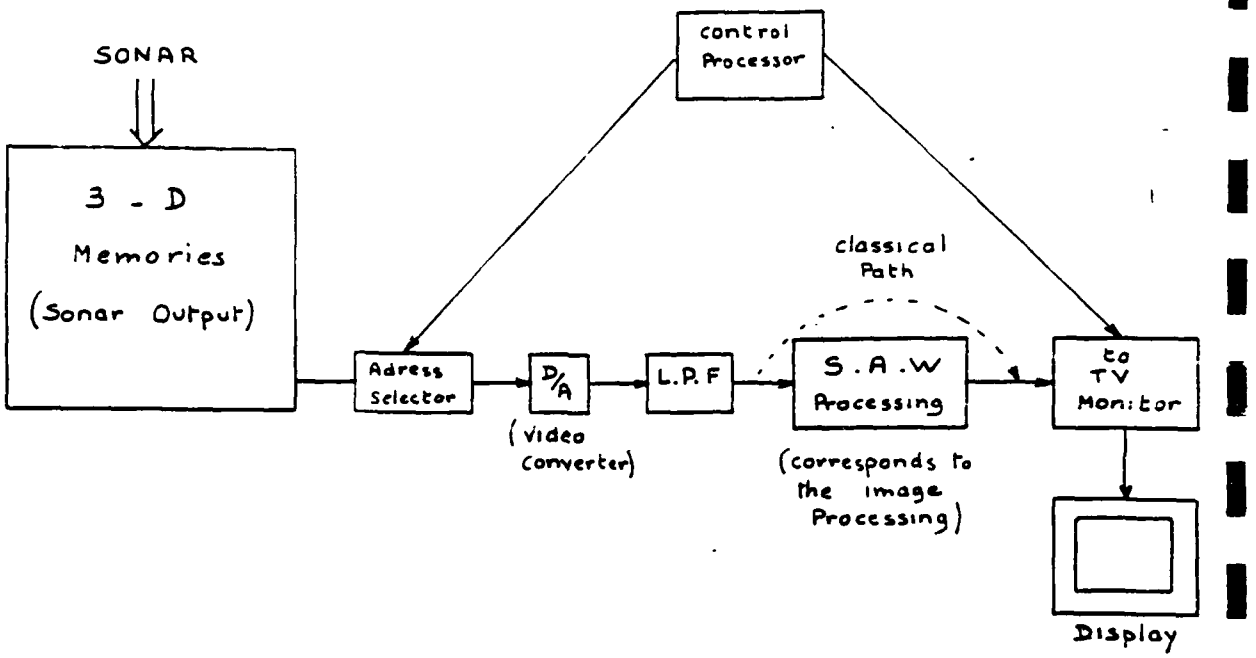

3.3 Partial conclusions

In this very brief section, we just recall the different promising features of S.A.W. use in sonar. It was established that sonar signal processing involves a lot of transversal FIR filters and Fourier transforms; these functions are well known applications of the S.A.W. technology. It was derived that several sonar functions like beamforming and spectral analysis could be efficiently implemented; moreover, some new features were described, which are hard to realize with digital computers; also, some possible adaptive beamforming or interference cancellation is possible with the use of the new programmable S.A.W. devices. This interesting capability, with the inherent fast speed, low volume and power consumption of these devices, may permit such fruitful signal processing in sonars where it was usually considered out of reach. Similarly, some image processing functions were proved to fit with S.A.W. filters, therefore, again, enlarging the capabilities of some small sonars. However, several points concerning S.A.W. processing will restrict the use of S.A.W. devices in sonar; they are the limited accuracy, dynamic range, the requirements for time compression, the need for A/D and D/A, and the different analog components that will be necessary (amplifiers, mixers). Thus, a trade-off has to be made which will determine the most promising systems for such use; this is adressed in the following chapters.

CHAPTER 4

Constraints and trade-offs

4.1 Accuracy and dynamic range limitations:

4.1.1 S.A.W. limitations [13,16,17,24,30]

So far, the accuracy and dynamic range limitations of analog components, and among them S.A.W., were just mentioned; let us detail a little further and explain roughly how and why. Usually, this limitation arises when these components are compared to digital implementations; indeed, it is generally assumed that an almost infinite accuracy or dynamic range is available on digital processors; this is only partially true; actually, the number of bits can be easily increased; however, it will always induce a loss in the speed of computations. Nevertheless, it is perfectly right that even fast digital components are more accurate and have a better dynamic range than analog circuits. In the remainder of this section, accuracy and dynamic range figures are given for S.A.W. devices and we try to explain where they come from.

Commonly, an equivalent accuracy of 6 to 10 bits is considered for S.A.W. devices; this corresponds

to an amplitude accuracy of 1.56 percent or a phase accuracy of about 10 degrees (average value of 8 bits). Actually, a phase and/or amplitude accuracy is measured on these devices and it is compared to that given by a finite word effect on digital computations; hence is obtained the 6 to 10 bits accuracy figure. For S.A.W. devices, the error is mainly due to phase inaccuracies. In section 2.1 was described how to design a transversal filter; particularly, the spatial sampling of the electrodes was related to the center frequency of the filter through an equation derived from Nyquist criterion: a finger electrode for each half wavelength. Basic mathematics proves that this procedure samples a sinusoidal waveform with a phaseshift of Π between two sampling points; the maximum amplitude signal represented by a two phase electrode is then when the phase are 0 and Π. As a matter of fact, slight defaults in the electrode design results in slight mislocations for some electrodes, leading therefore to some phase errors of the output signal Also the quality of the materials (inhomogeneities result in velocity changes, and hence phase mismatches), the electrode weight (again changes in velocity), and the wave diffraction (not truly planar wave between the launcher and receiver) are very critical. However, eventhough the phase disturbances are very important (especially for chirp filters), amplitude errors also occur, mainly because of the overlap technique. On the mask design, slight errors in the overlap result in amplitude inaccuracies that are usually not curable after deposition of the electrodes. This also creates the distortion of the wave crest [4,5], which can be solved by using techniques such as the dummy fingers. This last problem should be less important for P.S.A.W. because of the constant overlap and the a posteriori control with the biases; however, phase inaccuracies

will still exist. Finally, the design and manufacturing process result in an whole inaccuracy corresponding to an eight bit word equivalent; any application of S.A.W. devices has to deal with it.

On another hand, dynamic range limitations are usually reported to be the equivalent of the finite word length effect of a 10 to 15 bits processor; 10 corresponds to a non linear material for convolvers and 15 to a good substrate for linear filtering. The reasons for this figure are linked to the largest possible signal on the material and the smallest signal still above the internal noise. The largest signal is limited inherently on S.A.W. technology by the breakpoint of the material; since all the energy is confined into a quarter wavelength depth from the surface, the energy density can be very large, thus can create breaks onto the surface. However, it also depends on some parameters of the material and of the electrodes such as the radiation resistance and the capacitance of the transducers; this limits the power that a given signal generator (or amplifier) can put in the radiation resistance (this obviously depends on the matching circuit). Finally, we already mentioned these problems in section 2 for insertion losses; all these losses determine the largest signal; it was said earlier that -6 to -20 dB was typical. The smallest signal is limited by undesirable signals; we mentioned already the electromagnetic feedthrough, the bulk wave generation, the different echoes (on the edges of the crystal, or triple transit, on the electrodes themselves), etc.; [4] and [5] analyse these effects in details. Several means are available to fight against such phenomena; however there will always be residual ones. To get these undesireable signals under -80 dB is a good result; -90 or even -100 dB is the best you can

expect. Thus, an overall figure of, say, 12 bits (or 72 dB) for a dynamic range limitation may be adequate. Again, notice that no drastic change is to expect since all these are inherent limitations; any S.A.W. device has, more or less, such usage restrictions.

4.1.2 What are the performance requirements in sonar systems?

Now that the capabilities of S.A.W. devices were described, the sonar needs will be asserted in order to find out where a common ground could be. Nowadays, some people claim that floating point calculations are required for a sonar and a minimum of 24 to 28 bits is assumed. Let us detail a little this assumption: first of all, floating point quantization is required for large dynamic range computations, larger that what can offer the same number of bits in fixed format; here, the 24 bits would be split in a 16 bit mantissa and an 8 bit exponent; thus, the accuracy figure is given by the mantissa and the dynamic range by the exponent; therefore, the larger number would be 2 to the 256th in floating point format rather than 2 to the 24th for the fixed one [26]! Notice, that this corresponds to a dynamic range of 1536 dB, which is inconsistent with the physical phenomena, as is the 144 dB offered by the fixed point format. Actually, this dynamic range is required only for matrix inversions or eigenvalues type of computations; this calculus is very sensitive to the accuracy and dynamic range and therefore requires this number. However, this is not required by any kind of physical feature; thus, it is not necessary to have that for all the computations in the sonar. Now that was explained why such a high

number of bits was stated and that it was not required at the front end of a sonar, let us see what is common at the A/D conversion step.

A decade ago, sonars were working in a clipped mode, meaning that signals were represented by a 0 or a 1 according to their sign (clipping) just before or after the beamforming operation. Only thereafter was the number of bits increasing with the down-stream computations, allowing a greater dynamic range (see further for details). One can show that the phase of a signal may be perfectly represented with clipping; however, the amplitude is strongly affected, but in a known fashion. This kind of processing was yet satisfactory and proven roughly adequate for all kind of impulsing noise (such as active sonar transmissions). Little by little, as the technology was improving, sonars were using more and more significant bits for the encoding; a typical passive sonar, now in service, may have 8 bits for the encoding; soon to be in service are sonars with 12 bit encoding, even 16 bit. The limitation is due to the available technology and again, the trend is to have more and more, eventhough it is not always required for the front end calculations.

We are now going to investigate what is really available at the output of an antenna for a typical sonar. The ocean is a complex medium for the propagation of acoustic waves, and the wavefronts are very often distorted by such phenomena as multipaths, diffusion and inhomogeneities. Furthermore, once the vessel is in activity, the antenna is deformed by the water pressure or by the ship movements; therefore, the theoretical locations of the hydrophones are not always, if ever, espected. This results in an overall

inaccuracy of the coming wave that is inherent; there is no need, at least for the front end calculations, to shoot for a better accuracy than that. This figure is a little hard to find out; however, passive ranging sonars apparently measure phase changes reaching the limits of the acoustic wave, because it has been shown to be very dependant on the measurements situation. Consequently, a passive range measurement accuracy should give a reasonable figure; it seems from this that trying to outstand an accuracy of 10 degrees on the phase is somewhat silly in the frequency range from some hertz to 10 kHz, at least for conventional sonars. This corresponds to the accuracy we stated for a S.A.W. device. Therefore, it does seem to be possible to use such a device for the front end computations such as beamforming, filtering and spectral analysis.

The other aspect of the problem was the dynamic range; the clipped sonar experiences are rather promising for that aspect but this limitation is what causes the need of true encoding rather than clipping, although the latter is really inexpensive from a hardware point of view. The dynamic range that is to be expected for a sonar front end depends on the purpose of the sonar; it is obviously different for an active or passive sonar. Also, the dynamic range differs along the sonar signal processing chain, because the latter increases the signal to noise ratio; in order to be able to make good detection decisions, it is required to keep data that are representative of both the signal and noise levels. We will study that in several steps. On the preamplifier, the dynamic range is defined by the minimum and the maximum signals you expect to receive; for a passive case, a typical source emits between 100 and 200 dB/μPa, depending on its size and type; the minimum signal that is detectable is

typically 40 to 50 dB below the noise level for a powerful sonar; if we assume sea state 2 [27], that is 10 to 20 dB/μPa at 1 kHz; also, the distance of the target affects tremendously the signal level; spherical spreading (see [27] for more details) gives an attenuation of 20log(distance), that is 74 dB for five kilometers; then the overall range is around 110 dB if the largest signal is supposed to occur for a target at 5 kms; above this level, there is clipping which, in turn, spoils all the other signals; however, the figure is already very big and hard to get for a preamplifier. Some years ago, 60 dB was assumed correct; nowadays, 80 dB is more likely and future sonars will be equipped with preamplifiers having 100, even 120 dB dynamic range. Anyhow, again, we have to distinguish large passive sonars and medium size ones; the last ones, very likely, accept 70 to 80 dB. On the other hand, active sonars deal with echoes; they usually put out between 200 and 230 dB/μPa; however, the absorption (see [27]) is now 120 dB for one kilometer because of the round trip. Also, the expected gain is often less, thus leading to a minimum detectable level around 30 dB below the noise; this should give a 60 to 80 dB dynamic range level; it is more reasonable. Finally, an intercept receiver deals with active signals but with a one way trip; although the gain is usually very poor, a dynamic range of 100 to 120 dB is to be expected; however, being a less important equipment, the preamplifier may accept only 80 dB, for price sake. All other related equipments (see section 3.1.4) have generally a smaller dynamic range. Summarizing, at the preamplifier level, active sonar and intercept receivers are clipping the dynamic range to about 70 - 80 dB; therefore, S.A.W. devices should be compatible without too much trouble. On the other hand, passive sonars require much more and S.A.W. components do not

fit, except for low performances sonars (if the gain is decreased, the minimum detectable level and thus dynamic range is reduced).

So far, we only studied dynamic range at the preamplifier level; let us see what happens in the beamforming or the spectral analysis. The whole purpose of these operations is to take advantage of some knowledge about the signal to improve the signal to noise ratio; it involves its directionality on one hand, and some specific spectrum shape (CW for instance) on the other hand. Depending on the size of the array or the time length of the transform, the gain differs; it varies roughly as 10 times the logarithm (base 10) of the number of hydrophones or points of the transform; therefore, 30 dB of gain is very likely. For the beamformer, it does not change the dynamic range since we assumed that it was determined by the smaller and larger signal and not by some noise features; for the spectral analysis (or matched filter), it is important because noise data are to be kept without clipping the signal level; finally, a case by case approach must be taken for that point although some trade offs are possible.

Adaptive filtering and image processing were also shown to be promising for S.A.W. applications in sonar (section 3.2). In the first case, the dynamic range should accomodate the one of the preamplifier and then the S.A.W. one. On the other hand, the important accuracy is that of the coefficients rather than the one of the signal; this must be investigated for a specific application but an 8 bit accuracy is to be expected from the device. For image processing, the displays are often coded on 3 bits only; therefore, no dynamic range limitation occurs, at least for medium

size sonars; the 8 bit accuracy may be sufficient, but needs again to be investigated according to a specific algorithm.

4.1.3 Results and trade-offs

In the previous sections, the limitations for the S.A.W. components, in terms of accuracy and dynamic range have been seen; it was stated that an equivalent of 8 bits for the accuracy and 12 to 15 bits (therefore 72 to 90 dB) for the dynamic range was reasonable. On another hand, we attempted to derive what the sonar requirements were, for different configurations; the figures come either from what can be derived for the medium (through experiments) or from theoretical computations. Indeed, it was claimed that an 8 bit accuracy was enough for the front end computations, such as beamforming, and spectral analysis, because the stability of the wavefronts in the ocean was hardly giving more; only very modern passive systems with specific autocalibration of the antenna may do much better; furthermore, it was also stated that this accuracy was enough for the image processing algorithms, as they are envisionned now and that the case of adaptive filters has to be studied on specific examples.

The dynamic range problem is different. Passive sonars, at least large ones, require a dynamic range that outstands by far what S.A.W. technology can offer. A figure of 120 dB seems a good target for the coming years. Therefore, S.A.W. devices do not fit with modern passive sonars because of this constraint; moreover, it was already stated that these sonars could also be in

limit of the proposed accuracy. However, there are still some small low-performance passive sonars; these could accept a restricted 70 - 80 dB dynamic range. Nevertheless, it is not sure then that the computational flow is enough to justify the use of S.A.W. components. Active sonars, on another hand, seem to work with a smaller dynamic range than their passive homologues; 70 - 80 dB can be reasonably considered for an active sonar, thus rising no specific problem for S.A.W. technology. Also, intercept receivers are sonars that need a very large dynamic range; it is even more than large passive sonars. However, these receivers are usually low-cost equipments and the dynamic range is clipped on purpose to avoid the use of very expensive components. Consequently, it can be a good solution to use S.A.W. devices for it leads to an efficient implementation and could allow the same dynamic range as with conventional devices.

Finally, it turns out from dynamic range considerations mainly that the most promising applications of S.A.W. devices in sonar should be for active systems and specific equipments such as intercept receivers or even, imaging or mine sweeping sonars. Moreover, very often, in an active system, there is a modest passive sonar (which is a help for the active one) which could also fit for S.A.W. components. Therefore even shared functions, such as beamforming, could be realized this way; however, passive systems, small or large (where the passive function has the first priority), will hardly, if ever,be implemented with S.A.W. devices.

4.2 Interface Electronics

4.2.1 Problems associated with electronic components

It was mentioned in section 2.3 that using a S.A.W. device in a digital environment involves more than just the S.A.W. component itself. Figure 29 shows the components and connections required for both a temporal and spatial signal processing. Basically, A/D and D/A converters, low-pass filters, multiplexers and demultiplexers, and sometimes mixers (for the carrier modulation and demodulation) are needed. In the following, the problems that each of this component may rise will be shortly investigated in order to draw some limitations about S.A.W. use in sonar applications.

4.2.1.1 Analog to digital and digital to analog conversions

These components are the most important items for the scheme shown in figure 29, with the exception of the S.A.W. device itself. A very good overview of the different circuits and their problems is [23]. In order to focus our attention on the real problem, we first need to tell which categories of converters we are looking for; the important parameters are usually the speed of conversion, the size of the circuit and the accuracy or resolution. For the first point of view, very fast A/D and D/A converters are required; the frequency range of the S.A.W. devices is in the tens, even hundreds, of MHz; therefore, in order

Figure 29: Practical connections in using a S.A.W. component in a digital environment; (a) temporal processing; (b) spatial processing.

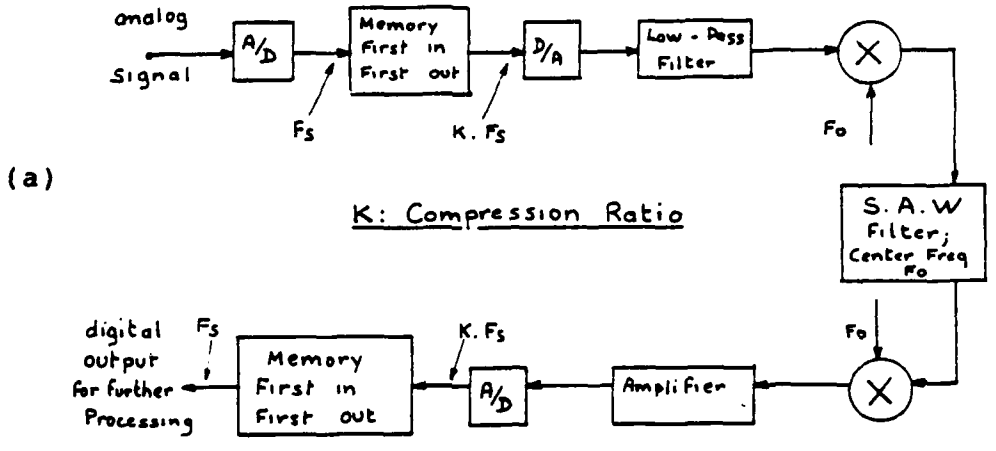

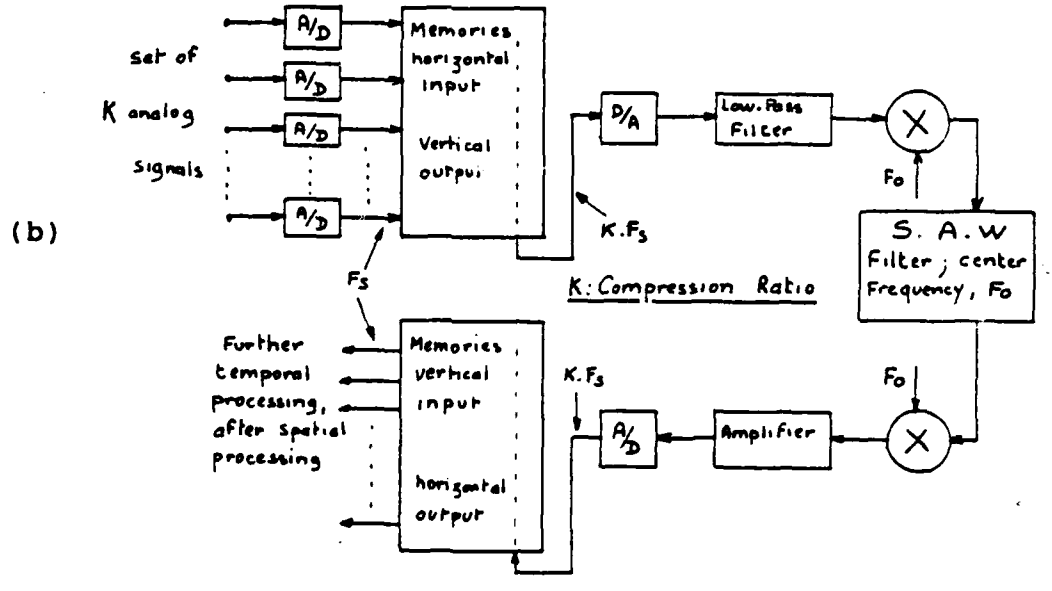

for a digital signal to become compatible with this frequency band, time compression is required and then fast conversions. Generally, D/A conversions can be realized in a much shorter time than their counterparts, because of their operating principles [23]. However, in our case, A/D conversions are required anyhow and this component sets some limits on the overall working speed. The second parameter, the size, is important because the whole purpose of this kind of operation is to save hardware; it is silly to shrink the functional hardware heavily and to increase greatly the interface one. We are then looking at integrated or at least hybrid versions of the converter. The third parameter, resolution, is less critical since we pointed out that S.A.W. devices were already limited; 8 or 10 bits of resolution should be enough for most applications.

According to [23], flash converters are the only ones that could achieve the involved conversion rate; 75 MHz data flow is possible, though extreme, on integrated flash converters. This may seem very fast but, yet, it represents only signals with 25 to 30 MHz bandwidth; therefore, this is just enough for this application and carrier modulation techniques may be required to match completely the SAW characteristics. The D/A converter on the other hand will be able to keep this pace because integrated versions exist having an 8 bit capability and a speed of conversion compatible with 100 MHz bandwidth signals. In the case of spatial signal processing, figure 30 emphasizes a solution to increase the compression factor with the available A/D converters. Basically, it takes advantages of the inherent parallelism to increase the overall flow speed by using several A/D converters.

Figure 30: Intrinsic parallelism in spatial processing

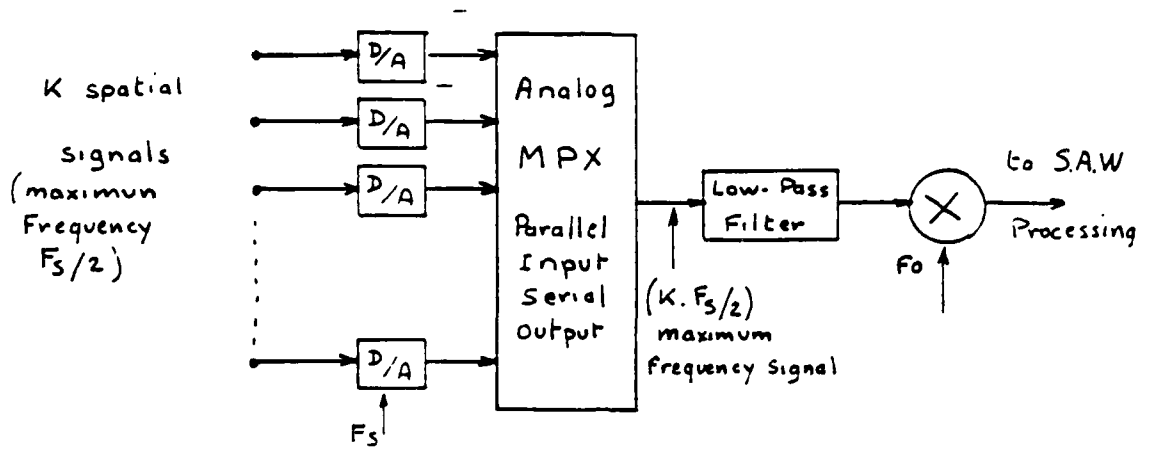

K: Compression Ratio

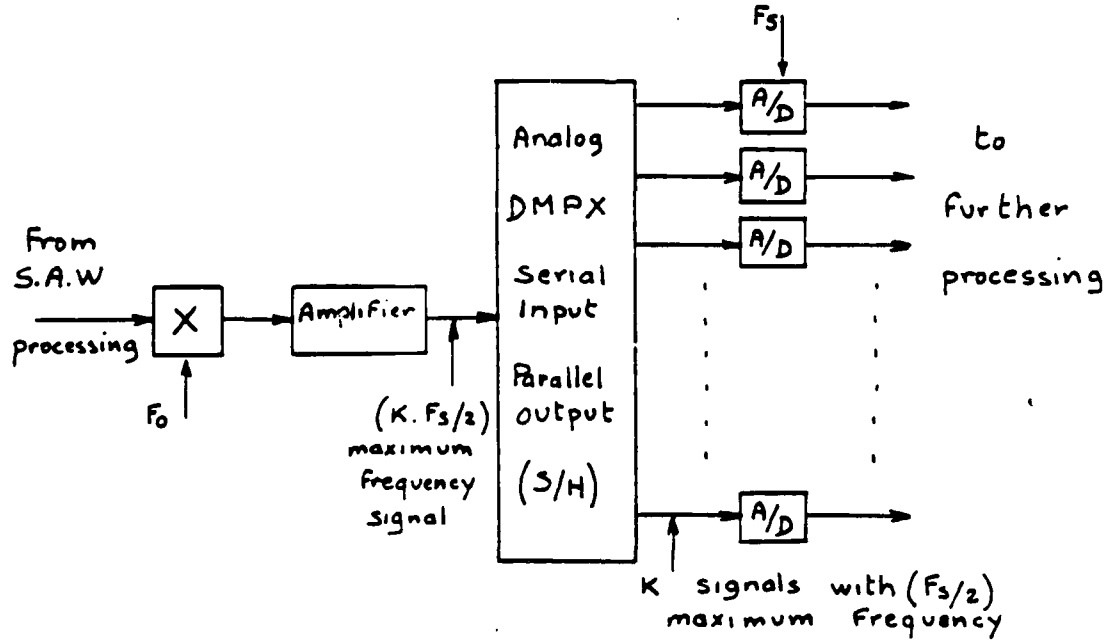

Several other problems are encountered when using A/D and D/A converters; there are mainly the quantization noises, the linearity errors for A/D, and glitching for the D/A. Some details can be found about these problems and their solutions in [23] and [26]; this explains why using an A/D and a D/A converter successively without any other component than a low-pass filter for smoothing would not result in an identical input and output. It is important to remember that it limits the number of conversions within a specified error allowance; this is a matter for the designer to decide how low this level should be, choose the adequate converters and to see how many conversions are possible. Emphatically, it means that a system cannot have S.A.W. devices in several points of the signal processing chain therefore leading to several consecutive conversions. Typically, it would be possible to have one or two functions assumed by such components, the remainder being digital. It was also noticed in section 3.2.1 that an important case was when no conversion takes place before the processing; hence, it is possible to achieve the function with only one set of conversions, which would have existed in any case to go to the digital domain (see figure 30).

4.2.1.2 Multiplexers and demultiplexers

These are also vital parts of the time compression scheme; two solutions are available depending on several factors; analog or digital multiplexers could be chosen. The first ones, as it was noticed earlier could provide a mean of increasing the compression ratio; on the other hand, the second kind is much more stable, with better insulation and

crosstalk reduction performances. However, again, the analog alternative allows a greater data flow than the digital one; then, it is a matter depending on the specific application and the speed to achieve. Nevertheless, it must be pointed out that analog solutions lead to some crosstalk that could or could not be tolerable.

4.2.1.3 Mixers

These components are required for the carrier modulation techniques; we pointed out that because of the speed of the A/D or D/A converters, they may be mandatory. Mixers usually have very large bandwidth capabilities (up to hundreds of MHz) but have poor quality performances; generally, the dynamic range is limited (between 50 and 60 dB); also, they are not always truly linear with respect to both input signals. Thus the overall performances of the system will be limited by these components if they are not chosen from the best breed. However, in the case of programmable S.A.W. devices, it was pointed out that an intrinsic mixing (true multiplication, this time) was available; therefore, better compactness and may be performances could be expected.

4.2.1.4 Filters

In order to get a thorough digital to analog conversion, a low-pass filter is required to smooth the steps present at the output of the D/A. This one has to be analog by nature and rejects all the spurious

components induced by the sampling; however, good quality analog filters are available and should not degrade the accuracy or dynamic range of the whole set.

4.2.2 Practical limitations

Now that the different problems induced by the interfacing electronics have been detailed (mainly the analog to digital and digital to analog conversions), the practical limitations of the use of S.A.W. components for sonar will be investigated.

First of all, it was shown that the speed of the converters, and mainly the analog to digital ones, imposes a limit on the time compression ratio, by setting an upper limit to the signal's frequency; if we assume that 75 MHz is a maximum limit for an integrated A/D converter, and suppose that this represents the baseband signal (already demodulated from the carrier), bandwiths greater than 25 to 30 MHz are not possible. It means that no more than 5000 signals at 5 kHz or 2500 at 10 kHz can be compressed on this converter. Actually, the compression ratio is clipped to 5000 for 5 kHz signals, and because of the data management, a little less than 5000 signals will be multiplexed. In other words, even if the S.A.W. component is capable of processing signals having bandwidths of hundreds of MHz, a sonar application does not allow an usage at more than 25 MHz. However, if the output signal is split into several components (spatial processing) the use of sample-and-hold devices and analog demultiplexers may allow a much faster rate; indeed, samplers and multiplexers may work at very high frequencies, a hundred of MHz at least [23]. This is

only true for a beamforming operation where the output is a composite signal where two consecutive samples are two different beams, being possibly sampled at a smaller rate than the original analog signal. In the case of temporal compression, it is not possible because the demultiplexing has to split segments of signals, each of them having still the full bandwidth. Figure 31 pictures this problem and the possibilities. Finally, time compression factor must be limited to 2500 or 5000 (which is already very large), except for beamforming. Subsequently, this limits the acceptable duration of processing. Considering 10 microseconds as typical on a S.A.W. device, it means that time segments longer than 50 milliseconds cannot be processed on a S.A.W. device with this scheme; exceptionally, a duration of 50 μs may be achieved, therefore giving a limit of 250 ms for the sonar signals. In other words, the time bandwidth product is typically about 250 for such processing, and specifically may rise up to 1250. This is a very strong constraint which is solely due to the analog to digital conversion process; however, except for beamforming and image processing, this has to be considered and seriously entails the possible S.A.W. applications in sonar.

Beamforming applications are not be affected by this limitation because of the intrinsic parallelism and, in the case of image processing, because D/A converters only are required; actually, update rate as high as 100 MHz are possible with these circuits therefore setting the limits where they are no more troublesome.

All the remaining electronics has to be considered for any practical application, but it should not set any particular hard constraint; the designer

Figure 31: Analog demultiplexing for temporal and spatial processing. Bandwidth considerations.

Temporal signal processing

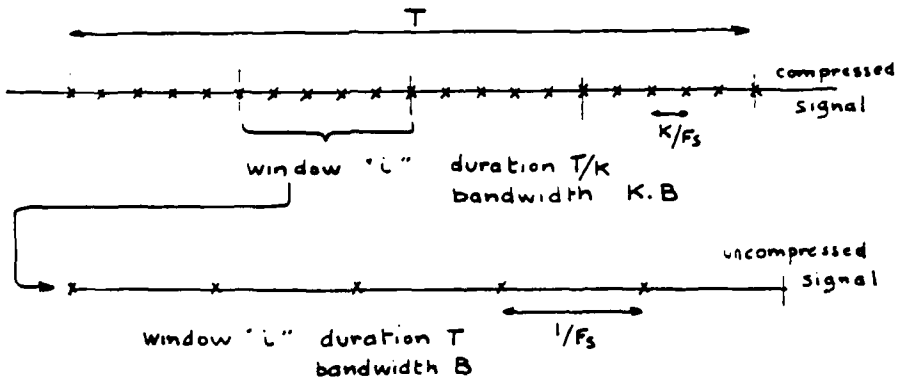

uncompressed signal obtained through an A/D converter at k.Fs (common to all windows) and an expansion in time by memory

Spatial Signal processing

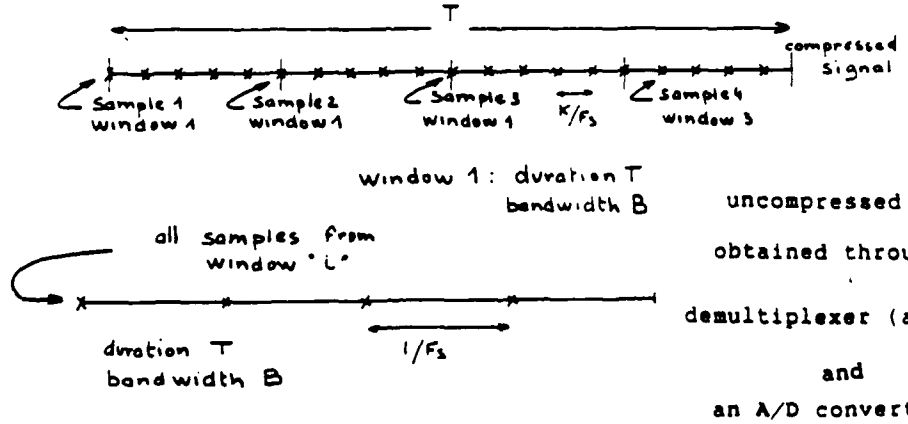

uncompressed signal obtained through a demultiplexer (analog) and an A/D converter at Fs (1 per window)

shall consider the different trade-offs in terms of accuracy and volume, because of all these extra components. Only this thorough study will decide whether this solution (S.A.W. component) is truly promising for some specific application.

4.3 Partial conclusions

In this brief section are summarized the different problems arisen by the performance limitations of S.A.W. devices and the necessary interfacing electronics. We will try to draw some practical conclusions; however, since some of them are very dependant of the technology (converters speed for instance), we will ponder them also simultaneously.

4.3.1 Limitations due to the characteristics of S.A.W. devices

It turns out from section 4.1 that S.A.W. devices offer an accuracy equivalent to an 8 bit digital word and an effective dynamic range of 70 to 80 dB. It was also said from empiric considerations that a typical sonar front end (with the exception of large modern passive sonars, where big improvements are expected) only requires an accuracy on the signal processing of about 8 bits. On the other hand, the dynamic range requirements are different depending on the kind of sonar. Passive sonars require a dynamic range between 80 and 120 dB; therefore, they are out of reach for S.A.W. devices. Active sonars are less

demanding and 70 to 80 dB is enough, thus matching S.A.W. features very well. Also in this category could be the passive subsystem of an active sonar (secondary function). Finally, intercept receivers need a very large dynamic range (100 to 120 dB) but their function, mainly detection, could accept some intended clipping for hardware's saving sake. Consequently, intercept receivers may accomodate S.A.W. devices very well. Other equipments such as sea bottom imagers or decoys have to be studied particularly to find out their requirements.

A last feature that should be checked is the temperature dependance of the S.A.W. devices. Although it depends on the material, this should not be too drastic, since such military components are in use in radars. The aging could also be considered; however, all these problems are well known of a S.A.W. devices manufacturer, and therefore should be solvable.

4.3.2 Interface electronics limitations

The results of our short investigation, mainly based on [23], is that the main limitation comes from the A/D converters speed; therefore, time compression is roughly limited to 5000, and more important, the time bandwidth product, BT, is typically 250, and specifically may rise to 1250! This restriction applies only for the temporal filtering (adaptive, Fourier transforms and image processing) but is only truly drastic for Fourier transforms; in other words, spectral analysis will not be possible with S.A.W. devices, except when such low gain as 250 is acceptable, or when the application tolerates very

large devices. This includes small systems as torpedoes, or active sonars (partially), and may be intercept receivers. Notice that any improvement in the A/D conversion techniques would change this conclusion; this may be likely to happen. All the remaining electronics affect somehow the whole signal processing function, in a way that should be apprehended by the designer, but do not set definite constraints.

4.3.3 Miscellaneous comments

In this section are made some other remarks concerning the use of S.A.W. components in sonar. First of all, let us point out one of the major problems of S.A.W. design, the electromagnetic feedthrough. This is true for any S.A.W. devices, could it be for radar or television. This corresponds to a signal going directly through the device, by radiation or capacitive coupling, without being affected by any specific acoustic features. We already mentioned that it was partly responsible for the limited dynamic range, but another fact is that it explains why those devices have to be mounted in specific packages, therefore possibly affecting the hardware connections. It must be a concern for the designer.

Another and last remark concerns the data throughput of the system. It was noticed how efficient these devices could be for signal processing. Computational speed of several hundreds Mops were claimed, with components as little as a standard hybrid IC. Let us recall that in order to justify a hybrid architecture (S.A.W. - digital) in a sonar, only hardware saving is an acceptable reason. Therefore, it

means that the system requires a large number of low frequency channels, in the same order than the time compression ratio. Hence, systems having less than 200 or 300 hundred signals with 10 kHz bandwidth should not be considered; notice also that the higher the frequency is, the smaller the number of channels is. Then, a torpedo working at 30 kHz will only require 50 to 100 hydrophones to be consistent with a S.A.W. implementation. For an intercept receiver working between 50 and 100 kHz with 20 channels, a S.A.W. implementation would be worthwhile.

CHAPTER 5

Some promising system applications

5.1 General considerations:

In this chapter, we investigate some promising sonar applications for the use of S.A.W. devices. The aim is not really to obtain the whole signal processing chart and implementation of these systems but rather to study on some specific cases what are the advantages, the trade-offs, and the problems. However, the applications were chosen among the most promising kinds of sonars for that purpose (see chapter 3) and by taking into account the different remarks from the chapter 4. The applications are mainly the results of different interviews of people at the N.O.S.C., at the N.U.S.C. and at E.D.O. Western Inc.. Nevertheless, none of these applications has any military actual interest; indeed no specific disclosure authorization is required. The different applications concern a torpedo active homing sonar, processing a linear towed array, an helicopter-borne dipping sonar, again an active one, with adaptive self-noise cancellation, and finally, an intercept receiver for medium size submarine. Each of

These applications is detailed in terms of signal processing charts, evaluation of parameters (frequency, bandwidth, number of hydrophones, etc.); then, a global computational load is derived by assuming conventional, but efficient, algorithms and some estimate of the hardware volume is attempted. Also, a S.A.W. component implementation of some of the signal processing functions is described, with all the necessary restrictions and at the end, a volume/quality comparison is estimated between the whole digital solution and the hybrid one.

5.2 Torpedo and linear array

5.2.1 Some details

Torpedoes are classical weapons in underwater warfare and linear towed arrays are now among the most classical and most powerful arrays. However, usually, torpedo's antennae are located at the front bow of the hull, without involving any kind of linear towed array. Indeed, the reason is linked to the little space available for electronics in a torpedo (rather have a bigger payload or more power-supplies) and to the difficulties encountered when trying to tow a linear array. This last reason is beginning to fade out, since this technology is evolving rapidly and people have more and more knowledge on this topic; then, before trying to address the first problem, small and compact electronics, let us clarify why a linear array on a torpedo could be promising.

The whole purpose of a linear array is to allow low, or even very low, operating frequencies without losing any resolution or gain on the antenna; it is well-known that the size of an antenna is determined by the acoustic wave-length of the operating frequency; with equal resolution and/or gain, the lower the frequency is, the larger the antenna is. An important fact to recall also is that in underwater acoustics the lower the frequency is, the larger the detection range is, because of absorption losses. Therefore, a torpedo using a low-frequency active sonar would be able to detect, and localize, a target from a farther point than with a normal torpedo sonar; that is one operating around 30 to 50 kHz. Actually, as the antenna is

located in the torpedo's bow, it is limited to about 20 inches in diameter, and thence the lower limit of the frequency for a given resolution. However, towing a linear array would allow the torpedo to use a large low-frequency sonar; for different reasons linked to propagation features in the ocean, a 5 kHz sonar could be optimal. In the following, we assume that the technological problems for the antenna manufacturing are solved and we address the signal processing problem; that is to find a solution to the electronics hardware problem. This application fits very well with this study, because it requires very compact and powerful hardware, low-power consumption and active sonar is typically suited for S.A.W. devices usage. A reasonable number of hydrophones, for such application, could be a hundred; thus, this is a very powerful active sonar and because of the low-frequency, a passive option is recommended in addition to the active primary function.

5.2.2 Signal processing chain analysis

In this section will be described briefly how the signal processing chain could be designed in order to perform the main straightforward functions.

For such application, the sonar functions are split into two groups corresponding to the target range; a first group, long distance detection and first localization, would be performed with either the passive low-frequency sonar or the active low-frequency one; the second group, attack homing and accurate localization, would be achieved conventionally with the bow high frequency active sonar. Only the first problem

is addressed.

Because the passive function is secondary and the active signal is a narrowband one, narrowband techniques are chosen. This induces that for the passive function, which cannot be simultaneous with the active part, the spectral analysis splits the band 1 to 5 kHz into narrow bands; however, the active function already needs this for the doppler measurements. A typical signal processing chain for the active and passive functions is shown in figure 32; the Fourier transform beamforming is adequate, because of its efficiency, and it is located before the narrowband decomposition to allow its use for both the active and passive chains; the number of points for the transform is at least 100, but will be fixed later since it differs from one implementation to another. However, for a digital implementation, 128 is likely the minimum. Because the torpedo is looking for targets being ahead of it, only a front sector needs to be covered; then, the downstream computations could be achieved on a reduced number of beams; say, the quarter of them looking ahead. The spectral Fourier transforms are linked either to the active signal duration (typically 100 ms at this frequency) or to the frequency resolution for the passive case (256 to 512). The detection occurs when the energy is reaching a threshold in one frequency cell; notice that the active signal has been transformed into baseband (naturally narrowband) but the passive one is directly analyzed. The active sonar gives also the azimuth (or pseudo one because of the array geometry) through the beam' s direction and the doppler (frequency measurement); the passive one gives just the pseudo azimuth.

Figure 32: Torpedo signal processing chain; active and passive primary functions

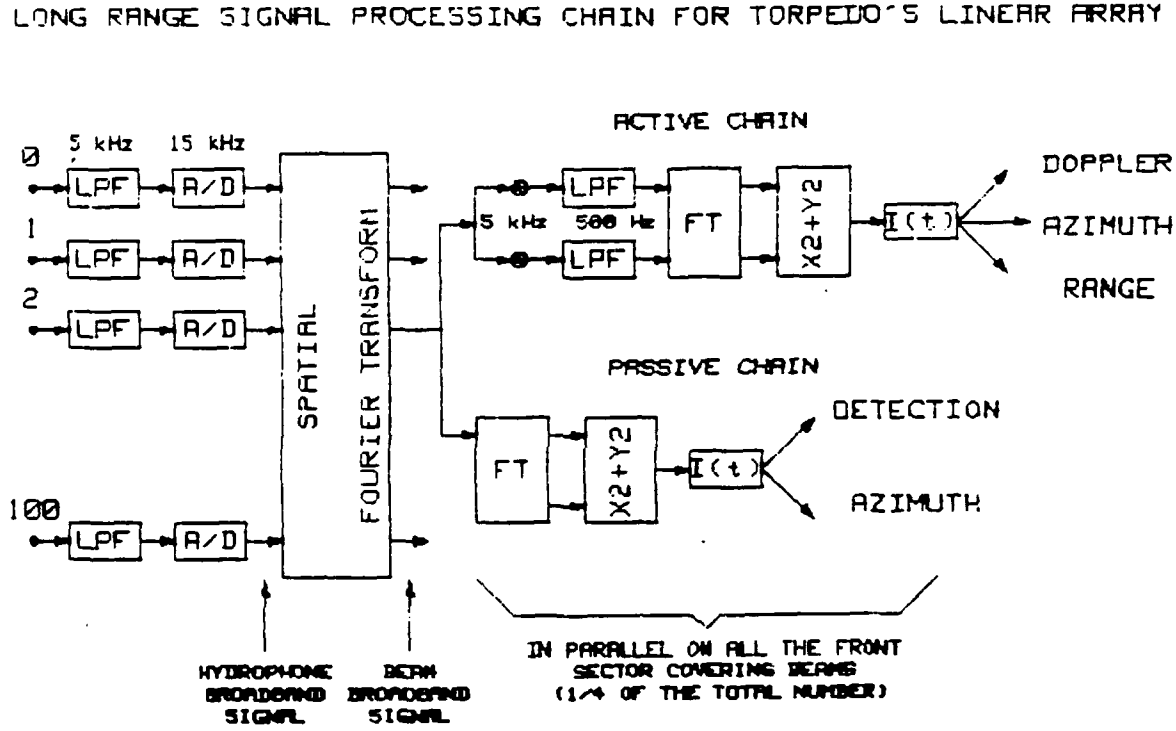

Notice also that such an application rises some questions; the torpedo usually searches for a target located in front of it; then, the torpedo itself, and mainly the engine noise, hides the useful signal; however, a distant homing torpedo generally moves at a shallow depth; this means that the main target (submarine) is not hidden because of the immersion depth difference; moreover, in active mode around 5 kHz, the noise of the torpedo should be attenuated (it usually peaks around 3 kHz). Furthermore, an adaptive cancelling feature could be imagined but will not be investigated. Anyway, torpedo's noise is known and the active transmission frequency may be chosen so that interferences are avoided.

5.2.3 Computational load for a digital processor

If the general scheme of figure 32 is assumed, and 128 beams are performed, the computational flow could be derived as follows; first the sampling frequency is required; a good figure would be three times the highest frequency, i.e. 15 kHz. Then, the number of operations by fast Fourier transform is required; it is, for a real signal transform:

$$M = N/4 \times \log_2(N) \times 10 \qquad (3)$$

where N is the transform length and 10 is the number of real operations per butterfly. From there and figure 32, the following figures are determined; the beamforming operation represents roughly 33 Mops for 123 points; it would represent 77 Mops for a 256

points. Besides, the temporal Fourier transforms are performed by segments; it means that N points are processed and eventually the next N points will be processed (without overlap). It is assumed that only 32 beams are consequently processed, because of the front coverage only. The active spectral analysis is designed for an active signal with 1 kHz bandwidth and 100 ms duration; then, 256 should be adequate; the load is therefore 3.84 Mops (complex FFT) (equation 4 is used, where M is from eq.3, F_s is the sampling frequency, and V the number of processed beams). For the passive case, with 256 points also (but a real one), the load is 9.6 Mops (still according to equation 4).

$$L = M \times F_s/N \times V \qquad (4)$$

The subsequent signal processing is negligible compared to the previous one; the total is thus about 48 Mops. Notice that the largest part is due to the beamforming. Finally, this kind of processing does not require a lot of dynamic range or accuracy; therefore, an 8 bit signal processor could achieve it. Dedicated hardware will certainly fill the available space in the torpedo, may be more! Using a Texas Instruments 320 circuit leads to about 10 Mops per circuit; therefore, 5 circuits are required, leading to about 5 electronic boards for the circuits and their interfaces. Anyhow, this processing is not compatible with the high frequency, small range functions; thus, another electronic hardware is needed, but all the space is occupied.

5.2.4 S.A.W. component solution

A S.A.W. component implemented solution is investigated here; it has been already noticed that it was adequate because of the involved signal processing. From figure 32, two functional blocks appear to be suitable for S.A.W. devices implementation: the beamforming operation and the spectral analysis. However, because of the small load of the spectral analysis (see section 5.2.3) and the requirements for time compression, D/A and A/D conversions, only the beamforming will be implemented this way. The scheme described in section 3.2.1 is chosen and the implementation of figure 33 is correct. Notice that, here, the choice for 256 beams (better resolution) would only cost some more A/D converters; actually, it is even more favorable because only a partial coverage is required. Then, with the same conversion hardware than the digital solution, 100 beams are possible, only scanning the front sector (1/4). This would correspond to a beamformer with 400 beams; the digital solution would thus be prohibitive.

Finally, the beamformer itself would be a chirp Fourier transformer; according to the 128 beams solution, the characteristics of the device would be then: compression ratio = 1000; T=10 microseconds (100 sensors, half a wavelength apart, leading to a duration of 100 times the half period); B=5 MHz and Fo=25 MHz; the duration to get a Fourier transform is then roughly 20 μs, far enough for what is needed. One chirp filter would be a piece of crystal of roughly 30 by 5 mm, therefore fitting into a hybrid IC package; 2 or 3 are needed for the thorough transform. The necessary interface (sampler, multiplexers, demultiplexers,

Figure 33: S.A.W. implementation for a torpedo

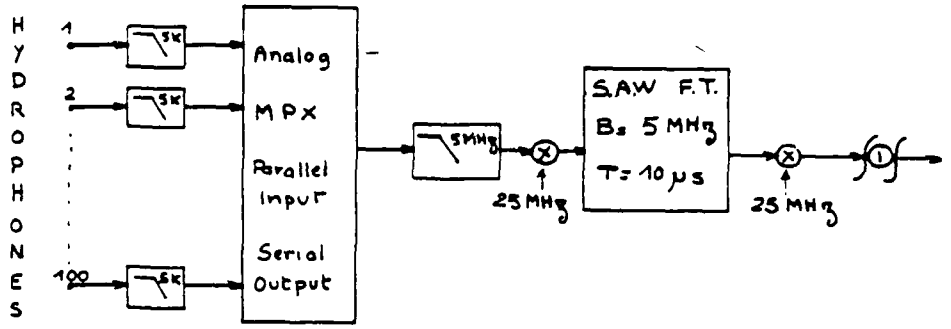

(1): transmission through cable link

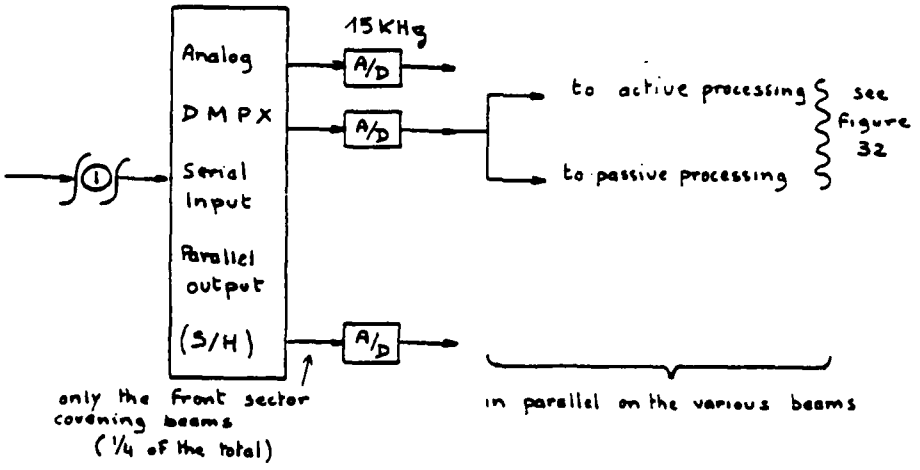

mixers) should fit also in a few IC packages. Thus, the whole beamforming function could be directly implemented in the towed array itself (it is assumed that the antenna is about 3 inches in diameter, because a smaller one would be useless for this application), as were actually the sampling, coding and multiplexing in the digital version. Beams would then be transmitted to the torpedo body, leaving the inner volume for the remainding electronics, and, possibly, other functions.

5.2.5 Partial conclusion

The purpose of this little study was to demonstrate a promising use for S.A.W. components in sonar. It was shown that for such application, the beamforming of a towed linear array, working at 5 kHz could be achieved, within the antenna itself, with a couple of standard IC's. Therefore, a computational burden of 33 Mops (or more if better angular resolution) would be saved, which hence saves a good amount of electronics (several boards). In this case, this saving was achieved without any loss of performance; indeed, it could allow the whole solution to exist as the digital alternative is certainly too expensive for a consumable product. Moreover, it allows an operating mode in addition to the normal active high frequency mode with very little additional electronics.

However, the shortness of the study should be kept in mind; many technical problems remain and it is not certain that such function could be achieved.

5.3 Helicopter dipping sonar

5.3.1 Adaptive cancellation of helicopter noise

Helicopter dipping sonars are very attractive since they permit a good survey of large ocean areas by sampling. The sonar usually consists in a dipping body, immerged while the helicopter is hovering, comprising the antenna itself and some digitizing and multiplexing electronics. The function is mainly active for two reasons: first, a quick detection, generally leading to an attack is required; second, a hovering helicopter makes an awful noise which spoils all the passive measurements and even the active ones. We will try to address this problem by proposing an attractive solution. The classical remedy is to design an antenna having an adequate directivity in the vertical plane, thus rejecting the helicopter noise usually coming from the top (in some cases, such as shallow water, there could also be some reflections on the bottom); 20 to 40 dB cancelling are achievable this way, depending on the antenna geometry and the beamforming. However, sometimes, more is required. Therefore, a cancelling of the self-noise by trying to subtract it would be adequate. According to [2], it is possible and it requires the scheme shown in figure 34; it assumes that each individual hydrophone would receive both the signal and the self noise, and it should be done on the beamformer output because it would need a different signal to noise ratio on the reference and input. The gain for such a process is about the signal to noise ratios difference; roughly, one can say that it would

Figure 34: Beamforming and interference cancellation; helicopter sonar case

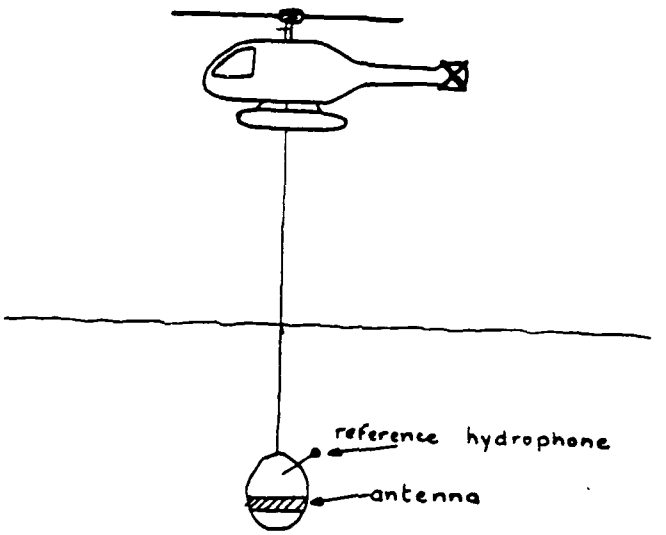

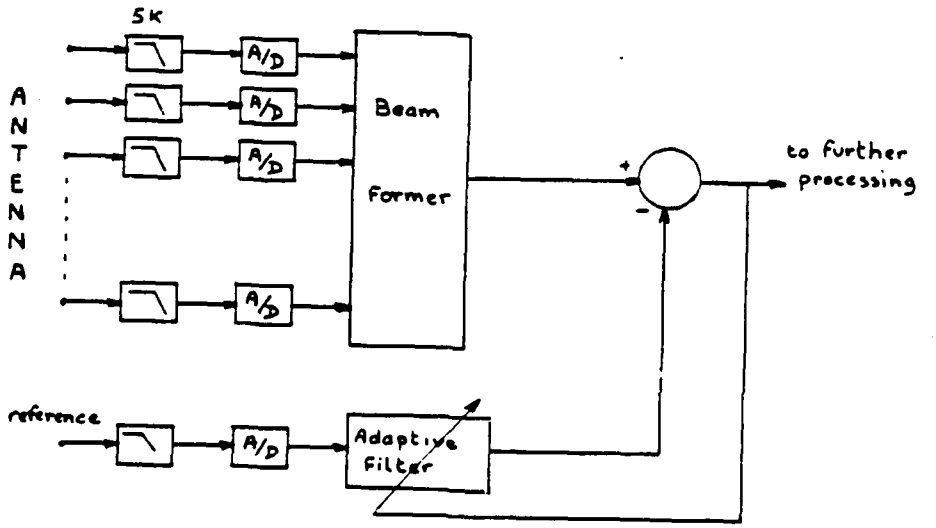

give an additional cancellation of the self noise of 10.log(N), where N is the number of hydrophones used for a beam.

For the remainder are assumed the following parameters: The sonar is operating at a central frequency of 5 kHz with a 1 kHz bandwidth in the active case and listening within 1 to 5 kHz in passive mode. The antenna comprises 30 hydrophones, 10 being used for each beam. The sampling frequency will be 15 kHz; only the beamforming and adaptive noise cancellation are described.

5.3.2 Signal processing analysis

A typical signal processing without any cancellation is shown in figure 35; the beamformer is a delay-sum one and the outputs are used for both the active and passive chains; the two modes are exclusive one from the other. Figure 36 shows the same signal processing with the addition of a noise cancelling feature; it must be situated after the beamformer (see [2] pp 315,316) and, in the helicopter case, a new reference must be used for each beam (the center hydrophone for instance). However, a typical sonar requires more beams than hydrophones, for the sake of redundancy and accuracy; 50 can be considered as adequate here. Therefore, 50 adaptive lines are required to compute the value to be subtracted from each beam.

Figure 35: Typical dipping sonar signal processing

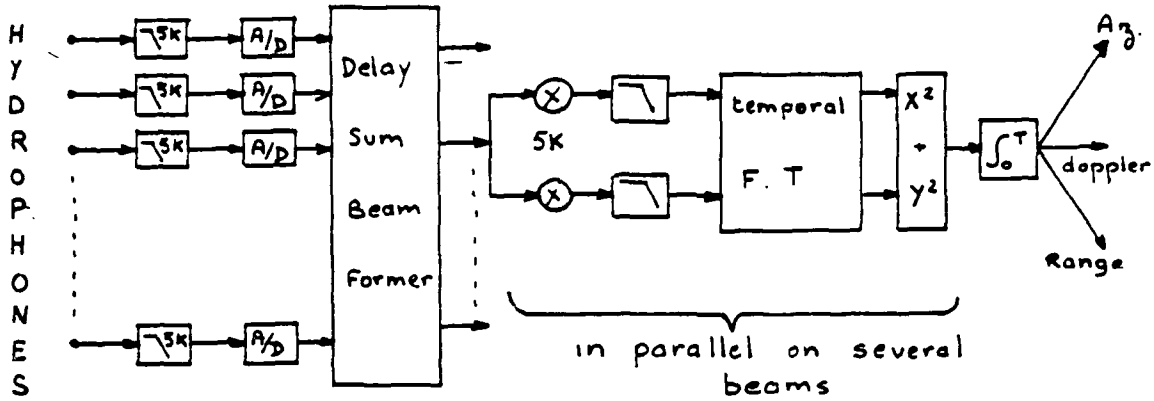

Figure 36: Addition of the adaptive self noise cancellation

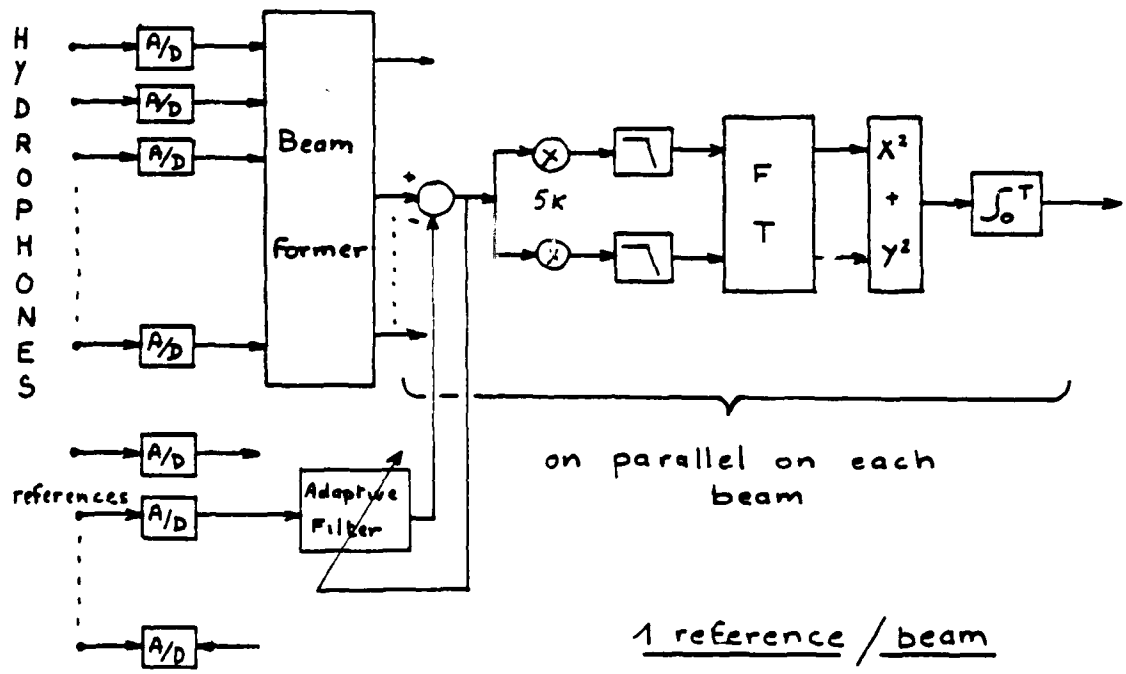

The adaptive filter could be implemented as a 50 taps transversal filter; a thorough study of the self noise features is needed to determine exactly the number of taps, but 50 represents a good average; indeed, it has nothing to do with the number of beams. The output of the subtracter is used for the subsequent processing and also for the error function for the adaptation. A typical 10 dB gain can be achieved in this case.

5.3.3 Digital and S.A.W. implementations

In this section is discussed a possible S.A.W. implementation of the described function; first of all, the number of operations per second that a digital implementation would require is determined. On the diagram shown in figure 36, the adaptive filter must give a data at the same sampling rate than the beamformer output, that is 15 kHz; each data is computed from 50 reference samples and represents one addition and one product per tap; then the total number of operation is multiplied by the number of beams (1 filter per beam). Therefore, equation (5) applies and the result is 75 Mops. This is not consistent with what a helicopter's sonar can afford as a matter of hardware capabilities (the beamforming itself, one of the most important operation only uses 45 Mops!). Notice that the adaptation algorithm itself is not taken into account. Several possibilities are available, and, moreover, the adaptation rate may be slowed down to limit the load. Furthermore, once the process converged and if the interference stays stationnary, no change is expected; therefore, the taps are unchanged; thus, the adaptation algorithm may be stopped. On another hand,

the transversal filtering is still required.

$$\text{Load} = 2 \times N_{beam} \times N_{tap} \times F_{sampling} \qquad (5)$$

A S.A.W. implementation is then the only alternative to implement such a function within a dipping sonar. The features of such an adaptive S.A.W. filter will now be discussed; for more details about it, see appendix 2. The generic scheme is indicated in figure 37. The duration of the filter for the sonar is 3.33 milliseconds; it must be shrunk to fit with the S.A.W. characteristics. Also, the A/D conversion, as was said, is limited to a 25 MHz signal; therefore, a compression factor of a thousand is chosen. This leads to a 3.33 μs filter with a 4 MHz bandwidth (size about 1.5 cm times 0.5 cm), because the input bandwidth is 1 to 5 kHz (see previous section). A 40 MHz carrier frequency is then adequate; notice that 50 taps are required for the filter, with or without time compression. However, the carrier modulation technique leads to a filter with 500 taps; among them, only 50 are consistent with the adaptive filtering, so each tap value is repeated 10 times. The time required for the filter to give an output is in the order of 3.5 μs; therefore, roughly nineteen 15kHz signals can be processed on the same filter. Thus, only 3 filters are required to process the 50 channels. In addition to that, memories (roughly 6 kilo bytes are needed), converters, a multiplexer, a demultiplexer, two mixers and a low-pass filter are required. Also of interest is the way to adapt the filter; figure 38 shows some details about it; according to section 2.2, only a D/A converter, some sample and holders and a multiplexer are required. This is still a reasonable hardware for such a function; it should represent 1 or 2 1/2 ATR electronic board.

Figure 37: S.A.W. implementation of the adaptive noise canceller

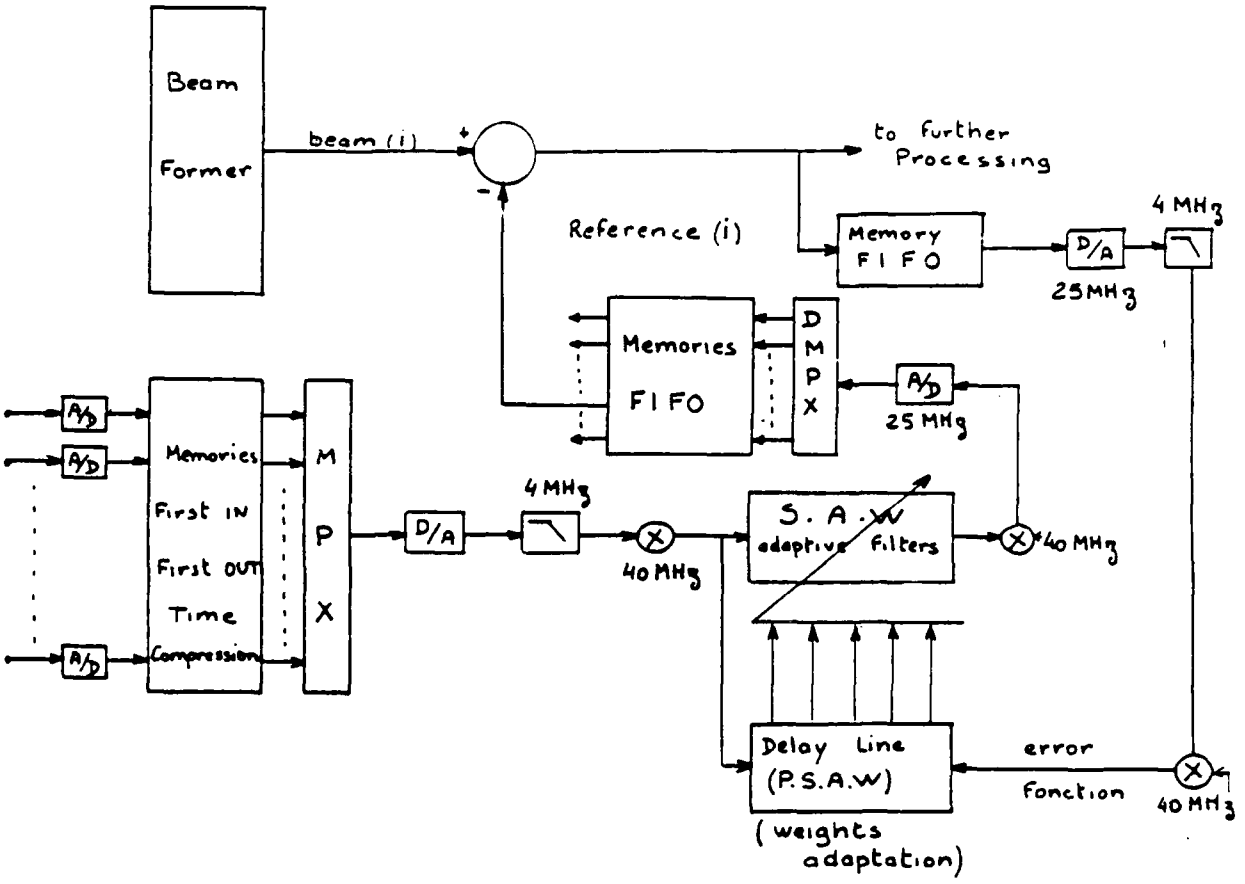

Figure 38: Adaptation process for the P.S.A.W. filter

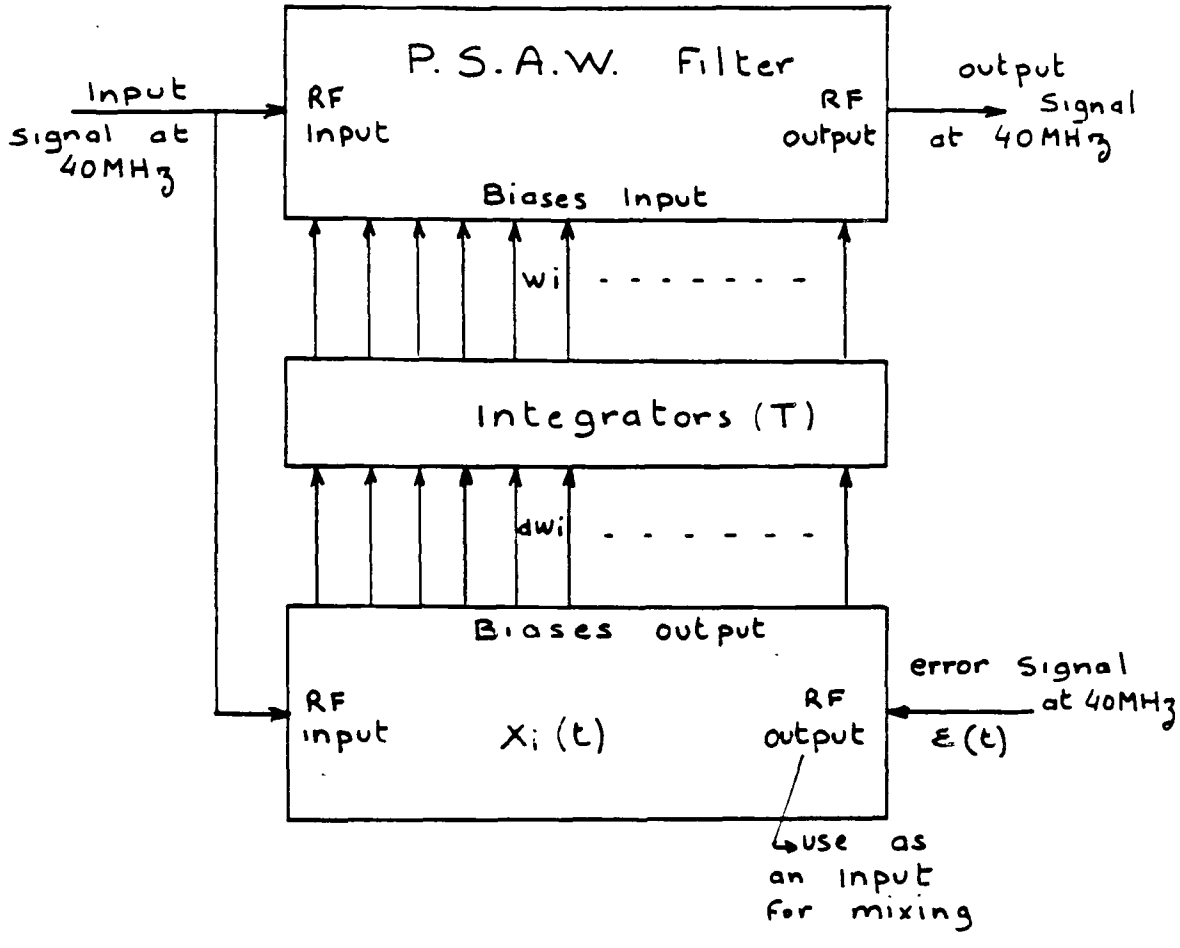

$$W_i = \int_0^T 2\mu \; \varepsilon(t) \; x_i(t) \; dt$$

5.3.4 Partial conclusion

So far, we described a very attractive application of adaptive S.A.W. filters in sonar; this dipping sonar application is promising because it helps to solve a big problem (i.e., the self noise coming from the hovering helicopter), without adding a lot of hardware. This is a very important requirement because weight and volume are very restricted for such sonars. Considering the digital implementation, it seems unreasonable and, therefore, not to be considered. However, the S.A.W. implementation truly offers a great opportunity.

Nevertheless, this application has to be studied in more details; particularly, the adaptive signal processing part needs to be detailed and this requires some data on the helicopter noise and the antenna; finally, a practical sonar case must be envisioned to enable a thorough study, which, only, may give some real insight on the promises of the described function.

AD-A130 910 ELASTIC DOMAIN WALL WAVES IN FERROELECTRIC CERAMICS AND 1/3
SINGLE CRYSTALS(U) STANFORD UNIV CA EDWARD L GINZTON
LAB OF PHYSICS B A AULD JUL 80 N00014-79-C-0222
UNCLASSIFIED F/G 20/2 NL

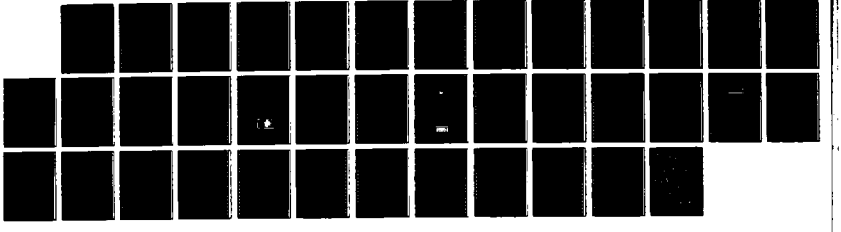

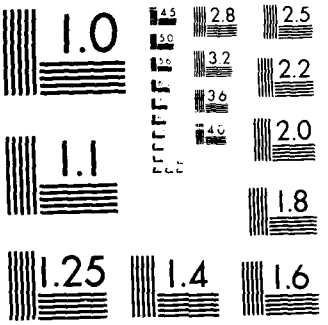
1.0
1.1
1.25
1.4
1.6
1.8
2.0
2.2
2.5
2.8
3.2
3.6
4.0
4.5
5.0

5.4 Intercept receiver

5.4.1 Some details

It was mentioned in section 3.1 that intercept receivers were adequate for the use of S.A.W. components. The large dynamic range could be reduced without too much loss in performances for the sake of hardware saving. Furthermore, it was said in [18] that one major problem for these equipments is the false alarm rate; this is due to the kind of expected signals and the fact that some mechanical vibrations are very similar to these signals. It happens that these mechanical vibrations are spatially very uncorrelated; therefore, a remedy to this problem consists in having different independant receivers that would confirm the detection of an acoustic wave, if any. It was already mentioned that these intercept receivers, dealing with high frequency impulsive noises, are built differently. Thus the hardware is specific to the application, and for such redundancy, each receiver would have its own processing, the synthesis being done by a general computer. The signal processing for such application is discussed in the following. Figure 39 pictures the principles of operation on a submarine.

Figure 39: Redundancy in intercept receiving

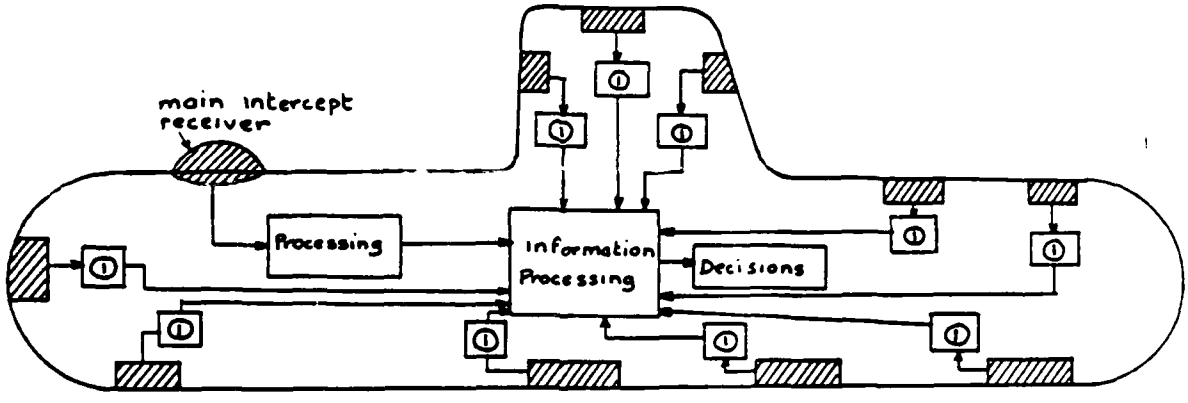

(1) Crude processing giving confirmations of detection (10 "confirmations" units here)

5.4.2 Signal processing analysis

In section 3.1.4 was given the general scheme of an intercept receiver. Here, the concern is the detection chain only and the requirements are the energy threshold, the frequency and an idea of the azimuth. Each independant receiver controls the whole frequency range but scans only a partial spatial sector, given by the directional hydrophones. A typical frequency range spans 10 to 100 kHz; usually, the signal is split into bands (generally corresponding to different hydrophone sizes), and consequently analyzed in spectral lines in each band. Here, only detection confirmations are expected and it may be worthwhile to directly analyze the full 10 - 100 kHz spectrum. With a sampling frequency of 300 kHz, a 1024 FT gives cells of about 300 Hz width; this should be enough for the purpose of these detectors. However, with digital processing, the equations (3) and (4) give a computational flow of 15 Mops; this is unthinkable for such a function. Nevertheless, since FT and S.A.W. component fit together, a S.A.W. implementation is worthy. The typical length of the analysis is 3.5 milliseconds. A compression ratio of 100 transforms it into a 35 μs duration and a 30 MHz signal, which is the upper limit for the A/D converter (see section 4.2). The large size of the device (35 μs) is here compatible with the specificity of the application. A S.A.W. Fourier transformer is then devisable; it would perform the FT in roughly 70 μs, leading to an equivalent computational rate of 360 Mops! Therefore, a single FT can process many parallel channels, i.e. different looking directions. Figure 40 shows the S.A.W. implementation for a group of 10 directional hydrophones. The size of each individual chirp filter

Figure 40: S.A.W. implementation and signal processing for a sparsed intercept receiver system; one group of ten is shown

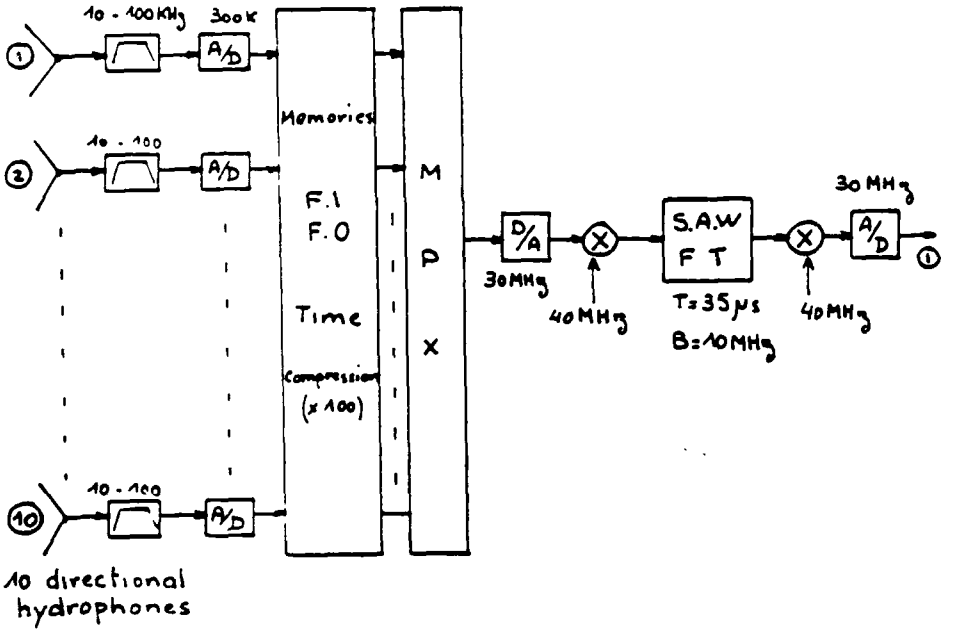

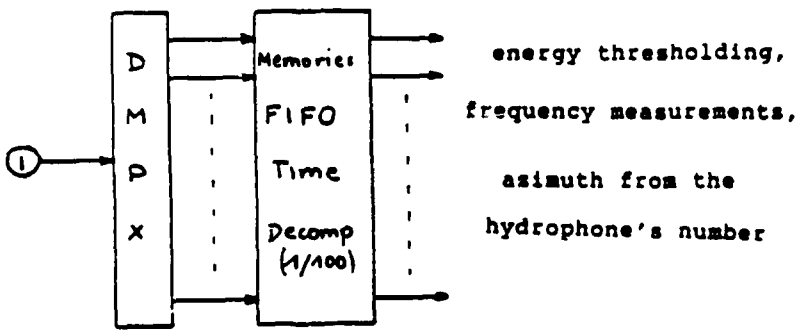

for the transform is roughly 10 cm by 1cm; however, for such FT, a R.A.C. implementation would be better [4,5,7,14] and roughly divide by two the length, while increasing slightly the overall width. Finally, such function could be implemented on two 1/2 ATR board, therefore leading to a very compact and fruitful harware.

5.4.3 Partial conclusion

It was shown that a particular intercept receiver system could take efficiently advantage of the S.A.W. component capability for Fourier transforms. The performance requirements for this system are compatible, especially for confirmations, with the S.A.W. capabilities. The high computational rate required for such application prevents it from being implemented digitally. One more time, S.A.W. components may allow the realization of an interesting but normally prohibitive function, at a reasonable cost. However, again, this is only a very brief overview of the problem and a thorough study could change the conclusion. Nevertheless, the purpose of this report is rather to point out the possibilities, advantages and drawbacks of S.A.W. use than to achieve a system.

CHAPTER 6

Some conclusions and openings

The present study intended to examine the different possibilities to use surface acoustic wave devices in a digital environment, and specifically for sonar signal processing. First of all were investigated the several points that could make a S.A.W. implementation promising for sonar. Some computational loads, the number of low-frequency channels and the capabilities of S.A.W. devices were derived to obtain some insights into these promises. Then, after recalling how a surface acoustic wave component is operating, the different achievable functions and the new possibilities offered by the concept of truly programmable or adaptive S.A.W. devices were listed. The interfacing of S.A.W. devices into a digital environment was investigated. It was derived that basically, two techniques, time compression and carrier modulation, were available for such purpose. However, the large discrepancy between the duration of sonar signals, though processed by segments, and the time length of a S.A.W. filter makes mandatory the use of time compression, at least before the carrier modulation. It was also shown that this technique involved only digital memories and multiplexers, and, indeed, did not require any extra component compared to a real-time digital implementation. Some performance figures were derived for the S.A.W. devices, in terms of computational speed, harware volume and consumption; these figures proved to outstand by a large factor the equivalent digital hardware for some specific functions such as transversal filtering (FIR), or Fourier transforms. On another hand were investigated different sonar signal processing chains in order to derive where using S.A.W. components could be fruitful. It was found that, sonar signal processing being mainly linear processing, several attractive functional blocks could be readily

implemented with S.A.W. devices. Different kinds of sonars, passive, active, or intercept receiver, were considered in order to discriminate the several possibilities in terms of frequency, performance requirements, and system standardization. Among the many attractive functional blocks were emphasized the beamforming operation for an equally spaced linear (or circular) array, the spectral analysis for detection purpose, the adaptive cancellation of some self generated noises and the two or three dimensional transversal filters involved for image processing. Some details were given about each of these applications. Nevertheless, using a S.A.W. component in a digital environment rises several constraints and trade-offs . These constraints were therefore investigated and the following points were made: First of all, these components, as many analog devices, are limited in terms of accuracy and dynamic range; some typical figures were assumed and compared to the real needs of a sonar; here again, the different varieties of sonar were separately investigated. It was shown that, except for the very recent large passive sonars, the accuracy of S.A.W. devices was consistent with what is available at the input of a sonar. Therefore, no real limitation was found on this aspect. However, it was shown that dynamic range was vastly changing for the different kind of sonars. The conclusions were that S.A.W. devices would not fit with passive sonars because of this limitation. On another hand, they would fit with active sonars and, allowing some performance losses, for intercept receivers. Also were investigated the limitations brought by the interfacing electronics. Although several components are involved, and each of them brings some specific problems, the real limitation occurs because of the A/D and D/A conversions, and especially of the first one: this prevents the time compression factors from soaring to the S.A.W. component needs and requires the use of carrier modulation techniques, in addition to the time compression. More important, it gives an upper limit to the time duration for signal processing, and

hence to the possible time bandwidth product. It was shown that 250 is a typical BT for such hybrid processing, and specifically, it may rise up to 1250, therefore losing some of the nice features, such as compactness. These limitations were introduced into the signal processing chain analysis for different systems in order to investigate some specially attractive applications. These applications were chosen because some of their characteristics were matching those envisionned for S.A.W. devices. Hence, a narrowband beamformer for a linear array on a torpedo system was shown to be promising. Also, an adaptive canceller for self generated noise on a helicopter dipping sonar was proved to have fruitful capabilities. Finally, an intercept receiver with sparsed antennae and distributed processing was investigated and nice capabilities were forecast.

In summary, in all of these specific applications, it was found that using S.A.W. devices may allow the realization of some fruitful functions that are possible with digital processing, but not compatible with hardware constraints. It should be noticed that, although these functions are very important, they are usually considered on these systems as a plus which should not change completely the hardware volume requirements; that is why S.A.W. implementation is so attractive. However, in a sonar system where such functions would be vital, it is certain that the digital solution, allowing better performances, would certainly be preferred. In fact, this consideration motivated our research of attractive applications: some functions that, though very promising and fruitful, were not mandatory. But, on a competitive international market, these "plus" may be a winning factor. Now that are recalled the different achievements of this study, it is important to synthesize these results and give some applicable rules or the use of S.A.W. components in sonar or some directions of further research for some specific applications. For this purpose, the case of a sonar designing

engineer will be considered, and it is assumed that this engineer is weighing the different advantages and drawbacks of using S.A.W. components into his application. First of all, what makes the use of S.A.W. devices wortwhile in sonar? In any case, the only true reason is the hardware savings, leading to more compactness and less power consumption; if this consideration is not of prime importance, there is no consistent reason for not using the more and more powerful digital technology. Moreover, it possesses nice features such as very good reproductibility, temperature and interferences insensitivity, software capabilities and so on. For the remainder is assumed that the hardware reduction is excessively important and thus the study worthwhile. The next important step to address is what kind of sonar is considered; it is for sure that if the main purpose of the sonar is a passive function, then the hardware constraint must be very strong to balance the drawbacks. As mentioned earlier, those are the dynamic range limitation to about 70 - 80 dB and the BT upper limit of 250. These are particularly important for a passive application because the dynamic range determines some of the detection performances; a typical BT is rather 500 to 1000, if not more, for the sake of performances. Finally, except for some very specific case, sonars having a passive main function are not to be considered further. However, this does not prevent a mainly active sonar, having a secondary passive subsystem, to use S.A.W. devices, even for shared functions such as beamforming. Now, the field is mainly restricted to active sonars and some specific equipments such as intercept receivers, sea bottom imagers, etc.. The following step is now to consider the number of low frequency channels, and thence, the computational load in order to see if it fits with S.A.W. devices. Usually, it will rather be too low rather than too high for S.A.W. capabilities, but this may still be attractive. The signal processing chain has also to be considered; as mentioned earlier, mainly Fourier transform and (adaptive or programmable) transversal filters are

available. Thus these functional blocks have to be identified; this is usually easy for sonar signal processing. If a couple of S.A.W. devices seem to be able to achieve the signal processing throughput where a powerful signal processor was required, it is time to investigate the interfacing electronics and its limits: Is the A/D conversion rate too high? Are there problems with the multiplexers, mixers, etc.? All these answers will determine the real promises of the potential application and give a better idea of the true hardware saving. In some cases, it could allow some specific function to be achieved where the digital solution was too expensive. The last, but not least, step is now to design or order the S.A.W. components; here, several problems may rise but, by working with the specialist people, a solution should be found. Actually, although leading to analog components with some drawbacks, this technology is very well understood and has been already used in several fields as radar or communications.

Finally, some further developments are likely to be done. Particularly, the image processing capability was emphasized as being attractive. However, no specific example was given, mainly because image processing is a whole science by itself. Also, designing an image processor for sonar (or radar) display involves to investigate accurately how a TV monitor works, since the S.A.W. filter would have to interact with it. Therefore, it seems that some studies are necessary in this area that should determine the potential applications. On another hand, it was already emphasized that detailing the use of S.A.W. devices in sonar would involve to specify accurately an application; it would be worthwhile in order to show the real promises to pick up an application (such as one described in section 5) and design it completely. Then a prototype could be realized to prove the whole thing. Finally, the adaptive signal processing seems to be promising for the union of sonar and S.A.W. processing. Here, some work is still

needed to adapt the large results on adaptive digital signal processing to its analog counterpart. Some more studies are also required on the truly programmable filters developped in Stanford. This is nowadays the major topic in Professor Auld's group and a prototype of an adaptive filter for TV application is under investigation.

To conclude, let us say that this study involved a field that was opened a decade ago; this report is nothing but another step in this field. We hope to have clarified some interesting opportunities, to have shown some nice available features with the union of an analog technique and a typically digital signal processing field. Let this work be a useful guide for some sonar engineers, desiring some knowledge about S.A.W. devices and also for S.A.W. specialists to get some more understanding about sonar developments.

APPENDIX 1

Bibliography

[1] A.V. Oppenheim, editor. "Applications of digital signal processing". Prentice-Hall. 1978.

[2] B. Widrow and S.D. Stearns. "Adaptive signal processing". Prentice-Hall Inc. - Signal processing series. 1985.

[3] S. Haykin, Editor. "Array signal processing". Prentice-Hall. 1985.

[4] David P. Morgan. "Surface Wave devices for signal processing". Elsevier - Amsterdam. 1985.

[5] Michel Feldmann and Jeannine Henaff. "Traitement du signal par ondes elastiques de surface". Masson - CNET, ENST. 1986.

[6] G.R. Laguna, P.F. Delval and B.A. Auld. "Electronic control of S.A.W. transduction in electrostrictive ceramics". Proceedings of the IEEE symposium on Ultrasonics. 1985.

[7] J.D. Maines and E.G. Paige. "Surface acoustic wave devices for signal processing applications". Proceedings of IEEE, Vol.64, No.5. May 1976.

[8] W.D. Squire, H.J. Whitehouse and J.M. Alsup. "Linear signal processing and ultrasonic transversal filters". IEEE transactions on microwave theory and techniques, Vol. MTT-17,

No.11. November 1969.

[9] C.Lardat, C. Legay and P. Tournois. "Applications des dispositifs a transfert de charges et de composants acoustiques a onde de surface au traitement du signal analogique". L'onde electrique, vol.57, No. 1 et 2. 1977.

[10] J.M. Alsup, R.W. Means and H.J. Whitehouse. "Real time discrete Fourier transforms using surface acoustic wave devices". IEE Conference Publication No.109. 1973.

[11] T.W. Bristol. "Analysis and design of surface acoustic wave transducers". IEE Conference Publication No.109. 1973.

[12] C. Atzeni and L. Masotti. "Linear signal processing by acoustic surface wave transversal filters". IEEE transactions on Microwave Theory and Techniques, Vol. MTT-21, No.8. August 1973.

[13] H. Gautier and P. Tournois. "Very fast signal processors as a result of the coupling of surface acoustic wave and digital technologies". IEEE Transactions on microwave theory and techniques, Vol. MTT-29, No.5. May 1981.

[14] M.A. Jack, P.M. Grant and J.H. Collins. "The theory, design and applications of surface acoustic wave Fourier transform processors". Proceedings of IEEE, Vol.68, No.4. April 1980.

[15] R.N. Bracewell. "The Fourier transform and its applications". Mc Graw Hill - 2d edition. 1986.

[16] J.M. Speiser and H.J. Whitehouse. "Dual chirp-Z transform". SPIE Vol.180 Real Time Signal Processing. 1979.

[17] H. Gautier and P. Tournois. "Signal processing using

surface acoustic wave and digital components". IEE Proceedings, Vol.127. April 1980.

[18] P.F. Delval, G.R. Laguna and B.A. Auld. "Systems applications of programmable electrostrictive transducers". Interim technical report -Ginzton laboratory - Stanford University. January 1986.

[19] G.R. Laguna. "Applications using electrically alterable material properties in large dielectric constant ceramics. Stanford University PhD thesis. June 1986.

[20] D.E. Oates, D.L. Smythe and J.B. Green. "SAW/FET programmable transversal filter with 100MHz bandwidth and enhanced programmability". Proceedings of the IEEE symposium on Ultrasonics. 1985.

[21] C.M. Panasik and D.E. Zimmerman. "A 16 tap hybrid programmable transversal filter using a monolithic Gaas dual gate FET array". Proceedings of the IEEE symposium on Ultrasonics. 1985.

[22] J.B. Green, G.S. Kino, J.T. Walker and J.D. Shott. "Novel programmable high speed analog transversal filter". IEEE Electronic devices letter, EDL-3. 1982.

[23] Engineering staff of Analog Devices Inc.. "Analog-Digital conversion handbook - 3rd edition". Prentice Hall. 1986.

[24] H. Gautier. "Digital processors using S.A.W. devices". Ultrasonics Symposium IEEE proceedings. 1981.

[25] H. Gautier et P. Tournois. "Processeurs ultrarapides employant les technologies a ondes acoustiques de surface et numeriques". 8eme GRETSI. Juin 1981.

[26] L.R. Rabiner and B. Gold. "Theory and applications of digital signal processing". Prentice Hall. 1975.

[27] R.J. Urick. "Principles of underwater sound - 3rd ed.". Mc Graw Hill. 1983.

[28] J.M. Speiser and H.J. Whitehouse. "Beamformer architectures ". Internal report - Naval Ocean Systems Center.

[29] D.R. Arsenault. "Wideband chirp-transform adaptive filter". Proceedings of the IEEE symposium on Ultrasonics. 1985.

[30] W.K. Pratt. "Digital Image Processing". John Wiley and sons Inc.. 1978.

[31] B.R. Hunt. "Digital image processing". Proc. IEEE, 63, 4, pp.693-708. April 1975.

[32] Y. Ichioka and N. Nakajima. "Iterative image restoration considering visibility". J.O.S.A., Vol.71, No.8. August 1981.

APPENDIX 2

A note on the signal processing applications of programmable surface acoustic wave devices, and specifically on the promises of an adaptive transversal filter

by P.F. Delval, and B.A. Auld
Stanford University

1. Introduction:

Surface acoustic wave (S.A.W.) devices are using the specific features of the propagation of surface acoustic waves on piezoelectric substrates in order to achieve some signal processing functions such as transversal filters and resonators [1,2]. Transversal filters are here envisioned in their general form; they involve a serie of delays (not necessarily equal), weightings (a_i) and a final summation. Figure 1(a) pictures this operation. With S.A.W. technology, a transversal filter is implemented using two acoustic transducers (a launcher and a receiver) (see figure 1(b)). The delays are achieved by taking advantage of the slow velocity of acoustic waves on solids (about 2000 m/s) and by spacing the different electrodes. The weigthings are conventionally determined by the overlap of two adjacent finger electrodes. This is perfect for fixed bandpass filters where the filter's characteristics are not to be changed (TV filters or radar ones). However, for more and more applications, the programmability of the filter transfer function is required. This is partly due to the competition of digital signal processing. Also very important is the impact of the adaptive signal processing; as the systems become more and more sophisticated, the way to model the mediums is less and less satisfactory; therefore adaptive signal processing, which tries continuously to adapt the model to the medium, is very attractive. Usually, an adaptive filter is achieved by using a programmable transversal filter and an adaptation algorithm. What is then required is a way of changing the weights of the filter according to the desired pattern. With conventional S.A.W. devices, this is not possible because of the implementation of the weights (once the electrodes are put on the substrate, it is very hard to make any change). Several people are working to solve this problem; this involves usually individually accessed electrodes and variable attenuations using FET circuits [3,4]. Despite the relative complexity of the electronics, the main drawback is the non linear relation between the actual weights and the command voltages. In this paper is described another concept to achieve the same result. In Stanford University was derived the idea that by electrically biasing a non piezoelectric but electrostrictive material, an induced piezoelectricity is achievable [5,6]. Therefore, by inducing a desired pattern, programmable weights are easily achieved; furthermore, the relation

Figure 1a: General form of a transversal filter:

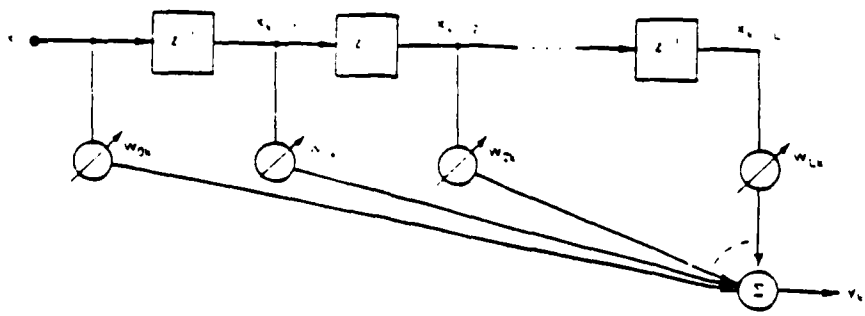

Figure 1b: S.A.W. implementation of a transversal filter:

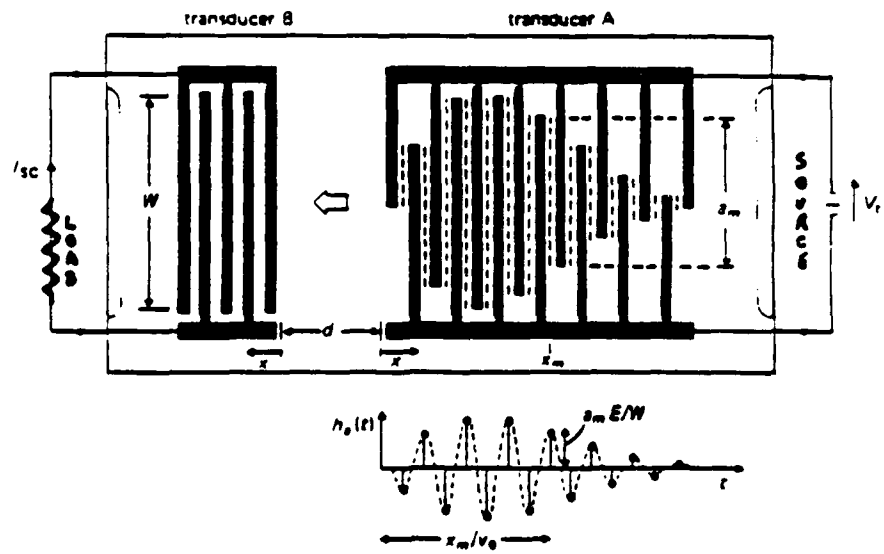

between the programmable coupling and the bias voltages is truly linear, with respect to the sign and magnitude. Thus, with straightforward electronics, adaptive or programmable filters can be realized.

In the following, the new physical concept is briefly reviewed, and some details about the design are given. Then, some promising component applications are investigated. A very attractive application, an adaptive S.A.W. filter for a TV image processing, is also described; it is nowadays under investigation at Stanford. Finally, some system applications of these components are evaluated and some conclusions projected.

2. Details on the principles and the design:

2.1 Overview of the principle

On conventional S.A.W. devices, the filter impulse response is determined, at the first order, by the spacing of the interdigital electrodes and the overlap of each pair. Comparing that to a digital transversal filter shows the following points: the input and output are analog, as are the weights; however, the delays are discrete, though not necessarily uniformly distributed (chirp filter [1,2]). The new concept has exactly the same features, except that the weights are not achieved by designing the overlap of two finger electrodes, but by controlling the piezoelectric coupling in that specific area. For this purpose, electrostrictive materials are used [5,6,7]. Piezoelectric materials satisfy the set of equations (1), where the d tensor is related to the piezoelectric coupling. On another hand, electrostrictive materials satisfy the set of equations (2) and are characteristic of any material having a center of symmetry. The Q tensor has generally very small coefficients, except for large dielectric solids (ϵ_r around several thousands).

$$D = \epsilon \cdot E + d : T \tag{1a}$$

$$S = s : T + d : E \tag{1b}$$

$$D = \epsilon \cdot E + 2 \cdot Q : T \cdot E \tag{2a}$$

$$S = Q : E^2 + s : T \tag{2b}$$

If two different electric fields are considered, E_1 and E_2, an electrostrictive material reacts to the square of the sum of the two fields. Actually, it is more complicated because all the electric field quantities are vectors. However, one can easily picture what is happening by considering them as scalar. With a proper electrode design, the quantities $Q \cdot E_1^2$ and $Q \cdot E_2^2$ have not the alternating polarity

that is necessary for launching a surface acoustic wave; therefore, only the $Q \cdot E_1 \cdot E_2$ term is responsible for the surface acoustic wave. If E_2 is considered as the conventional radio frequency (RF) field, applied on the inter digital transducer (IDT) electrodes, and E_1 is the biasing field, either applied on IDT electrodes too or on another set (see further for details), the $Q \cdot E_1$ combination is now similar to the d tensor in normal piezoelectrics. Equation (3) shows this result. The whole point is now that this d tensor is truly proportional to the applied biasing electric field, with respect to its sign and magnitude. A negative bias would result in a negative coupling. Therefore, by varying spatially and temporally the biasing field, different functions can be achieved and programmable or adaptive filters are readily available.

$$D = \epsilon \cdot E + (2 \cdot Q \cdot E_1) : T \tag{3a}$$

$$S = s : T + (2 \cdot Q \cdot E_1) : E_2 \tag{3b}$$

2.2 Filter design

Now that the basic principle is explained, the way to actually design such a filter is examined. As it was mentioned, two different electric fields must be applied on the material; the combination of these creates the function. However, the RF field must be set up as usually by using the IDT electrodes and the center frequency considerations are still the same. Then, in a first approach, the problem is to achieve the biasing field. The first attempted solution [5,6,7] gave good results although it does not allow a fine control of the impulse response. It consists in bottom plate electrodes which allow to bias the whole material. It is pictured in figure 2a. The thickness of the substrate, required for the Rayleigh nature of the wave (typically 10 lambdas), is responsible for the needed high biasing voltages and for the innaccuracy of the bias limits. However, it is still a good solution when bulk programming is required (i.e. whole section of the transducer, as opposed to control of each finger). In figure 2b is shown a possible improvement of the design by using a sandwich structure. The manufacturing is more complicated, but should be feasible. It has not been tested yet. Figure 2c represents a meander line structure. It allows low bias voltages along with individual controls if the connections are possible; indeed, air bridges for cross-connections are required. Finally, figure 2d shows what is the most promising solution. It allows low voltages along with individual controls; the design is rather simple since it corresponds to a split finger structure for conventional S.A.W. devices. The only remaining problem, present on all solutions, is the outside connection one; there are as many connections that programmable taps are desired. However, the hybrid circuit technology should be able to solve this problem. In the remainder, the last solution will mainly be considered; therefore, its design will be detailed, along with a basic physical explanation.

Figure 2: Biasing geometries. (a) top-bottom; (b) layered structure; (c) meander line; (d) Split finger transducer

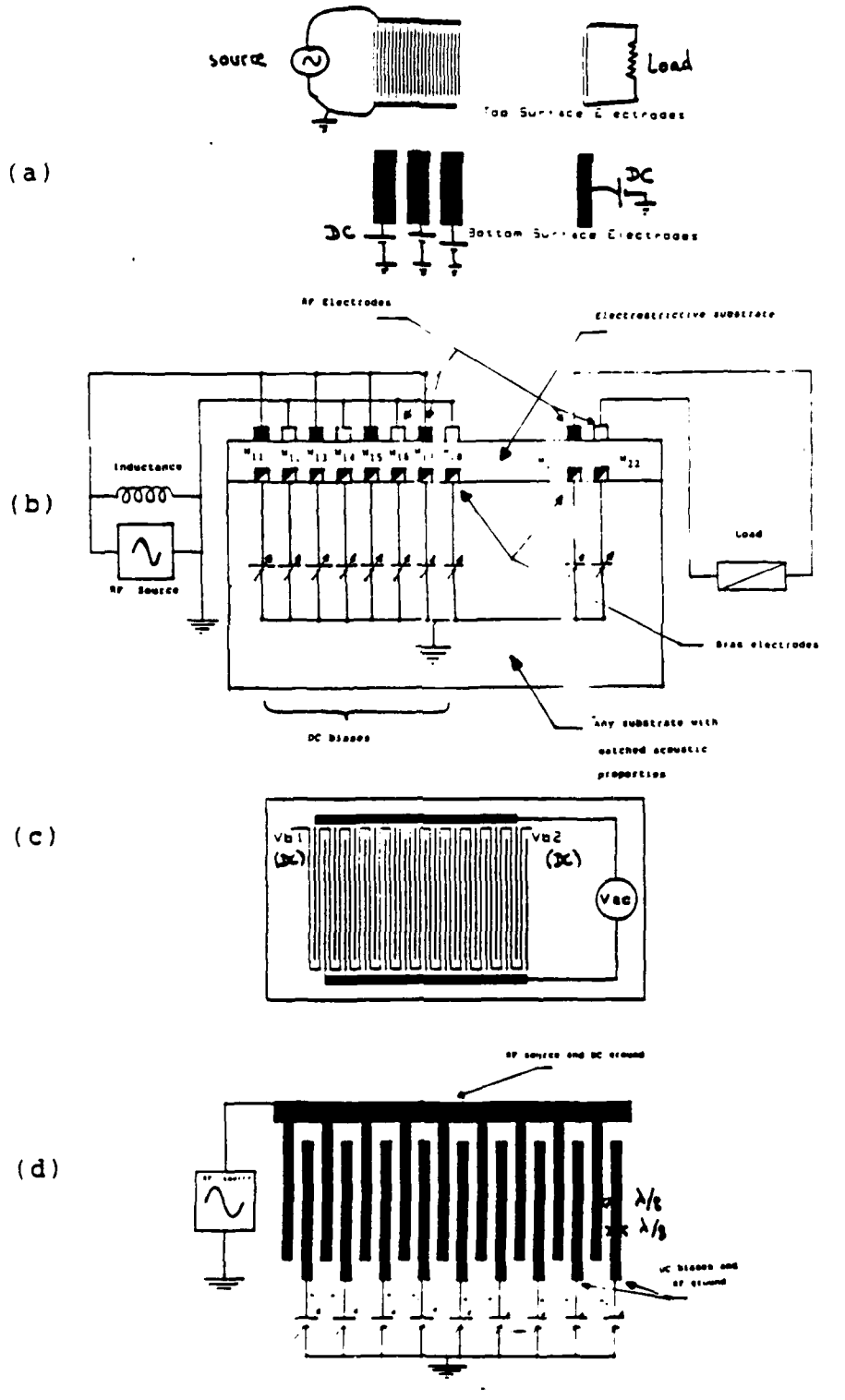

In order to get a basic and rough understanding of the transducer design for the split finger structure, the following remarks can be asserted: the forces that are created in the material, because of the electric fields have their magnitude proportional to the product of the magnitude of the applied fields, and its direction set up by the directions of the fields, as it is pictured in figure 3. Also, in order to generate a S.A.W., one needs to create an alternating set of forces, separated by half a wavelength (figure 3). Finally, the receiver works exactly the same way because of the reciprocity theorem [1,2].

Consequently, the design of a programmable transversal filter is done according to the following steps: first, the number of taps of the filter is determined; this may either involve the computation of the most requiring impulse function to be programmed, or, for adaptive filter, the number required by the problem itself (delay between reflected paths or interference features). Second, the center frequency of the filter is chosen; the signal center frequency is primarily important for this purpose, but some S.A.W. device considerations may lead to the choice of a different center frequency. In the latter case, where the signal is modulated prior to filtering and then demodulated, the signal undergoes an operation equivalent in the digital domain to an oversampling. Therefore, the impulse function of the filter undergoes the same oversampling; however, for the sake of the number of connections, taps may be connected in parallell. Actually, if 10 is the ratio between the signal and filter center frequency, and N the required number of taps (for signal purpose), then the filter needs $10 \cdot N$ taps but the taps are connected together 10 by 10 (see figure 4). Finally, the mask is made according to the center-frequency (one finger every $\lambda/8$, and width equal to gap) and the taps connected adequately as shown in figure 5.

A last but important point to mention is the following: the relation between the voltage and the effective tap value is linear; therefore, the only requirement for programming the filter is a variable DC power supply. It can be very efficiently implemented using a digital microcomputer and a D/A converter. Actually, considering the electrodes geometry, the current flowing into the circuit is nul as soon as the capacitance is charged. Thus, the circuit has a built-in holder on each electrode and a single D/A and an analog demultiplexer is enough to drive the filter, providing that the rate of the D/A is consistent with the programming speed.

Before detailing the applications, some constraints of these devices need to be pointed out. First, as all analog devices, there is a limited accuracy and dynamic range capability. Second, all S.A.W. devices have electromagnetic feedthrough problems, but especially these because of the high dielectric constant. Finally, the achieved electromechanical coupling is low, roughly twice the quartz figure with a biasing field of 1 MV/m or 30 Volts on a device working at 10 MHz, with the split finger geometry.

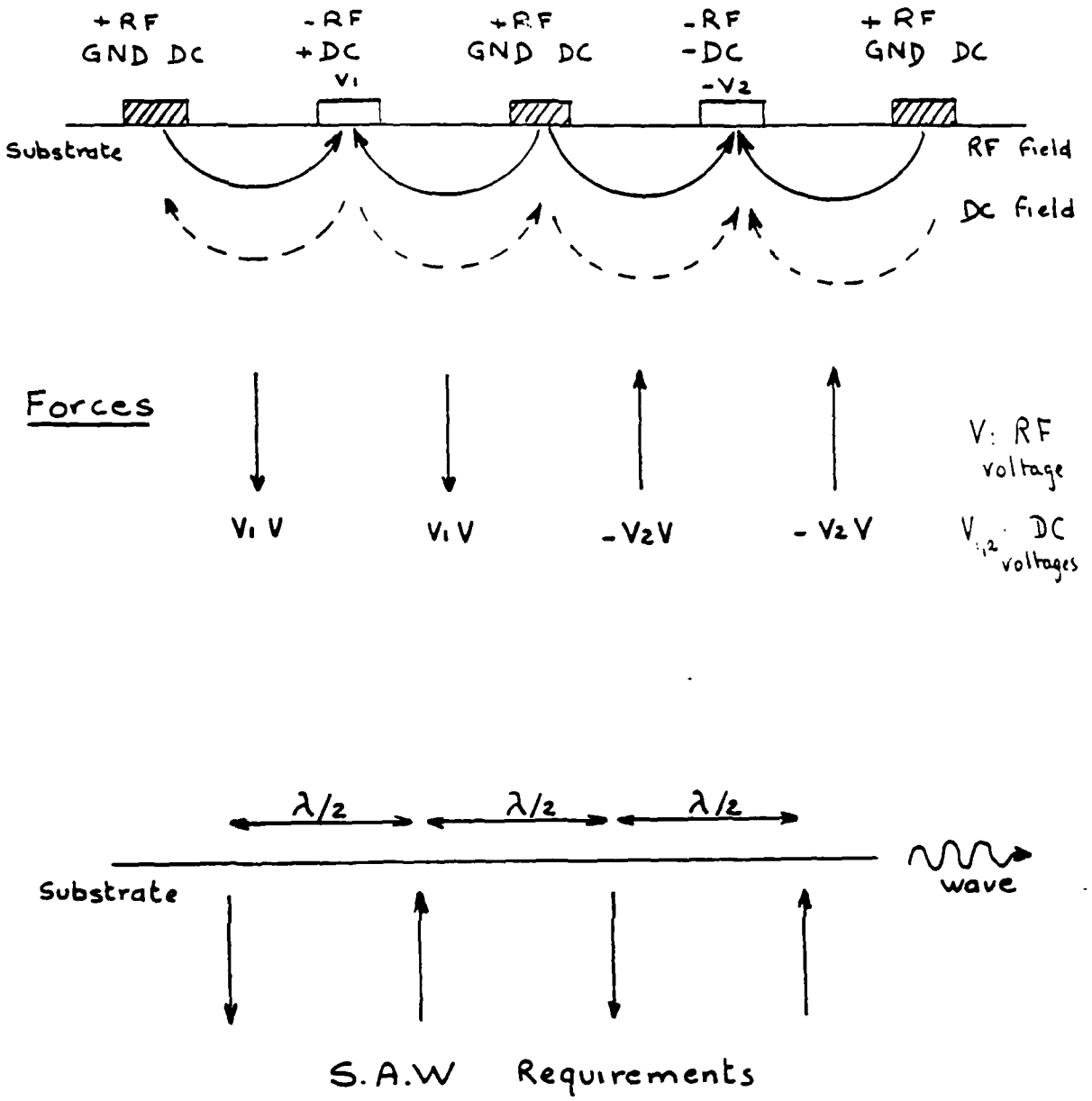

Figure 3: Fields and forces; S.A.W. requirements

Figure 4: Parallell taps

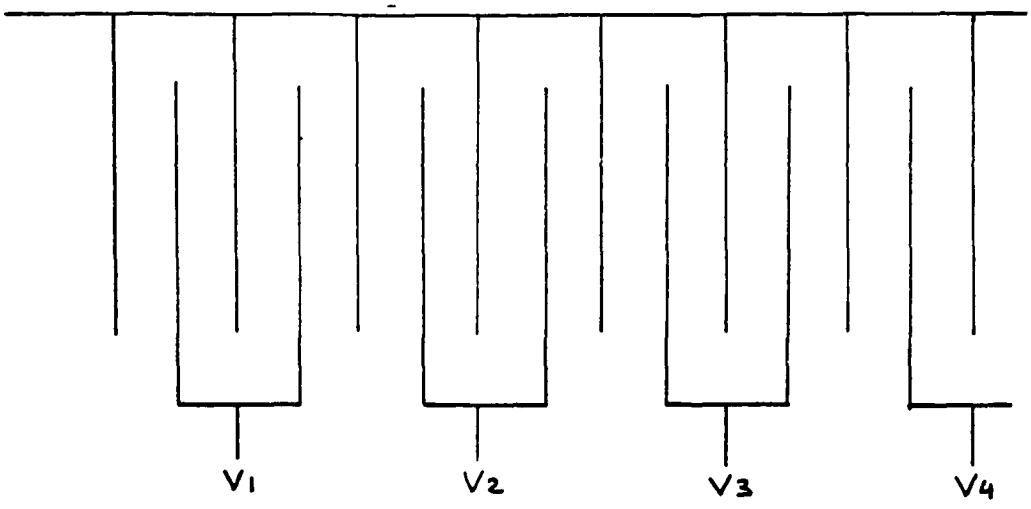

Figure 5: Mask and connections

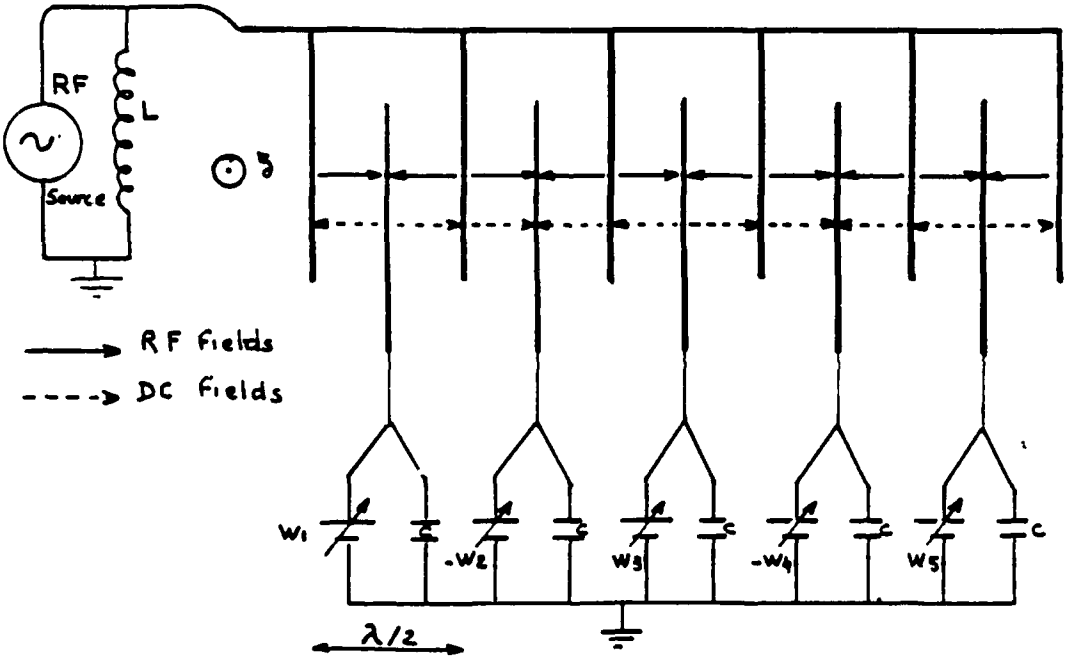

3. Some promising component applications:

We are now going to investigate the different promising component applications of these programmable S.A.W. devices. In a first part are described the different achievable functional blocks with their advantages. Then, a specific and very promising application, an adaptive transversal filter is prospected, along with the main features and principal use. This filter uses all of the different available features of a programmable S.A.W. device; therefore, it is also a very didactic example of this concept.

3.1 Achievable functional blocks

As mentioned previously, the main application of a S.A.W. device, programmable or not, is transverse filtering. However, since it is viewed in its most general form, it encompasses many more applications that what is usually envisioned for transversal digital filters. Indeed, there is no restriction such as uniform temporal sampling for a S.A.W. transversal filter. Therefore, frequency modulated signals are achieved easily by matching the spatial sampling to the desired waveform (see figure 6, chirp filter) [8]. As a matter of fact, this was one of the major S.A.W. application in radar (pulse compression). Also, the chirp filters are the major components into the design of a S.A.W. Fourier transformer (Figure 7). Then, all the applications of the Fourier transform in signal processing (spatial, temporal or image processing) are available with the fast capability of a S.A.W. device.

Actually, all these applications (and many more [1,2]) are also possible to realize with a programmable S.A.W. component. The resulting features are promising both from a component point of view (different functions on the same component) and from a system point of view (hybrid digital/S.A.W. processor having analog, programmable signal processing operators). It may be fruitful in a communication application to transmit different codes and allow the same component to perform the matched filtering operation by programming its impulse response. Also, programmable bandpass filters are achievable, leading to the capability of choosing one band among others (TV application for instance). The concept of impulse response programming is pictured in figure 8. On another hand, programmable and digitally compatible Fourier transformer may be easily designed with this technique. As a matter of fact, weighting of the analysis may be readily achieved by the bias control. Indeed, the weighting may be adjusted in real-time, therefore showing immediately the impact on the response. Fourier transform programming (for hybrid processor for instance) and weighting technique is shown in figure 9. Note that this weighting is also achievable with conventional S.A.W. devices but by using specific bilinear mixers.

The limitation of these components is their operating frequency. It is nowadays limited to tens of MHz, because of the substrate quality. However, even at this frequency, it outstands the digital capabilities for some specific signal processing

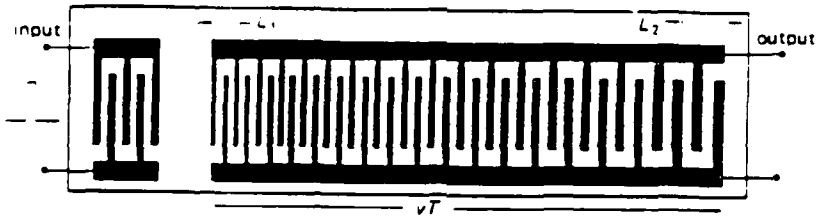

Figure 6: Chirp filter

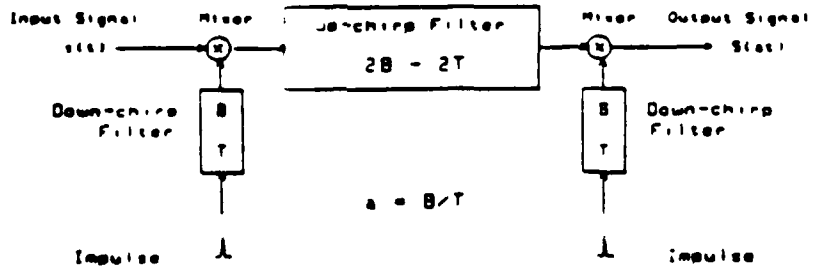

Figure 7: Fourier transform and chirp filters

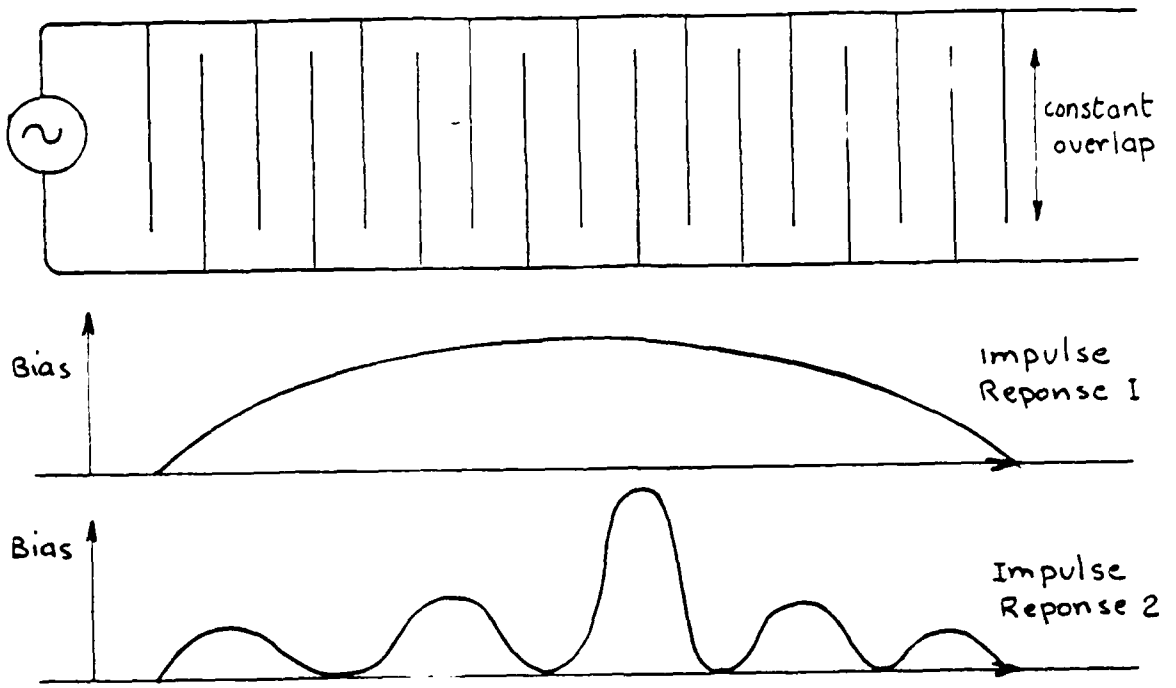

Figure 8: Impulse response programming

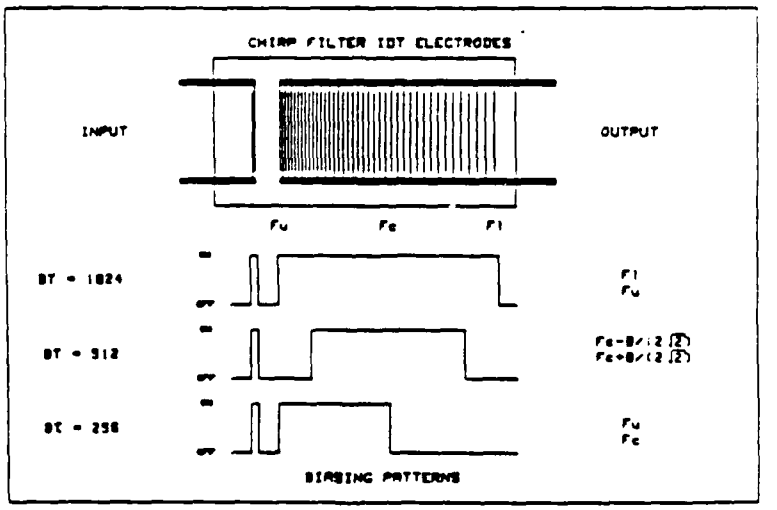

Figure 9: Fourier transform programming and weighting

blocks, generally with smaller and cheaper hardware. For instance, a bandpass filter at 20 MHz, having 100 taps (roughly 2.5 μs) has an equivalent speed of 500 mega operation per second. This filter is about 1 cm long and 3 mm wide. This is truly a very fast component.

3.2 Adaptive filter design

Adaptive filters may often be implemented with a variable weight transversal filter plus an adaptation algorithm [9]. The realization of such a filter with a programmable S.A.W. component is investigated in the following. The goal is to design a filter dealing with a multipath problem for a TV application. However, it is consistent with any adaptive signal processing. Indeed, the main concern is here the realization of the adaptive filter itself and few details are given about the adaptation process. It is envisioned only for the sake of clarity and in order to take the whole thing into account. Moreover, the LMS (least mean square) algorithm is considered because a thoroughly analog version is conceivable. According to [9], the scheme from figure 10 is adequate for the envisioned problem; the desired signal has to be estimated or created; this problem is not adressed here because of the nature of this paper; however, it is important to emphasize that, because of the inherent delay in a S.A.W. filter (between launcher and receiver transducers), the desired signal may need to be also delayed when it is derived from the input signal. Otherwise, the delay on the filtered signal (usually a few microseconds) would decorrelate the signal and the reference.

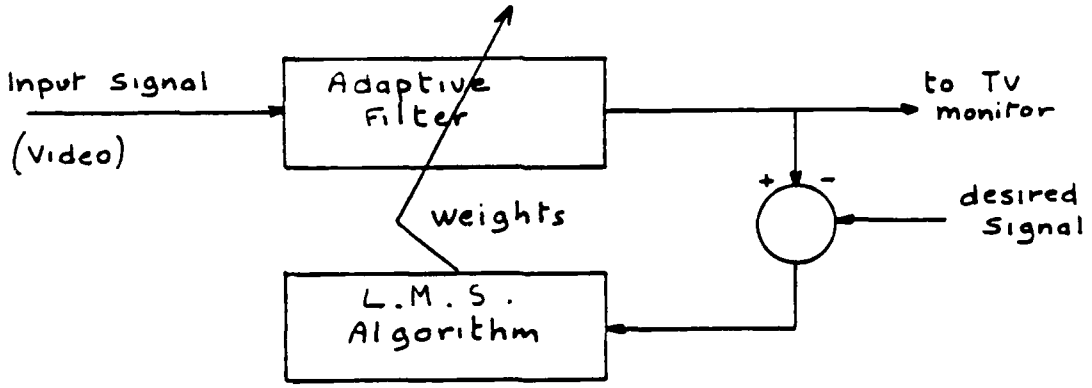

Figure 10: Adaptive filter algorithm

The conventional (digital) equations to be considered are recalled in (4) and (5). Y^k is the output of the filter at time "k"; X_i^k is the ith input sample at time "k" and the W_i^k are the different weights at time "k"; ϵ^k is the error function, d_k the desired signal and μ is the gain of the feedback loop, determining the speed of

convergence and misadjustment factor.

$$Y^k = \Sigma_i (W_i^k \cdot X_i^k) \tag{4}$$

$$W_i^k + 1 = W_i^k + 2 \cdot \mu \cdot \epsilon^k \cdot X_i^k \tag{5a}$$

$$\epsilon^k = Y^k - d^k \tag{5b}$$

For a S.A.W. filter, these equations have to be transformed into their continuous form, except for the input sample and weight numbering, because the latter stay discrete (finger pair locations). The basic idea is thus to keep all indices i and to transform the index k in a time variable t. These new equations are indicated in (6) and (7). The filter implementation follows this set of equations. It was already pointed out that equation (6) can be achieved through the use of a S.A.W. transversal filter. Equation (7) is possible to achieve using moderate electronics and the described programmable S.A.W. concept. The basic idea is to use two programmable S.A.W. filters, one truly working as a filter and the other as a variable delay line; if the two are identical, the $X_i(t)$ in eq. 7a are easily obtained. Figure 11 shows the basic implementation and figure 12 pictures a component either used as a filter or as a matched delay line.

$$Y(t) = \Sigma_i (W_i(t) \cdot X_i(t)) \tag{6}$$

$$\delta W_i(t)/\delta t = 2 \cdot \mu \cdot X_i(t) \tag{7a}$$

$$\epsilon(t) = Y(t) - d(t) \tag{7b}$$

Finally, the whole implementation is shown in figure 13. The output signal is split in two part, one going through the filter and the other through the delay line. The output is used to create the error signal through an operational amplifier, which is also achieving the μ factor (R_1/R_2). Then this signal is used as a bias signal for the delay line, taking advantage of the mixing capability of these programmable S.A.W. components. Each output of the delay line is now corresponding to the right hand term of equation (7a). A straightforward integrator, achieved through the use of an operational amplifier, finishes the signal processing loop and drives the bias of the actual filter; the low output impedance of an operational amplifier permits to put the bias electrodes to the ground for the high frequency signal (i.e. the input signal). Indeed, the input signal is modulated on the center frequency of the filter; a quick calculation shows that the error signal has the same carrier frequency, and thus,

Figure 11: Basic scheme for a LMS adaptive S.A.W. filter

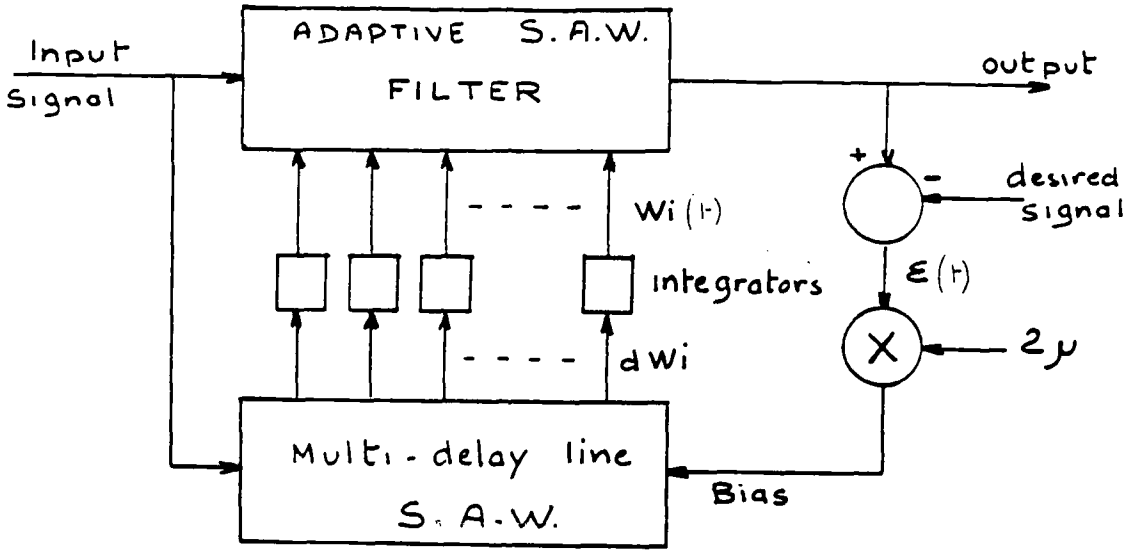

Figure 12: Programmable S.A.W. filter(a) and matched delay line(b)

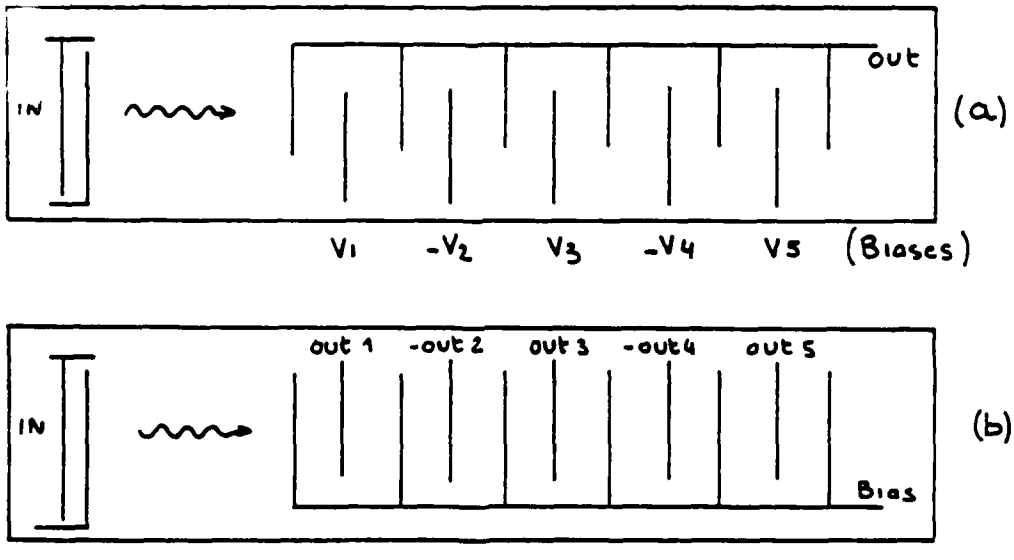

the weights are varying according to the useful signal frequency (demodulated); then, from the filter's point of view, the bias is a low frequency signal (TV video bandwidth for instance (5-6 MHz)). Finally, to end the connections, some inductors are added to put the top electrodes to ground for the biases.

A last point to emphasize is that the integrators have a time constant linked to the C and R_3 values. Indeed, these values affect the convergence rate of the filter. It means that, as opposed to digital filters where the analysis takes only μ into account, this time constant must be considered in the design process. Also, this time constant determines the higher frequency that is passed through the filter without being low-pass filtered. Finally, to emphasize the capability of this application, a TV case is considered and the equivalent digital computational load evaluated. Taking a filter with 750 taps (50 variable weights), working on VHF signals (5 MHz bandwidth on a 75 MHz carrier), would require two S.A.W. components fitting both on a 10 by 10 mm substrate (then fitting into an IC package). Adding the external electronics would lead to an implementation with a few hybrid packages. A digital implementation is not conceivable because the load would be around 1 giga operations per second! This adaptive filter is under investigation now and fruitful results are expected; however, several design problems are currently encountered.

4. System applications and some conclusions:

To conclude, some system applications of these programmable S.A.W. devices are prospected and the future of this component envisioned. There are four main signal processing functions that could be achieved with such components: bandpass filters, matched filters, Fourier transformers and adaptive transversal filters. These blocks are very common in several systems such as radar, communication, video transmission, medical imaging systems. geophysics, radio astronomy, sonar, etc.. Then, the application field is very wide but some other concepts like frequency range, dynamic range or accuracy considerations may allow or not the use of such components. Actually, video transmission and medical imaging are the most suitable fields for these components and it is likely that very fruitful implementations are conceivable. However, radar systems may use these components at an intermediate frequency processing; also, sonar or geophysics systems may use these components efficiently using a time compression scheme [10]. Moreover, some material improvements (and therefore an increase in frequency) are expected and hoped in order to enlarge the promises of this concept. They are likely because these electrostrictive materials have not been designed for that purpose; the promises may incite people to work on this problem and a very good quality one may exist. Finally, it seems to us that the most attractive application for this concept is the adaptive filter. Indeed, the others are also promising, but the programmability is only a "plus" that is not required necessarily. Contrariwise, adaptive signal processing is getting more and more interest, but is restricted nowadays to digitally implemented systems. The existence of an analog adaptive filter would surely open

new fields of applications. Furthermore, the digital compatibility, the linearity of the programming, the easy manufacturing and the mixing capability are truly keypoints. The described adaptive filter, which was entirely analog, is perfectly conceivable with other adaptation algorithm; direct methods, like eigenvectors, are truly achievable using a hybrid structure. Nevertheless, these components, and the concept itself, are still in their childhood. A lot of work is required before the described adaptive filter is actually working or implemented in TV sets. Yet, the prospects are already good and exciting and should definitely represent a breakthrough.

5. Bibliography:

[1] David P. Morgan. "Surface Wave devices for signal processing". Elsevier - Amsterdam. 1985.

[2] Michel Feldmann and Jeannine Henaff. "Traitement du signal par ondes elastiques de surface". Masson - CNET, ENST. 1986.

[3] D.E. Oates, D.L. Smythe and J.B. Green. "SAW/FET programmable transversal filter with 100MHz bandwidth and enhanced programmability". Proceedings of the IEEE symposium on Ultrasonics. 1985.

[4] J.B. Green, G.S. Kino, J.T. Walker and J.D. Shott. "Novel programmable high speed analog transversal filter". IEEE Electronic devices letter, EDL-3. 1982.

[5] G.R. Laguna, P.F. Delval and B.A. Auld. "Electronic control of S.A.W. transduction in electrostrictive ceramics". Proceedings of the IEEE symposium on Ultrasonics. 1985.

[6] G.R. Laguna. "Applications using electrically alterable material properties in large dielectric constant ceramics. Stanford University PhD thesis. June 1986.

[7] G.R. Laguna and B.A. Auld. "S.A.W. transduction in electrostrictive substrates". Proceedings of the 1986 ISAF symposium. June 1986.

[8] M.A. Jack, P.M. Grant and J.H. Collins. "The theory, design and applications of surface acoustic wave Fourier transform processors". Proceedings of IEEE, Vol.68, No.4. April 1980.

[9] B. Widrow and S.D. Stearns. "Adaptive signal processing". Prentice-Hall Inc. - Signal processing series. 1985.

[10] P.F. Delval. "Sonar applications of surface acoustic wave devices". Stanford University, Ginzton Laboratory internal report. August 1986

APPENDIX 3

Programmable coupling hydrophones

In this appendix will be described another potential application of electrostrictive ceramics for sonar; these ceramics, as it is pointed out in section 2.2, are non-piezoelectric; however, an induced piezoelectricity may be achieved by applying a bias voltage. Section 2.2 was describing one of the most potential applications, programmable surface acoustic wave devices; here will be presented the use of electrostrictive materials for programmable hydrophones. The basic idea is the same than for S.A.W. devices, that is to get a programmable electromechanical coupling coefficient; the mean is the same, to apply variable biasing voltage on the material, on top of the driving field. Promising applications of this technique were described in [18]: automatic gain control directly into the hydrophone, in order to shrink the dynamic range on the following preamplifier; a spatially controlled acoustic aperture, leading to the capability to implement weighting functions in the transducer. Figure A2.1 pictures the basic applications of this technique.

The main difference with the technique described in section 2.2 lay in the kind of desired acoustic waves; for hydrophones, bulk waves are expected, and therefore, the transducer's electrodes are different. Figure A2.2 shows two classical modes for driving the material, depending on the vibration mode (radial or transversal). The disposition of the electrodes, and the required condition that the

Figure A2.1: Basic applications: Automatic gain control and spatial aperture control

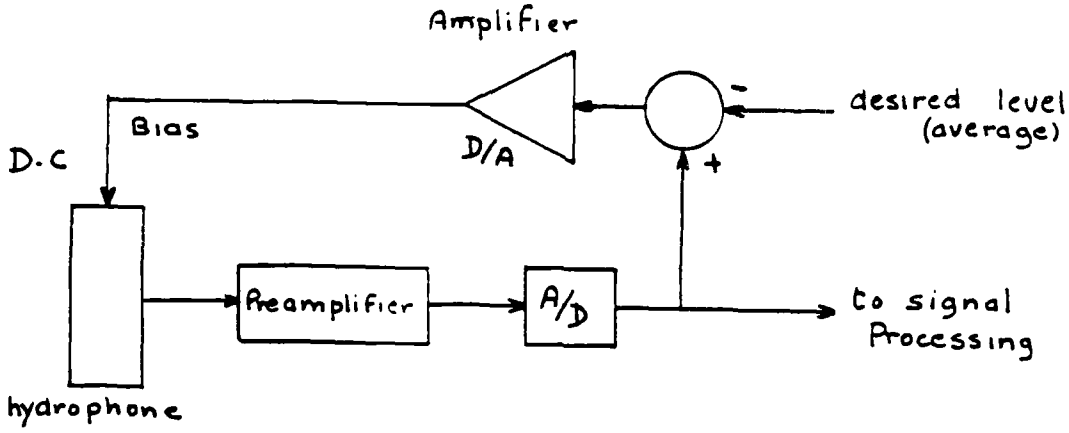

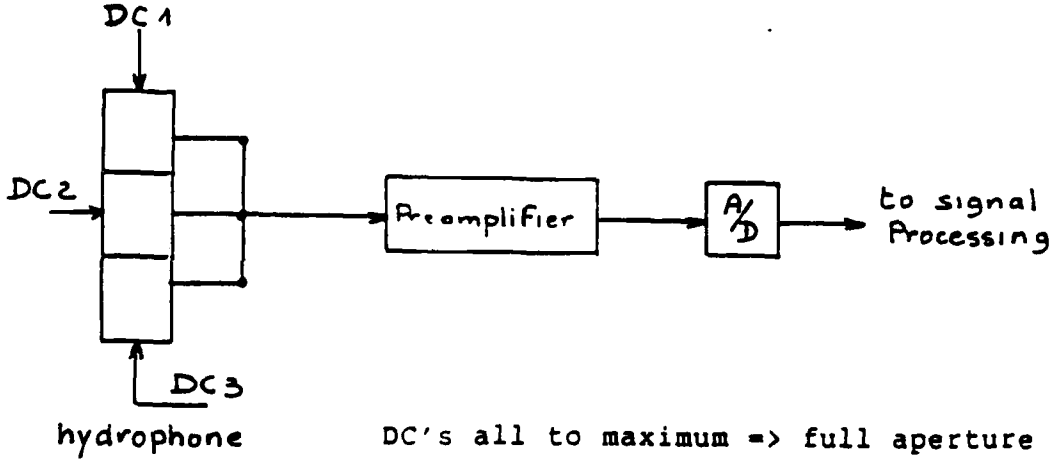

DC's all to maximum => full aperture

DC1 = DC3 = 0, DC2 = max. => central aperture

Figure A2.2: Typical electrode locations for hydrophones

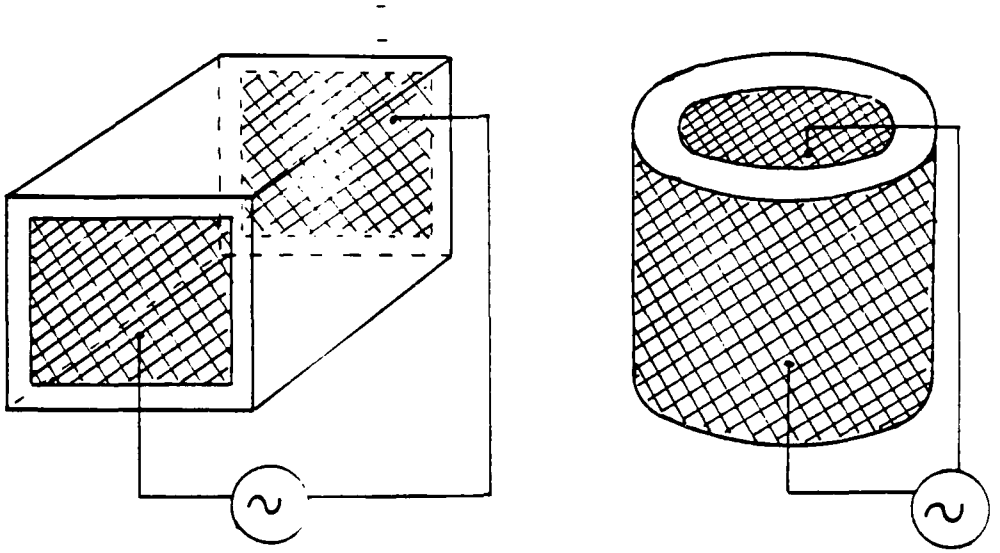

Figure A2.3: Various scheme to bias the material

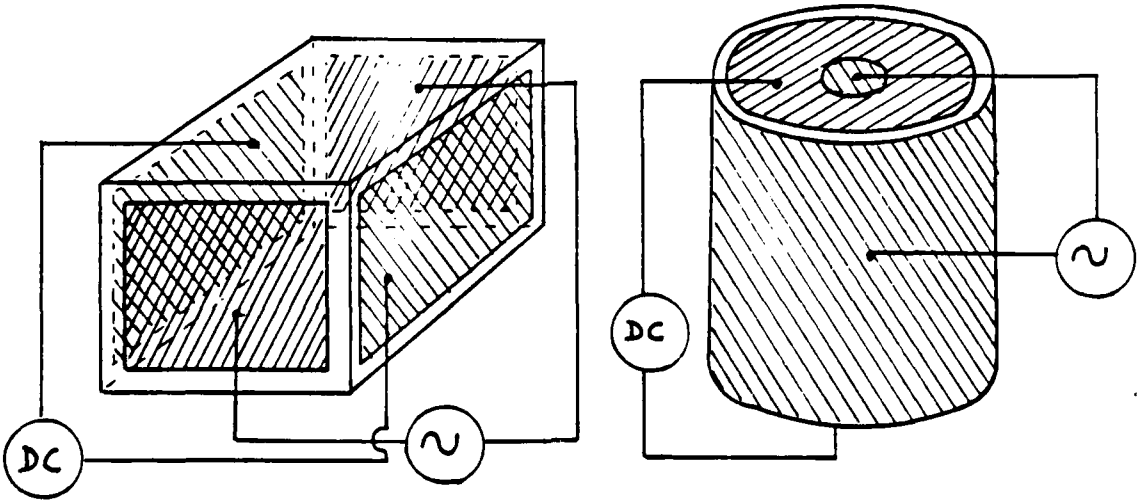

material is biased in the whole interaction volume, lead to the main constraint, that is almost the entire hydrophone needs to be biased; thus, because of the great distances between electrodes, high voltages will be required; according to the size of the hydrophone, they will vary between a few hundred volts and a thousand volts. Figure A2.3 describes the various possible ways to bias the material and therefore, launch bulk acoustic waves with the desired characteristics. Also, the size of an hydrophone is very often much larger than a S.A.W. device; then, is it possible to get this material in large enough pieces? The answer is that these materials can be manufactured as a powder, which is eventually included into an epoxy matrix to get a composite material. This way, large pieces of material are possible to obtain with the desired electrostrictive properties, and the nice and fruitful promises of composite structures.

Potential applications of this technique were, then, emphasized in [18]; however, it turned out that they are not truly promising. Among the different reasons for this are the high required voltages and the possibility to get the same effects with another method which does not require high voltages nor specific non-piezoelectric materials. Indeed, using conventional hydrophones and step gain preamplifier, the automatic gain control feature can be achieved; however, the real problem is that all these systems will be too slow to react to impulsive noises, which are the problematic ones for dynamic range limitations. On another hand, there are several techniques to get a spatially controlled acoustic aperture. Figure A2.4 pictures one possibility; eventhough it seems complicated, it is very simple to manufacture because of the relative large size of the hydrophones.

Moreover, according to the acoustician people in N.U.S.C., this spatial control is not really the big trend nowadays. Furthermore, this is already a big problem to get all the acoustic signals inside the submarine's hull, leading to many many holes. It seems unreasonable, for such a specific function, to complicate the problem, or worse add some holes, just to get some high DC voltage signals out of the hull. This will also increase the power consumption. Finally, it seems that such an idea, although promising in the principle, has no real potential application in sonar. However, it may have for other fields, such as medical ultrasonic imaging; but, this is another story.

Figure A2.4: Conventional ways to get programmable coupling hydrophones

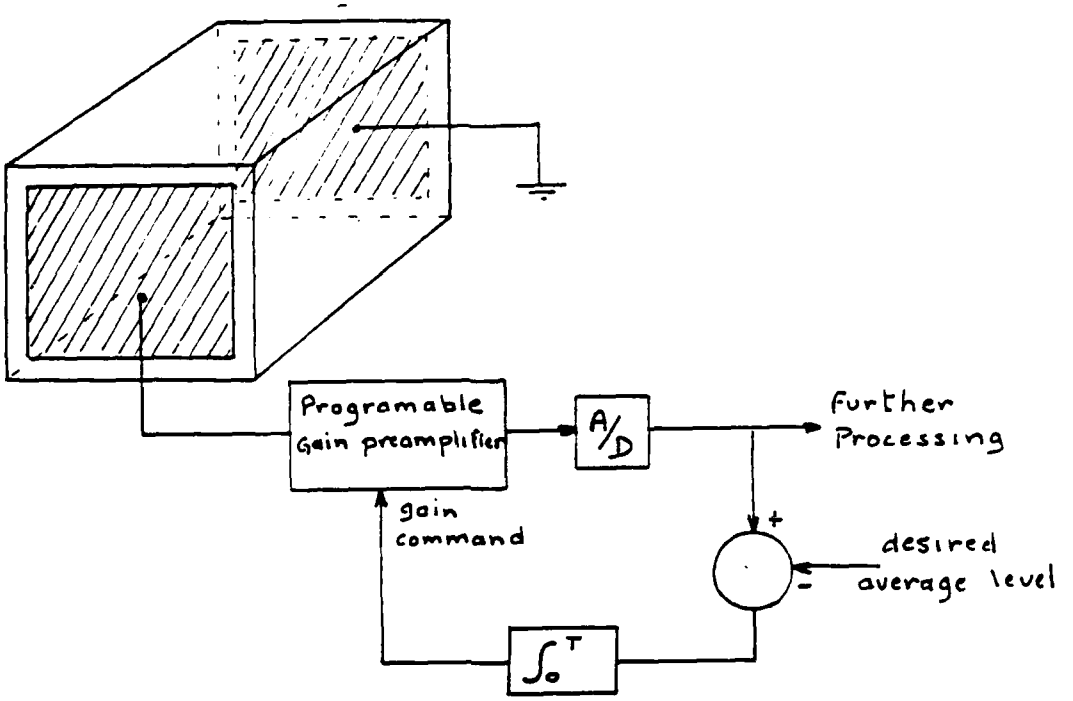

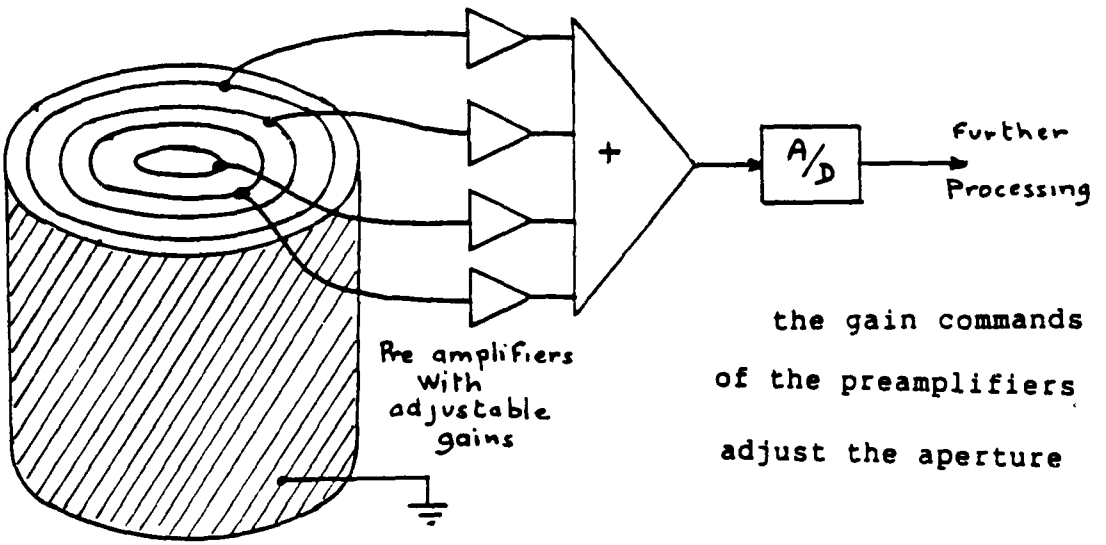

END

DATE

FILMED

DTIC

11-88